



Associate Directorate for Environmental Management

P.O. Box 1663, MS M992
Los Alamos, New Mexico 87545
(505) 606-2337

Environmental Management

P. O. Box 1663, MS M984
Los Alamos, New Mexico 87545
(505) 665-5658/FAX (505) 606-2132

Date: APR 25 2018
Refer To: ADEM-18-0013
LAUR: 18-23194

John Kieling, Bureau Chief
Hazardous Waste Bureau
New Mexico Environment Department
2905 Rodeo Park Drive East, Building 1
Santa Fe, NM 87505-6303

Subject: 2017 Sandia Wetland Performance Report

Dear Mr. Kieling:

Enclosed please find two hard copies with electronic files of the 2017 Sandia Wetland Performance Report. Los Alamos National Laboratory (the Laboratory) has prepared this report in response to requirements set forth in the document Work Plan and Final Design for Stabilization of the Sandia Canyon Wetland. The requirement to design a Sandia wetland monitoring program was previously set forth in the New Mexico Environment Department's (NMED's) Approval with Modification, Interim Measures Work Plan for Stabilization of the Sandia Canyon Wetland, in response to the Laboratory's Interim Measures Work Plan for Stabilization of the Sandia Canyon Wetland. The report was modified to consider comments from NMED in its Approval with Modifications [for the] 2016 Sandia Wetland Performance Report, dated September 11, 2017, and during a pre-report submittal meeting on January 22, 2018. The document also satisfies Appendix B, Milestones and Targets, Milestone 5, of the 2016 Compliance Order on Consent.

If you have questions, please contact Steve Veenis at (505) 667-0013 (veenis@lanl.gov) or Cheryl Rodriguez at (505) 665-5330 (cheryl.rodriguez@em.doe.gov).

Sincerely,

Enrique Torres, Program Director
Environmental Remediation Program
Los Alamos National Laboratory

Sincerely,

David S. Rhodes, Director
Office of Quality and Regulatory Compliance
Environmental Management
Los Alamos Field Office

ET/DR/SV

Enclosures: Two hard copies with electronic files – 2017 Sandia Wetland Performance Report (EP2018-0013)

Cy: (w/enc.)
Cheryl Rodriguez, DOE-EM-LA
Steve Veenis, ADEM ER Program

Cy: (w/electronic enc.)
Laurie King, EPA Region 6, Dallas, TX
Raymond Martinez, San Ildefonso Pueblo
Dino Chavarria, Santa Clara Pueblo
Steve Yanicak, NMED-DOE-OB, MS M894
emla.docs@em.doe.gov
Public Reading Room (EPRR)
ADESH Records
PRS Database

Cy: (w/o enc./date-stamped letter emailed)
lasomailbox@nnsa.doe.gov
Peter Maggiore, DOE-NA-LA
David Rhodes, DOE-EM-LA
Enrique Torres, ADEM ER Program
Randy Erickson, ADEM
Amanda White, ADEM ER Program
Jocelyn Buckley, ADESH-EPC-CP
Benjamin Roberts, ADESH-EPC-DO
William Mairson, ADESH/PADOPS
Craig Leasure, PADOPS

LA-UR-18-23914
April 2018
EP2018-0013

2017 Sandia Wetland Performance Report



Prepared by the Associate Directorate for Environmental Management

Los Alamos National Laboratory, operated by Los Alamos National Security, LLC, for the U.S. Department of Energy (DOE) under Contract No. DE-AC52-06NA253 and under DOE Office of Environmental Management Contract No. DE-EM0003528, has prepared this document pursuant to the Compliance Order on Consent, signed March 1, 2005. The Compliance Order on Consent contains requirements for the investigation and cleanup, including corrective action, of contamination at Los Alamos National Laboratory. The U.S. government has rights to use, reproduce, and distribute this document. The public may copy and use this document without charge, provided that this notice and any statement of authorship are reproduced on all copies.

2017 Sandia Wetland Performance Report

April 2018

Responsible project manager:

Steve Veenis		Project Manager	Environmental Remediation Program	4.19.18
Printed Name	Signature	Title	Organization	Date

Responsible LANS representative:

<i>for</i> Randall Erickson		Associate Director	Associate Directorate for Environmental Management	4/20/18
Printed Name	Signature	Title	Organization	Date

Responsible DOE EM-LA representative:

David S. Rhodes		Office Director	Quality and Regulatory Compliance	4-25-2018
Printed Name	Signature	Title	Organization	Date

EXECUTIVE SUMMARY

The 2017 Sandia wetland performance report is the fourth annual performance report following the 2012 to 2014 baseline that assessed the overall condition of the wetland at the head of Sandia Canyon in the context of the wetland's ability to prevent or minimize migration of contaminants of concern (i.e., chromium, polychlorinated biphenyls [PCBs], and polycyclic aromatic hydrocarbons) detected in wetland sediments as a result of historical releases at Los Alamos National Laboratory (LANL or the Laboratory). The geochemistry and physical stability of wetland sediments, along with the extent of wetland vegetation, are the key indicators of wetland conditions. The condition of the wetland is assessed to evaluate the effectiveness of the grade-control structure (GCS) completed in 2013 at the terminus of the wetland and to monitor changes to the Laboratory's operational practices that have affected outfall volumes discharging to the wetland. This report presents the results of monitoring conducted for surface water, alluvial groundwater, vegetation, and geomorphology between January and December 2017. The data are assessed relative to baseline conditions presented in the "Sandia Wetland Performance Report, Baseline Conditions 2012–2014" and the data presented in the "Sandia Performance Report, Performance Period April 2014–December 2014," "2015 Sandia Wetland Performance Report," and "2016 Sandia Wetland Performance Report" to identify any physical and geochemical changes that occurred during the 2017 monitoring period. Monitoring data include physical parameters (i.e., water level, temperature, dissolved oxygen, turbidity, pH) and water chemistry from 12 alluvial wells that monitor the alluvial groundwater in the wetland; surface water and storm water data from 2 gaging stations located upstream of the wetland and 1 gaging station located downstream; vegetation monitoring; and geomorphic change detection data from bank and thalweg surveys, repeat photos, and field observations.

The monitoring conducted during the performance period indicates the Sandia wetland remains stable following the installation of the GCS, even with generally lower, but variable, effluent volumes entering the wetland. The GCS continues to be effective in arresting headcutting at the terminus of the wetland. Groundwater within the shallow alluvium remains in a reducing condition, and no obvious detrimental temporal trends in chemistry have been observed. Water levels in the wetland remained similar over the last 4 yr, with a temporary drop in the easternmost transect during the summers. This decrease in water level was possibly a result of enhanced evapotranspiration associated with meteorological conditions and robust growth of additional wetland vegetation planted as part of the GCS restoration effort. Despite the observed decrease, water levels remained sufficiently high to sustain and allow some expansion of obligate wetland vegetation, and analytical results indicate alluvial groundwater remained in strongly reducing conditions in the eastern portion of the wetland immediately upgradient of the GCS. Even the upper portion of reach S-2 (the second reach down from the headwaters of Sandia Canyon and the reach that encompasses the Sandia wetland), which had previously seen a significant drop in the water table when the outfall was moved from a location that directly discharged into the wetland to an outfall (001) located upstream, retains reducing conditions at depth within alluvial groundwater. Storm water data indicate that the GCS has had a positive effect in reducing contaminant mobility, and this trend continued through 2017. Suspended sediment, PCBs, and chromium concentrations have decreased significantly compared with pre- and post-GCS data immediately downgradient of the wetland at gaging station E123, presumably from eliminating headcutting at the terminus of the wetland and from trapping efficiency because of the dense vegetation within the wetland.

Geomorphic change detection studies indicate the wetland is stable, with no significant geomorphic change experienced by the wetland between post-2016 monsoon to post-2017 monsoon season bank and thalweg survey data. A small amount of erosion was detected within the side channel located on the south side of reach S-2. This erosion has remobilized previously deposited sediment, advancing the fan north- and eastward, but has not resulted in significant loss of cattail vegetation in 2017. A log check dam was installed in September 2017 to reduce the sediment entering the wetland from the south side

channel, however more time will need to pass to determine the results of this mitigation. Overall, the thalweg was stable between 2016 and 2017, with minor lateral changes in thalweg position. The thalweg nick point has remained stable since 2015 with no indication of upstream erosion. Likewise, the plunge pool at the head of the reach has remained relatively stable. Even with sediment input from storm water runoff, the overall area seems unaffected. Based on erosion pin monitoring, the alluvial fan deposits from the Los Alamos County landfill have remained stable.

Vegetation perimeter mapping, cross-section transects, and photographic comparison suggest that the wetland is stable. Between 2016 and 2017, wetland vegetation area has expanded by approximately 2.5% over the whole study area, with most of the expansion occurring at the upstream end of the reach as new cattails and willows expanded along the stream channel.

Alluvial groundwater chemistry is stable and continues to indicate strong reducing conditions. Speciated arsenic and iron data collected from piezometers and alluvial wells installed in Sandia Canyon continue to confirm the reducing conditions of the wetland. Ongoing sampling of hexavalent chromium indicate it is at or below the method detection limit within the wetland.

Surface water and alluvial groundwater analytical data collected in 2017 were compared with New Mexico water-quality criteria and groundwater standards, respectively. Exceedances of water-quality criteria are presented in this report and are determined to be associated with historical Laboratory releases, runoff from developed areas in the upper watershed, naturally occurring chemicals, and/or with the natural reducing conditions of the wetland within the alluvial system.

Overall, 2017 monitoring indicates the wetland is physically more stable and discharging lower concentrations of contaminants of concern in storm water relative to baseline conditions. Alluvial groundwater chemistry data collected in 2017 continue to demonstrate the reducing conditions of the wetland sediment.

CONTENTS

1.0 INTRODUCTION 1

1.1 Project Goals 2

1.2 Timeline 3

1.3 Design and Function of the GCS 3

1.4 Sandia Canyon Outfalls and SERF 4

1.5 Monitoring Planned during the Performance Period 5

1.6 Conceptual Model for Assessing Wetland Performance 7

 1.6.1 Hydrologic Status 7

 1.6.2 Contamination in Wetland Sediment 8

 1.6.3 Cr(III) Stability in the Sandia Wetland 8

 1.6.4 Current State of the Sandia Wetland 9

2.0 MONITORING PERFORMED DURING THE 2017 MONITORING PERIOD 9

2.1 Monitoring of Surface Water 9

2.2 Monitoring of Alluvial System 10

2.3 Water-Level Monitoring 10

2.4 Geomorphic Monitoring 10

2.5 Vegetation Monitoring 10

2.6 Monitoring of the GCS 11

3.0 SUMMARY OF RESULTS FROM WETLAND PERFORMANCE METRICS 11

3.1 Key Monitoring Locations and Performance Metrics 11

3.2 Spatial and Temporal Geochemical Patterns 12

 3.2.1 Surface Water and Alluvial Groundwater Exceedances 13

3.3 Temporal and Spatial Trends in Water-Level 13

3.4 Geomorphic Trends in the Wetland 14

3.5 Spatial and Temporal Trends in Vegetation 14

3.6 Performance of GCS 14

3.7 2018 Monitoring Plan 14

3.8 Proposed Changes to Monitoring Plan from 2017 15

4.0 CONCLUSIONS 15

5.0 REFERENCES AND MAP DATA SOURCES 16

5.1 References 16

5.2 Map Data Sources 17

Figures

Figure 1.0-1 Locations of the Sandia GCS (headcut was located at the upper most sheet pile at the terminus of the wetland), NPDES outfalls, precipitation gage E121.9, alluvial wells, surface and storm water gaging stations, former Los Alamos County landfill, surrounding TAs, and reaches S-1N, S-1S, and S-2..... 19

Figure 1.2-1 Sandia Canyon wetland timeline..... 20

Figure 1.4-1 Daily, monthly average, and yearly average effluent release volumes (expressed as Kgal./d) for Outfall 001 from 2006 to December 2017, and daily effluent releases for Outfalls 03A027 and 03A199 from August 2007 to January 2010 and from November 2012 to December 2017..... 21

Figure 1.4-2 Daily water volumes (gpd) from November 2012 to December 2017 for effluent released from combined Outfalls 001 and 03A027 and Outfall 001 only 22

Figure 1.4-3 Updated process schematic for the power plant, SWWS, and SERF connections to Outfall 001 (current configuration)..... 23

Figure 1.4-4 Daily cooling water usage and discharge information for the SCC and Trinity cooling towers during 2017..... 24

Tables

Table 1.5-1 Completion Data for Alluvial Piezometers and Collocated Alluvial Wells 25

Table 1.5-2 Schema Crosswalk: Past Piezometers and Current Alluvial Wells 26

Table 1.5-3 Alluvial Groundwater Sampling and Analysis Plan for 2017 Sandia Wetland Stabilization Monitoring 26

Table 1.5-4 ISCO Bottle Configurations and Analytical Suites Calendar Year 2017 Storm Water Sampling Plan for E121, E122, and E123 27

Table 2.1-1 Field Data for Alluvial Locations and Surface Water Stations 2017 Sampling Events 28

Table 2.1-2 Precipitation, Storm Water Peak Discharge, and Samples Collected at Gaging Stations E121, E122, and E123 for Each Sample-Triggering Storm Event in 2017 30

Table 3.7-1 Proposed Sampling and Preservation Requirements for Sandia Wetland 31

Appendixes

Appendix A Acronyms and Abbreviations, Metric Conversion Table, and Data Qualifier Definitions

Appendix B 2016–2017 Geomorphic Changes in Sandia Canyon Reach S-2

Appendix C 2017 Wetland Vegetation Monitoring in Sandia Canyon Reach S-2

Appendix D Geochemical and Hydrologic Monitoring in Sandia Canyon

Appendix E 2017 Watershed Mitigations Inspections

Appendix F Analytical Data and 5-Min Stage, Discharge, and Precipitation Data (on CD included with this document)

1.0 INTRODUCTION

In response to liquid effluent released by the Los Alamos National Laboratory (LANL or the Laboratory), the Sandia wetland, located at the head of Sandia Canyon, has expanded from a relatively small footprint in the early 1950s to its current size, encompassing a wetland species vegetated area of 15,356 m², as of 2017 (calculated to include the total coverage of overlapping vegetation zones see Appendix C). Throughout the course of Laboratory operations, the wetland has been supported by continued effluent releases to the canyon. Contamination is present in wetland sediments because of historical releases from Laboratory operations (LANL 2009, 107453).

The Laboratory has prepared this “2017 Sandia Wetland Performance Report” in response to requirements set forth in the “Work Plan and Final Design for Stabilization of the Sandia Canyon Wetland” (LANL 2011, 207053). In that plan, the Laboratory proposed reporting of Sandia wetland monitoring data to the New Mexico Environment Department (NMED) by April 30 of each year. The requirement for designing a Sandia wetland monitoring program was previously set forth in NMED’s “Approval with Modification, Interim Measures Work Plan for Stabilization of the Sandia Canyon Wetland” (NMED 2011, 203806) in response to the Laboratory’s “Interim Measures Work Plan for Stabilization of the Sandia Canyon Wetland” (LANL 2011, 203454). The monitoring plan was provided in the work plan (LANL 2011, 207053) and is summarized in section 1.5 of this report. The monitoring plan is designed to identify physical or chemical changes in the Sandia wetland related to (1) the installation of a grade-control structure (GCS) at the terminus of the wetland (LANL 2013, 251743) and (2) changes in outfall chemistry and discharge volumes related to the Sanitary Effluent Reclamation Facility (SERF) expansion (DOE 2010, 206433).

This report assesses the overall condition and stability of the wetland in the context of the GCS at the terminus of the wetland, and changes to the volume and chemistry of effluent released into Sandia Canyon resulting from changes in the Laboratory’s water-management practices associated with SERF and National Pollutant Discharge Elimination System (NPDES) Outfall 001 (Figure 1.0-1). The results of monitoring conducted in 2017 for surface water, alluvial groundwater, vegetation, and geomorphology are presented herein. Data are assessed relative to baseline conditions presented in the “Sandia Wetland Performance Report, Baseline Conditions 2012–2014” (LANL 2014, 257590) and relative to data presented in the “Sandia Performance Report, Performance Period April 2014–December 2014” (LANL 2015, 600399), “2015 Sandia Wetland Performance Report” (LANL 2016, 601432) and the “2016 Sandia Wetland Performance Report” (LANL 2017, 602341) to identify any physical and geochemical changes during the monitoring period. Monitoring data include:

- Water levels and water chemistry from 12 alluvial wells that monitor the alluvial groundwater in the wetland
- Surface water and storm water data from 2 gaging stations located upstream of the wetland and 1 gaging station located downstream
- Vegetation monitoring, and
- Geomorphic change detection data from ground survey points and field observations.

Hexavalent chromium [Cr(VI)] was historically released into liquid effluent from the Technical Area 03 (TA-03) power plant at the head of Sandia Canyon from 1956 to 1972. Some of the Cr(VI) made its way to the regional aquifer beneath Sandia and Mortandad Canyons, and Cr(VI) concentrations in the regional aquifer presently exceed NMED groundwater standards and U.S. Environmental Protection Agency (EPA) maximum contaminant levels (MCLs). Historical releases of polychlorinated biphenyls (PCBs) from a former transformer storage area and polycyclic aromatic hydrocarbons (PAHs) from an asphalt batch plant also discharged to the wetland, which still contains an inventory of these contaminants. Sandia

Canyon wetland performance monitoring is related to the overall chromium remediation project because a large portion of the original chromium inventory and other contaminants (i.e., PCBs and PAHs, discussed in section 1.1 below) are currently sequestered in the wetland sediment. The results of characterization work conducted to date in Sandia Canyon are described in the “Investigation Report for Sandia Canyon” (hereafter, the Phase I IR) (LANL 2009, 107453) and in the “Phase II Investigation Report for Sandia Canyon” (hereafter, the Phase II IR) (LANL 2012, 228624).

New Mexico Water Quality Control Commission (NMWQCC) groundwater standards, EPA MCLs, NMED screening levels for tap water, and EPA regional screening levels for tap water were used to establish a set of screening values for evaluating monitoring data (D-3.3). Base-flow and storm water analytical results were screened against the appropriate surface water–quality standards in 20.6.4.900 New Mexico Administrative Code (D-2.1).

Information on radioactive materials and radionuclides, including the results of sampling and analysis of radioactive constituents, is voluntarily provided to NMED in accordance with U.S. Department of Energy policy.

1.1 Project Goals

The overall objective of this project is to monitor the physical and chemical stability of the Sandia wetland in the context of its inventory of contaminants of concern. Monitoring was initiated to evaluate the influence of the GCS (which was installed to reduce erosion at the terminus of the wetland) and anticipated decreases in discharge volume associated with the expansion of SERF on the discharge of contaminants.

Geochemical reducing conditions within the Sandia wetland converted some of the Cr(VI) released from 1956 to 1972 to stable, relatively insoluble trivalent chromium [Cr(III)]. A significant inventory of chromium as Cr(III), possibly around 15,000 kg, remains in wetland sediment (LANL 2009, 107453). Studies presented in the Phase I IR have shown the trivalent form of chromium is unlikely to oxidize and convert to mobile hexavalent chromium whether sequestered in the saturated reducing conditions of the wetland alluvium or exposed to oxygen upon dewatering of wetland sediments (LANL 2009, 107453). Maintaining the saturated reducing condition, however, is a prudent measure to ensure stability of the chromium inventory as trivalent chromium within the wetland sediment and alluvial groundwater.

The wetland also contains an inventory of PCBs and PAHs from historical Laboratory releases that have adsorbed to sediment within the wetland. This inventory will remain in place as long as the sediment remains physically stable. Abundant vegetation stabilizes sediments through root binding and also enhances deposition of suspended solids from storm water. PCBs in wetland sediment are primarily attributed to releases of PCBs from a transformer storage area, Solid Waste Management Unit 03-056(c). The PCB inventory in the wetland sediments is estimated to be 5.5 kg, 3.3 kg, 31.1 kg, and 24.4 kg for Aroclor-1242, Aroclor-1248, Aroclor-1254, and Aroclor-1260, respectively (LANL 2009, 107453). Four PAHs (benzo[a]anthracene, benzo[a]pyrene, benzo[b]fluoranthene, and indeno[1,2,3-cd]pyrene) were identified in the Phase I IR as being the most important for evaluating human health risk. PAHs are primarily attributed to releases from a former asphalt batch plant located upgradient of the wetland. The highest concentrations of benzo[a]anthracene and benzo[a]pyrene in sediment were found in investigation reaches S-1N and S-1S above the wetland (Figure 1.0-1). Much smaller concentrations, typically less than 1 mg/kg, have been measured in reach S-2, which includes the Sandia wetland (Figure 1.0-1).

The monitoring presented in this report is intended, in part, to assess the stabilizing impacts of the GCS on the eastern terminus of the wetland. Before the GCS was constructed, the terminus of the wetland had an active headcut (up to 3 m high). Installation of the GCS at the former active headcut has arrested it,

thereby stabilizing the grade (Figure 1.0-1). Stabilization of vegetation, hydrology, and geochemistry at the easternmost end of the wetland indicates the efficacy of the GCS, backing up groundwater because of its impervious subgrade face (section 1.3) (LANL 2015, 600399) and stabilizing the grade at the terminus of the wetland. Maintenance of physical and chemical stability will, in turn, help prevent potential physical mobilization of adsorbed contaminants associated with sediment and chemical mobilization of precipitated or reduced contaminants under changing geochemical conditions in groundwater (LANL 2011, 203454; LANL 2011, 207053).

The Sandia wetland has experienced generally decreased liquid outfall effluent volumes (both daily and annually) from NPDES-permitted Outfalls 001 and 03A027 as part of the SERF expansion project. As part of the SERF expansion, a portion of the effluent previously released to Sandia Canyon is now being rerouted to cooling towers at various facilities, including the Strategic Computing Complex (SCC) and the Trinity supercomputer. Though effluent releases to Sandia Canyon may be reduced further, discharge will be maintained at a minimum of 30,000 gpd during months when ET is highest, a level that is believed to be sufficient to maintain the ecologic, hydrologic, and geochemical functioning of the wetland—as described in the 100% Design Memorandum for Sandia Wetlands Stabilization Project prepared by Brown and Caldwell (LANL 2012, 240016). If future changes to effluent volume or chemistry are shown to adversely impact the wetland, adaptive management will be used to ensure wetland stability (e.g., engineered controls to manage sediment and water distribution to increase the area of wetland saturation).

More detailed background on the SERF-related outfall chemistry and discharge volume changes is provided in section 1.4. The monitoring plan and associated rationale designed to identify physical and chemical changes in the wetland are presented in section 1.5. A conceptual model for wetland performance is presented in section 1.6. Monitoring performed during the 2017 performance period is discussed in section 2. Detailed monitoring results are presented in Appendix D. Section 3 summarizes monitoring results in the context of wetland performance metrics and suggests proposed changes to the monitoring plan.

1.2 Timeline

A graphical timeline showing changes related to outfall discharge and chemistry, the construction of the GCS, the addition of piezometer and alluvial well monitoring locations, and associated sampling events is shown in Figure 1.2-1.

1.3 Design and Function of the GCS

The location of the GCS is shown in Figure 1.0-1. The overall objectives of the GCS were to arrest the headcut in the lower portion of the wetland and to maintain favorable hydrologic and geochemical conditions to minimize contaminant migration (LANL 2011, 203454, Figure 2.4-2). The GCS was designed to meet the following objectives:

- Minimize erosion during large flow events
- Provide an even grade to allow wetland expansion and further stabilization
- Be sufficiently impervious to prevent the draining of alluvial soils and promote a high water table
- Facilitate nonchannelized flow, and
- Support wetland function under potentially reduced effluent conditions.

The GCS transitions the grade approximately 11 vertical feet from the elevation of the wetland just upgradient of the former headcut location to the natural stream bed just upstream of gage E123. To maintain grade and to reduce the overall fill and size of a single structure, a set of three steel-sheet-pile walls was installed with decreasing elevation drops. Downstream of the third sheet-pile wall, a cascade pool was constructed of boulders and cobbles to transition to the final grade. The transition from the wetland above the GCS to the stream channel below is gradual, smooth, and stepped to prevent erosive flows that could scour and destabilize the stream reach below the structure (LANL 2013, 251743). The design of the GCS should allow for a reduction of outfall effluent discharge into the wetland without compromising the physical and geochemical function of the wetland, particularly of the eastern terminus where the GCS controls wetland water levels. The area behind the GCS was backfilled and wetland vegetation was planted to allow expansion of the wetland area. These measures physically stabilize the wetland by reducing sediment and associated contaminant transport into the lower sections of the canyon and should also maintain reducing conditions within the sediment near the terminus of the wetland, thus contributing to the goal of reducing potential contaminant transport (LANL 2013, 251743). A set of as-built diagrams for the GCS is presented in Appendix C of the completion report for the construction of the GCS (LANL 2013, 251743).

1.4 Sandia Canyon Outfalls and SERF

Outfalls have released liquid effluent to Sandia Canyon since the development of TA-03 in the early 1950s. There are currently three NPDES outfalls permitted to release to upper Sandia Canyon upstream of the wetland: Outfalls 001, 03A027, and 03A199 (EPA 2007, 099009, Figure 1.0-1). Effluent releases at these outfall discharge points are monitored in compliance with the Laboratory's industrial NPDES permit (Permit No. NM0028355, EPA 2014, 600257). Operational changes that impact these outfalls have occurred since mid-2012. Figure 1.4-1 shows daily, monthly, and yearly average effluent volumes from 2006 to 2017 for Outfall 001, which releases the greatest volume of effluent to Sandia Canyon. Figure 1.4-1 also shows daily releases from August 2007 to January 2010 and from November 2012 to December 2017 for the two smaller outfalls, Outfalls 03A027 and 03A199. (The record for these two outfalls is incomplete.) The 2015 Sandia wetland performance report discusses liquid effluent releases to Sandia Canyon from 2006, when the Laboratory's chromium investigation began, to 2015. Late 2015 to 2017 releases and operations are discussed below:

September 18, 2015, to March 7, 2016: Operational changes at the SERF plant resulted in increased discharge at Outfalls 001 and 03A027 in late 2015 and early 2016, as illustrated in Figures 1.4-1 and 1.4-2. During this time, incoming flows from the Sanitary Waste Water System (SWWS) plant increased, resulting in a corresponding increase in discharge at Outfall 001. In addition, the SERF plant discharged more effluent to Outfall 001 and sent less SERF-blended water for reuse in the SCC cooling towers. This combination of increases resulted in an additional 95,000 gallons per day (gpd) (58%) of effluent at Outfall 001 compared with the same period from September 2014 to March 2015. Makeup water for the SCC cooling towers was largely potable water (70%) rather than SERF-blended makeup water during this period (Figure 1.4-2). As a result, effluent volumes have increased by approximately 11,500 gpd at Outfall 03A027 because fewer cycles could be run using the silica-rich potable water. These changes represented a significant increase in the water input to the wetland but did not negatively affect wetland stability. Changes in water chemistry entering the wetland are discussed in Appendix D. The SERF product water has continued to be blended at a 4:1 ratio with SWWS effluent. However, a second blending point available near Outfall 001 was employed during this time period to mix SERF product water with SWWS effluent water; the blending of SERF to SWWS water (from the reuse and fire protection tank) at that point is not maintained at a constant ratio and likely has a higher ratio of SWWS water than usual when more water comes in from the SWWS plant.

March 8, 2016, to December 31, 2017: The operational changes at the SERF plant described above were temporary, and a return to reuse of SERF-blended water in the SCC cooling towers occurred on March 8, 2016. During this period, more than 99% of the water used by the SCC cooling towers was SERF-blended water. As a result, discharges at Outfall 001 decreased to an average of 152,000 gpd from March to December, 2016. Another operational change is also noted. Since September 9, 2016, discharges from the SCC cooling towers have been directed to Outfall 001 through the wet well (Figure 1.4-3) rather than to Outfall 03A027. Since then, including through the end of 2017, the SCC blowdown effluent volumes are accounted for in the Outfall 001 discharge volumes and releases to Outfall 03A027 have been zero. This change is illustrated in Figure 1.4-1, which shows discharges at Outfall 03A027 dropping to zero, and in Figure 1.4-2, which shows the “combined Outfalls 001 and 03A027” data (turquoise line) converging with the Outfall 001 data (dashed light-green line). This change in discharge location and in accounting for the SCC cooling tower blowdown volume is expected to be permanent; Outfall 03A027 will be used only during maintenance or in the event of an emergency.

The Trinity supercomputer was brought online for early access trial use late in 2016, and transitioned to full-scale use in July 2017. The long-term plan is that this computing facility will also use SERF-blended water for cooling. Cooling tower effluent from this new facility is discharged to Outfall 001, and discharge volumes from this source are accounted for in Outfall 001 data (i.e., the Outfall 001 effluent volumes shown in Figures 1.4-1 and 1.4-2 include these inputs). Figure 1.4-4 shows cooling water usage and discharge information for the SCC and Trinity cooling during 2017. During the trial phase before July, operations at Trinity were not continuous and potable makeup water was used for cooling. SERF-blended water was used for most of June to August, 2017, and again for most of December, 2017; otherwise potable water was used. While the SERF-blended water was used, the effluent volumes at Outfall 001 were on the order of 30,000 gpd less than when potable water was used.

Once the Trinity facility transitions to full-time use of SERF-blended makeup water, this change will result in a further decrease in discharge to Outfall 001 and therefore less surface water entering the wetland. The variability in effluent volumes and water chemistry that may be released to the wetland will depend on return flow from facilities to outfalls that release to the wetland.

1.5 Monitoring Planned during the Performance Period

The original monitoring plan for the Sandia wetland is described in section 6.0 of the “Work Plan and Final Design for Stabilization of the Sandia Canyon Wetland” (LANL 2011, 207053). Proposed revisions to the monitoring plan were presented in the “Sandia Wetland Performance Report, Baseline Conditions 2012-2014” (LANL 2014, 257590); in the “Sandia Wetland Performance Report, Performance Period April 2014–December 2014” (LANL 2015, 600399); in the “2015 Sandia Wetland Performance Report” (LANL 2016, 601432); and in the “2016 Sandia Wetland Performance Report” (LANL 2017, 602341).

The initial work plan (LANL 2011, 207053) called for a multiphased approach to monitoring to evaluate hydrologic and geochemical changes associated with the GCS and/or with the SERF expansion and subsequent effluent reduction:

- Evaluate changes in hydrology and key geochemical indicators to monitor the health of the wetland at 12 alluvial groundwater sampling locations
- Evaluate transport of metals and organic chemicals through the wetland by monitoring surface-water base flows and storm flows at 3 gaging stations
- Monitor vegetation every 2 yr via photographic survey, and
- Conduct periodic geomorphic surveys to evaluate erosion and aggradation of sediments within the wetland.

Monitoring of alluvial groundwater chemistry until February 2016 had been accomplished through a series of 13 drive- point 1-in.–inside diameter wells (henceforth denoted as “piezometers” because of their small well-casing diameter and method of installation) arranged in 4 transects in the wetland that were sampled quarterly. In the pilot sampling method comparison performed in 2015 and discussed in Appendix E of the “2015 Sandia Wetland Performance Report” (LANL 2016, 601432), alluvial wells were deemed the best method to obtain ample amounts of water and provide representative samples and field parameters. By October 2016, all the piezometers (prefix: SCPZ) were removed and replaced with 12 alluvial wells (prefix: SWA), placed in undisturbed locations adjacent to the piezometers with approximately the same screening depth (Table 1.5-1). These alluvial wells are constructed of a 2-in.– inside diameter polyvinyl chloride casing (PVC) and a 2-in. slotted PVC casing to act as a screen surrounded by a filter pack consisting of 1/20 silica sand. As the piezometers were gradually replaced with alluvial wells in 2016, water from the piezometers was sampled until the alluvial wells were installed. In 2017, only water from the alluvial wells was sampled. The alluvial well name will be used to refer to the approximate location shared by the former piezometers and the current alluvial wells (the piezometers and wells are cross-walked in Table 1.5-2) through the rest of this report.

The alluvial well (piezometer) transects are:

- Alluvial wells SWA-1-1 (SCPZ-1), SWA-1-2 (SCPZ-2/SWA-1), and SWA-1-3 (SCPZ-3) are located on a sand-and-gravel terrace near the active channel (c1 geomorphic unit) towards the western end of the wetland, which has experienced channel incision and dewatering relative to historical conditions. These alluvial systems are located on the c3 geomorphic unit (Figure D-4.0-1 and Appendix D for maps and definitions of geomorphic surfaces from the “2015 Sandia Wetland Performance Report” (LANL 2016, 601432)), away from the active channel and associated inset terrace (c2a geomorphic unit), which are locations of recent cattail expansion. Well SWA-1-1 is screened towards the base of alluvial fill, while the tops of the screens in wells SWA-1-2 and SWA-1-3 are approximately 6 ft and 3 ft below ground surface (bgs), respectively (Table 1.5-1).
- Wells SWA-2-4 (SCPZ-4), SWA-2-5 (SCPZ-5), and SWA-2-6 (SCPZ-6/SWA-2) form a transect in the widest portion of the wetland. The tops of the well screens are 2–3 ft bgs because the wetland water level is at or very near the ground surface at this transect. It is at these shallowest depths that deleterious changes in water level and sediment oxidation state, were they to occur, would be expected to manifest as a result of reduced effluent discharge. Similarly, the lateral margins of the wetland may dewater before the longitudinal axis of the wetland as a result of reduced effluent volumes. This effect could be most pronounced where the wetland is widest and water flux is most spread out. It is also at such locations that preferential flow paths within the alluvium may form.
- Wells SWA-3-7 (SCPZ-7), SWA-3-8 (SCPZ-8/SWA-3), and SWA-3-9 (SCPZ-9) are located in a narrow part of the wetland closer to its distal (eastern) end. This transect includes two shallow wells, SWA-3-7 and SWA-3-9, with the tops of the screens at 0.6 and 2.2 ft bgs, respectively, and the SWA-3-8 with the top of the screen at 4.8 ft bgs (Table 1.5-1). The wetland water level is at or just below the ground surface at this transect. These alluvial locations provide indications of changes near the surface of the wetland and at depth in a narrow portion of the wetland where preferential flow paths are less likely to develop.
- The final transect of wells SWA-4-10 (SCPZ-10), SWA-4-11 (SCPZ-11B), and SWA-4-12 (SCPZ-12/SWA-4) have responded most to the rewatering that has occurred at the eastern terminus of the wetland because of the effect of the GCS. The wetland water level is at or near the surface at this transect. Water was routed around this area during the period of construction of the GCS.

The 2017 sampling and analysis plan for the alluvial wells is provided in Table 1.5-3. Most of the analyses were designed as indicators of redox changes associated with potential dewatering of the wetland. Alluvial locations were instrumented with sondes for continuous monitoring of water levels, specific conductance, and temperature.

Samples from base flow were collected quarterly with the alluvial wells. The same analytical suites, with the addition of unfiltered metals, PCB congeners, PAHs, and suspended sediment concentration (SSC), were monitored in base flow at surface water gaging stations E121, E122, and E123 (Figure 1.0-1).

Flow rates into and out of the wetland are measured at gaging stations E121, E122, and E123 during sample-triggering storm events, as well as during base flow conditions. Analyses of storm water samples collected in 2017 were planned as presented in Table 1.5-4. Analytical results with data plots are discussed in Appendix D and analytical data is available on CD (Appendix F).

Since 2016, aerial LiDAR surveys are performed every three years, or if storm events with discharge greater than 50 cfs result in significant geomorphic changes in a year when a survey is not scheduled, with the next survey being scheduled for 2019. Ground-based global positioning system (GPS) surveying along geomorphic features of concern and monitoring of erosion pins is performed annually. Vegetation zone perimeters of the Sandia wetland and photographs from established locations are monitored from year to year and define the extent of obligate wetland species that depend upon saturated wetland conditions. Details of the monitoring scheme and the results from this vegetation monitoring are presented in Appendix C. This monitoring effort replaces and supersedes that originally proposed in the "Work Plan and Final Design for Stabilization of the Sandia Canyon Wetland" (LANL 2011, 207053).

The GCS is inspected twice a year and following rain events with discharges greater than 50 cubic feet per second (cfs) (LANL 2014, 600083). If erosion or any indications of instability are observed, appropriate actions will be taken to ensure continued stability and functionality of the GCS. The new controls installed upstream of the GCS where sediment was running into the wetland from a southern drainage were installed in September 2017, but damages were found during the December 2017 inspection. New controls were completed in January 2018 to protect from scouring in the southern drainage. The GCS inspections with photographs of the drainage controls are presented in Appendix E.

1.6 Conceptual Model for Assessing Wetland Performance

1.6.1 Hydrologic Status

The Sandia wetland is an effluent-supported cattail wetland. Surface water is generally present in a discrete channel (though in some areas surface water spreads from bank to bank) and passes through the wetland with a short residence time relative to alluvial groundwater (LANL 2009, 107453; LANL 2014, 257590). Wetland sediments are underlain by Bandelier Tuff upon which alluvial groundwater is perched. A water-balance analysis conducted in 2007 and 2008 showed little surface water loss (approximately 2% of both effluent and runoff) occurs through the wetland (LANL 2009, 107453). A direct-current (DC) electrical-resistivity-based geophysical survey found that large continuous areas of the wetland are underlain by highly resistive welded tuffs (Qbt 2 of the Tshirege Member of the Bandelier Tuff) that represent a significant barrier to the infiltration of alluvial groundwater into the subsurface (LANL 2012, 228624). In several areas, the survey also identified subvertical conductive zones that penetrate the upper bedrock units and, in some cases, appear to correlate with mapped fault and/or fracture zones. These conductive zones may represent present-day or historical infiltration pathways. However, the DC resistivity data do not differentiate between conductive zones that contain higher water content (possibly representing active infiltration) and wetted clay-rich fracture fill that may hinder infiltration.

Installation of the GCS has led to cessation of headcutting at the terminus of the wetland and has created an impermeable barrier to subsurface flow such that alluvial groundwater must resurface before exiting the wetland. Given the impermeable nature of this barrier and the largely impermeable tuff underlying the wetland, to the first order the system can conceptually be thought of as a bathtub that effectively holds water with excess water spilling over the GCS at the wetland terminus. Annual evaluation of base-flow rates confirms this “bathtub” assumption as rates entering and exiting the wetland are similar, although this assumption breaks down during storm events because of additional flow from subtributaries such as the former Los Alamos County landfill (Figure 1.0-1). However, as long as water inputs from the outfalls exceed wetland evapotranspiration, even significantly reduced outfall discharge may sustain water levels and sufficient saturation within wetland sediments. Extreme decreases in effluent input volumes into the wetland, however, could potentially result in wetland dewatering. The wetland sediment is typically saturated at the eastern end of the wetland; these conditions extend westward, but near- surface sediment is unsaturated at the margins and at the western end of the wetland. Over the last three years, there appears to be recovery of cattails in the west end of the wetland, which had been largely dewatered when the outfall that discharged directly into the wetland was relocated further upstream to the current location of Outfall 001. Channel meandering and sediment redistribution, however, are resulting in the reestablishment and expansion of cattails in this area (LANL 2016, 601432). Recent decreases in effluent volume to the wetland have not resulted in a lowering of the water table (dewatering) or decreased wetland vegetation cover (LANL 2016, 601432). The wetland vegetation community is important in mitigating storm water–related mobilization of contaminants through root binding and physical trapping of suspended sediments.

1.6.2 Contamination in Wetland Sediment

Detailed sediment mapping was performed during the Phase I IR (LANL 2009, 107453). Canyon reach S-2, which contains the Sandia wetland, contains high concentrations and proportions of the originally released contaminant inventory because of: (1) its proximity to contaminant sources; (2) the large volume of sediment deposited during the period of active contaminant releases; (3) the presence of high concentrations of organic matter in the wetland; and (4) the presence of large amounts of silt and clay (Figure 1.0-1). Contaminants commonly adsorb to, or are precipitated in association with, sediment particles or organic matter.

Chromium is the major inorganic contaminant of concern in the wetland that could be affected by both redox changes in the wetland and physical destabilization. Sections 1.0 and 1.1 present the background for chromium contamination in wetland sediments. Arsenic may also be released from wetland sediments upon dewatering (LANL 2009, 107453). Two groups of organic contaminants of concern, PCBs and PAHs, are primarily subject to physical transport in floods because of low solubility and a strong affinity for organic material and sediment particles. Important source areas for these contaminants are the former outfall for the power plant cooling towers in upper Sandia Canyon (chromium), a former transformer storage area along the south fork of Sandia Canyon (PCBs), and the former asphalt batch along the north fork of Sandia Canyon (PAHs) (LANL 2009, 107453).

1.6.3 Cr(III) Stability in the Sandia Wetland

The inventory of chromium contamination within the Sandia Wetland exists primarily in the form of Cr(III) because of reducing conditions. Alluvial saturation, along with significant amounts of solid organic matter (SOM) produced from wetland vegetation, results in reducing alluvial aquifer conditions as indicated by detectable concentrations of ammonia and sulfide, high dissolved iron and manganese concentrations, and low nitrate and sulfate in alluvial groundwater (LANL 2014, 257590; LANL 2015, 600399; LANL 2016, 601432; LANL 2017, 602341). Oxidation by manganese oxides under aqueous conditions is the primary

mechanism responsible for oxidation of Cr(III) to Cr(VI) (Rai et al. 1989, 249300). Complete oxidation of Cr(III) to Cr(VI) is likely to occur if the molar concentrations of Mn(IV) exceed those of Fe(II), Cr(III), and organic carbon. This situation, however, is unlikely within the active Sandia wetland because concentrations of total iron, consisting mainly of Fe(II), and SOM are present at much higher weight-percent concentrations than Mn(IV), which is usually present in the parts per million range (discussed in more detail in Appendix J of the Phase I IR (LANL 2009, 107453). In addition, drying and leaching experiments conducted on Sandia wetland sediments to quantify the potential release of Cr(VI) during drying of the wetland material showed that Cr(III) appears to remain stable, suggesting insufficient Mn(IV) is produced to oxidize appreciable amounts of Cr(III) to Cr(VI) (LANL 2009, 107453). Total “dissolved” chromium in leachates was primarily in the form of Cr(III), indicating most chromium measured in a filtered wetland performance monitoring sample occurs as colloids. This explanation is supported by analyses of Cr(VI), which is generally below the method detection limit (LANL 2016, 601432).

1.6.4 Current State of the Sandia Wetland

Data from geochemical studies presented in the Phase I IR (LANL 2009, 107453) and previous performance reports (LANL 2015, 600399; LANL 2016, 601432) indicate chromium in wetland sediments is predominantly geochemically stable as Cr(III) and is not likely to become a future source of chromium contamination in groundwater, especially if saturated conditions are maintained within the wetland. The mostly nondetects of Cr(VI) in the wetland water confirms that most if not all the chromium exists as Cr(III) (see results in Appendix D). Results from baseline monitoring of the wetland (LANL 2014, 257590) and from monitoring in 2014 (LANL 2015, 600399), 2015 (LANL 2016, 601432), and 2016 (LANL 2017, 602341) show that the Sandia wetland system is chemically and physically stable, with stable to increasing wetland vegetation cover in different parts of the system. Most importantly, results of storm-water monitoring from gage station E123 have shown a reduction of PCBs and chromium post-GCS installation.

2.0 MONITORING PERFORMED DURING THE 2017 MONITORING PERIOD

Quarterly sampling of Sandia wetland surface water and alluvial groundwater is coordinated with the Chromium Investigation monitoring group sampling conducted under the Interim Facility-Wide Groundwater Monitoring Plan. In 2017, performance sampling was conducted at 12 alluvial wells within the wetland (collocated to the piezometers where water was collected through 2016 [Table 1.5-2]) as well as at surface water gaging stations E121 and E122 [above the wetland] and E123 [below the wetland] (Figure 1.0-1).

2.1 Monitoring of Surface Water

Surface water gaging stations E121 and E122 are located in the upgradient western end of the Sandia Canyon watershed. Surface water gaging station E123 is located to the east immediately below the terminus of the wetland. Figure 1.0-1 shows the location of the gaging stations, outfalls, and the extent of the Sandia wetland. In 2017, gaging station E121 measured discharge from Outfall 001, Outfall 03A027, and storm water runoff from approximately 50 acres from TA-03. With changes at SERF in September 2016, discharge from SCC cooling towers is primarily directed to Outfall 001, with Outfall 03A027 used only for maintenance and emergency discharge (see Section 1.4). Gaging station E122 measures discharge from Outfall 03A199 and storm water runoff from approximately 50 acres from TA-03. Gaging station E123 measures surface water flow below the wetland, including discharge from all outfalls and storm water runoff from approximately 185 acres, 100 acres of which are from E121 and E122.

Tables 2.1-1 and 2.1-2 detail surface water base-flow sampling and field parameters, respectively, for samples collected in calendar year 2017 (see section 1.5).

In 2017, ISCO 3700 automated samplers attempted to collect storm water samples when discharge was greater than 10 cfs at gaging stations E121 and E123. For the beginning part of the 2017, the sampling discharge threshold was set to 10 cfs; however, by the beginning of July it was lowered to approximately 2.0 cfs because of the lack of significant storm water runoff in the channel where E122 is located. Base-flow and storm-flow samples in 2017 were analyzed based on the suites presented in Table 1.5-3 and Table 1.5-4, respectively. Samplers at E121, E122, and E123 were activated in May 2017, before the monsoon season, and turned off for the winter in November 2017. Stations E121 and E123 are equipped with a Sutron 9210 data logger, an MDS 4710 radio transceiver, and a Sutron Accubar bubbler. Station E122 is equipped with a Sutron 9210 data logger, an MDS 4710 radio transceiver, and a VEGAPULS 61 radar sensor. Stage is recorded every 5 min and transmitted to a base station where it is archived in a database. All three gaging stations are equipped with two automated ISCO samplers: one with a 24-bottle base for SSC analyses throughout the storm event, and one with a 12-bottle base for collection of chemistry samples (Table 1.5-4).

For each sample-triggering storm event in 2017, Table 2.1-2 shows precipitation at rain gage RG121.9, storm water peak discharge and whether a sample was collected at E121, E122, and E123 (Figure 1.0-1). Storm water discharge at E121 equaled or exceeded the trip level (10 cfs) five times in 2017 and samples were collected from five of those events. Discharge at E122 equaled or exceeded the newly lowered trip level (in July it was lowered to approximately 2.0 cfs) five times in 2017 and samples were collected from five of those events. Discharge at E123 exceeded the trip level (10 cfs) five times in 2017 and samples were collected from five of those events.

2.2 Monitoring of Alluvial System

Full suites were collected at all locations in each quarter. All analyses were performed off-site after the May round with the exception of sulfide which has a holding time of 24 h and was analyzed on site. Though often the sulfide holding time is exceeded, these data are still useful for interpreting redox conditions in the wetland. Actual sulfide concentrations are expected to be higher than those measured outside the holding time, so measured sulfide concentrations are conservative in terms of assessing redox conditions. Cr(VI) was measured at all alluvial wells and surface water locations (base flow) quarterly. As(III) and Fe(II) were measured quarterly in only the alluvial wells. The field parameter data from the surface water and alluvial wells are provided in Table 2.1-1.

2.3 Water-Level Monitoring

Water-level and temperature data collected by sondes are discussed in section D-4.0 in Appendix D. Sondes at alluvial well locations along transects 1 and 2 were sent in for routine calibration in mid-February 2017 and reinstalled at the beginning of April. Sondes in alluvial well locations along transects 3 and 4 were sent in for routine calibration in mid-March 2017 and reinstalled by the end of April. The sondes were left in the wells over the winter.

2.4 Geomorphic Monitoring

A full description of the approach and results for geomorphic surveys is presented in Appendix B.

2.5 Vegetation Monitoring

A full description of the approach and results for vegetation surveys is presented in Appendix C.

2.6 Monitoring of the GCS

Inspection results from monitoring of the GCS are presented in Appendix E.

3.0 SUMMARY OF RESULTS FROM WETLAND PERFORMANCE METRICS

Detailed results of performance metrics are presented in Appendix D and are summarized here.

3.1 Key Monitoring Locations and Performance Metrics

It is important to note that deleterious changes in any one metric do not necessarily represent a detriment to the overall function of the wetland and will not necessarily lead to contaminant release from wetland sediments. The wetland should be evaluated in terms of total system performance over time with multiple lines of evidence used to determine if the system is stable.

Gaging station E121 is a good location to monitor the integrated impacts of changing input chemistry and decreasing effluent volumes from Outfalls 001 and 03A027 in base flow. Gaging station E123 is the key integrating location of total wetland performance in mitigating discharges of contaminants of concern. Monitoring of storm water at E123 will reveal if anomalously high levels of sediment and contaminants (e.g., chromium, PCBs, PAHs) are mobilized during floods because of a reduction in chemical and/or physical stability in the wetland. Monitoring during base flow conditions will indicate changes in outfall chemistry and changes associated with wetland biogeochemistry and function. The metric for identifying deleterious impacts monitored at this location would be increases in base flow or storm water contaminant concentrations that occur year after year since the installation of the GCS.

The alluvial well array provides valuable water-level and alluvial groundwater chemistry data (Appendix D). These locations monitor potential changes associated with outfall volumes, evolving geomorphology, redistribution of reducing zones, and changes in chemistry of the outfall (in the case of more conservative constituents). The metrics for identifying deleterious impacts as monitored in the wells would be: (1) persistent increases in contaminant concentrations [e.g., Cr(VI)] and/or increases in oxidizing conditions as indicated by redox-sensitive species (e.g., decreased sulfide, increased sulfate); and (2) persistent decreases in water levels that have deleterious effects on obligate wetland vegetation.

Geomorphic change detection using ground-based surveys of the thalweg and the established erosion pins have proven to be the best method for evaluation of changes in geomorphology in the wetland (Appendix B).

The quantitative vegetation cross-sections and perimeter mapping over the year (Appendix C) are used to monitor both the physical stability and the saturation state of the wetland, as indicated by changes in obligate and facultative wetland vegetation. Increases in upland vegetation within the current extent of the wetland would indicate deleterious impacts on wetland function.

After calendar year 2018, 5 yr of post-GCS monitoring will have been conducted. In the 2018 performance report, a reduced, yet still robust, conceptual model for overall system performance that captures interannual variability will be proposed. This conceptual model will evaluate the full 5 yr of records following construction of the GCS and will capture the potential range of monitoring variability recorded in the Sandia wetland. In 2019, the Laboratory will continue to refine and improve the monitoring plan in an effort to fully identify, and monitor for, key criteria that are reliable proxies for wetland stability (e.g., vegetation, spatial contaminant trends, geomorphic stability, and key redox indicators).

3.2 Spatial and Temporal Geochemical Patterns

PCB and total chromium concentrations in both base flow and storm flow at E123 are significantly reduced since the GCS was constructed (Figure D-2.0-7). While PCB and total chromium concentrations in base flow and storm flow were significantly higher downgradient of the wetland (relative to upgradient locations E121 and E122) before the GCS was built, the concentrations are closer in magnitude upgradient and downgradient of the wetland since the GCS was constructed. The trend in PCBs and total chromium concentrations at all of the gaging stations, both in base flow and storm flow, indicate a general decrease over the past 7 yr or so, with a slight increase in 2017 in storm flow. The trends in PCBs and total chromium at E123 may be a result of continued growth of wetland vegetation, corresponding to stabilization of the sediment (Appendixes B and C); however, the decreasing trend at the upgradient locations may be a result of less intense precipitation and erosive runoff during the years following construction of the GCS. In 2017, the intense storm event on July 26 had high PCB and total chromium concentrations in storm flow, thus contributing to the slight increasing trend between 2016 and 2017.

PAHs were not analyzed in base flow or storm flow before the GCS was built. In base flow, all total PAH results were nondetections, with the exception of one sample collected at E123 in 2016 and one sample collected at E121 in 2017, and for which the total PAH concentrations were significantly lower than in storm flow. In storm flow, total PAH concentrations are similar upgradient and downgradient of the wetland. Overall, higher concentrations of PAHs were detected at E122 than at E121 and E123, suggesting the influence of the former asphalt batch plant near the northern fork of upper Sandia Canyon is still evident and is the most likely source of PAHs at the downstream gaging station, E123, because the low concentrations of PAHs at E121 do not indicate a source.

Indicators of base flow water quality show the impact of recent improvements in water quality because of the SERF upgrade (Appendix D-2.0). Redox indicators potentially show evidence of chemical reduction as surface water flows through the wetland (e.g., lower nitrate at gaging station E123 relative to E121). Base flow Cr(VI) concentrations at E121 and E122 are higher than at E123, indicating reduction occurring in the wetland (Figure D-2.0-5).

Low sulfate concentrations in alluvial groundwater relative to base flow, along with frequent detects of sulfide, emphasize the strong reducing nature of the wetland sediments. As sulfate reduction occurs at much lower redox potentials than the reduction of chromate, nitrate, iron, and so on, the wetland environment is highly favorable in terms of chemical stability of chromium as Cr(III). Several analytes clearly reflect reducing conditions in all alluvial locations throughout the wetland (sulfate, arsenic, iron, manganese, sulfide, and ammonium). For example, sulfide and ammonium are present at all locations and bound most of the redox ladder. Data indicate locations SWA-1-1, SWA-2-5, SWA-2-6, and SWA-2-8 seem to be the most reducing (based on alluvial arsenic, iron, manganese, and sulfate concentrations), while locations SWA-1-2, SWA-1-3, and perhaps SWA-2-4 are somewhat less reducing (based on alluvial manganese concentrations) (section D-3). SWA-3-7 continues to show the least reducing conditions in the wetland proper due to the shallow screening interval, with the top of the screen at 0.6 ft bgs while most other wells are at 3 ft bgs. While no preferential flow paths were identified in the alluvium, there do appear to be distinct geochemical domains in terms of redox conditions. It appears that the important easternmost transect is recovering from disturbance associated with installation of the GCS and is showing clear evidence of strongly reducing conditions (section D-3).

Only slight temporal increases in iron and manganese concentrations over the period of sampling may be the result of ongoing inputs of organic matter that continue to promote strong reducing conditions in the wetland (section D-3). No temporal trends were observed in chromium concentrations.

The speciated data continues to show highly reducing conditions in the wetland. Cr(VI) concentrations at or below the MDL indicate most of the chromium in the wetland is Cr(III), and most iron is Fe(II), the reduced form. It would be expected that all the total arsenic is As(III) as seen through 2016, but in 2017 there appears to be a discrepancy between total arsenic and As(III); this difference is believed to be an artifact of the analysis (see section D-3.2).

3.2.1 Surface Water and Alluvial Groundwater Exceedances

Base-flow and storm water analytical results from gaging stations E121, E122, and E123 in 2017 were screened against the appropriate surface water–quality criteria (SWQC) (see Section D-2.1). The two main sources of surface water that enter the wetland are discharges from outfalls and storm water runoff from the developed landscape within TA-03. This run-on sourced water influences the results from E121 and E122. Flow at E123 is composed of a mix of waters from E121, E122, runoff through the Sandia wetland, and urban runoff from the Laboratory and Los Alamos County. The exceedances detected in storm water in 2017 include aluminum, copper, gross-alpha, lead, total PCBs, and zinc; the exceedances detected in base flow in 2017 include only total PCBs and zinc. Most of the exceedances occurred in storm water (95), a lesser number occurred in perennial base flow (12).

A comparison of the average and maximum results from E121 and E122 to E123 shows that, with exception of PCBs, the Sandia wetland is not a source of pollutants that exceed New Mexico SWQC. Aluminum, copper, gross-alpha, lead, and zinc exceedances are attributed to urban runoff and naturally-occurring sediments routed to the wetlands from LANL (TA-03) and Los Alamos County. Some evidence exists for attenuation of zinc; however, results for other metals such as copper and lead exhibited no discernable trend in attenuation during 2017.

The alluvial system data from 2017 were screened to standards (section D-3.3 and Table D-3.3-1). Exceedances in alluvial groundwater included arsenic, chromium, iron, and manganese. Arsenic exceedances were observed at SWA-2-5 once and consistently at SWA-2-6 for all four monitoring rounds. We expect most of this arsenic to be As(III) under the geochemical conditions in the wetland alluvial aquifer. The higher total arsenic compared to As(III) in 2017 is believed to be an artifact of the analysis (see section D-3.2). Iron and manganese exceedances were observed and are expected due to the reducing wetland conditions and their positions on the redox ladder. Dissolved manganese is more persistent than iron due to manganese oxidation kinetics; and, it has been observed in surface water at E123 in the past. Most of the total chromium concentration in alluvial groundwater in the wetland is colloidal Cr(III), leading to exceedances; the measured Cr(VI) at the locations of the exceedances is at or below the minimum detection limit.

3.3 Temporal and Spatial Trends in Water-Level

Monitoring of water levels continues as a means to determine how operational effluent releases affect the overall wetland hydrology. Comparisons between the 2016 and 2017 water levels, shown in Figure D-4.0-2, indicate they have been relatively stable, even with changes in outfall volumes. Seasonal decreases in water levels are observed in a few wells in the easternmost transect, presumably as a result of high rates of evapotranspiration associated with warm temperatures and lower-magnitude precipitation events in the summers compared with those in the previous year (section D-2.0). The water levels in the alluvial system tend to stay stable because the relatively impermeable Bandelier Tuff bedrock base of the wetland, and an impermeable downgradient end (the GCS) keeps the water contained in the wetland. As such, as long as water inputs exceed wetland evapotranspiration, even significantly reduced outfall discharge may sustain water levels and sufficient saturation within wetland sediments. Decreased outfall discharge may manifest more in the surface water balance of the wetland than in alluvial groundwater levels.

3.4 Geomorphic Trends in the Wetland

Geomorphic change detection studies (Appendix B) indicate minor geomorphic change occurred between 2016 and 2017. Repeat GPS surveys in conjunction with field observations indicated that no significant geomorphic changes occurred in the wetland after the 2017 monsoon season. A small amount of deposition was detected in the plunge pool from storm runoff but has not affected the plunge pool area. The southern side channel continued to deposit sediment into the wetland but no significant loss of cattail vegetation was observed in 2017. Overall, the thalweg was stable between 2016 and 2017, with minor lateral changes in thalweg position. The thalweg nick point has remained stable since 2015 with no indication of upstream erosion. Three alluvial fans entering the wetland from the north (drainage from the former Los Alamos County landfill) remained relatively stable.

3.5 Spatial and Temporal Trends in Vegetation

Between 2016 and 2017, the wetland vegetation remains stable with a 2.5% overall expansion of obligate wetland species over the whole study area. The largest expansion was observed in the western-end of the wetland, with noticeable increases occurring in the satellite cattail populations by the plunge pool and in the field south of the channel in the Western Cattail Zone. The Northern Willow Zone continues to expand but the Central Cattail Zone remains generally unaffected with a stable and homogenous stand of cattails, which are only minimally affected by the deposition of sediment from the southern drainage. A slight decrease of GCS vegetation is observed in the GCS Wetland Vegetation Zone due to the spread of native cattails into that zone suggesting a further stabilization of the native Sandia wetland vegetation.

Vegetation monitoring documented in this report does not constitute a formal wetland delineation. For example, the occurrence of hydric soils has not been determined. The combined approach of monitoring the saturation status of the wetland through water-level measurements and redox chemistry, along with spatial and temporal patterns in obligate wetland vegetation, however, is sufficiently robust to evaluate the performance of the wetland. For example, should the wetland begin to dewater as a result of operational changes associated with the SERF, these changes would be noted immediately in water-level data and subsequently in alluvial groundwater chemistry and obligate wetland vegetation patterns.

3.6 Performance of GCS

Inspection results from monitoring of the GCS, presented in Appendix E, indicate that the GCS is stable and does not require corrective or mitigative actions. In fall 2017, several storm water controls were installed to capture sediment running off from a southern drainage into the wetland. Due to the completion date of the controls occurring near the end of the fiscal year, they were not included in the 2017 GCS inspections, but were photographed for reference (see Appendix E).

3.7 2018 Monitoring Plan

Surface water base flow and alluvial wells will be sampled as proposed in Table 3.7-1. Storm water sampling and off-site analysis will continue as presented in Table 1.5-4. If four storm water runoff events have been sampled at gaging station E121, E122, or E123 during the monitoring year, subsequent events with discharge less than the largest discharge of the sampled storm events will not be analyzed. This approach allows collection of representative data from each gaging location and ensures the largest storm water runoff event of the season is analyzed.

Perimeter mapping of wetland vegetation zones and photographs will continue aiding in the evaluation of the extent of obligate wetland vegetation. Future monitoring via the line-intercept method will occur biennially. Visual inspections will continue to occur annually and dictate whether further investigations

(i.e., via the line-intercept method, repeat photographs, or LiDAR surveys) are required for the monitoring year. Differential GPS surveys of the wetland vegetation perimeter will continue on an annual basis, as will qualitative photographic surveys of the wetland.

In 2018, geomorphic change will continue to be evaluated using post-monsoon ground-based surveys of the thalweg and monitoring of established erosion pins. If storm water peak discharge at E123 is greater than 50 cfs, a visual inspection of the wetland will occur to document qualitative geomorphic changes. If the visual observations or the thalweg survey indicate geomorphic changes that are not consistent with last year's observation, a LiDAR aerial flyover will be planned for the fall of 2018, and the processed data will be field-verified to ensure that geomorphic changes shown in a threshold DEM of difference comparison represent actual geomorphic changes.

3.8 Proposed Changes to Monitoring Plan from 2017

Changes for 2018 include the following:

- SWA-1-1 and SWA-4-11 will be sampled for arsenic and iron speciation during the May sampling round while all other alluvial locations will be sample only during the February round, in order to obtain four total rounds of speciated arsenic and iron from an off-site lab; and
- A post-monsoon walk-down of the Sandia wetlands will be organized in conjunction with NMED to observe potential changes to vegetation, geomorphology, and any potential problem areas.

4.0 CONCLUSIONS

This performance period covers the fourth year following baseline monitoring. The monitoring performed during the performance period indicates that the Sandia wetland is stable and expanding following installation of the GCS. Yearly comparisons of analytical results indicate that the wetland is discharging lower concentrations of contaminants of concern in storm water since construction of the GCS. Even with periods of lower effluent volumes entering the wetland and periods of evapotranspiration, the alluvial system remains stable and wetland sediments remain highly reducing, with no detrimental temporal trends in chemistry noted. Even the upper portion of reach S-2 (the second reach down from the headwaters of Sandia Canyon and the reach that encompasses the Sandia wetland), which had been previously dewatered and is outside the current footprint of the wetland, retains reducing conditions in alluvial groundwater at depth and has observed an expanse in vegetation.

Despite overall reduced effluent volumes, water levels remain sufficiently high to sustain and promote the expansion of the obligate wetland vegetation. Continuing vegetation monitoring in future years will be valuable in assessing wetland performance, with abundant wetland vegetation promoting sediment stability and preserving reducing conditions. No large-scale, systematic erosion has been noted in the wetland, and the system seems to be highly stable from a physical perspective. The GCS has arrested headcutting at the terminus of the wetland. Planted wetland vegetation has rapidly established around the GCS, and wetland vegetation is expanding in the upper portion of the system. Storm water data indicate that the GCS has had a positive impact on contaminant mobility. Suspended sediment, PCBs, and chromium concentrations have decreased at E123 post-GCS, presumably due to cessation of headcutting at the terminus of the wetland.

Ongoing monitoring will continue to allow the Laboratory to assess changes within the Sandia wetland related to the GCS, changes in effluent chemistry, and decreases in effluent volumes and discharge rates. The Laboratory will respond with an adaptive management strategy should adverse changes be noted.

5.0 REFERENCES AND MAP DATA SOURCES

5.1 References

The following reference list includes documents cited in this report. Parenthetical information following each reference provides the author(s), publication date, and ERID or ESHID. This information is also included in text citations. ERIDs were assigned by the Associate Directorate for Environmental Management's (ADEM's) Records Processing Facility (IDs through 599999), and ESHIDs are assigned by the Environment, Safety, and Health Directorate (IDs 600000 and above). IDs are used to locate documents in the Laboratory's Electronic Document Management System and in the Master Reference Set. The NMED Hazardous Waste Bureau and ADEM maintain copies of the Master Reference Set. The set ensures that NMED has the references to review documents. The set is updated when new references are cited in documents.

DOE (U.S. Department of Energy), August 24, 2010. "Final Environmental Assessment for the Expansion of the Sanitary Effluent Reclamation Facility and Environmental Restoration of Reach S-2 of Sandia Canyon at Los Alamos National Laboratory, Los Alamos, New Mexico," U.S. Department of Energy document DOE/EA-1736, Los Alamos Site Office, Los Alamos, New Mexico. (DOE 2010, 206433)

EPA (U.S. Environmental Protection Agency), June 8, 2007. "Authorization to Discharge under the National Pollutant Discharge Elimination System, NPDES Permit No. NM 0028355," Region 6, Dallas, Texas. (EPA 2007, 099009)

EPA (U.S. Environmental Protection Agency), August 12, 2014. "NPDES Permit No. NM0028355 Final Permit Decision," U.S. Environmental Protection Agency Region 6, Dallas, Texas. (EPA 2014, 600257)

LANL (Los Alamos National Laboratory), October 2009. "Investigation Report for Sandia Canyon," Los Alamos National Laboratory document LA-UR-09-6450, Los Alamos, New Mexico. (LANL 2009, 107453)

LANL (Los Alamos National Laboratory), May 2011. "Interim Measures Work Plan for Stabilization of the Sandia Canyon Wetland," Los Alamos National Laboratory document LA-UR-11-2186, Los Alamos, New Mexico. (LANL 2011, 203454)

LANL (Los Alamos National Laboratory), September 2011. "Work Plan and Final Design for Stabilization of the Sandia Canyon Wetland," Los Alamos National Laboratory document LA-UR-11-5337, Los Alamos, New Mexico. (LANL 2011, 207053)

LANL (Los Alamos National Laboratory), March 2012. "100% Design Memorandum For Sandia Wetlands Stabilization Project," Los Alamos National Laboratory, Los Alamos, New Mexico. (LANL 2012, 240016)

- LANL (Los Alamos National Laboratory), September 2012. "Phase II Investigation Report for Sandia Canyon," Los Alamos National Laboratory document LA-UR-12-24593, Los Alamos, New Mexico. (LANL 2012, 228624)
- LANL (Los Alamos National Laboratory), December 2013. "Completion Report for Sandia Canyon Grade-Control Structure," Los Alamos National Laboratory document LA-UR-13-29285, Los Alamos, New Mexico. (LANL 2013, 251743)
- LANL (Los Alamos National Laboratory), June 2014. "Sandia Wetland Performance Report, Baseline Conditions 2012–2014," Los Alamos National Laboratory document LA-UR-14-24271, Los Alamos, New Mexico. (LANL 2014, 257590)
- LANL (Los Alamos National Laboratory), December 15, 2014. "2014 Annual Monitoring Report for Sandia Canyon Wetland Grade-Control Structure (SPA-2012-00050-ABQ)," Los Alamos National Laboratory letter and attachments (ENV-DO-14-0378) to K.E. Allen (USACE) from A.R. Grieggs (LANL), Los Alamos, New Mexico. (LANL 2014, 600083)
- LANL (Los Alamos National Laboratory), April 2015. "Sandia Wetland Performance Report, Performance Period April 2014–December 2014," Los Alamos National Laboratory document LA-UR-15-22463, Los Alamos, New Mexico. (LANL 2015, 600399)
- LANL (Los Alamos National Laboratory), April 2016. "2015 Sandia Wetland Performance Report," Los Alamos National Laboratory document LA-UR-16-22618, Los Alamos, New Mexico. (LANL 2016, 601432)
- LANL (Los Alamos National Laboratory), April 2017. "2016 Sandia Wetland Performance Report," Los Alamos National Laboratory document LA-UR-17-23076, Los Alamos, New Mexico. (LANL 2017, 602341)
- NMED (New Mexico Environment Department), June 9, 2011. "Approval with Modification, Interim Measures Work Plan for Stabilization of the Sandia Canyon Wetland," New Mexico Environment Department letter to G.J. Rael (DOE-LASO) and M.J. Graham (LANL) from J.E. Kielling (NMED-HWB), Santa Fe, New Mexico. (NMED 2011, 203806)
- Rai, D., L.E. Eary, and J.M. Zachara, October 1989. "Environmental Chemistry of Chromium," *Science of the Total Environment*, Vol. 86, No. 1–2, pp. 15–23. (Rai et al. 1989, 249300)

5.2 Map Data Sources

Rain Gages; Los Alamos National Laboratory; ER-ES Surface Hydrology Group; 2017.

WQH NPDES Outfalls; Los Alamos National Laboratory, ENV Water Quality and Hydrology Group; Edition 2002.01; 01 September 2003.

Alluvial Well Locations; Los Alamos National Laboratory, Waste and Environmental Services Division; Locus EIM database pull; 2017.

Paved Road Arcs; Los Alamos National Laboratory, FWO Site Support Services, Planning, Locating and Mapping Section; 06 January 2004; as published 29 November 2010.

Grade Control Structure and Cascade Pool; Los Alamos National Laboratory; ER-ES Engineering Services; as published, project 14-0015; 2017.

Structures; Los Alamos National Laboratory, FWO Site Support Services, Planning, Locating and Mapping Section; 06 January 2004; as published 29 November 2010.

Former Los Alamos County Landfill; Los Alamos National Laboratory; ER-ES Engineering Services; as published, project 14-0015; 2017.

Canyon Reaches; Los Alamos National Laboratory, ENV Environmental Remediation and Surveillance Program, ER2002-0592; 1:24,000 Scale Data; Unknown publication date.

Technical Area Boundaries; Los Alamos National Laboratory, Site Planning & Project Initiation Group, Infrastructure Planning Office; September 2007; as published 13 August 2010.

Orthophotography, Los Alamos National Laboratory Site, 2014; Los Alamos National Laboratory, Site Planning and Project Initiation Group, Space and Site Management Office; 2014.

Contours, 20 and 5-ft intervals; as generated from 2014 LiDAR elevation data; Los Alamos National Laboratory, ER-ES; as published, project 14-0015; 2017.

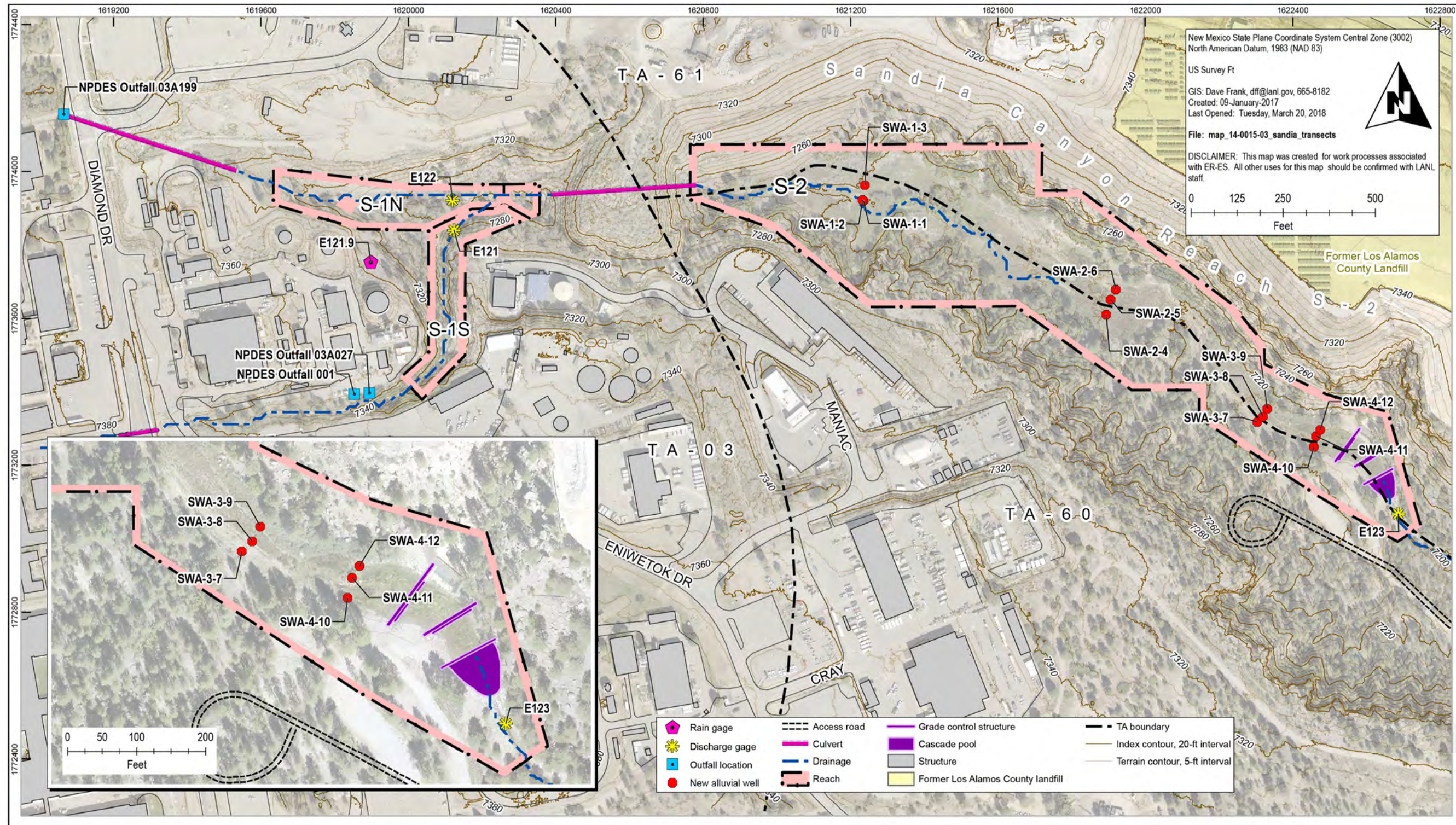
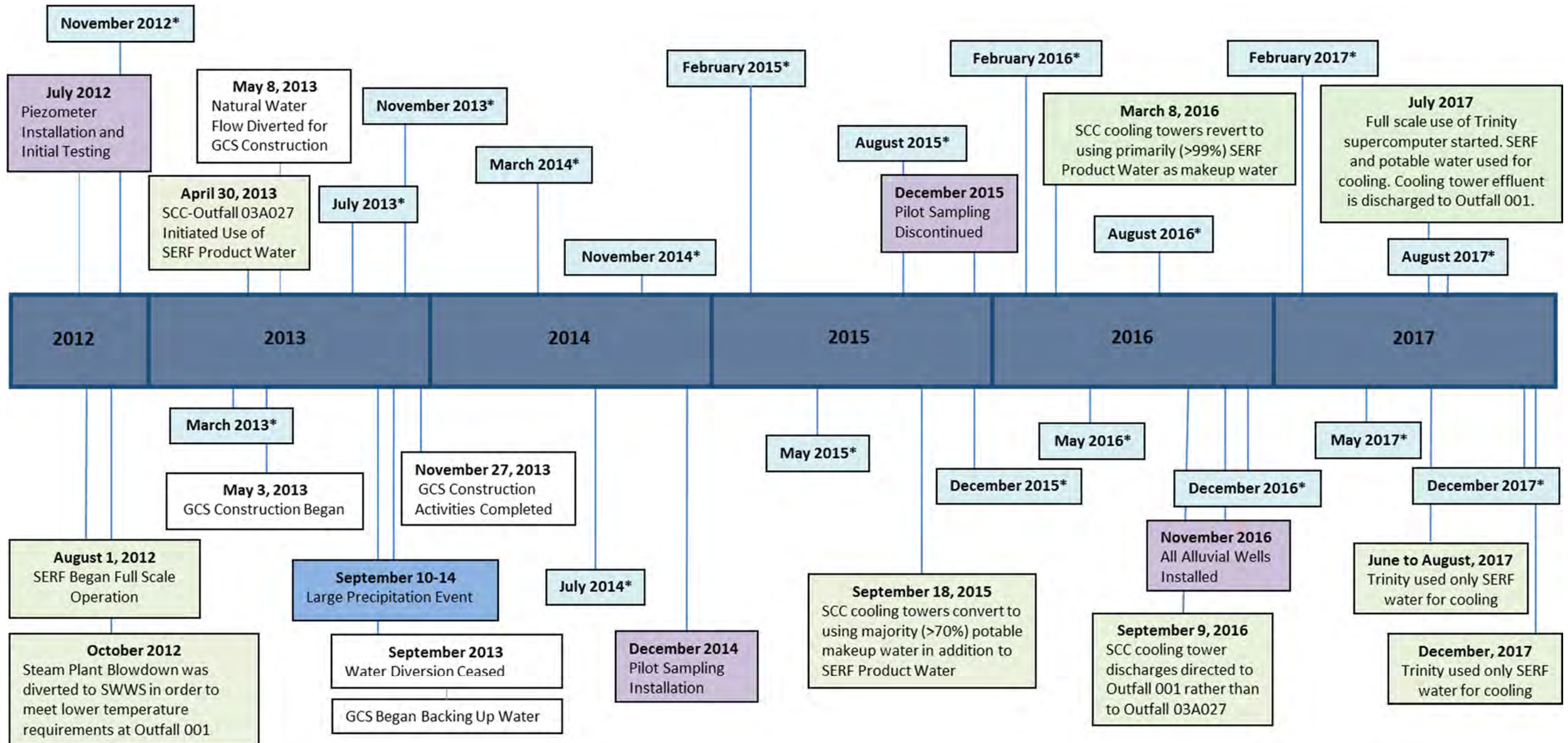


Figure 1.0-1 Locations of the Sandia GCS (headcut was located at the upper most sheet pile at the terminus of the wetland), NPDES outfalls, precipitation gage E121.9, alluvial wells, surface and storm water gaging stations, former Los Alamos County landfill, surrounding TAs, and reaches S-1N, S-1S, and S-2.



*Quarterly alluvial and surface water sampling

Figure 1.2-1 Sandia Canyon wetland timeline. Types of events are grouped by color.

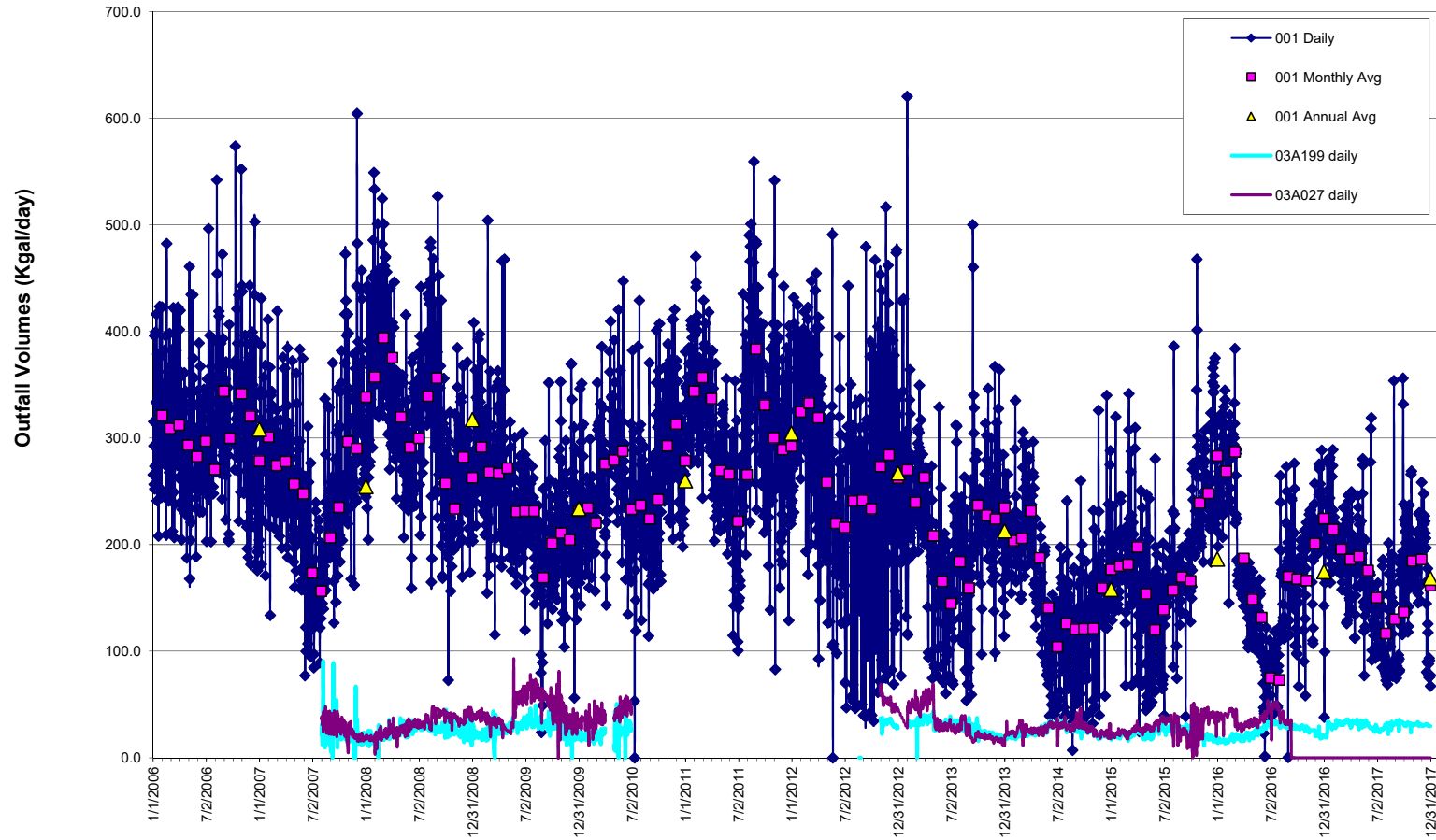


Figure 1.4-1 Daily, monthly average, and yearly average effluent release volumes (expressed as Kgal./d) for Outfall 001 from 2006 to December 2017, and daily effluent releases for Outfalls 03A027 and 03A199 from August 2007 to January 2010 and from November 2012 to December 2017. No discharges to Outfall 03A027 have occurred since September 2016.

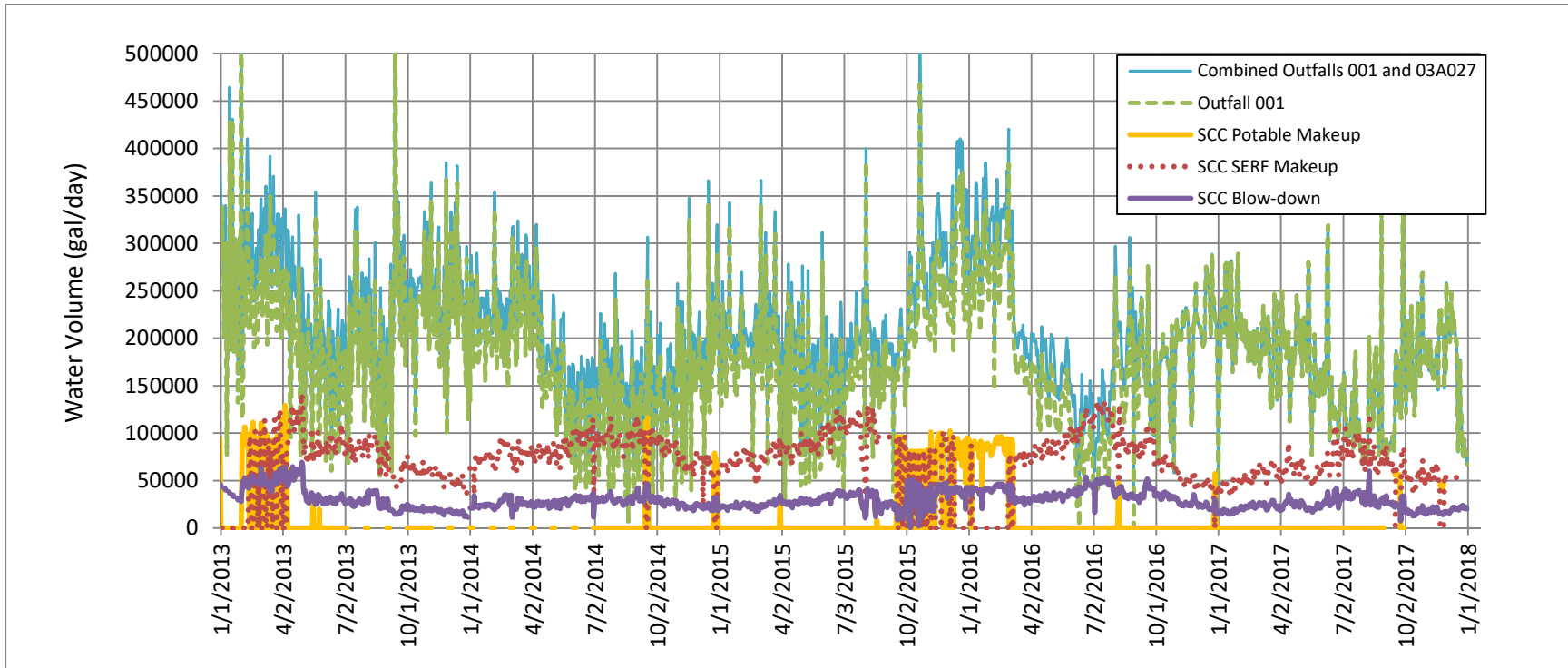


Figure 1.4-2 Daily water volumes (gpd) from November 2012 to December 2017 for effluent released from combined Outfalls 001 and 03A027 and Outfall 001 only. Also included are effluent (blowdown) volumes from the SCC cooling towers and makeup water sources (potable or SERF-blended water) used at the SCC cooling towers. The SCC cooling tower blowdown was released to Outfall 03A027 until September 8, 2016; since September 9, 2016, the blowdown has been released to Outfall 001.

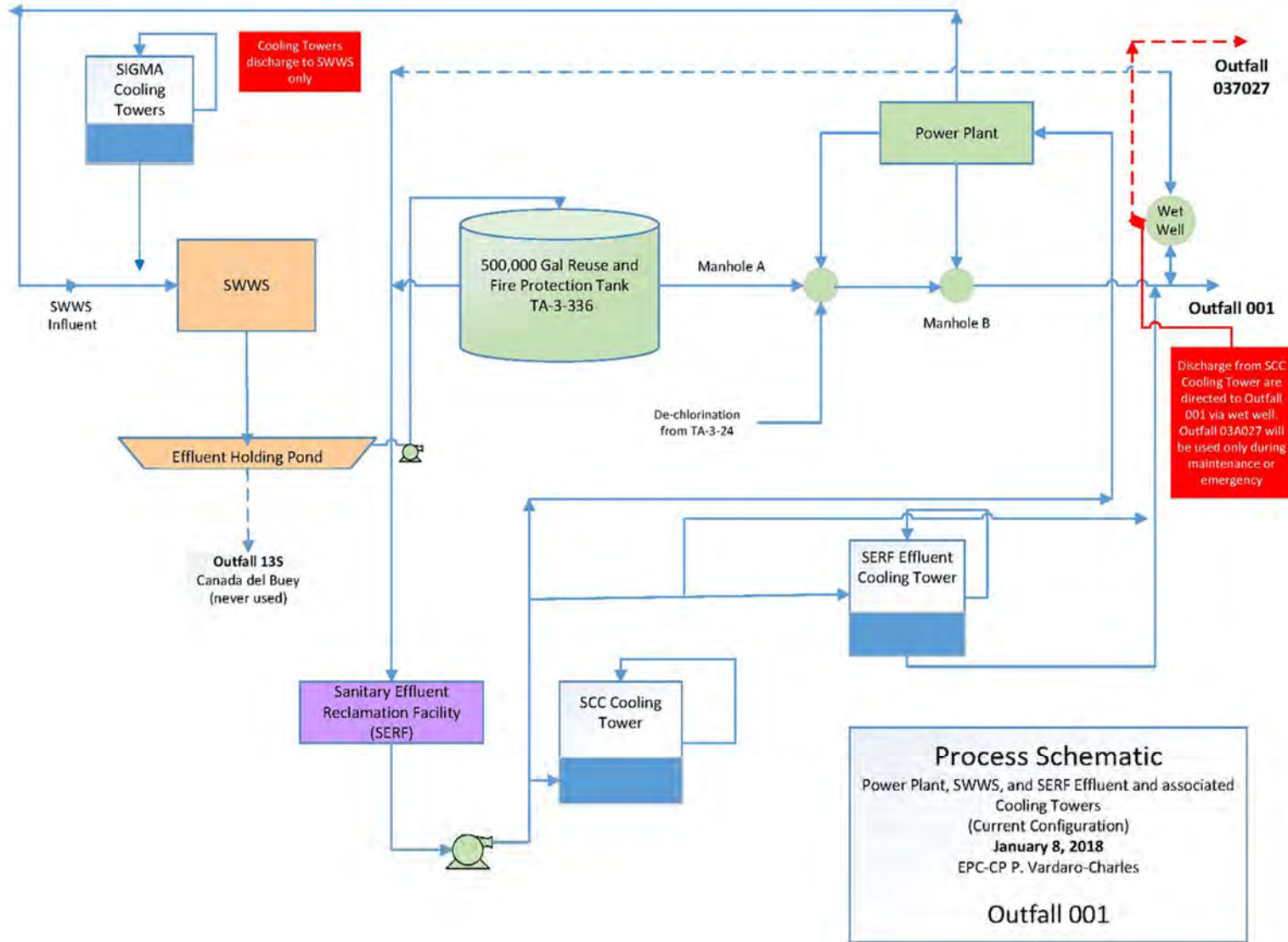


Figure 1.4-3 Updated process schematic for the power plant, SWWS, and SERF connections to Outfall 001 (current configuration)

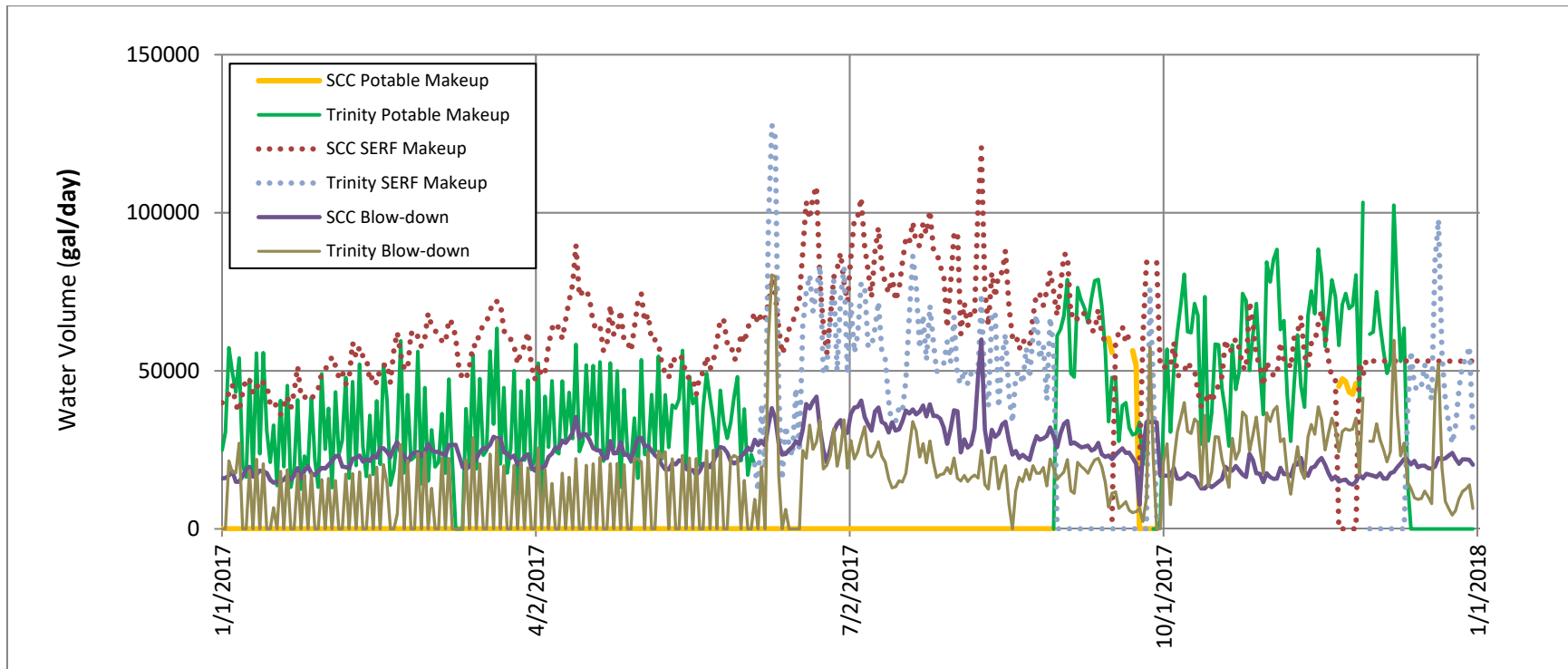


Figure 1.4-4 Daily cooling water usage and discharge information for the SCC and Trinity cooling towers during 2017. Included are effluent (blowdown) volumes from the SCC and Trinity cooling towers and makeup water sources (potable or SERF-blended water) used at the SCC and Trinity cooling towers. During 2017, all SCC and Trinity cooling tower blowdown was released to Outfall 001.

**Table 1.5-1
Completion Data for Alluvial Piezometers and Collocated Alluvial Wells**

Piezometers													
	SCPZ-1	SCPZ-2	SCPZ-3	SCPZ-4	SCPZ-5	SCPZ-6	SCPZ-7	SCPZ-8	SCPZ-9	SCPZ-10	SCPZ-11(A)	SCPZ-11(B)	SCPZ-12
Total length (ft)	20.5	11.4	8.3	8.3	8.3	8.3	8.3	11.4	8.3	8.3	8.3	8.3	8.3
Stick up (ft)	4.36	3.26	3.19	3.16	2.64	3.18	4.32	4.78	3.35	4.01	3.8	4.48	3.77
Top of screen (ft bgs)	13.8	6.0	3	3	3	3	1.6	5.3	3	3	3	1	3
Total depth (ft bgs)	16.2	8.3	5.4	5.4	5.4	5.4	4.0	7.6	5.4	5.4	5.4	5.4	5.4
Alluvial Wells													
	SWA-1-1	SWA-1-2	SWA-1-3	SWA-2-4	SWA-2-5	SWA-2-6	SWA-3-7	SWA-3-8	SWA-3-9	SWA-4-10		SWA-4-11	SWA-4-12
Ground elevation (ft amsl*)	7239.9	7240.0	7239.2	7223.3	7223.0	7222.9	7212.7	7213.1	7212.9	7209.6		7210.8	7210.5
Total length (ft)	18.33	13.17	9.37	9.00	8.96	8.22	6.84	10.68	8.22	8.44		7.93	8.19
Stick up (ft)	2.33	4.14	3.02	3.00	2.96	2.1	3.24	2.88	3.02	3.94		1.93	2.2
Top of screen (ft bgs)	13.0	6.03	3.0	3.0	3.0	3.12	0.6	4.8	2.2	2.5		3	2.99
Bottom of screen (ft bgs)	15.5	8.53	5.5	5.5	5.5	5.62	3.1	7.3	4.7	5		5.5	5.49
Total depth (ft bgs)	16.0	9.03	6.0	6.0	6.0	6.12	3.6	7.8	5.2	5.5		6	5.99

Note: Alluvial wells shown below collocated piezometer.

*amsl = Above mean sea level.

**Table 1.5-2
Schema Crosswalk: Past Piezometers and Current Alluvial Wells**

Piezometer	To	Alluvial Well	Date of Alluvial Well Installation
SCPZ-1	→	SWA-1-1	8/19/2016
SCPZ-2	→	SWA-1 / SWA-1-2*	12/18/2014
SCPZ-3	→	SWA-1-3	7/21/2016
SCPZ-4	→	SWA-2-4	7/20/2016
SCPZ-5	→	SWA-2-5	7/20/2016
SCPZ-6	→	SWA-2 / SWA-2-6*	12/16/2014
SCPZ-7	→	SWA-3-7	4/27/2016
SCPZ-8	→	SWA-3 / SWA-3-8*	12/16/2014
SCPZ-9	→	SWA-3-9	4/28/2016
SCPZ-10	→	SWA-4-10	4/27/2016
SCPZ-11B	→	SWA-4-11	7/19/2016
SCPZ-12	→	SWA-4 / SWA-4-12*	12/15/2014

* SWA-1, SWA-2, SWA-3, and SWA-4 were pilot wells installed in December 2016; SWA-1-2, SWA-2-6, SWA-3-8, SWA-4-12 are the same wells relabeled in 2015.

**Table 1.5-3
Alluvial Groundwater Sampling and Analysis Plan
for 2017 Sandia Wetland Stabilization Monitoring**

Suite	Frequency	Comment
Metals ^a (filtered)	Quarterly	Includes redox-sensitive metals Fe, Mn, Cr, As.
Anions ^b (filtered)	Quarterly	Includes redox-sensitive anions, sulfate and nitrate; nitrate is a wetland vegetation nutrient
Sulfide (unfiltered)	Quarterly	Redox indicator (reduction of sulfate)
Alkalinity/pH (unfiltered)	Quarterly	Organic matter degradation
Ammonia (unfiltered)	Quarterly	Indicator of organic matter degradation; wetland vegetation nutrient
DOC ^c (filtered)	Annually	Organic matter degradation (collected in August 2017)
Fe(II) (filtered)	Quarterly	Indicator of Fe(III) reducing to Fe(II)
As(III) (filtered)	Quarterly	Indicator of As(V) reducing to As(III)
Cr(VI) (unfiltered)	Quarterly	Indicator of Cr(III) oxidizing to Cr(VI)

^a Metals consists of the following suite: Ag, Al, As, B, Ba, Be, Cd, Co, Cr, Cs, Cu, Fe, K, Li, Mg, Mn, Na, Ni, Pb, Rb, Se, Si, Sr, Ti, Tl, U, V, Zn, Hg, Mo, Sb, Sn, Th.

^b Anions consists of the following suite: Br, F, Cl, NO₂, NO₃, PO₄, SO₄, C₂O₄H₂ (oxalic acid).

^c DOC = Dissolved organic carbon.

Table 1.5-4
ISCO Bottle Configurations and Analytical Suites
Calendar Year 2017 Storm Water Sampling Plan for E121, E122, and E123

Sample Bottle (1 L)	Start Time (min) 12-Bottle ISCO	Analytical Suites 12-Bottle ISCO	Start Time (min) 24-Bottle ISCO	Analytical Suites 24-Bottle ISCO
1	Peak+10	SSC ^a ; particle size	Trigger	SSC
2	Peak+12	PCBs ^b (UF ^c) Part 1 ^d	Trigger+2	SSC
3	Peak+14	TOC ^e (UF), DOC ^f (F ^g) + chloride (F) + sulfate (F) + alkalinity (UF) + pH (UF)	Trigger+4	SSC
4	Peak+16	PCBs (UF) Part 2	Trigger+6	SSC
5	Peak+18	TAL ^h metals + B + U + hardness (F/UF)	Trigger+8	SSC
6	Peak+20	PAH ⁱ (UF)	Trigger+10	SSC
7	Peak+22	SVOC ^j (UF)	Trigger+12	SSC
8	Peak+24	Gross alpha (UF)	Trigger+14	SSC
9	Peak+26	SSC	Trigger+16	SSC
10	Peak+28	Extra bottle	Trigger+18	SSC
11	Peak+30	Extra bottle	Trigger+20	SSC
12	Peak+32	Extra bottle	Trigger+22	SSC
13	n/a ^k	n/a	Trigger+24	SSC
14	n/a	n/a	Trigger+26	SSC
15	n/a	n/a	Trigger+28	SSC
16	n/a	n/a	Trigger+30	SSC
17	n/a	n/a	Trigger+50	SSC
18	n/a	n/a	Trigger+70	SSC
19	n/a	n/a	Trigger+90	SSC
20	n/a	n/a	Trigger+110	SSC
21	n/a	n/a	Trigger+130	SSC
21	n/a	n/a	Trigger+150	SSC
23	n/a	n/a	Trigger+170	SSC
24	n/a	n/a	Trigger+190	SSC

Notes: E121 = Sandia right fork at Pwr Plant, E122 = Sandia left fork at Asph Plant or South fork of Sandia at E122, E123 = Sandia below Wetlands. The 12-bottle ISCO begins collection 10 mins after the peak discharge (i.e., "Peak+10") and the 24-bottle ISCO begins collection as soon as water is detected by the liquid level actuator (i.e., "Trigger").

^a SSC = Suspended sediment concentration.

^b PCBs = Polychlorinated biphenyls.

^c UF = Unfiltered.

^d Bottles 2 and 4 are to be sent to the lab together for one PCBs analysis.

^e TOC = Total organic carbon.

^f DOC = Dissolved organic carbon.

^g F = Filtered through a 0.45- μ m membrane.

^h TAL = TAL metals are Ag, Al, As, Ba, Be, Ca, Cd, Co, Cr, Cu, Fe, Hg, K, Mg, Mn, Na, Ni, Pb, Sb, Se, Tl, V, and Zn; hardness is calculated from calcium and magnesium, components of the TAL list.

ⁱ PAH = Polycyclic aromatic hydrocarbons.

^j SVOC = Semivolatile organic compounds.

^k n/a = Not applicable.

Table 2.1-1
Field Data for Alluvial Locations and Surface Water Stations 2017 Sampling Events

Location Name	Date	Dissolved Oxygen (mg/L)	Oxidation-Reduction Potential (mV)	pH	Specific Conductance (μS/cm)	Temperature (°C)	Turbidity (NTU ^a)
Surface Water Stations							
E121	2/22/2017	8.29	NR ^b	8.47	536	14.5	3.9
E121	5/22/2017	7.62	NR	8.25	549.7	16.8	1.3
E121	8/10/2017	6.97	199.5	7.86	409.5	20.6	0.3
E121	11/28/2017	7.68	NR	8.01	366.6	13.8	0.3
E122	2/22/2017	8.3	NR	8.48	392.8	15	1.4
E122	5/22/2017	7.97	NR	8.35	392.5	18.1	1.6
E122	8/10/2017	6.35	222	8.15	397	20.4	0.5
E122	11/28/2017	7.28	NR	8.11	344.8	13.8	0.2
E123	2/22/2017	10.12	NR	7.78	601	9	1
E123	5/22/2017	7.65	NR	7.99	445.6	13.9	1.4
E123	8/10/2017	7.53	201.2	7.95	416.9	18	2.9
E123	11/28/2017	9.81	NR	7.89	373.6	6.4	0.5
Piezometers and Alluvial Wells							
SWA-1-1	2/23/2017	0.73	-134.3	7.01	604	11.4	2.1
SWA-1-1	5/24/2017	0.5	-136.3	7.04	850	11.9	3.3
SWA-1-1	8/16/2017	0.47	-145.9	7.01	672	13.2	0.4
SWA-1-1	11/29/2017	0.54	-157.8	7.21	579	13.5	6
SWA-1-2	2/23/2017	0.63	-68	7.03	900	6.6	6.1
SWA-1-2	5/24/2017	0.86	-95.5	7.54	426.8	12.4	4.9
SWA-1-2	8/16/2017	0.92	-87.2	6.97	425.2	17.7	2.4
SWA-1-2	11/29/2017	0.94	-91.4	7.33	387.3	10.8	7.4
SWA-1-3	2/23/2017	0.73	-107.3	6.77	997	5	5.6
SWA-1-3	5/24/2017	0.77	-122.4	7.11	450.1	12.9	5.9
SWA-1-3	8/16/2017	0.98	-105.9	6.55	469.4	17.4	2.5
SWA-1-3	11/29/2017	0.89	-98.2	6.99	382.6	8.4	8.5
SWA-2-4	2/23/2017	0.46	-85.7	7.06	880	6.9	1.3
SWA-2-4	5/24/2017	0.99	-61.5	7.04	469	12.8	1
SWA-2-4	8/15/2017	0.62	-79.9	6.93	485.6	15.6	0.6
SWA-2-4	11/29/2017	0.63	-107.6	7.02	416	8.8	0.2
SWA-2-5	2/23/2017	0.46	-163.8	7.28	524	10.6	5.9
SWA-2-5	5/24/2017	0.79	-141.8	7.24	686	11.5	2.8
SWA-2-5	8/15/2017	0.71	153.6	7.27	652	11.9	1.1
SWA-2-5	11/29/2017	0.56	-170.7	7.28	563	10.8	3.2
SWA-2-6	5/24/2017	0.71	-144.7	7.12	659	10.5	1.8

Table 2.1-1 (continued)

Location Name	Date	Dissolved Oxygen (mg/L)	Oxidation-Reduction Potential (mV)	pH	Specific Conductance (μ S/cm)	Temperature ($^{\circ}$ C)	Turbidity (NTU ^a)
Piezometers and Alluvial Wells (continued)							
SWA-2-6	2/23/2017	0.55	-162.2	7.19	525	8.1	7.4
SWA-2-6	8/15/2017	1.04	-151.3	7.02	668	12	1.6
SWA-2-6	11/29/2017	0.35	-165	7.28	570	8.8	3
SWA-3-7	2/24/2017	0.55	-52	6.33	990	1.9	14.5
SWA-3-7	5/23/2017	0.64	-52.3	6.42	721	9.2	1.4
SWA-3-7	8/16/2017	0.77	-122.6	6.42	634	15.9	2.2
SWA-3-7	11/30/2017	0.9	-25.4	6.32	819	5.1	0.9
SWA-3-8	2/24/2017	0.58	-120.3	6.94	601	4.9	1.2
SWA-3-8	5/23/2017	0.52	-94.1	6.84	656	7.9	1
SWA-3-8	8/16/2017	0.71	-111.9	6.87	605	12.6	1.5
SWA-3-8	11/30/2017	0.83	-95.1	6.87	612	7.7	4.2
SWA-3-9	2/24/2017	0.44	-117.5	6.72	622	4.3	0.7
SWA-3-9	5/23/2017	0.57	-95.7	6.57	680	8.3	1.8
SWA-3-9	8/16/2017	0.64	-111.1	6.83	627	12.8	1.2
SWA-3-9	11/30/2017	0.65	-97.5	6.72	584	7.1	3.5
SWA-4-10	2/24/2017	2.89	-25.9	6.3	789	4	14
SWA-4-10	5/23/2017	1.35	-66.1	6.39	698	9.6	21.1
SWA-4-10	8/15/2017	0.99	48.3	6.15	621	15.3	8.5
SWA-4-10	11/30/2017	3.31	-79.9	6.6	545	8.6	11
SWA-4-11	2/24/2017	0.81	-95	7.13	617	2.7	15.4
SWA-4-11	5/23/2017	0.69	-76.3	6.67	450.1	11	12
SWA-4-11	8/15/2017	1	-119.3	6.54	483.3	17.4	1
SWA-4-11	11/30/2017	0.44	-81.8	6.72	376.8	5.1	4.7
SWA-4-12	2/24/2017	0.58	-80.8	6.32	830	3.1	2.2
SWA-4-12	5/23/2017	0.78	-78.8	6.84	449.6	11	1.4
SWA-4-12	8/15/2017	1.28	-94.8	6.52	565	16.2	1.08
SWA-4-12	11/30/2017	0.41	-82.8	6.68	405.7	6.2	1.21

^a NTU = Nephelometric turbidity unit.

^b NR = Not recorded.

**Table 2.1-2
Precipitation, Storm Water Peak Discharge, and Samples Collected at
Gaging Stations E121, E122, and E123 for Each Sample-Triggering Storm Event in 2017**

Storm Event Date	RG121.9 Total Precipitation (in.)	E121 Peak Discharge (cfs)	E122 Peak Discharge (cfs)	E123 Peak Discharge (cfs)
6/6	0.3	26 S ^a	2.3 BT ^b	16 S
6/25	0.3	20 S	2.8 BT	30 S
7/18	1.0	36 S	5.3 S ^c	14 S
7/26	0.6	87 S	9.1 S	78 S
7/27	0.3	6.8 BT	1.9 S	8.4 BT
7/29	0.4	30 S	4.7 S	29 S
8/21	0.2	9 BT	1.8 S	10 CT ^d

^a S = Sample was collected. These discharge levels are shaded in green to emphasize those events for which discharge exceeded the trip level and samples were collected.

^b BT = Below 10-cfs trip level, no sample collected.

^c Trip level at E122 was lowered to approximately 2.0 cfs.

^d CT = Close to 10-cfs trip level, no sample collected. Stage measurement sensors can have inaccuracies ± 2 cfs.

**Table 3.7-1
Proposed Sampling and Preservation Requirements for Sandia Wetland**

Analytical Suite	Analytical Method	Sample Type ^a	Frequency	Filtered ^b	Preservation	Field Storage	Holding Time	Ideal Volume	Minimum Volume	Comment
Alluvial Wells										
Cr(VI) Speciation	IC-ICPMS:Metals	W	Qtrly	Y	NH ₄ OH/(NH ₄) ₂ SO ₄ buffer to pH > 9.0 - 9.5; zero headspace	<4°C	28 days	125 mL	125 mL	— ^c
As(III) Speciation	IC-ICPMS:Metals	W	Qtrly	Y	Pre-preserved with EDTA/acetic acid solution; minimal headspace	<4°C	28 days	125 mL	125 mL	—
Fe(II) and Fe(III) Speciation	SM:3500 and SM:3500 Fe-B	W	Qtrly	Y	Preservative at collection (preservative, 4% degassed 6M HCl, provided in vial)	<4°C	2 days for Fe(II)	2 x 40 mL glass amber bottles	40 mL	—
Target Analyte List (TAL) Metals	SW-846:6010C and SW-846:6020 EPA:245.2 (Hg)	W	Qtrly	Y	Nitric acid	<4°C	6 mo 28 Days for Hg	1 L	300 mL	—
Anions	EPA:300.0	W	Qtrly	Y	None	<4°C	28 Days	125 mL	50 mL	—
Ammonium, Nitrate-Nitrite, Phosphorus	EPA:350.1 (NH ₃ -N) EPA:353.2 (NO ₃ +NO ₂ -N) EPA:365.4 (PO ₄ -P)	W	Qtrly	Y	H ₂ SO ₄	<4°C	28 Days	250 mL	100 mL	—
Alkalinity/pH	EPA:150.1 (pH) EPA:310.1 (Alkalinity)	W	Qtrly	N	None	<4°C	ASAP ^d	125 mL	125 mL	—
DOC	SW-846:9060	W	Annually	Y	None	<4°C	28 Days	40 mL	40 mL	August sample event
EES Sulfide	SW-846:9215	W	Qtrly	N	Sulfide buffer pH 12	<4°C	24 hr	15 mL	15 mL	Short holding time – On-site analysis
Surface Water Base Flow at Gages E121, E122, and E123										
PAH Congeners	EPA:625	WS	Qtrly	N	Na ₂ O ₃ S ₂ if residual Cl is present	<4°C	7 days	3 L	1 L	Amber glass with Teflon lid
PCB Congeners	EPA:1668C	WS	Qtrly	N	None	<4°C	1 yr	3 L	1L	—
TAL Metals (F)	SW-846:6010C and SW-846:6020 EPA:245.2 (Hg)	WS	Qtrly	Y	Nitric acid	<4°C	6 mo 28 Days for Hg	1 L	300 mL	—
TAL Metals (UF)	SW-846:6010C and SW-846:6020 EPA:245.2 (Hg)	WS	Qtrly	N	Nitric acid	<4°C	6 mo 28 Days for Hg	1 L	300 mL	—
Chromium (Cr VI) speciation	IC-ICPMS:Metals	WS	Qtrly	F	NH ₄ OH / (NH ₄) ₂ SO ₄ (liquid) buffer 1 mL to 100mL of sample	<4°C	14 days	100 mL	100 mL	—
EES Sulfide	EPA:376.2	WS	Qtrly	N	Sulfide buffer pH 12	<4°C	24 hr	15 mL	15 mL	On-site analysis
Anions	EPA:300.0	WS	Qtrly	Y	None	<4°C	28 Days	125 mL	50 mL	—
Ammonium, Nitrate-Nitrite, Phosphorus	EPA:350.1 (NH ₃ -N) EPA:353.2 (NO ₃ NO ₂ -N) EPA:365.4 (PO ₄ -P)	WS	Qtrly	Y	H ₂ SO ₄	<4°C	28 Days	250 mL	100 mL	—
Alkalinity/pH	EPA:150.1 EPA:310.1	WS	Qtrly	N	None	<4°C	ASAP	125 mL	125 mL	—
SSC	ASTM:D3977-97	WS	Qtrly	N	None	no requirement	n/a ^e	1 L	1 L	—
DOC	EPA:415.1	WS	Annually	Y	None	<4°C	28 Days	40 mL	40 mL	August sample event

^a W = Alluvial groundwater samples; WS = base flow water samples.

^b Y= Filtered using 0.45-µm pore size; N= nonfiltered.

^c — = None.

^d ASAP = As Soon As Possible.

^e n/a = not applicable.

Appendix A

*Acronyms and Abbreviations,
Metric Conversion Table, and Data Qualifier Definitions*

A-1.0 ACRONYMS AND ABBREVIATIONS

3-D	three-dimensional
amsl	above mean sea level
bgs	below ground surface
cfs	cubic foot per second
DC	direct current
DEM	digital elevation model
DGPS	differentially corrected global positioning system
DOC	dissolved organic carbon
DoD	DEM of difference
EES	Earth and Environmental Sciences (Laboratory group)
EPA	Environmental Protection Agency (U.S.)
ESH	Environment, Safety, and Health
F	filtered
FAC	facultative plant
FACU	facultative upland plant
FACW	facultative wetland plant
FIS	fuzzy inference system
GCD	geomorphic change detection
GCS	grade-control structure
gpd	gallons per day
gpm	gallons per minute
GPS	global positioning system
HH-OO	human health-organism only
IR	investigation report
LANL	Los Alamos National Laboratory
LiDAR	light detection and ranging
MCL	maximum contaminant level
MDL	method detection limit
MF	membership function
MY	monitoring year
NI	no indicator status
NMED	New Mexico Environment Department

NMWQCC	New Mexico Water Quality Control Commission
NPDES	National Pollutant Discharge Elimination System
NTU	nephelometric turbidity unit
OBL	obligate wetland plant
PAH	polycyclic aromatic hydrocarbon
PCB	polychlorinated biphenyl
PVC	polyvinyl chloride
RMSE	root-mean-square error
RPD	relative percent difference
SCC	Strategic Computing Complex
SERF	Sanitary Effluent Reclamation Facility
SOM	solid organic matter
SSC	suspended sediment concentration
SVOC	semivolatile organic compound
SWMU	solid waste management unit
SWQC	surface water–quality criteria
SWWS	Sanitary Waste Water System
TA	technical area
TAL	target analyte list
TDS	total dissolved solids
TKN	total Kjeldahl nitrogen
TOC	total organic compound
TSS	total suspended sediment
UF	unfiltered
UPL	upland plant
VE	vertical exaggeration

A-2.0 METRIC CONVERSION TABLE

Multiply SI (Metric) Unit	by	To Obtain U.S. Customary Unit
kilometers (km)	0.622	miles (mi)
kilometers (km)	3281	feet (ft)
meters (m)	3.281	feet (ft)
meters (m)	39.37	inches (in.)
centimeters (cm)	0.03281	feet (ft)
centimeters (cm)	0.394	inches (in.)
millimeters (mm)	0.0394	inches (in.)
micrometers or microns (μm)	0.0000394	inches (in.)
square kilometers (km^2)	0.3861	square miles (mi^2)
hectares (ha)	2.5	acres
square meters (m^2)	10.764	square feet (ft^2)
cubic meters (m^3)	35.31	cubic feet (ft^3)
kilograms (kg)	2.2046	pounds (lb)
grams (g)	0.0353	ounces (oz)
grams per cubic centimeter (g/cm^3)	62.422	pounds per cubic foot (lb/ft^3)
milligrams per kilogram (mg/kg)	1	parts per million (ppm)
micrograms per gram ($\mu\text{g}/\text{g}$)	1	parts per million (ppm)
liters (L)	0.26	gallons (gal.)
milligrams per liter (mg/L)	1	parts per million (ppm)
degrees Celsius ($^{\circ}\text{C}$)	$9/5 + 32$	degrees Fahrenheit ($^{\circ}\text{F}$)

A-3.0 DATA QUALIFIER DEFINITIONS

Data Qualifier	Definition
U	The analyte was analyzed for but not detected.
J	The analyte was positively identified, and the associated numerical value is estimated to be more uncertain than would normally be expected for that analysis.
J+	The analyte was positively identified, and the result is likely to be biased high.
J-	The analyte was positively identified, and the result is likely to be biased low.
UJ	The analyte was not positively identified in the sample, and the associated value is an estimate of the sample-specific detection or quantitation limit.
R	The data are rejected as a result of major problems with quality assurance/quality control (QA/QC) parameters.

Appendix B

2017 Geomorphic Changes in Sandia Canyon Reach S-2

CONTENTS

B-1.0 INTRODUCTION B-1

B-2.0 HYDROLOGIC EVENTS DURING THE 2017 MONSOON SEASON..... B-1

B-3.0 GROUND-BASED SURVEY METHODS OF THE SANDIA WETLAND B-1

B-4.0 RESULTS AND DISCUSSION B-2

 B-4.1 Thalweg Characterization B-2

 B-4.2 Plunge Pool Characterization B-2

 B-4.3 Channel Bank Characterization B-3

 B-4.4 Alluvial Fan Characterization B-3

B-5.0 CONCLUSIONS AND RECOMMENDATIONS B-4

B-6.0 REFERENCES AND MAP DATA SOURCES B-4

 B-6.1 References B-4

 B-6.2 Map Data Sources B-5

Figures

Figure B-1.0-1 Sandia Canyon reach S-2 orthophoto with gage station E123, alluvial wells, and survey locations mentioned in report, including channel banks, thalweg, alluvial fans, and the plunge pool..... B-7

Figure B-4.1-1 Thalweg profile in Sandia Canyon comparing 2016 and 2017 survey data B-8

Figure B-4.1-2 Lower end of reach S-2 highlighting position of thalweg in relation to alluvial fan extent B-9

Figure B-4.2-1 Plan view of plunge pool in Sandia Canyon reach S-2..... B-10

Figure B-4.3-1 Upper portion of reach S-2 displaying 1 yr bank and thalweg comparisons, path of overbank flows, and erosion pin data B-11

Figure B-4.3-2 Map of reach S-2 highlighting overbank flow features in the northcentral portion of the reach B-12

Figure B-4.4-1 Map of reach S-2 highlighting two alluvial fans in the northcentral part of the reach ... B-13

Figure B-4.4-2 Map of reach S-2 highlighting net change documented at erosion pins in their respective groups..... B-14

Figure B-4.4-3 Map of reach S-2 highlighting alluvial fan extent and erosion pin data for locations on the southeastern side of the Sandia wetlands B-15

Tables

Table B-4.1-1 Thalweg Sinuosity B-17

Table B-4.2-1 Plunge Pool Area and Growth Assessment..... B-17

Attachments

Attachment B-1 2017 Photographs of Geomorphic Conditions in Sandia Canyon Reach S-2

Attachment B-2 2017 Geomorphic Changes in Sandia Canyon Reach S-2 Survey Data
(on CD included with this document)

B-1.0 INTRODUCTION

This report evaluates geomorphic changes that occurred from October 2016 to November 2017 in reach S-2, above the Sandia Canyon grade-control structure (GCS) within the Los Alamos National Laboratory (LANL or the Laboratory). Geomorphic change was evaluated using post-monsoon ground-based surveys of the thalweg, channel banks, plunge pool, and alluvial fans. Results from those surveys are presented in this appendix, representing change over the 2017 monsoon season. Figure B-1.0-1 shows site locations discussed in this appendix. Attachment B-1 contains photographs of areas of erosion and deposition in Sandia Canyon reach S-2.

B-2.0 HYDROLOGIC EVENTS DURING THE 2017 MONSOON SEASON

Discharge in 2017 was similar to the 2016 discharge at all gage stations, being near or well below the mean for the 10-yr period of record. There were 7 sample-triggering storm events in 2017, with the largest runoff-producing event occurring following heavy rains on July 26, 2017 (see Section 2.1 and Table 2.1-3 in the main text for more details).

B-3.0 GROUND-BASED SURVEY METHODS OF THE SANDIA WETLAND

The 2017 post-monsoon channel thalweg, channel banks, plunge pool, and downslope extent of the southern alluvial fan were surveyed using ground-based methods to document change. These features were surveyed using real-time kinematic differentially corrected GPS surveying equipment. The alluvial fans on the northern edge of the wetland were also monitored via erosion pins during the 2017 monsoon season.

As in 2016, the 2017 longitudinal channel thalweg profile was surveyed for the entire study reach (Figure B-1.0-1). While the thalweg location is challenging to define in some areas (e.g., dense cattail vegetation) of the reach because of channel branching, a best-estimate location was determined for comparison with the 2016 data. For each thalweg survey point, the distance along the thalweg was calculated as the straight-line distance between the plunge pool and that point. This distance is referred to as the “canyon distance.” Data tables of thalweg survey points and distances and ArcGIS shape files are included in Attachment B-2. The 2017 thalweg gradient and map-view location were compared with 2016 data for all reach sections where data were available.

Channel banks were initially surveyed in 2015 to document baseline conditions. Channel bank surveys were repeated in 2017 at the western end of reach S-2 as well as the eastern end that drains the wetland area. In the central portion of the reach, where flow is diffused and there is standing water, there are no prominent channel banks. Data tables of channel survey points and ArcGIS shape files are included in Attachment B-2.

The plunge pool perimeter was surveyed at the lateral extent of the ponded area. The 2017 results are compared with the 2016 survey of the same area. Data tables of plunge pool survey points and ArcGIS shape files are included in Attachment B-2.

Three alluvial fan deposits on the north side and one on the south side of reach S-2 were monitored in 2017. Alluvial fans on the northern edge of the wetland were monitored using erosion pins during the 2017 monsoon season. The lateral extent of the southern alluvial fan deposit was surveyed for comparison with the 2016 survey of the same area. Flow generally occurs on the fans within 2–4-inch-wide and 2–3-inch-deep channels. Erosion pins are placed near or on these channels to track the places most likely to experience geomorphic changes (Photo B1-1, Attachment B-1). Erosion pins record episodic erosion and deposition. Since the pins are monitored on a quarterly basis all changes are

inferred to be the result of the cumulative effect of the rainfall events during a given quarter. Erosion pins are installed on a given feature and then the height from the top of the pin to the ground is measured. A washer is placed on the pin and the height is then measured from the washer to the pin top. During a monitoring period, the washer cannot physically move upwards, therefore it serves as the overall estimation of erosion or deposition at that location. An increase in the height of the washer from the pin top since the last measurement is interpreted as erosion occurring at that location. If it is observed that the washer is covered, the distance from the ground to the pin top has decreased and the distance between the ground and the pin top is interpreted as the amount of deposition that has occurred at that location.

B-4.0 RESULTS AND DISCUSSION

Reach S-2 underwent minor geomorphologic changes during the 2017 monsoon season. Repeat GPS surveys and erosion pin data support the conclusion that features within the reach have remained stable since they were last surveyed in the fall of 2016. The monsoon season of 2017, being generally average to below average in its intensity of rainfalls, has resulted in minor annual changes to morphology of monitored features and caused no significant geomorphic changes within Reach S-2.

B-4.1 Thalweg Characterization

In 2017, the channel thalweg profile was again surveyed as a continuous feature from the plunge pool to gage station E123. In the central cattail zone, the thalweg remains challenging to identify as a distinct channel because of diffuse flow and channel branching within the active wetland. Where a main channel was not distinct, the thalweg of the most established channel branch was surveyed.

The channel thalweg profile (Figure B-4.1-1) compares 2016 and 2017 post-monsoon survey data displayed with a vertical exaggeration (VE) of 13 times. Overall, the 2017 thalweg profile closely matched the 2016 thalweg profile, indicating continued stability of the reach.

Between 2016 and 2017, minor lateral changes occurred in the thalweg position over the entire reach (Figure B-1.0-1) with sinuosity of the thalweg path increasing by 7.8% since last year (Table 4.1-1). In the western area, where banks are present, the continued establishment of cattails below a steep cut bank has caused the thalweg to meander approximately 7 ft to the north creating a slight departure from the 2015 and 2016 paths.

Repeat surveys of the small nick point upstream of alluvial well transect No. 4 have demonstrated stability of that feature since 2015 (Figure B-4.1-2; LANL 2016, 601432).

B-4.2 Plunge Pool Characterization

The shape and areal extent of the plunge pool did not significantly change during the 2017 monsoon season (Figures B-1.0-1 and B-4.2-1). The 2017 perimeter survey generally shows slight variations compared to 2016. One notable change is the deposition of sediments derived from storm runoff immediately south of the culvert into the plunge pool. The input of sandy alluvium to this location has allowed a small population of cattails located there to flourish and double in size from 2016 to 2017 (see Appendix C Figure C-3.0-1). This deposit has not affected the overall area of the plunge pool in 2017, as total area increased at a stable rate, similar to that of 2015 and 2016 (see Table B 4.2-1).

B-4.3 Channel Bank Characterization

Stream banks below the plunge pool area show minimal changes between surveys (Figures B-1.0-1 and B-4.3-1). Slight differences between the bank surveys are attributed to different interpretations of what constituted the most important breaks in slope between surveys and do not reflect significant bank erosion or deposition, as confirmed by field observations (e.g. Photo B1-2, Attachment B1).

Overbank flow features were observed and baseline surveys were established in reach S-2. In September of 2017 flow in reach S-2 exceeded 50 cfs resulting in alternate flow paths within reach S-2.

An abandoned channel between the northern alluvial fans and the wetland was reoccupied with overbank flow during the September 2017 storm event (Figure B-4.3-2 and Photo B1-3 in Attachment B1). Small deposits of gravel have formed on the margin of the cattails in response to the flow re-entering the main wetland (Photo B1-4 in Attachment B1). Other occurrences of overbank flow took place in the upper portion of reach S-2 at and just upstream of alluvial well transect No. 1 (Figure B-4.3-1). One occurrence highlights the location of a floodstage channel surface where erosion pin EP04-MY16 detected approximately 0.11 feet of net erosion in 2017 due to the reoccupation of this side channel (Photo B1-5 in Attachment B1). Overbank flow also took place immediately downstream of the snag on the south side of the main channel (Photo B1-6 in Attachment B1) and flowed directly toward the largest population of cattails in the meadow of redtop grass south of the channel, presumably contributing to the expansion of the cattail population in this area (See Appendix C Figure C-3.1-1).

B-4.4 Alluvial Fan Characterization

Alluvial fans within reach S-2 were monitored throughout 2017 for geomorphic changes. Visual inspection and erosion pin data demonstrate that no significant changes occurred on the alluvial fans within reach S-2 during the monsoon season. Changes in erosion pin height are presented and discussed in this section. These measurements were used to assess the character and magnitude of geomorphic change that may occur on the alluvial fans in reach S-2.

Changes in erosion pin height of the northern alluvial fans are presented in Figures B-4.3-1 and B-4.4-1. Results from 2016-Quarter 3 through 2018-Quarter 1 are presented in graphs within Figures B-4.3-1, B-4.4-1, B-4.4-2, and B-4.4-3. Data from erosion pins in reach S-2 has been tabulated to show the magnitude of cumulative deposition and erosion for each quarter (e.g.: +0.07ft of deposition, -0.01 ft of erosion, and a resultant net deposition of 0.06 ft). Figure B-4.4-2 displays the trend in net change of all pins located in reach S-2.

Measurements from erosion pins recorded during 2017 indicate that the fans on the north side of the wetland (Figures B-4.3-1 and B-4.4-1) experienced punctuated, runoff induced change but remained relatively stable throughout the 2017 monsoon season. Alluvial fans on the northern side of reach S-2 continued to revegetate during 2017. Erosion pins indicate that the fans did not significantly aggrade during the 2017 monsoon season or increase in lateral extent.

On the south side, alluvial fan sediments continued to advance eastward into the wetland due to contribution from a side channel that is spatially coincident with the edge of the central cattail zone (Figure B-4.4-3). The fan on the south side of reach S-2 that had previously impacted cattail growth (LANL 2016, 601432) has advanced approximately 4 ft farther north into the wetland and another 15 ft east but has not resulted in the destruction of any cattails. Based on the vegetation perimeter mapping presented in Appendix C, the cattails of the central cattail zone began revegetating the 2015 sand/gravel lobe (see Figure C-3.0-1 in Appendix C). The lobe of sediment on the downstream (easternmost) end of the fan has extended approximately 15 ft past the previous extent mapped in 2016, and is generally coincident with the margin of the wetland boundary (Figure B-4.4-3).

B-5.0 CONCLUSIONS AND RECOMMENDATIONS

Repeat GPS surveys in conjunction with field observations indicate that between 2016 and 2017 no significant geomorphic change occurred in reach S-2.

Repeat surveys of the channel thalweg indicate few, minor changes (largely in map-view position) between the 2016 and 2017 surveys and overall suggest thalweg stability. GPS surveying also indicates that the plunge pool also remained stable from 2016 to 2017. Channel bank surveys were conducted at the western- and easternmost parts of the study area (the only areas in the reach with prominent channel banks). Channel surveys below the plunge pool area and below gage E123 show minimal change between surveys. Based on 2017 erosion pin monitoring, the downslope extent of alluvial fan deposits on the northern side of the reach below the former Los Alamos County landfill has remained stable. On the south side of the canyon, a side channel entering reach S-2 has continued to redistribute sandy gravel within the alluvial fan and into the wetland. The continued advancement of the alluvial sediments in 2017 has not resulted in any significant vegetation (cattail) loss.

In 2018, geomorphic change will continue to be evaluated using post-monsoon ground-based surveys of the thalweg and monitoring of established erosion pins. If storm water peak discharge at E123 is greater than 50 cfs, a visual inspection of the wetland will occur to document qualitative geomorphic changes. If the visual observations or the thalweg survey indicate geomorphic changes that are not consistent with last year's observation, a LiDAR aerial flyover will be planned for the fall of 2018; and, the processed data will be field-verified to ensure that geomorphic changes shown in a threshold DEM of difference comparison represent actual geomorphic changes.

B-6.0 REFERENCES AND MAP DATA SOURCES

B-6.1 References

The following reference list includes documents cited in this appendix. Parenthetical information following each reference provides the author(s), publication date, and ERID or ESHID. This information is also included in text citations. ERIDs were assigned by the Associate Directorate for Environmental Management's (ADEM's) Records Processing Facility (IDs through 599999), and ESHIDs are assigned by the Environment, Safety, and Health Directorate (IDs 600000 and above). IDs are used to locate documents in the Laboratory's Electronic Document Management System and in the Master Reference Set. The NMED Hazardous Waste Bureau and ADEM maintain copies of the Master Reference Set. The set ensures that NMED has the references to review documents. The set is updated when new references are cited in documents.

LANL (Los Alamos National Laboratory), April 2016. "2015 Sandia Wetland Performance Report," Los Alamos National Laboratory document LA-UR-16-22618, Los Alamos, New Mexico. (LANL 2016, 601432)

B-6.2 Map Data Sources

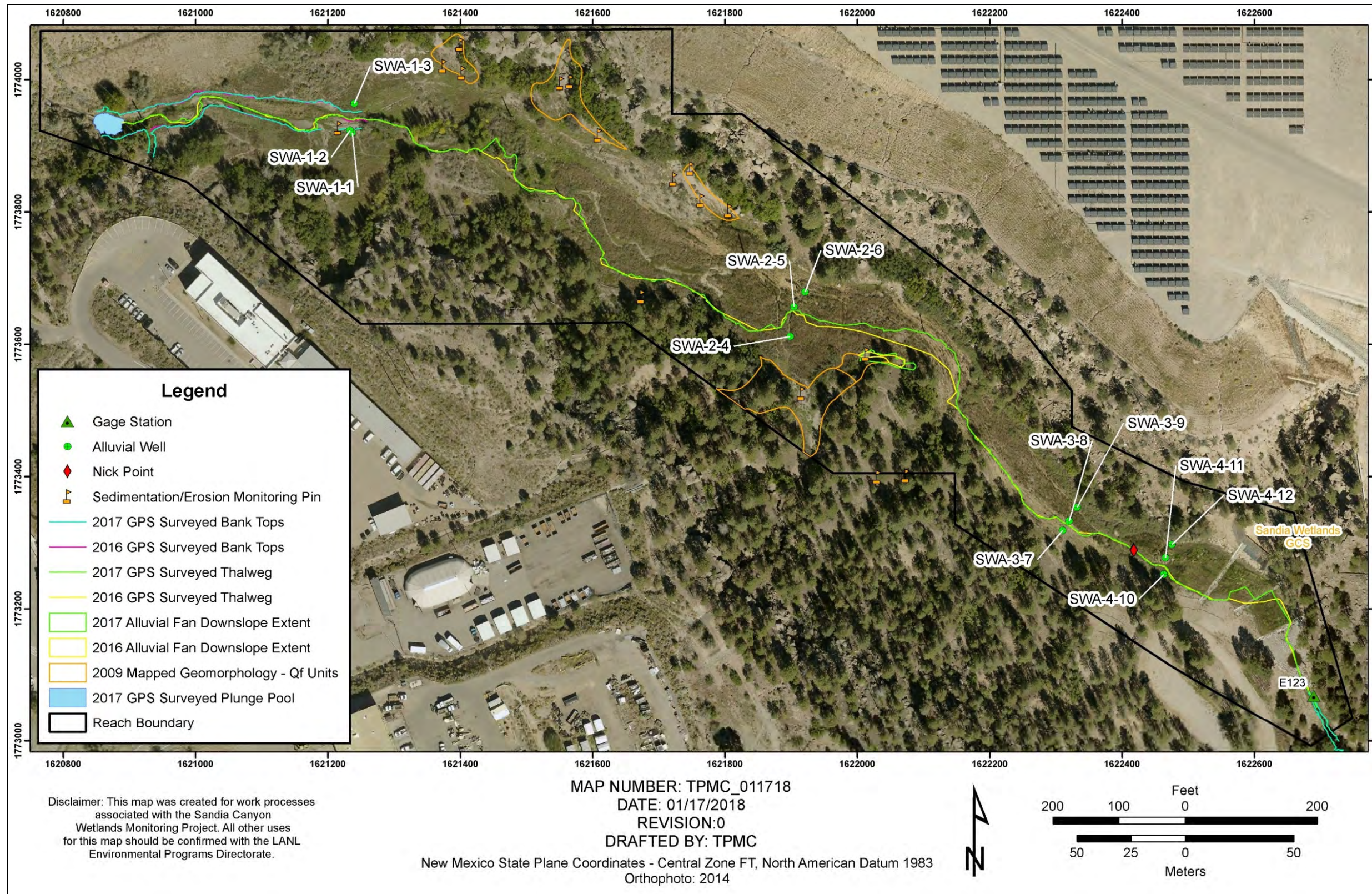
The following list provides data sources for maps included in this appendix.

Gaging stations; Los Alamos National Laboratory, Waste and Environmental Services Division; 1:2,500; March 19, 2011.

LANL area orthophoto; Los Alamos National Laboratory, 2014.

Geomorphic Reach Boundary, Los Alamos National Laboratory, Earth and Environmental Science, GISLab, 2009.

Geomorphology Units; Los Alamos National Laboratory, Earth and Environmental Sciences, GISLab, 2009.



Note: Qf (alluvial fan) consists of relatively young sands, gravel, and cobbles made up of Bandelier Tuff and pumice fragments and quartzite gravels.

Figure B-1.0-1 Sandia Canyon reach S-2 orthophoto with gage station E123, alluvial wells, and survey locations mentioned in report, including channel banks, thalweg, alluvial fans, and the plunge pool

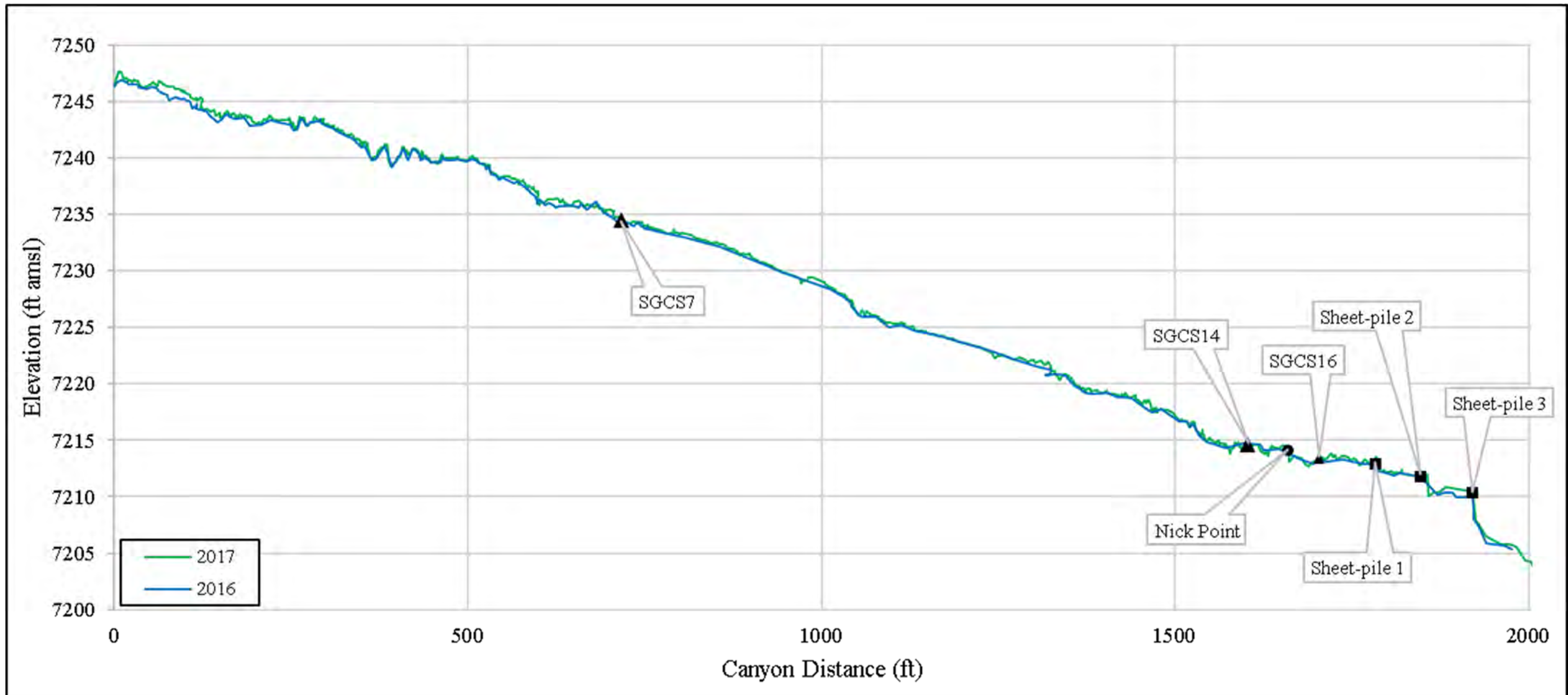


Figure B-4.1-1 Thalweg profile in Sandia Canyon comparing 2016 and 2017 survey data

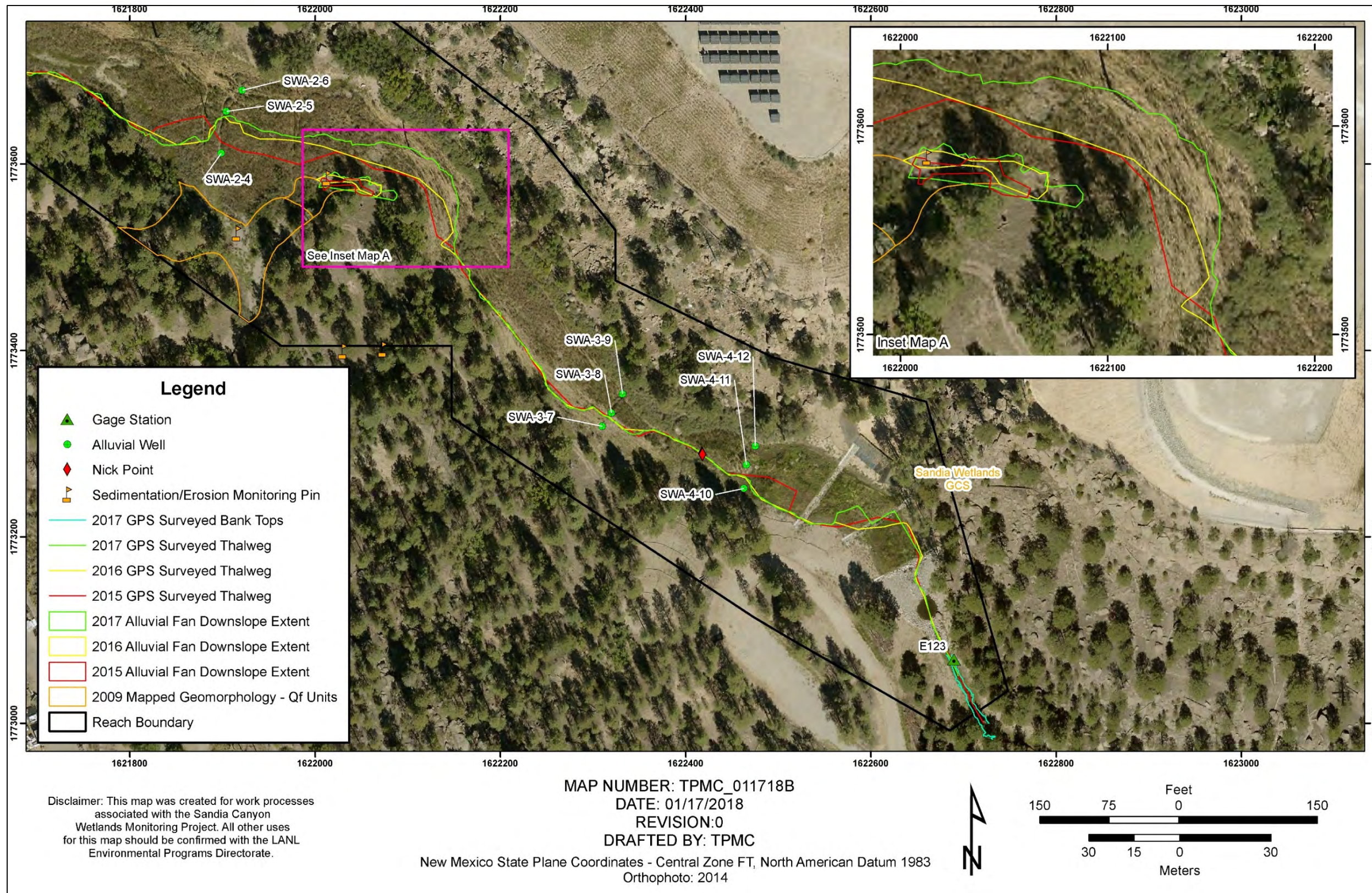


Figure B-4.1-2 Lower end of reach S-2 highlighting position of thalweg in relation to alluvial fan extent

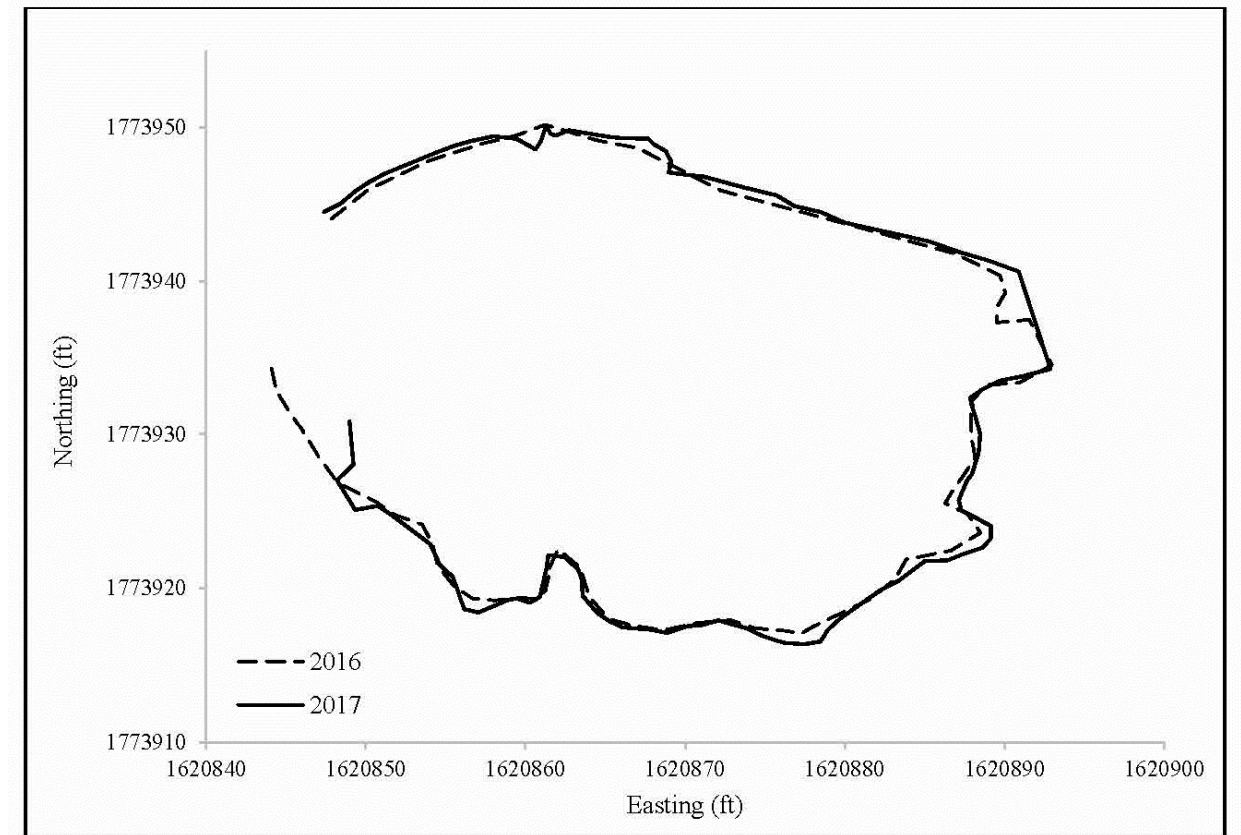


Figure B-4.2-1 Plan view of plunge pool in Sandia Canyon reach S-2

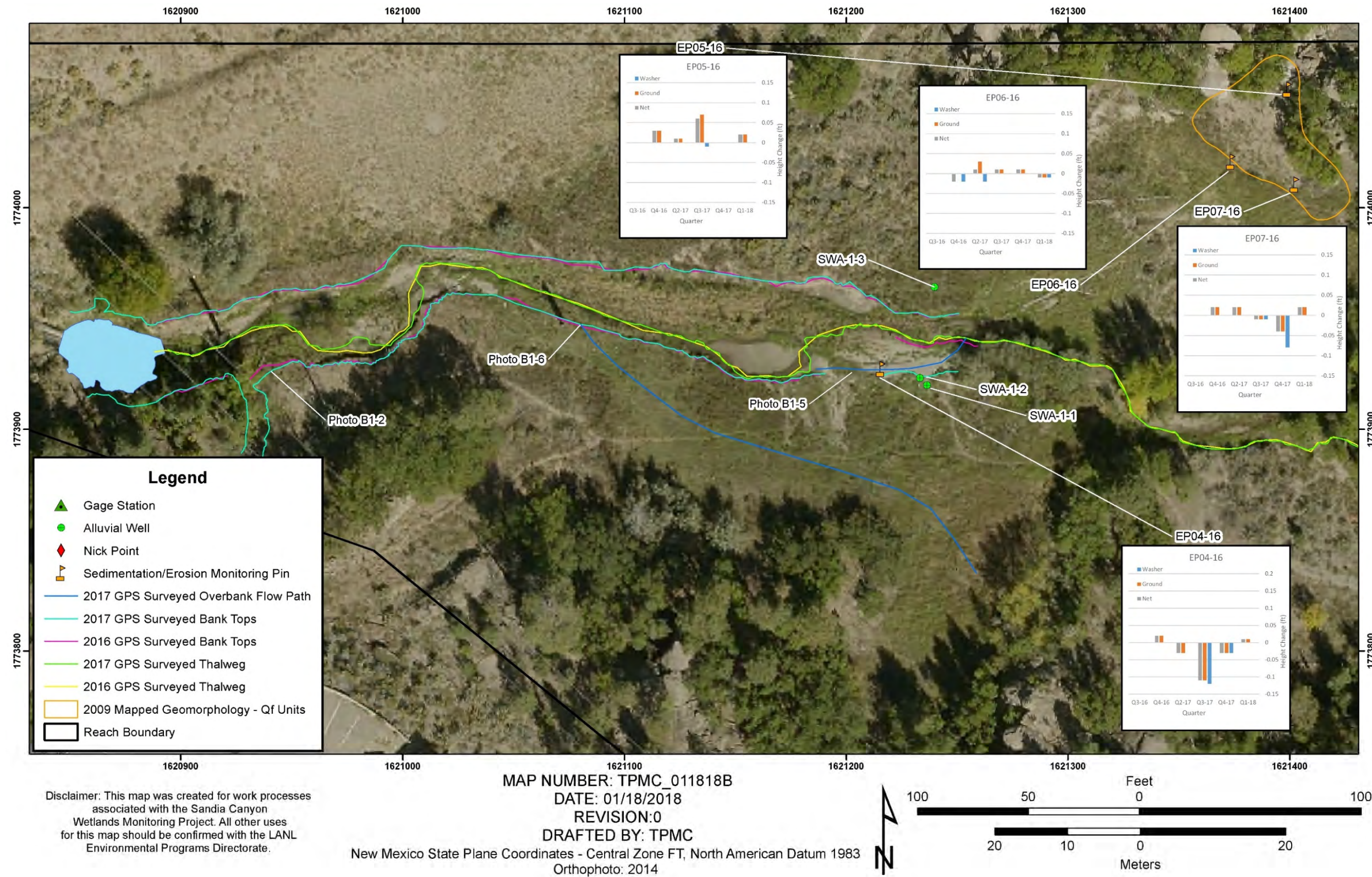


Figure B-4.3-1 Upper portion of reach S-2 displaying 1 yr bank and thalweg comparisons, path of overbank flows, and erosion pin data

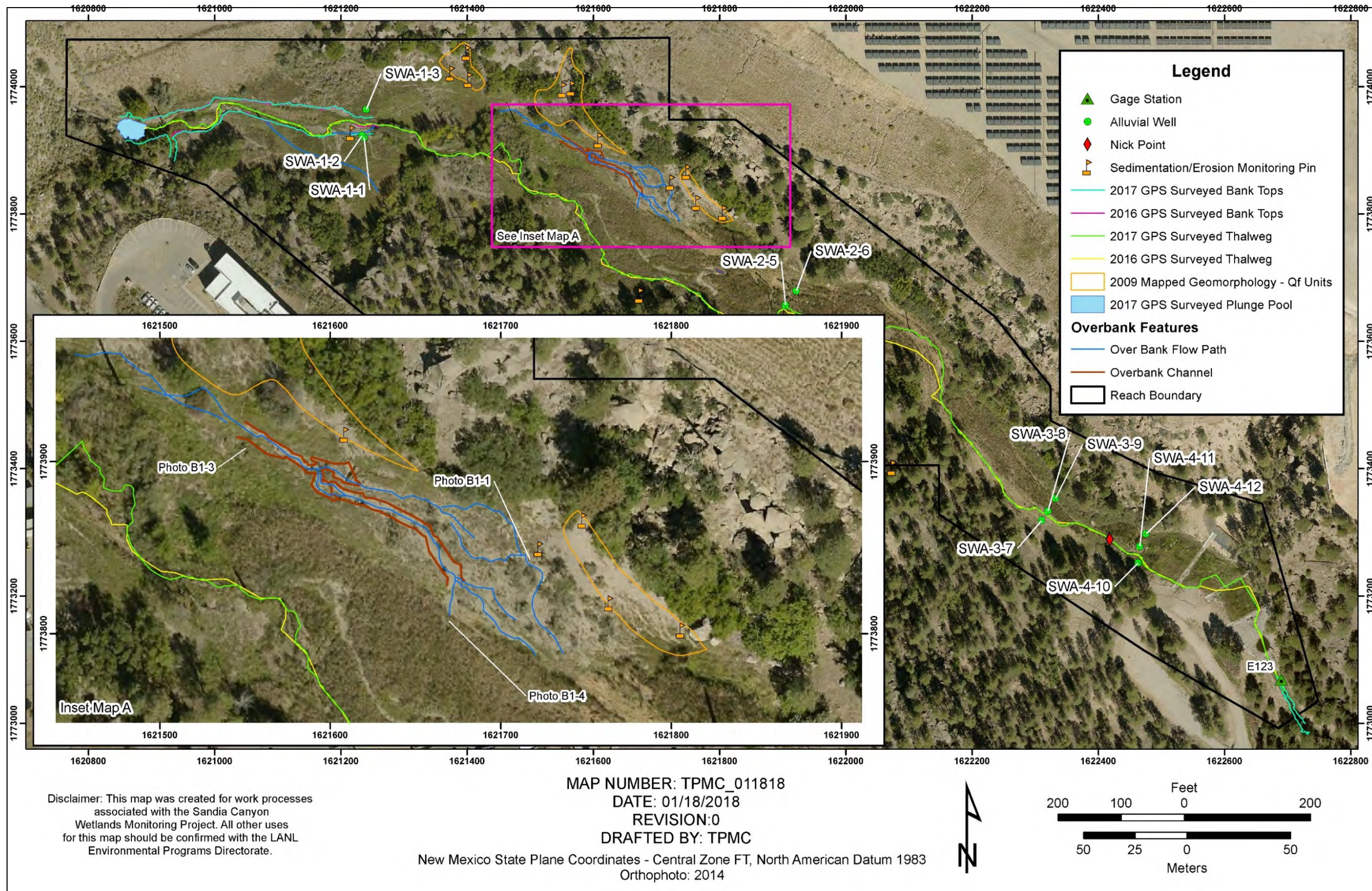


Figure B-4.3-2 Map of reach S-2 highlighting overbank flow features in the northcentral portion of the reach

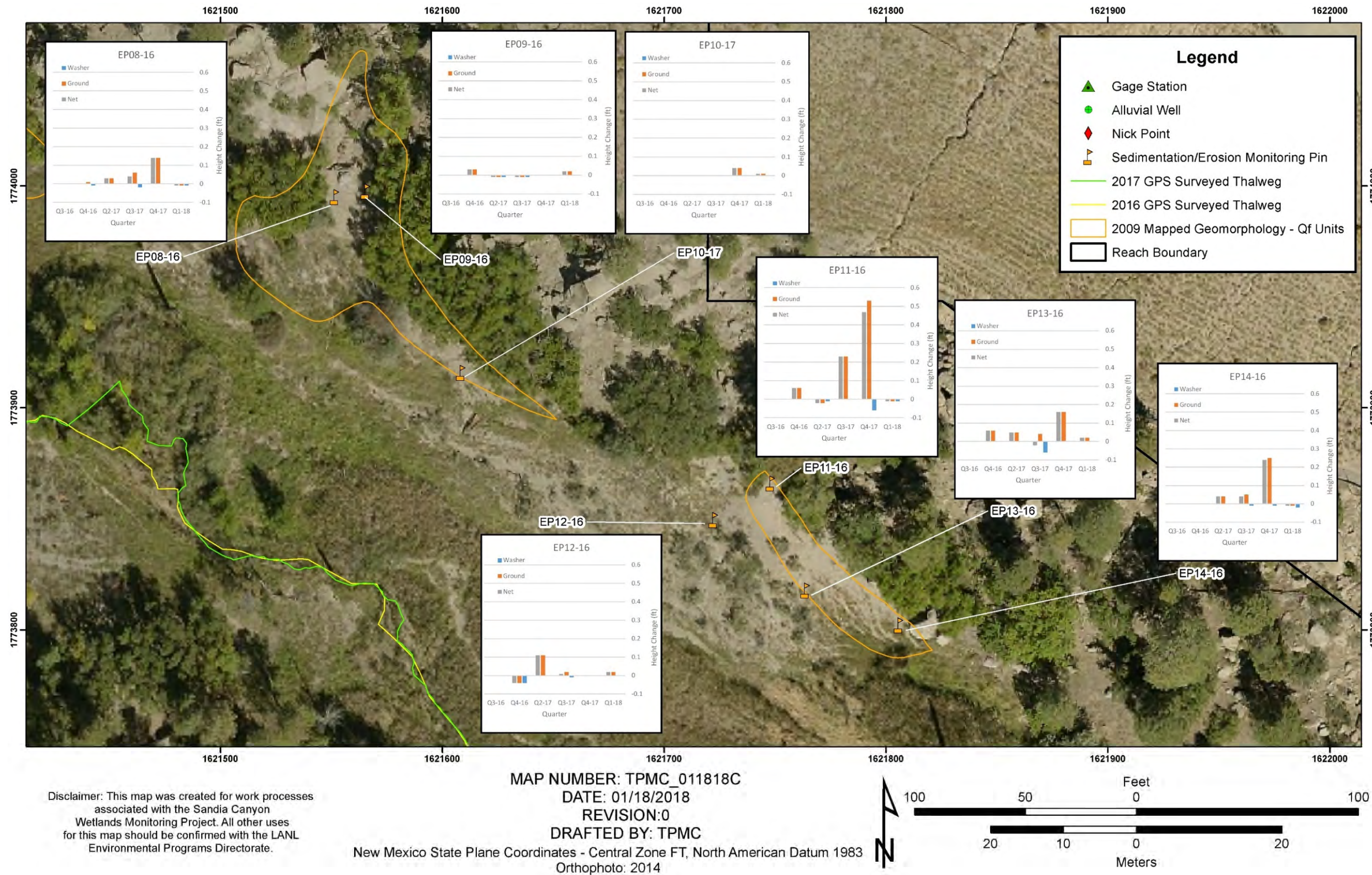


Figure B-4.4-1 Map of reach S-2 highlighting two alluvial fans in the northcentral part of the reach

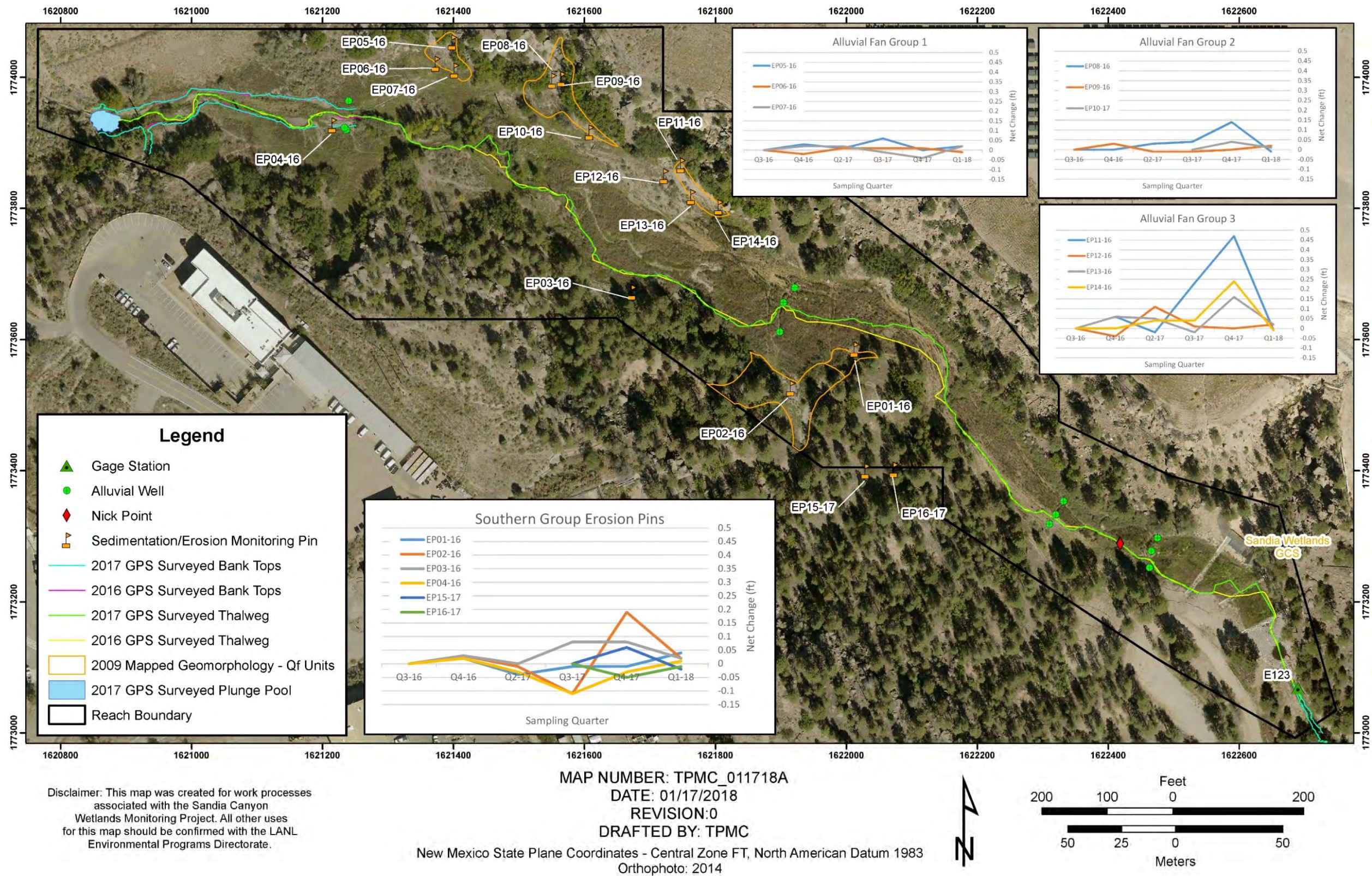


Figure B-4.4-2 Map of reach S-2 highlighting net change documented at erosion pins in their respective groups

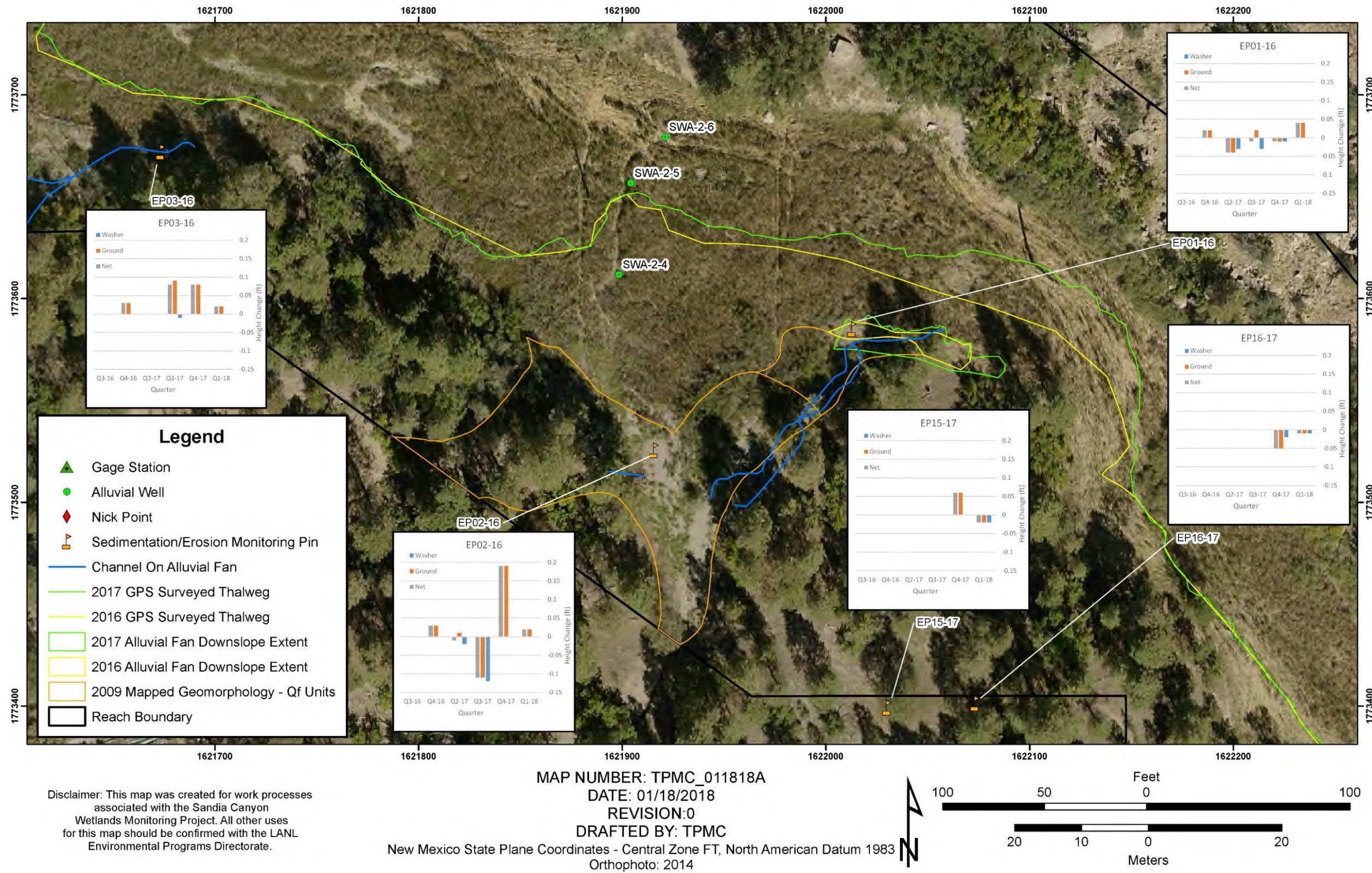


Figure B-4.4-3 Map of reach S-2 highlighting alluvial fan extent and erosion pin data for locations on the southeastern side of the Sandia wetlands

**Table B-4.1-1
Thalweg Sinuosity**

Year	Length (sq ft)	Sinuosity	% Change in Sinuosity
2017	2538.86*	1.27	7.8
2016	2355.94	1.18	-4.6
2015	2468.67	1.23	n/a

*Straight line distance from plunge pool to gage station E123 is 2000.26ft

**Table B-4.2-1
Plunge Pool Area and Growth Assessment**

Year	Area (sq ft)	Area (sq m)	% Change in Area From Previous Year	Rate of Change (sq. ft./ yr)
2017	1124.2	104.4	1.9	20.81
2016	1103.4	102.5	2.4	25.58
2015	1077.9	100.1	3.4	35.35
2014	1042.5	96.9	18.5	162.98
2013*	879.5	81.7	na	na

*2013 is baseline survey year for plunge pool perimeter mapping

Attachment B1

*2017 Photographs of Geomorphic Conditions
in Sandia Canyon Reach S-2*



Photo B1-1 Example of erosion pin placement in reach S-2. February 2018 photo looking to north.



Photo B1-2 Example of bank survey interpretation of break in slope. No evidence of erosion based on field check. February 2017 photo looking northeast.



Photo B1-3 Overbank flow in previously abandoned channel between northern alluvial fans and wetland. February 2017 photo looking east.



Photo B1-4 Deposition of gravels at eastern termination of side channel (Photo B1-3) into wetland. February 2017 photo looking southeast.



Photo B1-5 Example of 2017 overbank flow into a side channel. Erosion pin (orange cap) located in center of picture detected 0.25 in of net change (erosion) February 2018 photo looking east parallel to side channel flow.



Photo B1-6 Debris piles as evidence of overbank flow that has continued to provide water to the cattail islands in the redtop grass meadow south of the wetland (See Appendix C Figure 3.1-1). February 2018 photo looking southeast parallel to side channel flow toward cattail island populations.

Attachment B-2

*2017 Geomorphic Changes in
Sandia Canyon Reach S-2 Survey Data
(on CD included with this document)*

Appendix C

*2017 Wetland Vegetation Monitoring
in Sandia Canyon Reach S-2*

CONTENTS

C-1.0 INTRODUCTION C-1

C-2.0 VEGETATION MONITORING METHODS C-1

 C-2.1 Line-Intercept Method..... C-2

 C-2.1-1 Plant Species Indicators..... C-2

 C-2.1-2 Vegetative Canopy Cover and Species Composition C-2

 C-2.1-3 Obligate Zone Delineation and Characterization C-3

 C-2.2 Wetland Vegetation Perimeter Mapping..... C-3

C-3.0 MONITORING RESULTS AND DISCUSSION C-4

 C-3.1 Comprehensive Species List..... C-4

 C-3.2 Vegetative Canopy Cover and Species Composition..... C-4

 C-3.3 Obligate Zone Delineation and Characterization..... C-5

 C-3.4 Wetland Vegetation Area..... C-6

C-4.0 CONCLUSIONS AND RECOMMENDATIONS C-8

C-5.0 REFERENCES AND MAP DATA SOURCES C-9

 C-5.1 References C-9

 C-5.2 Map Data Sources C-10

Figures

Figure C-1.0-1 Locations of cross-sections, piezometers, sheet piles, and thalweg profiles in Sandia Canyon reach S-2 C-11

Figure C-3.0-1 2017 and 2016 vegetation perimeter mapping comparison results at Sandia Canyon reach S-2 C-12

Figure C-3.1-1 Upper wetland area highlighting cattail populations C-13

Figure C-3.3-1 Spatial distribution of obligate species on transects SGCS-3a and SGCS-3b in Sandia Canyon Reach S-2 C-14

Figure C-3.3-2 Spatial distribution of obligate species on transects SGCS-4 and SGCS-5 in Sandia Canyon Reach S-2 C-15

Figure C-3.3-3 Spatial distribution of obligate species on transects SGCS-7 and SGCS-9 in Sandia Canyon Reach S-2 C-16

Figure C-3.3-4 Spatial distribution of obligate species on transects SGCS-11 and SGCS-12 in Sandia Canyon Reach S-2 C-17

Figure C-3.3-5 Spatial distribution of obligate species on transects SGCS-14 and SGCS-16 in Sandia Canyon Reach S-2 C-18

Figure C-3.3-6 Spatial distribution of obligate species on transects SGCS-19, SGCS-20, and SGCS-21 in Sandia Canyon Reach S-2 C-19

Figure C-3.4-1 Three-year (2014–2017) comparison of wetland vegetation perimeters C-20

Tables

Table C-2.1-1 Wetland Plant Species Indicator Definitions C-21

Table C-3.1-1 2017 Comprehensive Species List C-21

Table C-3.1-2 2015 to 2017 Species Composition Percentage by Life Form C-23

Table C-3.1-3 2015 to 2017 Species Composition Percentage by Indicator Status..... C-24

Table C-3.2-1 2015 to 2017 Percent Canopy Cover and Percent Species Composition for Each
Transect (Entire Length) C-24

Table C-3.2-2 2015 to 2017 Ranked Order of Species Composition Summary C-25

Table C-3.3-1 2015 to 2017 Vegetation Survey Transect Length and Percentage of Obligate
Zone C-27

Table C-3.3-2 2015 to 2017 Comparison of Canopy Cover to the Vegetative and Nonliving
Presence along Transects in Obligate and Non-Obligate Zones C-28

Table C-3.4-1 2017 Wetland Vegetation Zone Summary C-29

Attachments

Attachment C-1 2016 and 2017 Photographs of Sandia Wetland Vegetation Monitoring

Attachment C-2 2017 Vegetation Survey Data (on CD included with this document)

Attachment C-3 2017 Rank Order of Percent Canopy Cover and Individual Species Composition
Summary Tables (on CD included with this document)

C-1.0 INTRODUCTION

This appendix evaluates vegetation changes that occurred in Sandia Canyon reach S-2 within Los Alamos National Laboratory (LANL or the Laboratory). The vegetation survey data collected in 2017 documents vegetation conditions in reach S-2 for the purpose of annual vegetation monitoring. This appendix compares the previous 2015 transect and 2016 survey data with subsequent survey data obtained in fall 2017 to satisfy the annual vegetation monitoring requirements (LANL 2017, 602341).

Vegetation surveys are performed in detail because the vitality of wetland species is a good indicator of redox and saturation conditions over a spatial distribution that cannot be easily measured by other point data techniques such as alluvial well/piezometer monitoring. Specifically, the presence of obligate wetland vegetation implies persistent saturation. Persistent saturation and contribution of organic matter from wetland vegetation are highly favorable to producing and maintaining reducing conditions. This appendix evaluates data from thirteen transects in reach S-2 in order to define the species type, density, and indicator status (probability the plant occurs in the wetland) of the vegetation present. Perimeter mapping of wetland vegetation is also performed and is supplemented with annual photographic comparisons to help evaluate the extent of obligate wetland vegetation and the establishment of overbank vegetation and their ability to compete for any remaining bare ground. Figure C-1.0-1 shows the geographic locations of transects discussed in this appendix while Figure C-3.0-1 shows the perimeter extent of mapped wetland species. Attachment C-1 presents photographs taken in 2016 and 2017 that compare vegetation conditions in Sandia Canyon reach S-2. Attachment C-2 presents vegetation survey data collected in 2017. Attachment C-3 presents the rank order of 2017 percent canopy cover and individual species composition summary tables for the 2017 surveys.

C-2.0 VEGETATION MONITORING METHODS

The line-intercept method (Coulloudon et al. 1999, 600337) and vegetation perimeter mapping were used for the 2017 vegetation survey in reach S-2 of Sandia Canyon. A total of 13 transects (Figure C-1.0-1) were surveyed in mid- to-late August to capture vegetation at maximum growth. The vegetation survey transect locations were selected to capture representative sections of the Sandia wetland and the engineered GCS areas of revegetation. Ten transects were surveyed to compare with baseline vegetation surveys performed in 2014 and again in 2015. Transects SGCS-3A, SGCS-3B, and SGCS-5, were conducted as baseline vegetation surveys in 2015 and were repeated in 2017. Transects SGCS-3A, SGCS-3B, SGCS-4, SGCS-5, and SGCS-7 are located in the western part of reach S-2 (Figure C-1.0-1). Transects SGCS-9, SGCS-11, and SGCS-12 are centrally located and were established to monitor encroachment of willows and sediment into the central cattail zone. The five transects in the eastern region of reach S-2 focus on the GCS: SGCS-14 and SGCS-16 are located above the GCS; transects SGCS-19, SGCS-20, and SGCS-21 are located upstream of Sheet Piles 1, 2, and 3, respectively, and are used to monitor revegetation efforts following installation of the GCS (LANL 2014, 600083). The resulting data set from the 2017 line-intercept transect survey provides a comprehensive species list, quantifies vegetative canopy cover and species composition along transects, and allows for the delineation and characterization of the wetland area. Vegetation perimeter mapping documents the spatial distribution and areal extent of targeted wetland species.

C-2.1 Line-Intercept Method

Vegetation canopy cover and species composition data were collected using the line-intercept method (Coulloudon et al. 1999, 600337). A species intercept occurs when a species crosses the vertical plane containing the tape measure (e.g. Photos C-1-1 and C-1-2 in Attachment C-1). The intercepted tape distances of all plant species along the established transect are recorded as well as the occurrence of nonliving categories such as logs, rocks, bare ground, and open water (channels), (see Attachment C-2). Nonliving objects are recorded only if the intercepted area along the transect is devoid of vegetation; that is, the occurrence of bare ground or logs is not recorded if vegetation canopy is also present. Canopy cover from different and overlapping species is accounted for by recording the tape intercept distances for both species. Overlapping species along a transect are common and any interception with the tape distance must be recorded (e.g. Photo C-1-2 in Attachment C-1). Species not identified in the field are sampled for later identification using taxonomic keys. Raw survey species identification and tape distance data are included electronically as Attachment C-2 (on CD included with this document).

C-2.1-1 Plant Species Indicators

The 'Wetland Plant Species Indicator' status provides the probability that a species occurs within a wetland ecosystem versus outside a wetland ecosystem. For this report, this status was used to delineate wetland zones from zones outside the wetland in the S-2 reach of Sandia Canyon. For instance, a cattail (*Typha latifolia*), an abundant species in the study area is an obligate wetland species (OBL) that is expected to occur "almost always (estimated probability of >99%) in wetlands and rarely (estimated probability of <1%) in non-wetlands" (Reed 1988, 600338). Therefore, this species helps to delineate the boundary of the wetland. Other relevant indicator types for this report are facultative wetland plants (FACW), facultative plants (FAC), facultative upland plants (FACU), and obligate upland plants (UPL). Complete definitions for these indicator types can be found in Table C-2.1-1 and were assigned to each species found in the study area according to Reed (1988, 600338). Any species newly identified in 2017 that is not listed in Reed, 1988 has been categorized according to an updated version of the national wetland plant list (USACE 2016, 602997). It is important to note that not all species identified in the 2017 survey were updated to the 2016 standards for ease of comparing the 2015 report data to the 2017 data.

Plants that do not have an indicator status (NI) for wetland systems are usually species that are never or very rarely found in wetland systems and, therefore, are not given a wetland indicator status. Thus, throughout this report, "obligate," when used alone, refers to obligate wetland plants but not to obligate upland plants.

C-2.1-2 Vegetative Canopy Cover and Species Composition

For an individual species, canopy cover percentage is calculated by summing all intercept lengths over which the species is present and expressing this total as a proportion of tape length (Coulloudon et al. 1999, 600337). The vegetative canopy cover is the sum of individual species canopy cover percentages for all living categories and can be greater than 100% because of overlap of different plant species. For example, consider a 100 ft long transect containing only two species. Species A covers 50 ft and species B covers 70 ft (with a 20-ft overlap). Species A has 50% canopy cover $[(50 \text{ ft}/100 \text{ ft}) \times 100]$, species B has 70% canopy cover $[(70 \text{ ft}/100 \text{ ft}) \times 100]$, and the vegetative canopy cover for the transect as a whole is 120% (50% + 70%). A vegetative canopy cover greater than 100% is common where low vegetation occurs under a higher, over-story canopy.

Species composition is determined by dividing the species intercept length by the total intercept length of all species and non-living categories (Coulloudon et al. 1999, 600337). This ratio is reported as a percentage. The sum of all individual species composition and nonliving composition percentages will always be 100%. In the above example, the total intercept length is 120 ft (100 ft (transect length) + 20 ft (overlap)), therefore the species composition of species A is 42% $[(50 \text{ ft}/120 \text{ ft}) * 100]$ and the species composition of species B is 58% $[(70 \text{ ft}/120 \text{ ft}) * 100]$.

C-2.1-3 Obligate Zone Delineation and Characterization

For the reporting purpose of this appendix, the wetland zone, also referred to as the obligate zone, is defined as the area bound by obligate species (OBL). Therefore, the classification of obligate and non-obligate zones define the geographic extent of the wetland as it relates to the occurrence of specific species. The differentiation between the obligate and non-obligate zones allows analysis of vegetation as related to the occurrence in the wetland. Using line-intercept transect data, the obligate zone is designated to be the section of each transect between the first and last identified obligate species. The non-obligate zone is the area bordering the obligate zone and is usually topographically higher than the wetland zone where saturation is less likely to occur. While both zones can contain non-obligate (FACW, FAC, FACU, UPL, and NI) species, only the obligate zone can contain obligate species.

In this appendix, three metrics are reported to characterize the obligate zone. The first metric is the percentage of transect in the obligate zone, calculated by dividing the length of the obligate zone by the total transect length and then converting the quotient to a percentage. The second metric is the percentage of obligate zone with obligate occurrence, which is the vertical projection of obligate presence within the obligate zone expressed as a percentage. This metric is calculated by first determining the sections of the line within the obligate zone that are covered by any OBL species. This metric is based on the presence or absence of a species, so a section of transect is considered to be covered by OBL whether it contains one or many OBL species. The combined length of sections covered by OBL is divided by the obligate zone length and converted to a percentage. The third metric is the vegetative canopy cover in the obligate zone. This is calculated by summing the intercept lengths of all living categories (OBL and non-OBL), dividing by the length of the obligate zone, and then converting the quotient to a percentage.

For example, consider an obligate zone that extends from 20 ft to 70 ft on a 100-ft transect. OBL species A covers 20 ft to 50 ft, OBL species B covers 30 ft to 50 ft, FACW species C (a non-OBL species) covers 50 ft to 60 ft, and OBL species D covers 60 ft to 70 ft. The percent of transect in the obligate zone is 50% $[(70 \text{ ft} - 20 \text{ ft})/100 \text{ ft}] * 100$. The percent of the obligate zone with obligate occurrence is 80% $[(50 \text{ ft} - 20 \text{ ft}) + (70 \text{ ft} - 60 \text{ ft})/50 \text{ ft}] * 100$. The vegetation canopy cover in the obligate zone is 140% $[(30 \text{ ft} + 20 \text{ ft} + 10 \text{ ft} + 10 \text{ ft})/50 \text{ ft}] * 100$.

C-2.2 Wetland Vegetation Perimeter Mapping

Vegetation perimeter mapping was used to document the spatial distribution and areal extent of targeted wetland species (Figure C-1.0-1). Through the comparison of annual perimeter maps, success of wetland zones can be quantified based on the areal extent of specific wetland obligate zones. Vegetation perimeter mapping documents targeted cattails, coyote willows, and grade-control structure (GCS) wetland species. These targeted areas are defined by wetland obligate species, or species expected to occur almost always (estimated probability of >99%) in wetland systems. While these targeted species represent the majority of vegetation in their designated zone, many other species (both wetland obligate and non-obligate) species coexist within the same zones. In some instances (western end of reach S-2), targeted species were intermixed with other plant species and/or are discontinuous. When a gap in the

targeted species was encountered along the length of the reach, the survey perimeter (i.e., polygon) was closed. While most of these targeted species were of sufficient concentration to be easily identified as a mappable unit, no spatial density interpretations of the interior of the mapped perimeters are implied. Surveys were conducted using a differentially corrected global positioning system (DGPS). Raw survey data (x and y coordinates using the New Mexico State Plane coordinate system and elevations of all survey points) for surveyed perimeters are included electronically as Attachment C2 (on the CD included with this document).

Photograph points that were established at both the north and south ends of each vegetation transect (see Attachment C1 for photos) were used to qualitatively compare annual changes in vegetation. Vegetation growth (height) and species diversity can be analyzed qualitatively from these comparison photographs documenting changes from 2016 to 2017.

C-3.0 MONITORING RESULTS AND DISCUSSION

Annual measurements collected from a total of 13 transects during August 2017 yielded quantifiable data for comparison to the previous 2015 vegetation survey. Results show high overall species diversity and high abundance of wetland species. Wetland vegetation perimeter maps, obligate zone delineation and characterization, a comprehensive species list, and vegetative canopy cover and species composition are reported in the following sections and associated tables and figures. Figure C-3.0-1 shows the locations of the vegetation cross-sections and perimeter wetland vegetation mapping results. A representative photo of each transect as they appeared in calendar years 2016 and 2017 is presented in Attachment C-1, Photographs C1-1 through C1-13.

C-3.1 Comprehensive Species List

Table C-3.1-1 catalogs species symbol, scientific name, common name, indicator category, life form, and obligate/non-obligate classification for each of the 81 observed species, 14 of which were newly identified, for the 2017 survey compared with 72 species along the same 13 transects surveyed in 2015 (LANL 2014, 257590). A total of five species (yarrow, Northern reedgrass, indian rice grass, scarlet globemallow, and swamp verbena) present in the 2015 survey were absent along all transect lines in 2017; therefore, Table C-3.1-1 contains only those species identified along transects in 2017 and is not necessarily an exhaustive list of all species present in Sandia Canyon reach S-2.

Graminoid and forb life forms represent 34.6% and 44.4% of the overall 81 observed species, which is comparable to 2015 (Table C-3.1-2). The remaining vegetation consist of shrubs (1.1%), trees (8.6%) and vines (1.2%), and make up the majority of non-obligate species. Of the total 13 OBL indicator species there are: eight graminoid species, four forb species, and only one shrub species (Table C-3.1-2). The breakdown of wetland indicator status by percentage of total species is: 16.1% OBL indicators, 14.8% FACW indicators, 16% FAC indicators, 17.3% FACU indicators, 4.9% UPL indicators, and 30.9% have NI status (Table C-3.1-3).

C-3.2 Vegetative Canopy Cover and Species Composition

Attachment C-3 provides the rank order of percent canopy cover and composition for individual species or nonliving categories identified along each transect. Total vegetative canopy cover and composition as well as total nonliving cover and composition are also presented at the bottom of each table.

Three 2015 baseline surveys were repeated in the upstream part of the Sandia wetland at locations SGCS-3A, SGCS-3B, and SGCS-5. Vegetative species composition on these transects ranged from 97% to 99%, which is an overall increase from the baseline value range of 93-97% in 2015. Vegetative canopy cover on all three transects remains above 100%, with a trend of increasing vegetative canopy cover downstream in the mixed cattail/willow zone (Table C-3.2-1). This trend is probably the result of the stream becoming less channelized downstream, allowing for a wider obligate area and more multistory plant communities.

Repeat surveys of 10 other previously surveyed transects also show an increase in vegetative canopy cover from 2015 to 2017 with the exception of SGCS-11 and SGCS-14, which decreased by <3%. The increase in vegetative cover for all other transects ranges from 4% to 80%, with the largest increases in cover occurring on transects SGCS-20 (80.1%) and SGCS-19 (77.5%), both of which cross the Sandia GCS and on transects SGCS-3B (71.6%) and 5 (58.8%) in the cattail/willow zone. The smallest increase in cover (4%) occurred on transect SGCS-21 in between sheet piles 2 and 3 of the GCS.

Transects SGCS-9 and SGCS-11 had small increases (<1%) in nonvegetative cover compared to 2015, that is, these two transects have developed slightly more bare ground or open water since the previous surveys. All other transects show a decrease in nonvegetative cover, meaning vegetation has grown in areas of bare ground or open water since 2015. All 13 transects surveyed in 2017 have vegetative canopy cover greater than 100% (Table C-3.2-1), which is attributed to smaller forb species occurring within dense cattail stands and beneath willows in the obligate area and, to a lesser degree, small forb species occurring beneath trees outside the obligate area.

Table C-3.2-2 lists the top three most abundant (ranked composition) species within each transect, omitting nonvegetative categories (algae, water, bare ground, litter, logs). In 8 of the 13 transects, an obligate indicator species is the most abundant. Furthermore, in 2 of those 7 transects, the species with second greatest composition is also an obligate indicator. Between the 2015 and 2017 surveys, the most abundant species type remained unchanged on 9 transects. In contrast, the species type for the second and third rank species was largely inconsistent between the two surveys with only five and three species, respectively, persisting over the two-year period.

C-3.3 Obligate Zone Delineation and Characterization

Table C-3.3-1 presents the transect length, obligate zone length, and the percent of transect in the obligate zone. Table C-3.3-2 presents the vegetative canopy cover, vegetation presence, and nonvegetative presence, expressed as percentages, for the obligate and non-obligate zones as well as the obligate occurrence within the obligate zone. For a visual representation of these numbers, Figures C-3.3-1 through C-3.3-6 show topographic profiles, obligate zone boundaries of the 2017 and the 2015 surveys, distribution of obligate species (all OBL indicators binned) within the obligate zone, and distribution of two individual obligate species (broad-leafed cattail and coyote willow) for each transect.

Many variables are required to describe actual change to a complex system like the wetland in Sandia Canyon. For example, SGCS-3B doubled in obligate zone length from 2015 to 2017. This dramatic increase is the product of two small isolated cattail stands located in the southern extent of the transect and represent discontinuous growth along SGCS-3B. The obligate zone length alone might suggest that the space over which obligate species grew increased by 56ft from 2015 to 2017. However, taking into account the 20% decrease in obligate zone occurrence we see that these species have only been identified along an additional 11.2 ft of the transect.

In contrast, SGCS-11, underwent the largest decrease (20 ft) in obligate zone length but increased to a 100% obligate occurrence. These numbers demonstrate that the length along which obligate species are present has decreased but there is no longer any discontinuous growth. The loss in obligate zone length can be attributed to die-off of coyote willow where larger trees and understory vegetation out-compete the willows in the southern extent of the transect as it moves upslope and into unsaturated ground.

In addition to small amounts of spatial growth to the obligate zone in several other transects, there is also evidence that the obligate zones are becoming more densely filled with obligate species. For example, the obligate zone length for SGCS-19 not only increased by two feet but the obligate occurrence percentage increased by 35.6%. Similarly, the percent obligate occurrence in the obligate zone increased significantly (>5%) on transects SGCS-3A, SGCS-3B, SGCS-19, SGCS-20, and SGCS-21 (Table C-3.3-2). The vegetative presence in the obligate zone also increased on most of these transects, further indicating that obligate species formed multistory plant communities or filled in areas without vegetation since 2015. Additionally, vegetative canopy cover in the obligate area ranges from 123% to 325% and vegetative canopy cover in the non-obligate area ranges from 99% to 191% (Table C-3.3-2). These numbers reflect a small increase in overall vegetative canopy cover since the 2015 survey, where the same parameters ranged from 116% to 265% and 60% to 187% respectively, further demonstrating that multi-story plant communities are being established throughout the study area.

C-3.4 Wetland Vegetation Area

The perimeter of wetland vegetation was surveyed using DGPS. Four distinct zone types were mapped in 2017 and are labelled in the map legend of Figure C-3.0-1: (1) Cattail, (2) Willow, (3) Mixed Cattail/Willow, and (4) GCS Wetland Vegetation. Mapping of these zones results in 6 distinctive features: (1) Western Cattail Zone which includes the cattail populations in the meadow of redtop grass as well as the population bordering the western edge of the plunge pool, (2 & 3) Mixed Cattail/Willow Zones (central and west), (4), Central Cattail Zone (5) Northern Willow Zone, and (6) GCS Wetland Vegetation Zone (Figure C-3.0-1). The area encompassed by feature type and percent change are provided in Table C-3.4-1.

The Western Cattail Zone is a narrow zone of cattails with no willows that parallels the open channel at the head of the study area and encompasses an area of 760 m². Cattails inhabit the channel from the western edge of the Western Mixed zone all the way upstream to the plunge pool (Figure C-3.0-1). The West Cattail Zone perimeter has expanded 17.6% since 2016 (Table C-3.4-1). Increases in areal coverage of this feature were observed moving southwards onto higher flow stage surfaces just upstream of the first transect of alluvial wells as well as north and south along the continuously flowing channel. Other noticeable areas of increase occurred at satellite populations of cattails in the Western Cattail zone. The five satellite populations of cattails identified at the plunge pool and in the field of giant redtop grass south of the Western Cattail Zone increased to cover approximately 46 m² of area (Figure C-3.1-1).

The Northern Willow Zone, located along the northern extent of the Central Cattail Zone, encompasses 1585 m², an expansion of 7.5% since 2016 (Table C-3.4-1). Growth in 2017 saw continued competitive advancement of willows into the established Central Cattail Zone as well as continued upslope advancement onto the cliff base of the northern wall of Sandia Canyon.

There are two Mixed Cattail/Willow Zones: one (Central Mixed Cattail/Willow Zone) located on the south central edge and the second (Western Mixed Cattail/Willow Zone) located on the northwestern extent of the Central Cattail Zone. Together they encompass 2251 m² in 2017 (Figure C-3.0-1). These zones are primarily dominated by coyote willows with several lanceleaf cottonwood trees as well as stands of cattails along the stream channel and vegetative boundaries. These areas in reach S-2 show a decrease of 11.2% in areal extent from that of 2016.

The Upper Mixed Cattail/Willow Zone perimeter near SGCS-4 and SGCS-3B has expanded by 11% since 2016, largely from willow growth to the south of the stream channel (Figures C-3.0-1 and C-3.1-1 and Table C-3.1-1). This perimeter has continued annual expansion (LANL 2016, 601432) as a result of new willow growth west and south of the originally mapped 2014 zone of mixed cattails and willows (Figure C-3.1-2).

The Central Mixed Cattail/ Willow Zone was originally mapped on the south side of the Central Cattail Zone in 2015 (Figure C-3.0-1). This area, including the inner boundary, was surveyed again in 2017 (Figure C-3.0-1). The mixed area is dominated by willows on the south and has a gradational contact into strictly cattails to the north. This interior contact of the mixed zone with the Central Cattail Zone was surveyed in 2017 using new benchmarks that allowed for stronger GPS signal in this area (LANL 2016, 601432). This area remains relatively stable with an approximately 1% increase in areal coverage over 2016's surveyed footprint.

The Central Cattail Zone encompassed 10155 m², a decrease of 4% since 2016 (Table C-3.4-1). Despite this decrease, the Central Cattail Zone has continued to thrive as a stable vegetative unit in 2017 and exhibits minor growth expanding its outer boundary to the south near the GCS while staying relatively the same everywhere else (Figure C-3.0-1). This zone remained a stable and homogenous stand of broad-leaved cattails during 2017. During the 2015 monsoon season, a side channel on the south side of the Central Cattail Zone deposited a small amount of sandy gravel into the wetland, burying a small patch of cattails. Monitoring of this feature in 2016 included installing erosion pins on the established channel to determine if alluvium was advancing farther out into the Central Cattail Zone perimeter. Continued monitoring of this feature during the 2017 monsoon season has demonstrated that storm runoff is still depositing alluvium into the wetland area at this location. Annual surveys of the cattail boundary at this location have determined that the storm deposits have had only a minimal effect on the ability of cattails to effectively repopulate the area. Results from the erosion pins show the fan is relatively stable, but sediments are continually advancing eastward along the channel, which is spatially coincident with the edge of the central cattail zone. Monsoon season flow events have seen the development of small 4–6- inch-deep channels on the alluvial fan in question and erosion/aggradation of its surface approx. ±0.2 ft over Q3 and Q4 of 2017 near erosion pin EP04-MY16 (see Appendix B Section B-4.4).

Monitoring, via erosion pins, of the alluvial fans on the north side of the wetland continued throughout 2017. Measurements recorded in 2017 indicate the fans on the north side of the wetland did not significantly change in spatial extent nor in terms of aggrading of alluvial fan surfaces. Measurements collected during 2017 indicate a range of erosive events on the scale of -0.01 ft to -0.06 f. and aggrading events of 0.01 ft to 0.5 ft with the most significant changes occurring near the head of the easternmost alluvial fan. Non-wetland vegetation has steadily revegetated alluvial fan surfaces since the initial mapping of these features, making it difficult to map the downslope extent of the active fan. Runoff flow on the fans typically occurs in narrow 2–4-inch-deep by 4–6 in wide channels. Erosion pins are placed to monitor activity nearby those active flow areas.

Gravel bars devoid of wetland vegetation were surveyed in the middle of the Central Cattail Zone in 2015 (Figure C-3.0-1). These gravel bars were approximately 1–2 ft above the water surface in the wetland at the time of survey and were populated with grasses and small shrubs such as rubber rabbitbrush (LANL 2016, 601432). Observations from the fall of 2017 of previously mapped gravel bars indicate they are still populated by graminoid species, rubber rabbitbrush, and thistle species. A very narrow trail exists on the top of the gravel bars with no vegetation; otherwise, the gravel bars are revegetating with primarily non-obligate wetland species.

The GCS Wetland Vegetation Zone surrounding the GCS encompasses 1185 m², a reduction of 10% from 2016. This reduction is accounted for by a change in the location of the line separating the Central Cattail Zone from the GCS Wetland Vegetation Zone (Figure C-3.0-1). There is no longer a distinct boundary separating the western edge of the GCS vegetation area from the eastern edge of the established wetland of the Central Cattail Zone. The distinction between the two zones is estimated in the field by the assumed location of the westernmost edge of the first sheet pile in the GCS. Despite mapping the GCS zone as smaller in 2017, lateral expansion of this zone has continued during 2017, with wetland obligate species continuing to revegetate the banks of the GCS area.

C-4.0 CONCLUSIONS AND RECOMMENDATIONS

This appendix presents the annual vegetation monitoring surveys of Sandia Canyon reach S-2. Vegetation data were collected along 13 transects to support calculations, including species composition and vegetative canopy cover percentages, obligate zone delineation and characterization, and wetland vegetation area extent. The areal extent of the wetland system in the upstream areas begins as a narrow zone adjacent to a defined channel and gradually expands across a much wider area into the Central Cattail zone and continues to the GCS. Between 2016 and 2017, the wetland vegetation area has expanded by approximately 2% over the whole study area, with most of the expansion occurring at the upstream end of the reach as new cattails and willows expanded along the stream channel.

Obligate zone delineation and characterization parameters help clarify the significance of observed differences in the system occurring between consecutive surveys, and give us a better understanding of how the wetland is evolving in real time. Obligate species (cattails) occurring outside of the primary wetland area (SGCS-3B) (Figure C-3.1-1) indicate that discontinuous areas adjacent and areas immediately south of the Western Cattail zone are saturated enough to support wetland vegetation; in addition, that wetland species can compete with upland species in that location. Furthermore, an increase in vegetative canopy cover in the obligate zone along 11 of the 13 transects shows growth of and/or relative stability throughout all four zones of the study area. Significant increases in vegetative canopy cover with decreases in non-vegetative composition along SGCS-19, SGCS-20, and SGCS-21 suggest that the GCS has been efficient in stabilizing water and sediment transport allowing for the generation of a healthy wetland system.

Steadily increasing data trends derived from the line intercept method in 2014, 2015, and 2017 and vegetation perimeter mapping in 2014, 15, 16, & 17 (Figure C-3.1-2) indicate a stable and growing wetland that is unlikely to regress unless a significant change is incurred by the system. Future monitoring via the line-intercept method will occur biennially. Visual inspections will continue to occur annually and dictate whether further investigations (i.e., via the line-intercept method, repeat photographs, or LiDAR surveys) are required for the monitoring year. Differential GPS surveys of the wetland vegetation perimeter will continue on an annual basis, as will qualitative photographic surveys of the wetland.

C-5.0 REFERENCES AND MAP DATA SOURCES

C-5.1 References

The following reference list includes documents cited in this appendix. Parenthetical information following each reference provides the author(s), publication date, and ERID or ESHID. This information is also included in text citations. ERIDs were assigned by the Associate Directorate for Environmental Management's (ADEM's) Records Processing Facility (IDs through 599999), and ESHIDs are assigned by the Environment, Safety, and Health Directorate (IDs 600000 and above). IDs are used to locate documents in the Laboratory's Electronic Document Management System and in the Master Reference Set. The NMED Hazardous Waste Bureau and ADEM maintain copies of the Master Reference Set. The set ensures that NMED has the references to review documents. The set is updated when new references are cited in documents.

Cobrain, D., April 3, 2013. FW: Sandia Wetland cross sections. E-mail message to D. Katzman (LANL) from D. Cobrain (NMED), Santa Fe, New Mexico. (Cobrain 2013, 256726)

Coulloudon, B., K. Eshelman, J. Gianola, N. Habich, L. Hughes, C. Johnson, M. Pellant, P. Podborny, A. Rasmussen, B. Robles, P. Shaver, J. Spehar, and J. Willoughby, 1999. "Sampling Vegetation Attributes," Interagency Technical Reference 1734-4, Cooperative Extension Service, U.S. Department of Agriculture Forest Service (National Resource Conservation Service), and U.S. Department of the Interior Bureau of Land Management, Denver, Colorado. (Coulloudon et al. 1999, 600337)

LANL (Los Alamos National Laboratory), October 2009. "Investigation Report for Sandia Canyon," Los Alamos National Laboratory document LA-UR-09-6450, Los Alamos, New Mexico. (LANL 2009, 107453)

LANL (Los Alamos National Laboratory), September 2011. "Work Plan and Final Design for Stabilization of the Sandia Canyon Wetland," Los Alamos National Laboratory document LA-UR-11-5337, Los Alamos, New Mexico. (LANL 2011, 207053)

LANL (Los Alamos National Laboratory), June 2014. "Sandia Wetland Performance Report, Baseline Conditions 2012–2014," Los Alamos National Laboratory document LA-UR-14-24271, Los Alamos, New Mexico. (LANL 2014, 257590)

LANL (Los Alamos National Laboratory), December 15, 2014. "2014 Annual Monitoring Report for Sandia Canyon Wetland Grade-Control Structure (SPA-2012-00050-ABQ)," Los Alamos National Laboratory letter and attachments (ENV-DO-14-0378) to K.E. Allen (USACE) from A.R. Grieggs (LANL), Los Alamos, New Mexico. (LANL 2014, 600083)

LANL (Los Alamos National Laboratory), April 2015. "Sandia Wetland Performance Report, Performance Period April 2014–December 2014," Los Alamos National Laboratory document LA-UR-15-22463, Los Alamos, New Mexico. (LANL 2015, 600399)

LANL (Los Alamos National Laboratory), April 2016. "2015 Sandia Wetland Performance Report," Los Alamos National Laboratory document LA-UR-16-22618, Los Alamos, New Mexico. (LANL 2016, 601432)

LANL (Los Alamos National Laboratory), April 2017. "2016 Sandia Wetland Performance Report," Los Alamos National Laboratory document LA-UR-17-23076, Los Alamos, New Mexico. (LANL 2017, 602341)

Reed, P.B.J., September 1988. "National List of Plant Species That Occur in Wetlands: 1988 National Summary," Biological Report 88(24), U.S. Department of the Interior, Fish and Wildlife Service, Washington D.C. (Reed 1988, 600338)

USACE (U.S. Army Corps of Engineers), May 12, 2016. "Western Mountains, Valleys & Coast 2016 Regional Wetland Plant List," The National Wetland Plant: 2016 Wetlands Ratings to R.W. Lichvar, D.L. Banks, W.N. Kirchner, and N.C. Melvin. (USACE 2016, 602997)

C-5.2 Map Data Sources

Gaging stations; Los Alamos National Laboratory, Waste and Environmental Services Division; 1:2,500; March 19, 2011.

LANL area orthophoto; Los Alamos National Laboratory, 2014.

Geomorphic Reach Boundary, Los Alamos National Laboratory, Earth and Environmental Science, GISLab, 2009.

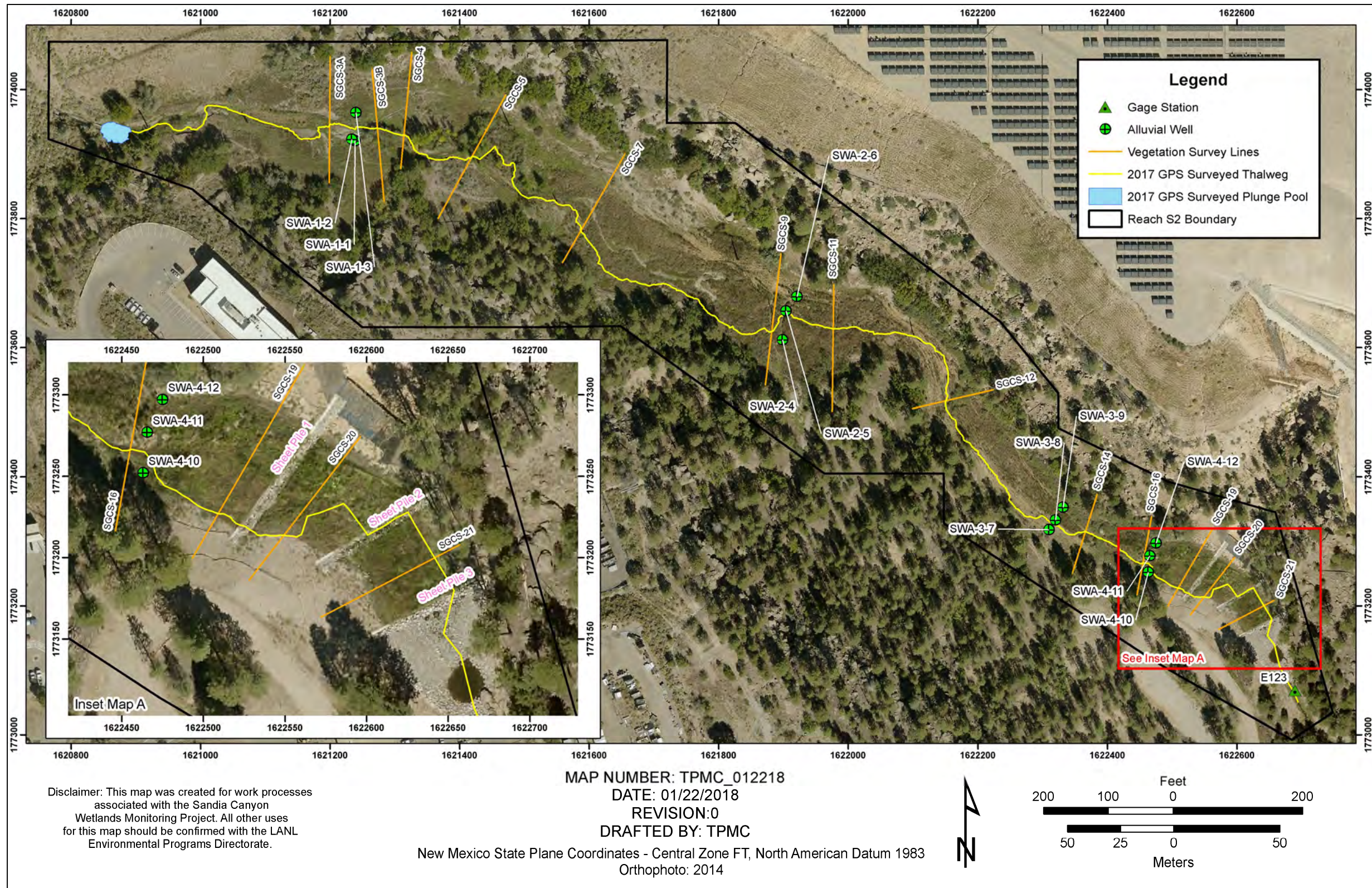


Figure C-1.0-1 Locations of cross-sections, piezometers, sheet piles, and thalweg profiles in Sandia Canyon reach S-2

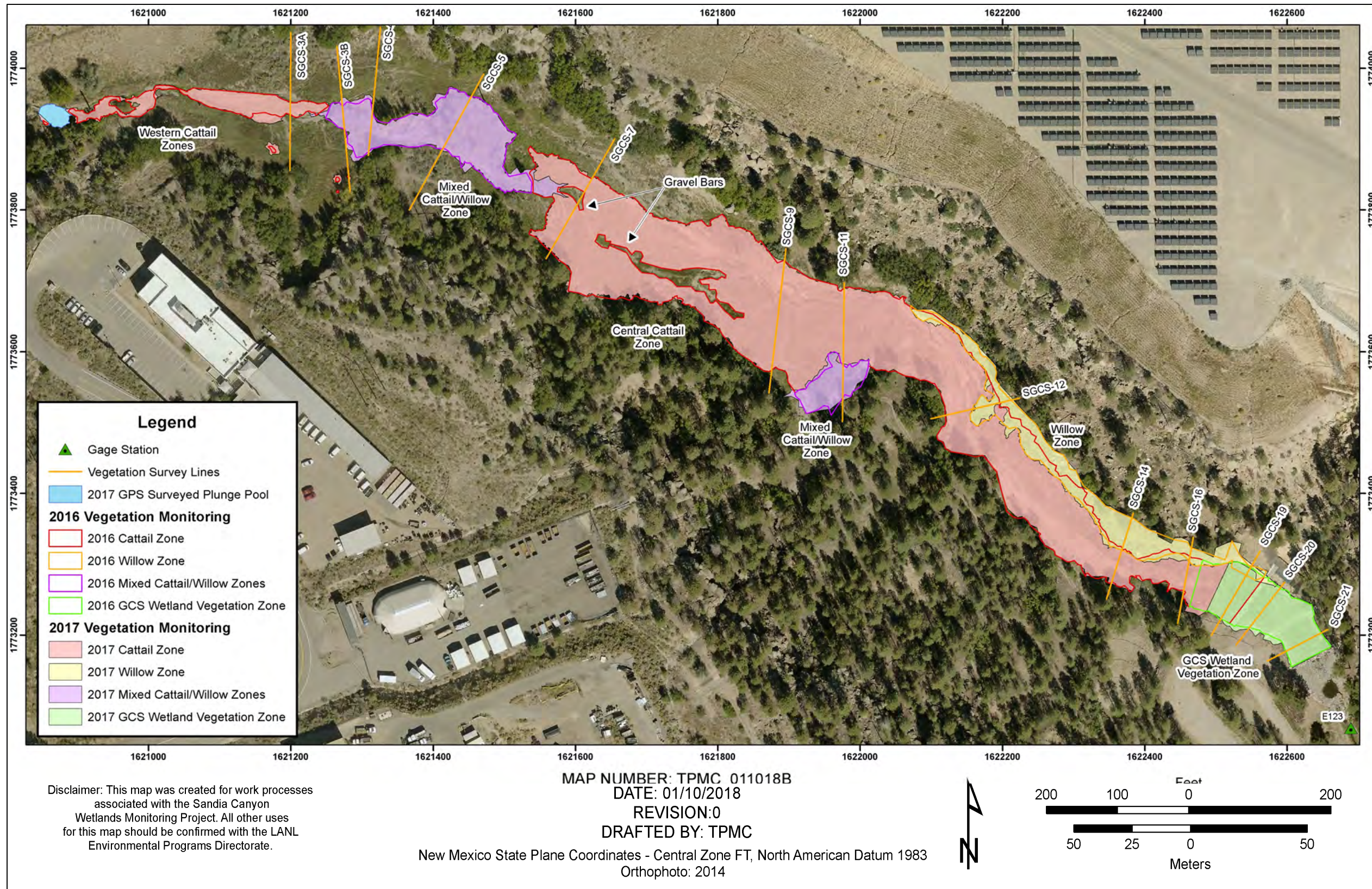


Figure C-3.0-1 2017 and 2016 vegetation perimeter mapping comparison results at Sandia Canyon reach S-2

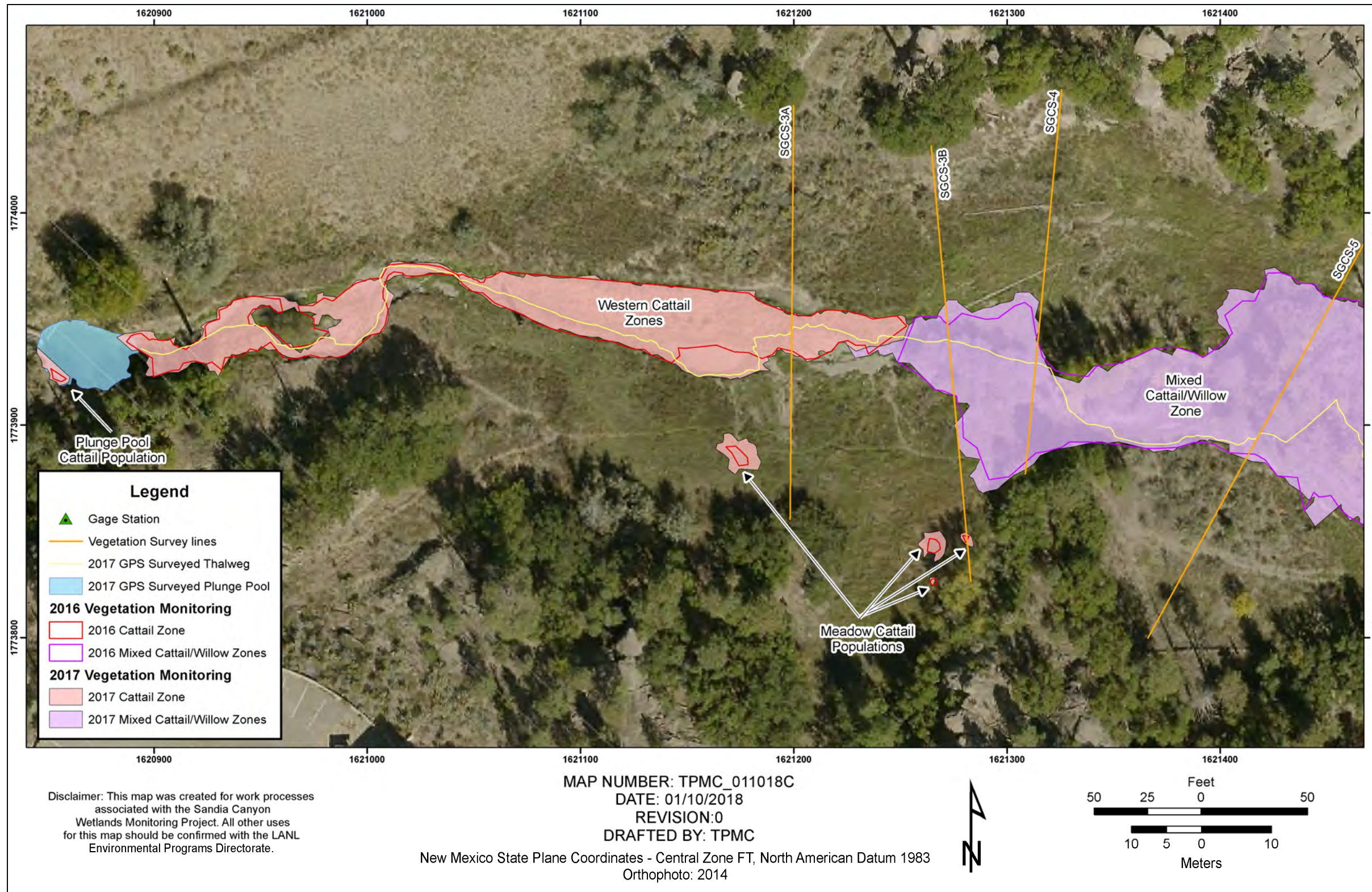
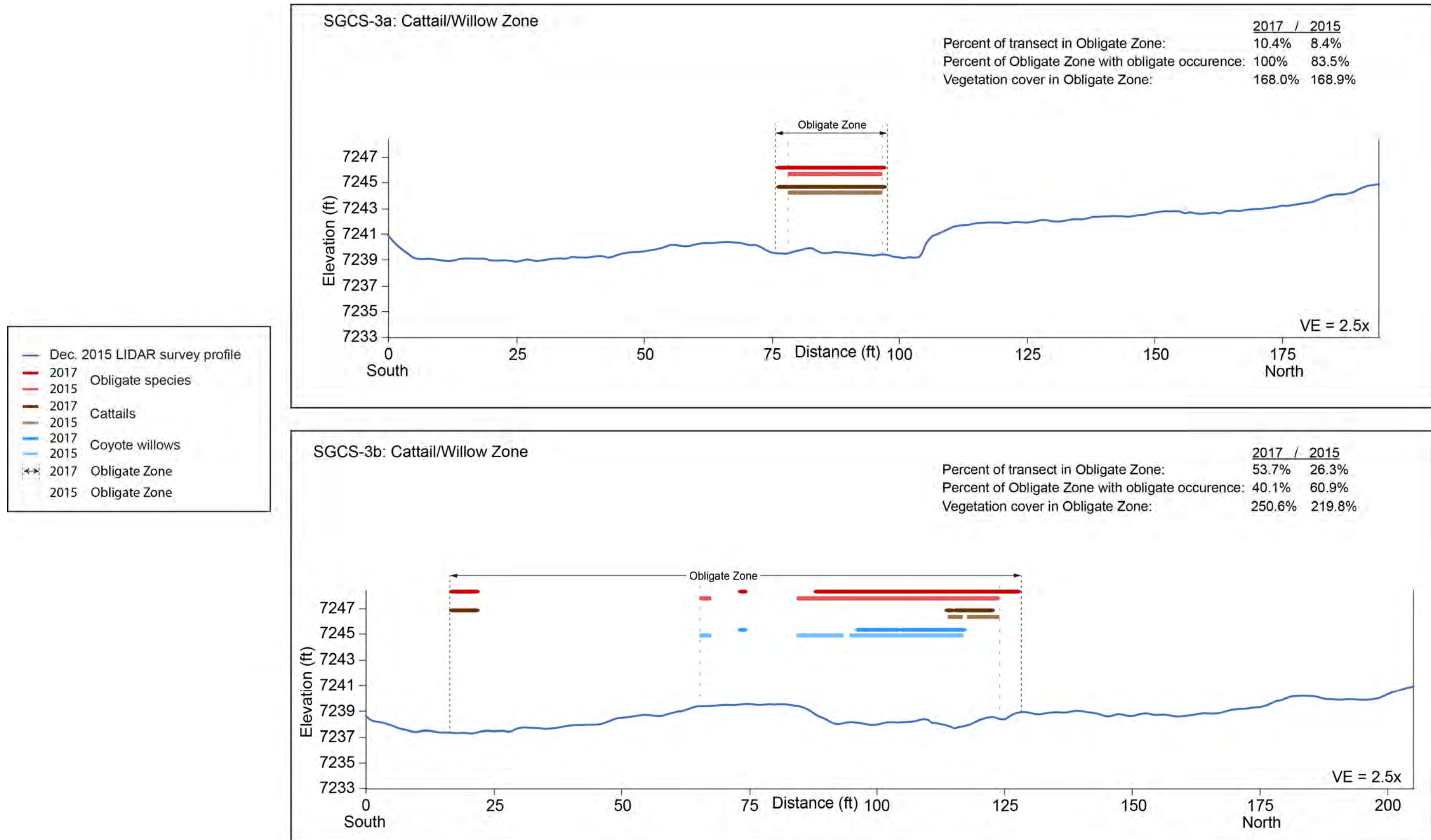
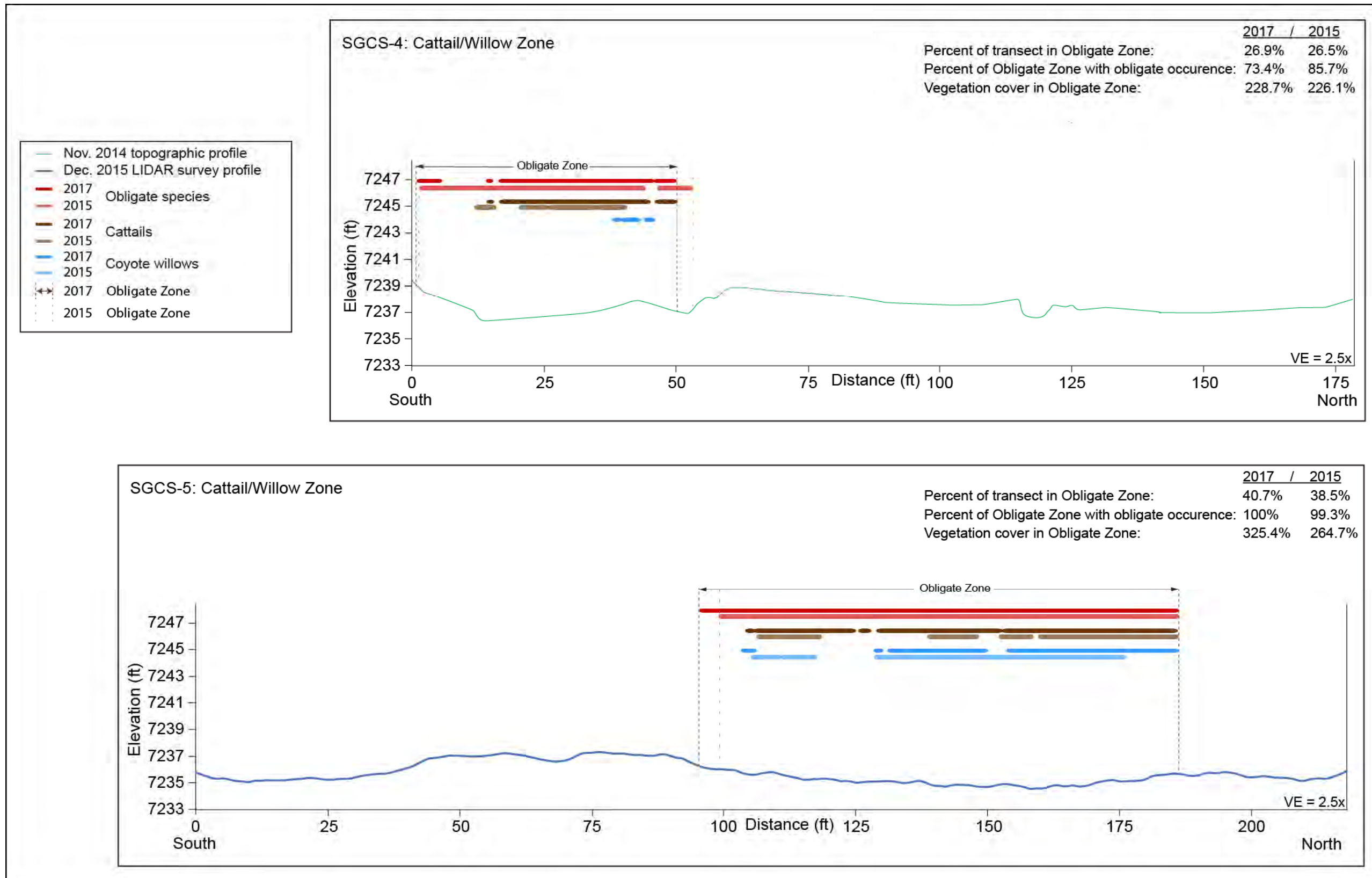


Figure C-3.1-1 Upper wetland area highlighting cattail populations



Note: Topographic profiles extracted from 2015 LiDAR survey based DEM.

Figure C-3.3-1 Spatial distribution of obligate species on transects SGCS-3a and SGCS-3b in Sandia Canyon Reach S-2



Note: Topographic profile for SGCS-5 extracted from 2015 LiDAR survey based DEM.

Figure C-3.3-2 Spatial distribution of obligate species on transects SGCS-4 and SGCS-5 in Sandia Canyon Reach S-2

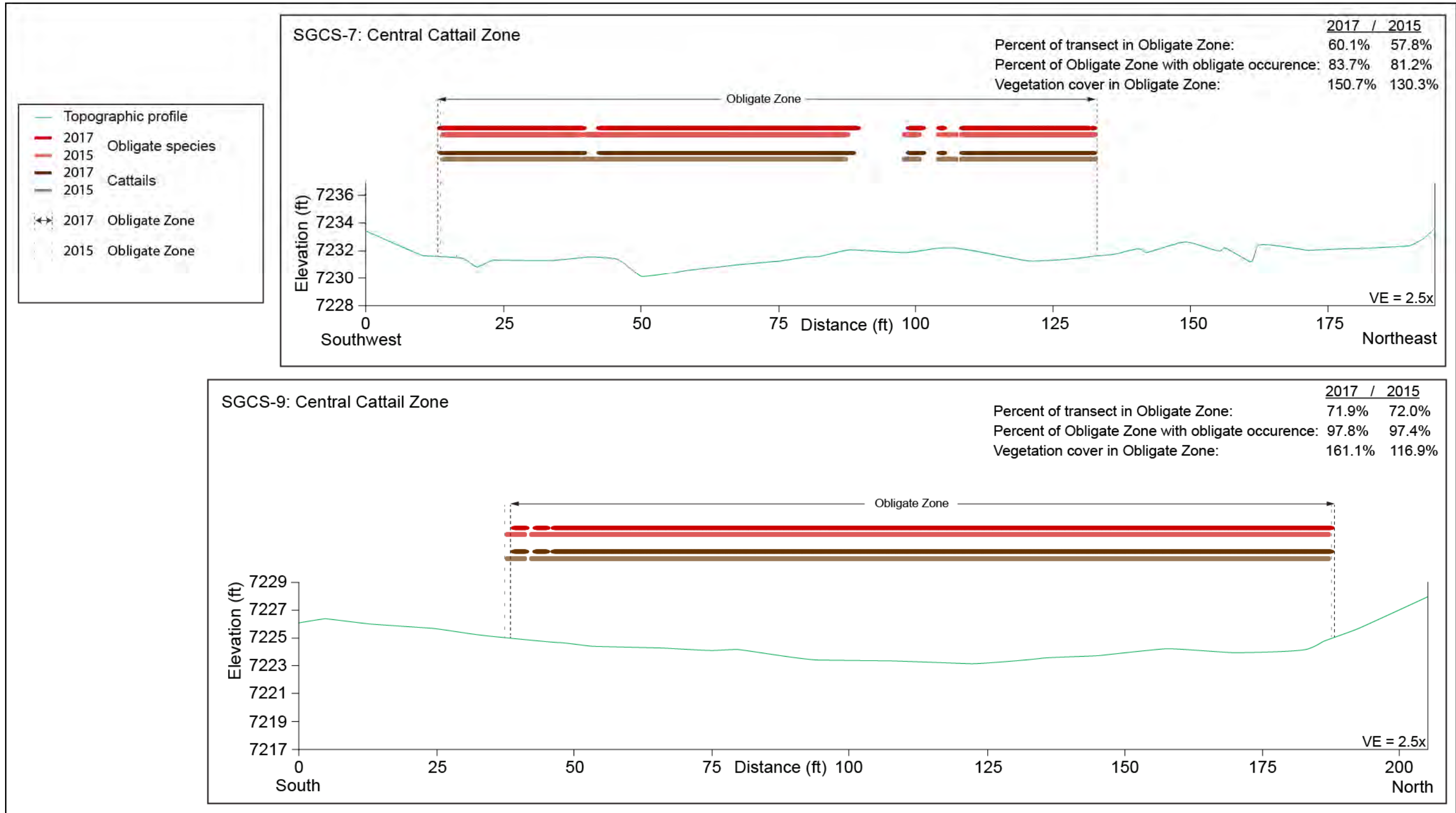


Figure C-3.3-3 Spatial distribution of obligate species on transects SGCS-7 and SGCS-9 in Sandia Canyon Reach S-2

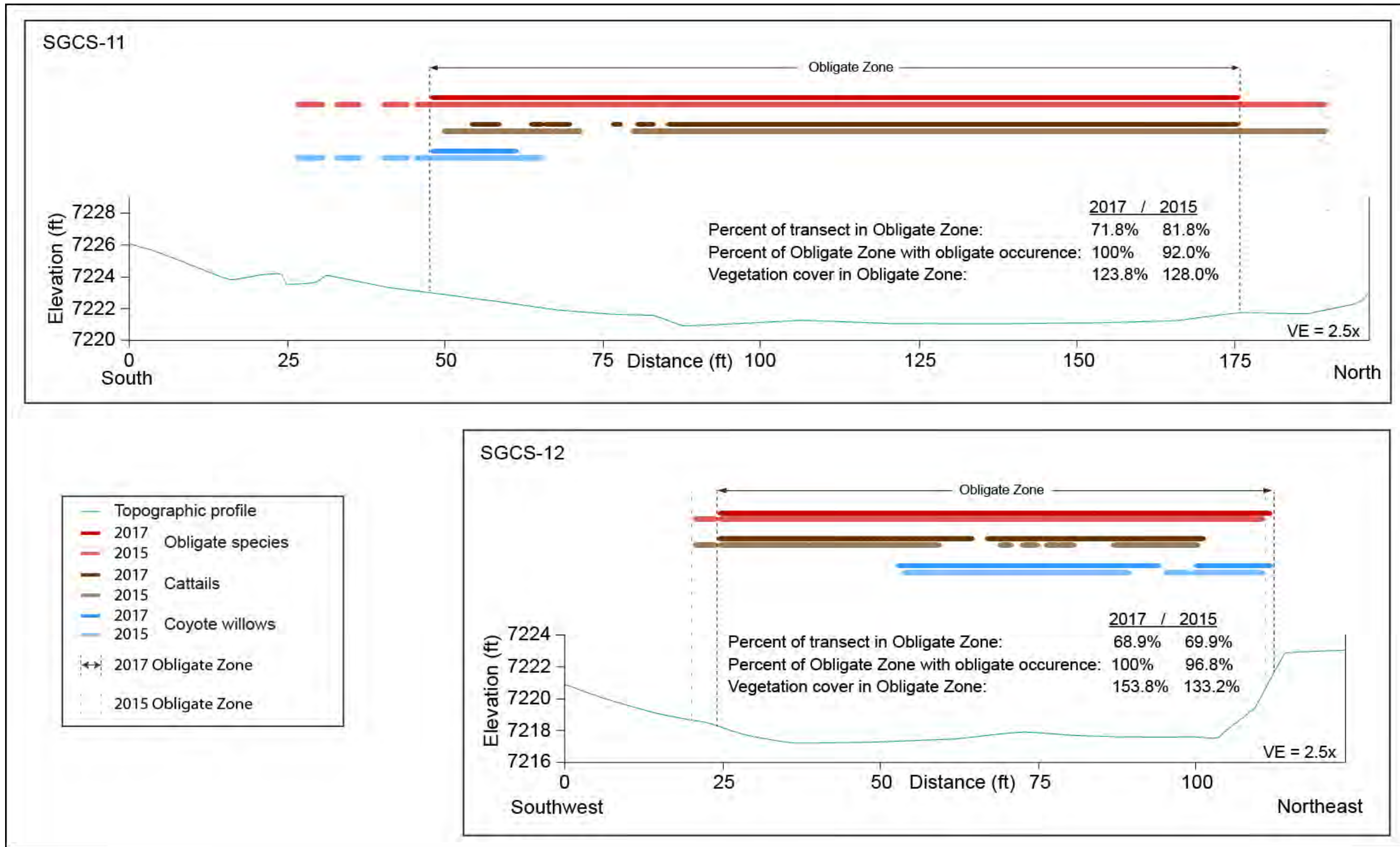


Figure C-3.3-4 Spatial distribution of obligate species on transects SGCS-11 and SGCS-12 in Sandia Canyon Reach S-2

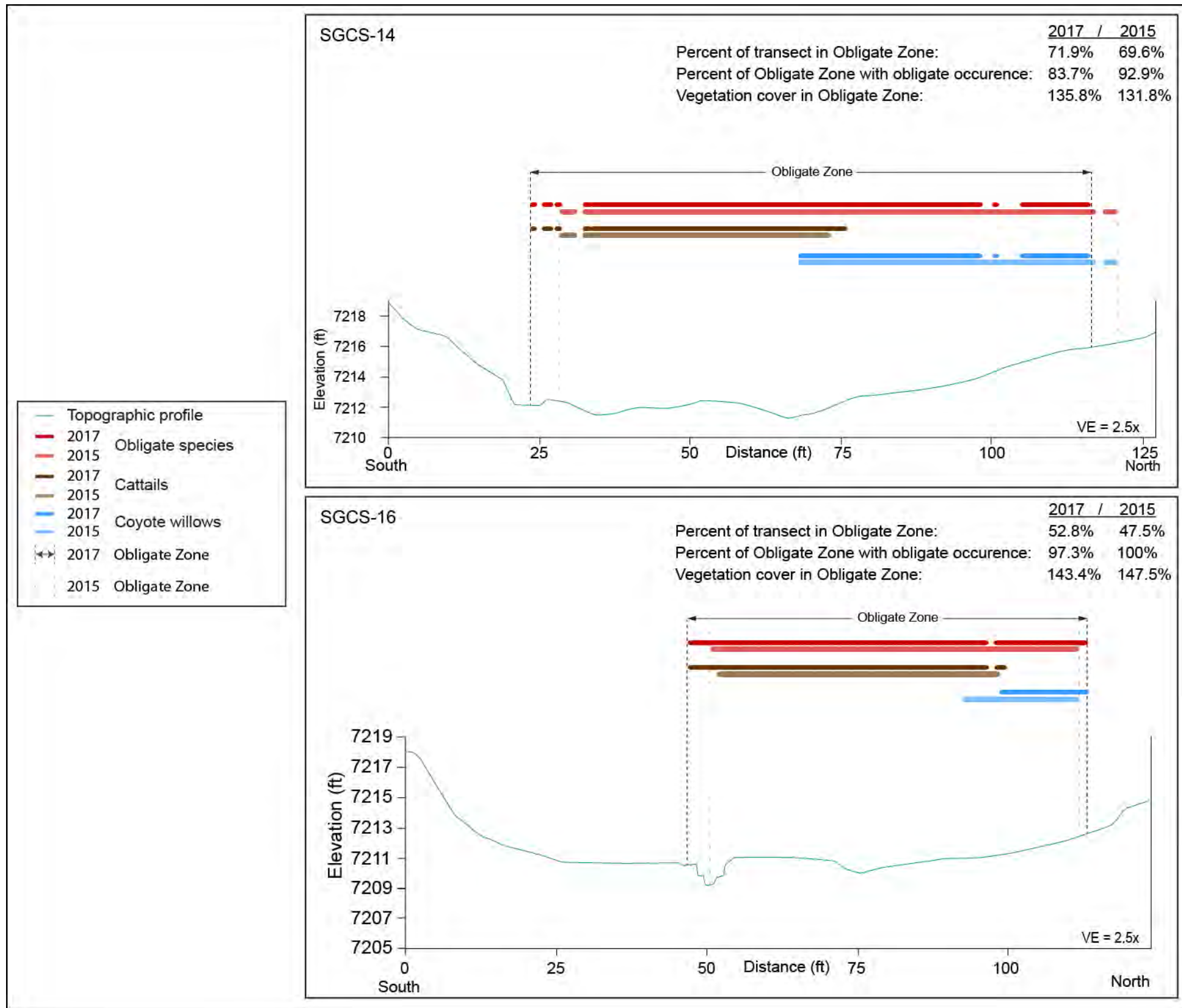


Figure C-3.3-5 Spatial distribution of obligate species on transects SGCS-14 and SGCS-16 in Sandia Canyon Reach S-2

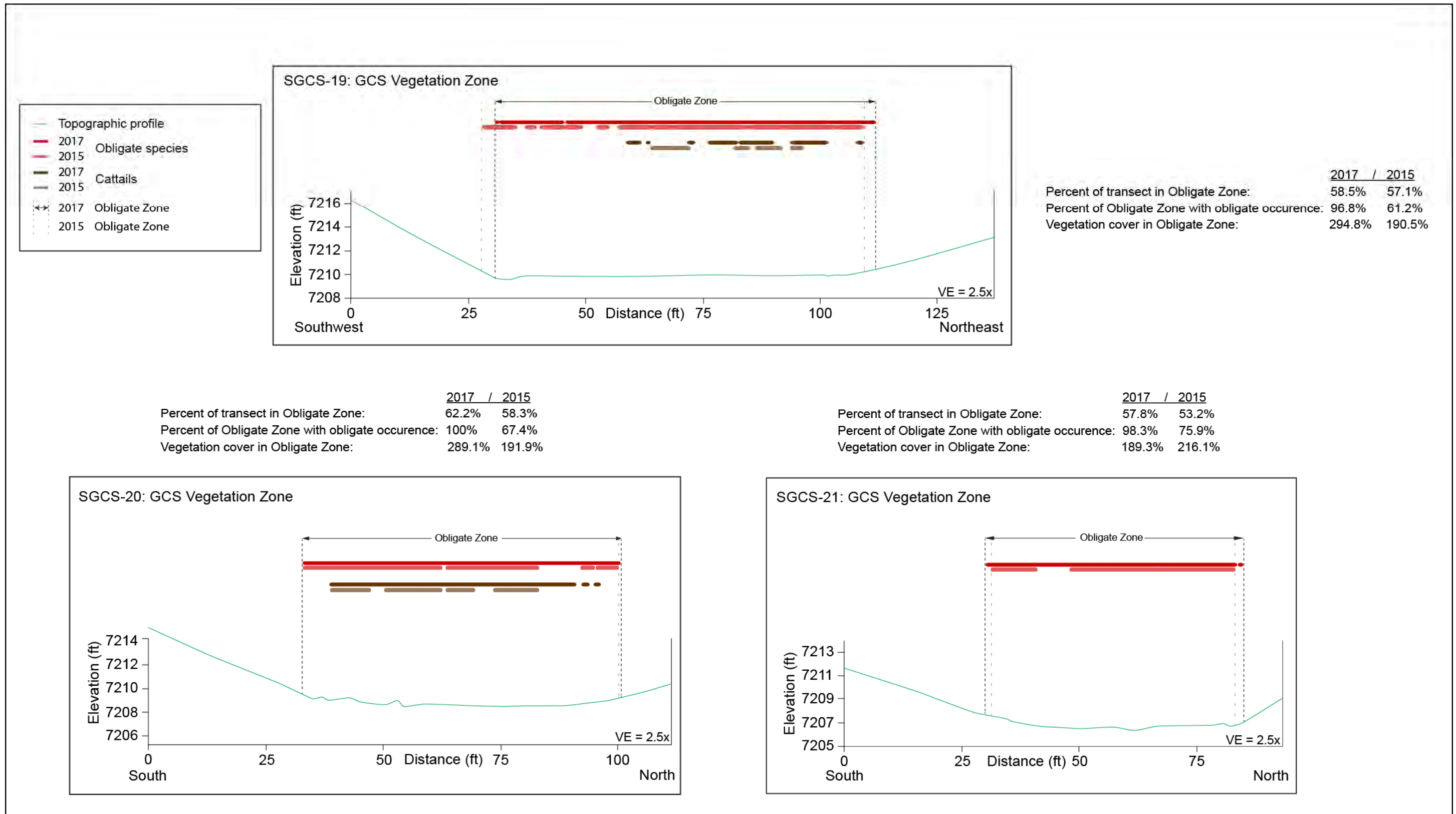


Figure C-3.3-6 Spatial distribution of obligate species on transects SGCS-19, SGCS-20, and SGCS-21 in Sandia Canyon Reach S-2

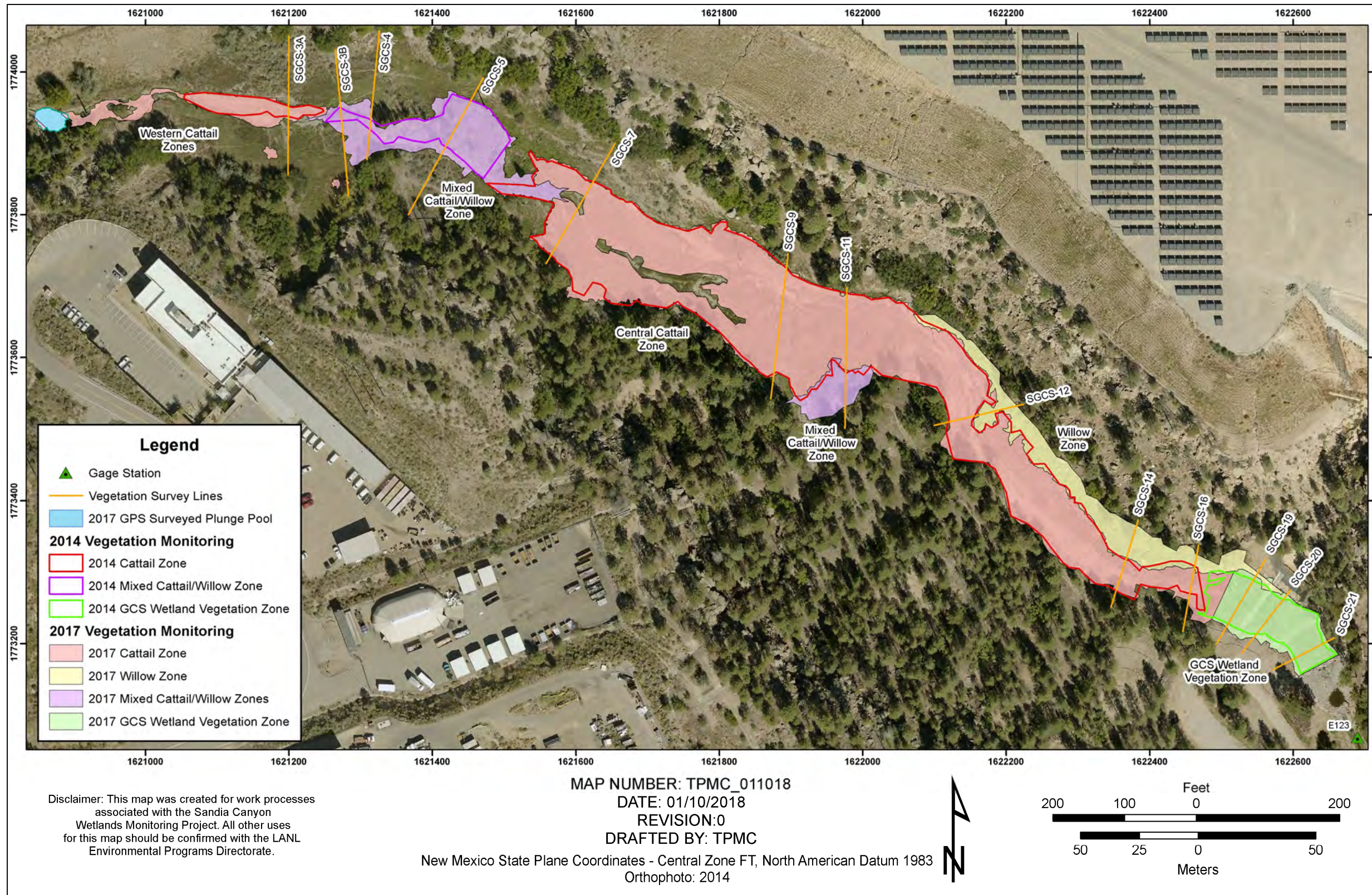


Figure C-3.4-1 Three-year (2014–2017) comparison of wetland vegetation perimeters

**Table C-2.1-1
Wetland Plant Species Indicator Definitions**

Indicator Acronym	Full Title	Definition*
OBL	Obligate Wetland Plants	Occur almost always (estimated probability of >99%) in wetlands but occasionally are found in non-wetlands (estimated probability of <1%).
FACW	Facultative Wetland Plants	Usually occur in wetlands (estimated probability of 67% to 99%) but occasionally are found in non-wetlands (estimated probability 1% to 33%).
FAC	Facultative Plants	Share an equal likelihood (estimated probability 33% to 67% of occurring in either wetlands or non-wetlands.
FACU	Facultative Upland Plants	Usually occur in non-wetlands (estimated probability 67% to 99%) but occasionally are found in wetlands (estimated probability 1% to 33%).
UPL	Obligate Upland Plants	Occur almost always (estimated probability >99%) in non-wetlands.
NI	No Indicator Status	Unable to determine indicator status.

*Source: Reed (1988, 600338).

**Table C-3.1-1
2017 Comprehensive Species List**

Symbol ^a	Scientific Name	Common Name	Indicator Category ^{b, c, d}	Lifeform	Classification
ACNE	<i>Acer negundo</i>	boxelder	FACW	Tree	Non-Obligate
AGGI	<i>Agrostis gigantea</i>	giant redtop	FACW	Graminoid	Non-Obligate
AMDI	<i>Amauriopsis dissecta</i>	yellow ragweed	NI	Forb	Non-Obligate
AMPS	<i>Ambrosia psilostachya</i>	Cuman ragweed	NI	Forb	Non-Obligate
ANGE	<i>Andropogon gerardii</i>	big bluestem	FACU	Graminoid	Non-Obligate
ANPA4 ^a	<i>Antennaria parvifolia</i>	small-leaf pussytoes	NI ^d	Forb	Non-Obligate
ARFR4 ^a	<i>Artemisia frigida</i>	prairie sagebrush	NI ^d	Shrub	Non-Obligate
ARLU ^a	<i>Artemisia ludoviciana</i>	white sagebrush	UPL ^c	Forb	Non-Obligate
ASSP	<i>Asteraceae Spp.</i>	thistle	FACW	Forb	Non-Obligate
BASA	<i>Baccharis salicifolia</i>	seep willow	FACW	Shrub	Non-Obligate
BEFE	<i>Berberis fendleri</i>	Colorado barberry	NI	Forb	Non-Obligate
BOCU	<i>Bouteloua curtipendula</i>	sideoats grama	NI	Graminoid	Non-Obligate
BOGR	<i>Bouteloua gracilis</i>	blue grama	NI	Graminoid	Non-Obligate
BRAN	<i>Bromus anomalus</i>	nodding brome	NI	Graminoid	Non-Obligate
BRTE	<i>Bromus tectorum</i>	cheatgrass	NI	Graminoid	Non-Obligate
BUDA	<i>Buchloe Dactyloides</i>	buffalograss	FACU	Graminoid	Non-Obligate
CAAQ	<i>Carex Aquatilis</i>	water sedge	OBL	Graminoid	Obligate
CABR ^a	<i>Carex brevior</i>	short-beaked sedge	FAC	Graminoid	Non-Obligate
CAUT ^a	<i>Carex utriculata</i>	Northwest Territory sedge	OBL	Graminoid	Obligate
CHNA	<i>Chrysothamnus nauseosus</i>	rubber rabbitbrush	NI	Shrub	Non-Obligate
CIIN ^a	<i>Cichorium intybus</i>	chicory	NI ^d	Forb	Non-Obligate

Table C-3.1-1 (continued)

Symbol ^a	Scientific Name	Common Name	Indicator Category ^{b,c,d}	Lifeform	Classification
COBO ^b	<i>Conyza bonariensis</i>	hairy fleabane	FACU	Forb	Non-Obligate
CYFE ^d	<i>Cyperus fendlerianus</i>	Fendler's sedge	FAC	Forb	Non-Obligate
DAGL	<i>Dactylis glomerata</i>	orchard grass	FACU	Graminoid	Non-Obligate
ELAN	<i>Elaeagnus angustifolia</i>	Russian olive	FACW	Tree	Non-Obligate
ELEL	<i>Elymus elymoides</i>	squirreltail	UPL	Graminoid	Non-Obligate
EPCI	<i>Epilobium ciliatum</i>	fringed willowherb	FACW	Forb	Non-Obligate
ERCI	<i>Erodium cicutarium</i>	redstem stork's bill	NI	Forb	Non-Obligate
GECA ^{3a}	<i>Geranium caespitosum</i>	purple cluster crane's bill	FAC ^c	Forb	Non-Obligate
GLBO	<i>Glyceria Borealis</i>	small floating mannagrass	OBL	Graminoid	Obligate
HEAN ^a	<i>Helianthus annuus</i>	common sunflower	FAC	Forb	Non-Obligate
HOJU	<i>Hordeum jubatum</i>	foxtail barley	FAC	Graminoid	Non-Obligate
IPAG	<i>Ipomopsis aggregata</i>	scarlet gilia	NI	Forb	Non-Obligate
JUBA	<i>Juncus balticus</i>	Baltic rush	OBL	Graminoid	Obligate
JULO	<i>Juncus longistylus</i>	longstyle rush	FACW	Graminoid	Non-Obligate
JUSC	<i>Juniperus scopulorum</i>	Rocky Mountain juniper	NI	Tree	Non-Obligate
JUTE ^a	<i>Juncus tenuis</i>	poverty rush	FACW	Graminoid	Non-Obligate
JUTO	<i>Juncus Torreyi</i>	Torrey's rush	FACW	Graminoid	Non-Obligate
KOMY	<i>Kobresia myosuroides</i>	Ballardi bog sedge	FACU	Graminoid	Non-Obligate
KOSC	<i>Kochia scoparia</i>	mock cypress	FAC	Forb	Non-Obligate
LASE	<i>Lactuca serriola</i>	prickly lettuce	FACU	Forb	Non-Obligate
LEMI	<i>Lemna minor</i>	common duckweed	OBL	Forb	Obligate
LILE	<i>Linum lewisii</i>	Lewis flax	NI	Forb	Non-Obligate
LUAR	<i>Lupinus argenteus</i>	silvery lupine	UPL	Forb	Non-Obligate
MEOF	<i>Melilotus officinalis</i>	yellow sweet clover	FACU	Forb	Non-Obligate
MIGL	<i>Mimulus glabratus</i>	roundleaf monkey flower	OBL	Forb	Obligate
MIGU	<i>Mimulus guttatus</i>	seep monkey flower	OBL	Forb	Obligate
MUMO	<i>Muhlenbergia montana</i>	mountain muhly	UPL	Graminoid	Non-Obligate
MUWR ^a	<i>Muhlenbergia wrightii</i>	spike muhly	FACU	Graminoid	Non-Obligate
OECO ^{2a}	<i>Oenothera coronopifolia</i>	pink evening primrose	NI ^d	Forb	Non-Obligate
OEEL	<i>Oenothera Elata</i>	Hooker's evening primrose	FACW	Forb	Non-Obligate
PAQU	<i>Parthenocissus quinquefolia</i>	Virginia creeper	FAC	Vine	Non-Obligate
PASM	<i>Pascopyrum smithii</i>	western wheatgrass	FAC	Graminoid	Non-Obligate
PELE	<i>Penstemon lentus</i>	handsome beardtongue	NI	Forb	Non-Obligate
PHAR	<i>Phalaris arundinacea</i>	reed canyon grass	OBL	Graminoid	Obligate
PIPO	<i>Pinus ponderosa</i>	ponderosa pine	FACU	Tree	Non-Obligate
POAC	<i>Populus acuminata</i>	lanceleaf cottonwood	FAC	Tree	Non-Obligate
POHI	<i>Potentilla hippiana</i>	wooly cinquefoil	NI	Forb	Non-Obligate
POOL	<i>Portulaca Oleracea</i>	common purslane	FAC	Forb	Non-Obligate
POPR	<i>Poa pratensis</i>	Kentucky bluegrass	FACU	Graminoid	Non-Obligate

Table C-3.1-1 (continued)

Symbol ^a	Scientific Name	Common Name	Indicator Category ^{b,c,d}	Lifeform	Classification
POTR	<i>Populus tremuloides</i>	quaking aspen	FACU	Tree	Non-Obligate
PRVI	<i>Prunus virginiana</i>	Chokecherry	FACU	Shrub	Non-Obligate
QUGA	<i>Quercus gambelii</i>	Gambel oak	NI	Tree	Non-Obligate
RICE	<i>Ribes cereum</i>	wax currant	FAC	Shrub	Non-Obligate
ROWO	<i>Rosa woodsii</i>	Woods' rose	FACU	Shrub	Non-Obligate
RUCR	<i>Rumex crispus</i>	curly dock	FACW	Forb	Non-Obligate
RUID	<i>Rubus idaeus</i>	American red raspberry	FAC	Forb	Non-Obligate
SAEX	<i>Salix exigua</i>	narrowleaf (coyote) willow	OBL	Shrub	Obligate
SAIR	<i>Salix irrorata</i>	bluestem willow	FACW	Shrub	Non-Obligate
SCAC	<i>Scirpus Acutus</i>	hardstem bulrush	OBL	Graminoid	Obligate
SCPU	<i>Schoenoplectus pungens</i>	common threesquare	OBL	Graminoid	Obligate
SCTA	<i>Scirpus Tabernaemontani</i>	softstem bulrush	OBL	Graminoid	Obligate
SEVA	<i>Securigera varia</i>	purple crown vetch	NI	Forb	Non-Obligate
SIIR*	<i>Sisymbrium Irio</i>	London rocket	NI	Forb	Non-Obligate
SPAN3 ^a	<i>Sphaeralcea angustifolia</i>	narrow leaf globemallow	NI ^d	Forb	Non-Obligate
SPCO-B	<i>Sporobolus contractus</i>	spike dropseed	NI	Graminoid	Non-Obligate
TAOF	<i>Taraxacum officinale</i>	common dandelion	FACU	Forb	Non-Obligate
THMO ^a	<i>Thermopsis montana</i>	mountain goldenbanner	FAC	Forb	Non-Obligate
TYLA	<i>Typha latifolia</i>	broad-leaved cattail	OBL	Forb	Obligate
VETH	<i>Verbascum thapsus</i>	common mullein	NI	Forb	Non-Obligate

^a Species first observed along transects in 2017

^b Source: Reed (1988, 600338) unless otherwise noted.

^c Source: Luchvar (2016)

^d Source: USDA

Table C-3.1-2
2015 to 2017 Species Composition Percentage by Life Form

Year	Species Count	Tree	Shrub	Graminoid	Forb	Vine
Overall						
2015	72	9.7%	12.5%	36.1%	40.3%	1.4%
2017	81	8.6%	11.1%	34.6%	44.4%	1.2%
Obligate Species						
2015	12	0%	8.3%	58.3%	33.3%	0%
2017	13	0%	7.7%	61.5%	30.8%	0%
Non-Obligate Species						
2015	60	11.7%	13.3%	31.7%	41.7%	1.7%
2017	68	10.3%	11.8%	29.4%	47.1%	1.5%

**Table C-3.1-3
2015 to 2017 Species Composition Percentage by Indicator Status**

Year	Obligate Wetland Plants (OBL)	Facultative Wetland Plants (FACW)	Facultative Plants (FAC)	Facultative Upland Plants (FACU)	Obligate Upland Plants (UPL)	No Indicator Status (NI)
2015 ^a	16.7%	16.7%	12.2%	19.4%	5.6%	29.2%
2017 ^b	16.1%	14.8%	16.0%	17.3%	4.9%	30.9%

^a n = 72 species.

^b n = 81 species.

**Table C-3.2-1
2015 to 2017 Percent Canopy Cover and
Percent Species Composition for Each Transect (Entire Length)**

Transect	Year	Percent Canopy Cover		Percent Species Composition	
		Vegetative	Non-Vegetative ^a	Vegetative	Non-Vegetative ^a
SGCS-3A ^b	2015	109.9%	7.9%	93.3%	6.7%
	2017	143.5%	4.2%	97.2%	2.8%
SGCS-3B ^b	2015	142.5%	8.3%	94.5%	5.5%
	2017	214.1%	1.7%	99.2%	0.8%
SGCS-4	2015	159.1%	6.8%	95.9%	4.1%
	2017	179.0%	3.1%	98.3%	1.7%
SGCS-5 ^b	2015	170.7%	5.0%	97.2%	2.8%
	2017	229.5%	2.1%	99.1%	0.9%
SGCS-7	2015	120.1%	15.1%	88.8%	11.2%
	2017	155.7%	4.0%	97.5%	2.5%
SGCS-9	2015	136.7%	0.0%	100.0%	0.0%
	2017	163.9%	0.5%	99.7%	0.3%
SGCS-11	2015	125.7%	5.0%	96.2%	3.8%
	2017	124.9%	5.6%	95.7%	4.3%
SGCS-12	2015	126.4%	5.2%	96.1%	3.9%
	2017	138.3%	5.5%	96.2%	3.8%
SGCS-14	2015	138.3%	5.9%	95.9%	4.1%
	2017	135.6%	4.6%	96.7%	3.3%
SGCS-16	2015	147.6%	6.4%	95.9%	4.1%
	2017	166.1%	0.0%	100.0%	0.0%
SGCS-19	2015	150.7%	13.6%	91.7%	8.3%
	2017	228.2%	1.8%	99.2%	0.8%
SGCS-20	2015	137.2%	23.9%	85.2%	14.8%
	2017	217.3%	8.9%	96.0%	4.0%
SGCS-21	2015	168.5%	11.7%	93.5%	6.5%
	2017	172.5%	1.6%	99.1%	0.9%

^a Nonvegetative categories: algae, logs, litter, bare ground, water.

^b Baseline surveyed conducted in 2015.

**Table C-3.2-2
2015 to 2017 Ranked Order of Species Composition Summary**

Transect	Year	Species Rank 1			Species Rank 2			Species Rank 3		
		Species ^a	Indicator Status	Composition	Species ^a	Indicator Status	Composition	Species ^a	Indicator Status	Composition
SGCS-3A ^b	2015	giant redtop	FACW	29.3%	dragon sagewort	NI	23.9%	rubber rabbitbush	NI	9.4%
	2017	giant redtop	FACW	32.0%	cheatgrass	NI	21.5%	dragon sagewort	NI	13.3%
SGCS-3B ^b	2015	giant redtop	FACW	37.2%	dragon sagewort	NI	10.8%	purple crown vetch	NI	9.0%
	2017	giant redtop	FACW	33.1%	lanceleaf cottonwood	FAC	8.6%	common threesquare	OBL	8.4%
SGCS-4	2015	giant redtop	FACW	33.7%	western wheatgrass	FAC	19.8%	common threesquare	OBL	14.3%
	2017	giant redtop	FACW	39.3%	western wheatgrass	FAC	24.5%	broad-leafed cattail	OBL	9.5%
SGCS-5 ^b	2015	common threesquare	OBL	15.0%	giant redtop	FACW	14.9%	narrowleaf (coyote) willow	OBL	12.9%
	2017	giant redtop	FACW	21.8%	common threesquare	OBL	14.6%	broad-leafed cattail	OBL	14.6%
SGCS-7	2015	broad-leafed cattail	OBL	36.0%	giant redtop	FACW	29.7%	curly dock	FACW	3.0%
	2017	broad-leafed cattail	OBL	31.7%	giant redtop	FACW	29.5%	western wheatgrass	FAC	8.0%
SGCS-9	2015	broad-leafed cattail	OBL	51.3%	giant redtop	FACW	11.4%	Russian olive	FACW	9.4%
	2017	broad-leafed cattail	OBL	42.8%	giant redtop	FACW	30.2%	Russian olive	FACW	7.1%

Table C-3.2-2 (continued)

Transect	Year	Species Rank 1			Species Rank 2			Species Rank 3		
		Species ^a	Indicator Status	Composition	Species ^a	Indicator Status	Composition	Species ^a	Indicator Status	Composition
SGCS-11	2015	broad-leafed cattail	OBL	47.6%	giant redbtop	FACW	13.0%	narrowleaf (coyote) willow	OBL	9.4%
	2017	broad-leafed cattail	OBL	44.5%	giant redbtop	FACW	17.5%	water sedge	OBL	12.5%
SGCS-12	2015	broad-leafed cattail	OBL	29.2%	narrowleaf (coyote) willow	OBL	27.9%	ponderosa pine	FACU	9.9%
	2017	broad-leafed cattail	OBL	40.7%	narrowleaf (coyote) willow	OBL	29.0%	ponderosa pine	FACU	7.4%
SGCS-14	2015	narrowleaf (coyote) willow	OBL	25.8%	broad-leafed cattail	OBL	21.4%	ponderosa pine	FACU	21.2%
	2017	broad-leafed cattail	OBL	24.3%	narrowleaf (coyote) willow	OBL	22.7%	ponderosa pine	FACU	19.7%
SGCS-16	2015	broad-leafed cattail	OBL	23.5%	yellow sweet clover	FACU	13.7%	ponderosa pine	FACU	11.6%
	2017	broad-leafed cattail	OBL	24.3%	western wheatgrass	FAC	18.5%	giant redbtop	FACW	11.1%
SGCS-19	2015	giant redbtop	FACW	30.1%	yellow sweet clover	FACU	13.5%	hardstem bulrush	OBL	8.6%
	2017	giant redbtop	FACW	26.2%	common threesquare	OBL	18.7%	softstem bulrush	OBL	17.5%
SGCS-20	2015	giant redbtop	FACW	25.9%	broad-leaf cattail	OBL	14.1%	Torrey's rush	FACW	7.5%
	2017	broad-leafed cattail	OBL	21.2%	giant redbtop	FACW	20.7%	hardstem bulrush	OBL	15.8%
SGCS-21	2015	Torrey's rush	FACW	22.1%	wedge sedge	OBL	15.1%	yellow sweet clover	FACU	13.8%
	2017	common threesquare	OBL	32.4%	giant redbtop	FACW	18.1%	western wheatgrass	FAC	12.2%

Note: Table omits nonvegetative categories: algae, logs, litter, bare ground, water.

^a Common name used

^b Baseline surveyed conducted in 2015.

Table C-3.3-1
2015 to 2017 Vegetation Survey Transect Length and Percentage of Obligate Zone

Transect	Year	Total Transect Length (ft)	Obligate Zone Length (ft)	Percent of Transect in the Obligate Zone
SGCS-3A*	2015	195.1	16.4	8.4%
	2017	195.0	20.3	10.4%
SGCS-3B*	2015	206.1	54.3	26.3%
	2017	205.9	110.5	53.7%
SGCS-4	2015	178.9	47.4	26.5%
	2017	178.7	48.1	26.9%
SGCS-5*	2015	220.7	85.0	38.5%
	2017	220.2	89.6	40.7%
SGCS-7	2015	194.9	112.7	57.8%
	2017	194.6	118.8	61.0%
SGCS-9	2015	205.0	147.7	72.0%
	2017	206.2	148.2	71.9%
SGCS-11	2015	196.9	161.0	81.8%
	2017	196.9	141.4	71.8%
SGCS-12	2015	125.7	87.9	69.9%
	2017	126.6	87.2	68.9%
SGCS-14	2015	127.8	88.9	69.6%
	2017	127.9	91.9	71.9%
SGCS-16	2015	123.9	58.9	47.5%
	2017	124.1	65.5	52.8%
SGCS-19	2015	137.2	78.3	57.1%
	2017	137.2	80.3	58.5%
SGCS-20	2015	111.6	65.1	58.3%
	2017	111.8	69.5	62.2%
SGCS-21	2015	93.5	49.7	53.2%
	2017	93.5	54.0	57.8%

* Baseline surveyed conducted in 2015.

Table C-3.3-2
2015 to 2017 Comparison of Canopy Cover to the Vegetative and
Nonliving Presence along Transects in Obligate and Non-Obligate Zones

Transect	Year	Obligate Zone				Non-Obligate Zone		
		Vegetative Canopy Cover	Obligate Occurrence	Vegetative Presence	Non-Vegetative Presence ^a	Vegetative Canopy Cover	Vegetative Presence	Non-Vegetative Presence ^a
SGCS-3A ^b	2015	168.9%	83.5%	100.0%	0.0%	104.5%	92.3%	7.6%
	2017	168.0%	100.0%	100.0%	0.0%	140.6%	96.8%	3.2%
SGCS-3B ^b	2015	219.8%	60.9%	96.4%	3.6%	113.1%	93.1%	6.9%
	2017	250.6%	40.1%	99.9%	0.1%	171.9%	98.2%	1.8%
SGCS-4	2015	226.1%	85.7%	97.2%	2.8%	133.5%	95.0%	5.0%
	2017	228.7%	73.4%	100.0%	0.0%	160.6%	97.4%	2.6%
SGCS-5 ^b	2015	264.7%	99.3%	100.0%	0.0%	111.8%	93.2%	6.8%
	2017	325.4%	100.0%	100.0%	0.0%	163.7%	97.8%	2.2%
SGCS-7	2015	130.3%	81.2%	89.8%	10.2%	104.7%	87.1%	12.9%
	2017	150.7%	83.7%	98.8%	1.2%	163.6%	95.7%	4.3%
SGCS-9	2015	116.9%	97.4%	100.0%	0.0%	187.8%	100.0%	0.0%
	2017	161.1%	97.8%	100.0%	0.0%	171.0%	99.0%	1.0%
SGCS-11	2015	128.0%	92.0%	100.0%	0.0%	115.3%	80.7%	19.3%
	2017	123.8%	100.0%	100.0%	0.0%	127.7%	86.5%	13.5%
SGCS-12	2015	133.2%	96.8%	99.2%	0.8%	110.3%	87.1%	12.9%
	2017	153.8%	100.0%	100.0%	0.0%	104.1%	85.6%	14.4%
SGCS-14	2015	131.8%	92.9%	94.9%	5.1%	153.7%	98.1%	1.9%
	2017	135.8%	83.7%	96.1%	3.9%	135.0%	98.4%	1.6%
SGCS-16	2015	147.5%	100.0%	95.1%	4.9%	147.7%	96.6%	3.4%
	2017	143.4%	97.3%	100.0%	0.0%	191.5%	100.0%	0.0%
SGCS-19	2015	190.5%	61.2%	96.5%	3.5%	96.4%	80.9%	19.1%
	2017	294.8%	96.8%	99.7%	0.3%	134.3%	97.8%	2.2%
SGCS-20	2015	191.9%	67.4%	97.7%	2.3%	60.7%	54.3%	45.7%
	2017	289.1%	100.0%	100.0%	0.0%	99.3%	80.8%	19.2%
SGCS-21	2015	216.1%	75.9%	98.2%	1.8%	114.4%	84.9%	15.1%
	2017	189.3%	98.3%	99.1%	0.9%	149.6%	99.0%	1.0%

^a Nonvegetative categories: algae, logs, litter, bare ground, water.

^b Baseline surveyed conducted in 2015.

**Table C-3.4-1
2017 Wetland Vegetation Zone Summary**

Zone Name	2016 Area (m²)	2017 Area (m²)	% Change	Comments
West Cattail	646	760	+17.6%	Expansion of meadow cattail populations and new growth onto flood stage channel surface.
Cattail/Willow	2023	2251	+11.2%	Continued growth of willow populations within cattail dominated areas, specifically in the northeast (downstream) section of the wetland.
Central Cattail	10623	10155	-4.4%	Continued growth of willow populations within cattail dominated areas, specifically in the northeast (downstream) section of the wetland.
GCS Vegetation	1298	1185	-8.7%	Southeastward (downstream) expansion of cattails toward the GCS structure.
North Willow	1474	1585	+7.5%	Willows continue to advance further into central cattail area, as well as upslope on the northern wetland margin.
Sum Area of zones	16065	15936	n/a	Differences in 'sum of areas' and 'total wetland area' are a result of overlap between the GCS, Central cattail, and Mixed areas.
Total wetland area*	14981	15356	+2.5%	Total wetland areal coverage continues to increase.

* Calculated to include the total coverage of overlapping zones

Attachment C-1

*2016 and 2017 Photographs
of Sandia Wetland Vegetation Monitoring*

C1-1



Photo C1-1 SGCS-3A baseline photograph looking north; (left) September 2016 and (right) August 2017

C1-2



Photo C1-2 SGCS-3B baseline photograph looking south; (left) September 2016 and (right) August 2017



Photo C1-3 SGCS-4 photographs looking north; (left) September 2016 and (right) August 2017

C1-4



Photo C1-4 SGCS-5 baseline photograph looking north; (left) September 2016 and (right) August 2017

C1-5



Photo C1-5 SGCS-7 photographs looking south; (left) September 2016 and (right) August 2017

C1-6



Photo C1-6 SGCS-9 photographs looking north; (left) September 2016 and (right) August 2017



Photo C1-7 SGCS-11 photographs looking north; (left) September 2016 and (right) August 2017



Photo C1-8 SGCS-12 photographs looking north; (left) September 2016 and (right) August 2017



Photo C1-9 SGCS-14 photographs looking north; (left) September 2016 and (right) August 2017



Photo C1-10 SGCS-16 photographs looking north; (left) September 2016 and (right) August 2017

C1-10

C1-11



Photo C1-11 SGCS-19 photographs looking north, upstream of sheet pile 1; (left) September 2016 and (right) August 2017



Photo C1-12 SGCS-20 photographs looking north, between sheet pile 1 and 2; (left) September 2016 and (right) August 2017



Photo C1-13 SGCS-21 photographs looking north, upstream of sheet pile 3; (left) September 2016 and (right) August 2017

Attachment C2

*2017 Vegetation Survey Data
(on CD included with this document)*

Attachment C-3

*2017 Rank Order of Percent Canopy Cover and
Individual Species Composition Summary Tables
(on CD included with this document)*

Appendix D

Geochemical and Hydrologic Monitoring in Sandia Canyon

CONTENTS

D-1.0 INTRODUCTION	D-1
D-2.0 ANALYTICAL RESULTS FROM SURFACE WATER GAGING STATIONS E121, E122, AND E123	D-1
D-2.1 Screening Surface and Storm Water to Surface Water Quality Criteria.....	D-5
D-3.0 ANALYTICAL RESULTS FROM ALLUVIAL SYSTEM	D-6
D-3.1 Non-redox Sensitive Species	D-7
D-3.2 Redox Sensitive Species	D-7
D-3.3 Screening Alluvial Groundwater Results to Groundwater Standards.....	D-9
D-4.0 WATER-LEVEL RESULTS FROM ALLUVIAL SYSTEM	D-10
D-5.0 REFERENCES	D-11

Figures

Figure D-2.0-1	Time-series plot showing chloride concentrations at gaging stations E121 and E123 and National Pollutant Discharge Elimination System– (NPDES-) permitted Outfall 001.....	D-13
Figure D-2.0-2	Time-series plot showing nitrate plus nitrite as nitrogen concentrations at gaging stations E121 and E123 and NPDES Outfall 001.....	D-13
Figure D-2.0-3	Time-series plot showing silicon dioxide concentrations and TDS at gaging stations E121 and E123 and NPDES Outfall 001.....	D-14
Figure D-2.0-4	Time-series plot showing manganese concentrations at gaging stations E121 and E123.....	D-14
Figure D-2.0-5	Time-series plot showing total chromium and Cr(VI) concentrations at gaging stations E121 and E123.....	D-15
Figure D-2.0-6	Time-series plots from 2010 to 2017 showing discharge at E121, E122, and E123 and total discharge from Outfalls 001, 03A027, and 03A199; solid black horizontal lines indicate approximate base flow discharge at the surface-water gaging stations, which vary throughout the 8-yr period.....	D-17
Figure D-2.0-7	Box-and-whisker plots of peak discharge, TSS/SSC, PCBs, unfiltered chromium and Cr(VI), and PAHs for base flow and storm flow at gaging stations E121, E122, and E123, pre- and post-construction of the GCS, respectively, in 2015, 2016, and 2017	D-18
Figure D-2.0-8	Hydrographs of storm water discharge at E121, E122, and E123 during each sample-triggering storm event in 2017	D-20
Figure D-2.0-9	Storm- and base flow discharge correlations with SSC, total PCBs, total chromium, and total PAHs from 2014 to 2017 at E121, E122, and E123 with standardized residual outliers removed; the red dashed lines are 2 times the standard error (2×SE) of the estimate, as noted with the equation of the line and the Pearson's correlation coefficient (R^2).....	D-23
Figure D-2.0-10	Annual mass flux (top) and annual mass flux normalized by runoff volume (bottom) for sediment at gaging stations E121 (blue), E122 (orange), and E123 (green) from 2014 to 2017	D-25

Figure D-2.0-11	Annual mass flux (top) and annual mass flux normalized by runoff volume (bottom) for total PCBs at gaging stations E121 (blue), E122 (orange), and E123 (green) from 2014 to 2017	D-26
Figure D-2.0-12	Annual mass flux (top) and annual mass flux normalized by runoff volume (bottom) for total chromium at gaging stations E121 (blue), E122 (orange), and E123 (green) from 2014 to 2017	D-27
Figure D-2.0-13	Annual mass flux (top) and annual mass flux normalized by runoff volume (bottom) for total PAHs at gaging stations E121 (blue), E122 (orange), and E123 (green) from 2014 to 2017	D-28
Figure D-3.0-1	Chloride concentrations in Sandia wetland surface water and alluvial system	D-29
Figure D-3.0-2	Sulfate concentrations in Sandia wetland surface water and alluvial system	D-30
Figure D-3.0-3	Sulfide concentrations in Sandia wetland surface water and alluvial system	D-31
Figure D-3.0-4	Iron concentrations in Sandia wetland surface water and alluvial system	D-32
Figure D-3.0-5	Manganese concentrations in Sandia wetland surface water and alluvial system....	D-33
Figure D-3.0-6	Ammonium concentrations in Sandia wetland surface water and alluvial system	D-34
Figure D-3.0-7	Arsenic concentrations in Sandia wetland surface water and alluvial system	D-35
Figure D-3.0-8	Chromium concentrations in Sandia wetland surface water and alluvial system.....	D-36
Figure D-4.0-1	Water levels recorded by sondes located in the alluvial system plotted with precipitation data from the E121.9 weather station and total daily volume of flow in surface water gaging station E121 in 2016 and 2017	D-37
Figure D-4.0-2	Time series of water level and temperature in alluvial system in 2016 and 2017	D-38

Tables

Table D-2.0-1	Travel Time of Flood Bore, Peak Discharge, Increase or Decrease in Peak Discharge, and Percent Change in Peak Discharge from Upgradient to Downgradient of the Wetland for Each Sample-Triggering Storm Event in 2017	D-39
Table D-2.0-2	Calculated Sediment Yield and Runoff Volume at Gaging Stations E121, E122, and E123 for Each Sample-Triggering Storm Event from 2014 to 2017	D-40
Table D-2.1-1	Analytical Exceedances in Surface Water at Gaging Stations E121, E122, and E123.....	D-43
Table D-2.1-2	Summary of 2017 Base Flow and Storm Water SWQC Exceedances	D-46
Table D-3.4-1	Analytical Exceedances in the Alluvial System	D-47

D-1.0 INTRODUCTION

The geochemical and hydrologic analytical results from performance monitoring of the Sandia wetland are presented and evaluated herein (Appendix F contains all the analytical and hydrologic data). Construction and subsequent revegetation of the Sandia grade-control structure (GCS) and the implementation of monitoring were undertaken by Los Alamos National Laboratory (LANL or the Laboratory) not with the objective of reducing concentrations of contaminants in water to specific values; therefore, the comparison between analytical results and water-quality standards or other criteria presented in sections D-2.1 and D-3.4 are not for the purpose of evaluating compliance with regulatory requirements.

D-2.0 ANALYTICAL RESULTS FROM SURFACE WATER GAGING STATIONS E121, E122, AND E123

As noted in the baseline performance report (LANL 2014, 257590), similar base flow chemistry for many constituents between upgradient and downgradient locations indicates a relatively short residence time for surface water and little interaction (exchange) with alluvial groundwater. This finding is evident for chloride, nitrate plus nitrite, and silica, which are indicators of water quality in outfall discharge in the context of chemistry from Outfall 001 (Figures D-2.0-1 to D-2.0-3). Improvements in water chemistry discharged from Outfall 001 are obvious for chloride and silica (as inferred from concentrations at E121) and also for total dissolved solids (TDS), a general indicator of water quality in outfall discharge (Figures D-2.0-1 to D-2.0-3). Manganese, a sensitive redox indicator, is discussed because this base flow constituent shows some evidence for temporal trends (Figure D-2.0-4). Hexavalent chromium, also a contaminant of concern along with total chromium, is also discussed (Figures D-2.0-5). Base flow and storm flow data for three key contaminants associated with wetland sediments, polychlorinated biphenyls (PCBs), chromium, and polycyclic aromatic hydrocarbons (PAHs) are discussed below.

In terms of indicators of improved water quality associated with the Sanitary Effluent Reclamation Facility (SERF) expansion, concentrations have continued to stabilize in 2017 with no strong base flow temporal concentration trends for filtered chloride and nitrate (Figures D-2.0-1 and D-2.0-2, respectively). However, the patterns observed post-SERF expansion (August 2012) are similar at both gaging stations and Outfall 001 (Figures D-2.0-1 and D-2.0-2). Interestingly, nitrate has consistently lower concentrations at gaging station E123 relative to station E121 (Figure D-2.0-2). This finding is expected because nitrate is not only a water-quality indicator, it is also a plant nutrient and a redox-sensitive species that may be reduced and assimilated during surface water transport through the wetland. The peak increases in nitrate at the Outfall 001 are reflected in base flow nitrate concentrations (Figure D-2.0-2). These increases are likely related to an increase in Sanitary Waste Water System (SWWS) nitrate-containing effluent in Outfall 001 water until March 2016, however, the reason for the peak in late 2016 is unclear. Surface water base flow silicon dioxide concentrations are plotted in Figure D-2.0-3. TDS is also plotted as a general indicator of water quality associated with outfall discharge. The effect of the SERF expansion on both parameters is represented by a clear drop in concentration (Figure D-2.0-3).

Among redox-sensitive species, dissolved manganese in base flow at gaging station E123 appears to be showing overall improvement in water quality through time (Figure D-2.0-4). The cause of periodic spikes in manganese concentrations at E123 is not clear. Following completion of the GCS, manganese concentrations have remained generally lower. Manganese at E123 could represent either colloidal Mn(IV) and/or dissolved Mn(II). Manganese in alluvial groundwater will tend to be present as mobile Mn(II) and, given the slow oxidation kinetics, may not fully oxidize to less soluble Mn(IV) in the time between alluvial groundwater surfacing (at the headcut pre-GCS or at the upper impermeable wall post-GCS) and reaching gaging station E123 immediately downstream. Generally, lower manganese concentrations post-GCS are likely the result of some combination of cessation of headcutting at the

terminus of the wetland, which would reduce colloidal transport of Mn(IV), and altered alluvial groundwater dynamics, which could affect Mn(II) concentrations and oxidation kinetics. Because the wetland is still saturated (section D-4.0), it is unlikely that trends in manganese concentrations at downstream gaging station E123 reflect changes in redox conditions within the wetland. Further monitoring may explain the cause of the overall decrease through time. Dissolved concentrations of manganese are consistently higher at gaging station E123 relative to E121 because alluvial groundwater in the wetland has high manganese concentrations, probably as Mn(II) and possibly because of colloidal transport of Mn(IV). Greater mobilization of Mn(IV) colloids during construction of the GCS could account for the large spike in manganese concentration before the GCS was completed (Figure D-2.0-4).

Background concentrations of approximately 5–6 µg/L Cr(VI) occur in regional aquifer waters (LANL 2007, 095817). Because potable water is derived from the regional aquifer, it provides a starting point for expected concentrations of Cr(VI) in sanitary waste water before modifications occur at SWWS, SERF, or the cooling towers where potable water is used. Water from Outfall 03A027 analyzed for Cr(VI) in September 2015 showed a concentration of 6.41 µg/L (unfiltered), and the result falls within expected values for potable water. Cr(VI) has been detected in unfiltered samples at gaging station E121 with values up to 7.76 µg/L in May 2016. At E123, most values of Cr(VI) have been below or at the detection limit, with the highest measured value of 1.33 µg/L with a detection limit at 1 µg/L. In 2017 there were three detected Cr(VI) values as the minimum detection limit was lowered to 0.152 µg/L but all values were below 1 µg/L. Hexavalent chromium shows evidence of attenuation as it is transported through the wetland; multiple detections of Cr(VI) at E121 tend to become nondetections by the time they reach gaging station E123 (Figure D-2.0-5).

Surface water at gaging stations E121, E122, and E123 is perennial; thus, the results for primary contaminants PCBs, chromium, and PAHs are separated into base flow and storm flow components. Figure D-2.0-6 shows the discharge measured at E121, E122, and E123 from 2010 to 2017 and the varying base flow at each station during this period. This figure also shows the total discharge from the three outfalls and the influence of discharge on each gaging station, particularly E121 and E123. For both base flow and storm flow, box-and-whisker plots of peak discharge, suspended sediment concentration (SSC)/total suspended sediments (TSS), PCBs, chromium, and PAHs are presented in Figure D-2.0-7.

SSC, PCBs, chromium, and PAHs are discussed in the context of peak discharge and are used as key parameters to track the performance of the GCS. Results from gaging stations E121 and E122, which monitor most of the surface water flow into the wetland, and gaging station E123, which monitors surface water flow out of the wetland, are plotted together to show changes in surface water discharge and chemistry from upgradient to downgradient of the wetland (Figure D-2.0-7). These plots show the range of concentrations and represent a historical baseline before GCS construction (pre-GCS), during the first year of performance monitoring after GCS construction (post-GCS), and in 2015, 2016, and 2017. Multiple years of data are needed to fully delineate the performance metrics for the GCS.

In Figure D-2.0-7, storm flow discharge is expectedly greater than base flow discharge for all the gaging stations. At E121 and E123, base flow discharge is highly dependent on the outfall effluent discharge rate (Figure D-2.0-6); thus, the reduction in this rate from pre- to post-GCS and the seasonal fluctuations in this rate in 2015, 2016, and 2017 are reflected in the base flow discharge, more so at E121 than at E123 because of the damping effect of the wetlands on the discharge. Gaging station E122 base flow discharge is fairly stable throughout the years, although it reduced slightly in 2017. One of the objectives of the GCS is to reduce the peak discharge of the storm flow, which can cause erosion and thus movement of contaminants. The storm flow peak discharge from upstream (E121 and E122) to downstream (E123) of the GCS was reduced post-GCS, in 2015, 2016, and 2017. It is also important to note that precipitation in 2015, 2016, and 2017 was generally less intense than in 2013 and 2014, thus possibly attributing to the

reduction in storm flow peak discharge. However, the wetland alone attenuates the storm flow peak discharge, as can be noted during pre-GCS conditions.

Hydrographs for the 7 sample-triggering storm events recorded at E121, E122, and E123 from June 6 to August 21, 2017, are presented in Figure D-2.0-8. During these storm events, tributaries downstream of E121 and E122 can contribute significant flow. Table D-2.0-1 presents the timing of the transmission of flood bore, or peak, from E121 and E122 downstream to E123. In 2017, the average time of transmission from E121 to E123 and from E122 to E123 is approximately 76 min and 72 min, respectively. This finding indicates storm water from both upgradient stations flows through the wetland in approximately the same amount of time and quite rapidly, although not as rapidly as during 2014 (approximately 40-min average travel time between E121 and E122 to E123) when precipitation events were more intense.

In Figure D-2.0-7, the sediment content in base flow is lower than storm flow, significantly so for TSS (compare pre-GCS TSS for base flow and storm flow) and slightly so for SSC. This is typical for storm water because of the greater erosive energy associated with the increase in discharge. Note that base flow was sampled for TSS pre-GCS and SSC beginning in 2016, and storm flow was sampled for TSS pre-GCS and SSC post-GCS on. As expected, storm flow SSC at E121 and E122 is not significantly different pre- to post-GCS; however, at E123, storm flow SSC is significantly reduced after construction of the GCS and continues to remain low through 2016, possibly because of a cessation of headcutting at the terminus of the wetland. This reduction is noteworthy because contaminants in the wetland are strongly sorbed to sediments, and a reduction in SSC should be associated with a reduction in contaminant migration. In 2017, there was a fairly intense storm event (1 inch in 30 mins) centered over Sandia and Mortandad Canyons on July 26. The intensity of the July 26 storm contributed to high SSCs during the storm, but SSCs during the remainder of 2017 were consistent with SSCs measured during 2015 and 2016. In 2015, 2016, and 2017, sediment content at E121 and E122 is less than that measured during the pre- or post-GCS period. This result is most likely because of the lack of more intense precipitation and erosive runoff during these years.

The box-and-whisker plots in Figure D-2.0-7 indicate that PCB and total chromium concentrations in both base flow and storm flow at E123 are significantly reduced since the GCS was constructed. While PCB and total chromium concentrations in base flow and storm flow were significantly higher downgradient of the wetland (relative to upgradient locations E121 and E122) before the GCS was built, the concentrations are closer in magnitude upgradient and downgradient of the wetland since the GCS was constructed. The trend in PCBs and total chromium concentrations at all of the gaging stations, both in base flow and storm flow, indicate a general decrease over the past 7 yr or so, with a slight increase in 2017 in storm flow. The trends in PCBs and total chromium at E123 may be a result of continued growth of wetland vegetation, corresponding to stabilization of the sediment (Appendixes B and C); however, the decreasing trend at the upgradient locations may be a result of less intense precipitation and erosive runoff during the years following construction of the GCS. In 2017, the intense storm event on July 26 had high PCB and total chromium concentrations in storm flow, thus contributing to the slight increasing trend between 2016 and 2017.

Total PAH was computed using the 18 most prominent PAHs, and nondetections were considered zero. PAHs were not analyzed in base flow or storm flow before the GCS was built. In base flow, all total PAH results were nondetections, with the exception of one sample collected at E123 in 2016 and one sample collected at E121 in 2017, and for which the total PAH concentrations were significantly lower than in storm flow. In storm flow, total PAH concentrations are similar upgradient and downgradient of the wetland. Overall, higher concentrations of PAHs were detected at E122 than at E121 and E123, suggesting the influence of the former asphalt batch plant near the northern fork of upper Sandia Canyon is still evident and is the most likely source of PAHs at the downstream gaging station, E123, because the low concentrations of PAHs at E121 do not indicate a source.

Fairly consistent correlations exist between SSC, total PCBs, total chromium, total PAHs, and discharge, as presented in Figure D-2.0-9. Correlations show that as discharge increases, the concentrations of these constituents increase. There are exceptions to this regular correlation (e.g., E121 for SSC and E122 for total chromium). In general, however, these relationships show that discharge is a good indicator of sediment and associated contaminant transport. The relationships shown in Figure D-2.0-9 were obtained after removing data points when the ISCO sampler malfunctioned and removing outliers using the standardized residual outlier method. These relationships were used to calculate the mass flux as follows. The line of best fit was used to calculate the approximate concentrations of sediment, total PCBs, total chromium, and total PAHs every 5 min using the following:

$$y_{n,i} = m_n x_i + b_n \quad \text{Equation D-1}$$

where $y_{n,i}$ is the calculated concentration of each constituent n every 5 min or time step i ; n = SSC, total PCBs, total chromium, or total PAHs; x_i is the discharge at each time step i ; and m_n and b_n are each constituent's linear equation parameters (slope and y-intercept, respectively). The annual mass flux was then computed as the area under the 5-min concentration curve multiplied by the discharge:

$$\text{mass flux}_{x_n} = \sum_{i=1}^I \left(\frac{y_{n,i+1} + y_{n,i}}{2} \right) * (t_{i+1} - t_i) * x_i \quad \text{Equation D-2}$$

where t_i is the time of the discharge measurement at time step i and the annual mass flux was computed as the sum of the mass for calendar years 2014 through 2017.

Figures D-2.0-10 through D-2.0-13 show the estimated annual mass flux from 2014 to 2017 at each gaging station for sediment, total PCBs, total chromium, and total PAHs, respectively. Also shown in these figures is the annual mass flux normalized by annual runoff volume for each constituent. Sediment flux into the wetland is greater than the sediment flux out, which was also observed in the SSC box plots in Figure D-2.0-7, and indicates sediment is no longer being moved near the former headcut and the GCS is performing well. According to the normalized plots, storm water runoff from the E121 watershed is more sediment-laden than runoff from the E122 or E123 watersheds, again indicating a reduction in sediment load through the wetland.

Total PCB and chromium flux out of the wetland is slightly greater than the PCB and chromium flux into the wetland in 2014, 2015, and 2017, suggesting a small amount of PCBs and Cr(III) is being entrained in the surface water through the wetland. In 2016, this trend was reversed, most likely because of the lack of intense storm events during 2016. The absence of any clear, continuing trend in PCB or chromium flux at E123 may be an indication that the wetland has stabilized after construction of the GCS. E121 also has no clear trend in PCB or chromium flux over time. PCB and chromium flux at E122 has remained fairly stable over time. The total PCBs wetland inventory [the sum of 5.5 kg, 3.3 kg, 31.1 kg, and 24.4 kg for Aroclor-1242, Aroclor-1248, Aroclor-1254, and Aroclor-1260, respectively (LANL 2009, 107453), see section 1.1] is plotted in Figure D-2.0-11. Note that Aroclors were used to compute the total PCBs inventory, while congeners were used to compute the annual mass flux. Thus, they are not directly comparable; but, the wetland inventory provides perspective on the magnitude of annual flux of PCBs into and out of the wetland. The total chromium wetland inventory (approximately 15,000 kg of chromium as Cr(III) [LANL 2009, 107453], see section 1.1) is plotted in Figure D-2.0-12. Note that the inventory is computed for Cr(III) while the total chromium concentrations were used to compute the annual mass flux. Thus, they are not directly comparable; but, the wetland inventory provides perspective on the magnitude of annual flux of chromium into and out of the wetland. Also, most of the chromium in the wetland exists as Cr(III) (section 1.6.3); thus, this comparison is reasonable.

PAH flux out of the wetland is slightly greater than the PAH flux into the wetland, indicating a small amount of PAHs is being entrained in the surface water through the wetland. Note that the relationships

between total PAHs and discharge, which is the foundation of the mass flux calculations, are not very good for E121 or E123; thus, there is significant uncertainty associated with the flux.

In addition to using the relationship between SSC and discharge to estimate annual sediment flux, the actual sediment flux for each sampled storm event was also computed using SSC measurements (Table D-2.0-2). The relationship between sediment volume and runoff volume for storm flow tends to be a stronger relationship than sediment volume and peak discharge, and for all of upper Sandia Canyon this relationship is $R^2=0.54$:

$$\text{sediment volume} = 0.153 * \text{runoff volume}^{1.227} \quad \text{Equation D-3}$$

D-2.1 Screening Surface and Storm Water to Surface Water Quality Criteria

Base flow and storm water collected and analyzed in 2017 at gaging stations E121, E122, and E123 were screened against the appropriate surface water–quality criteria (SWQC) in 20.6.4.900 New Mexico Administrative Code. Chronic aquatic life criteria for hardness-dependent metals (i.e., aluminum, cadmium, copper, lead, and zinc) were calculated using concurrent hardness values for samples collected for storm water and average hardness values for base flow.

Sample results that exceed SWQC are presented in Table D-2.1-1. Base flow exceedances were observed for total PCBs and zinc. Exceedances in storm water were observed for aluminum, copper, gross alpha, lead, total PCBs, and zinc.

The Sandia wetland receives urban runoff water from developed areas within Technical Area 03 (TA-03) at the Laboratory, which impacts water-quality results from E121 and E122. Developed areas in and around the Laboratory are documented sources of contaminants exceeding SWQC, including aluminum, copper, lead, zinc, and PCBs, as determined by storm water runoff monitoring (LANL 2012, 219767; LANL 2013, 239557). Therefore, exceedances of SWQC for these constituents at E121 and E122 are likely partially derived from these developed areas within TA-03. In addition, E121 and E122 may be influenced by historical releases from solid waste management units (SWMUs) upgradient of these monitoring locations.

Gaging station E123 is located at the lower terminus of the Sandia wetland. Base flow water at E123 is composed of outfall discharges upstream of E121 and E122 and any exchange between the alluvial aquifer and surface water flowing through the Sandia wetland. Storm flow at E123 is composed of outfall discharges upstream of E121 and E122 and storm water runoff from urban areas that drain the watersheds surrounding the Sandia wetland during precipitation events. Storm water flows through the Sandia wetland where the sediment-bound contaminant inventory may be entrained and contribute to the chemical signature of the water collected at E123. Comparing results from E121 and E122 with E123 is useful in evaluating exceedances to determine if the Sandia wetland may be a source of constituents exceeding SWQC. Table D-2.1-2 provides summary statistics for each analyte exceeding SWQC for all three gaging stations, E121, E122, and E123, in the respective media (base flow or storm water) in 2017.

Table D-2.1-2 shows that the maximum exceedance result for filtered aluminum at E123 is greater than E121 and E122 for storm water. Aluminum is not a contaminant of concern associated with the Sandia wetland (LANL 2011, 203454), and is considered to be associated with the natural background geology. LANL studies of storm water runoff at background reference watersheds on the Pajarito Plateau have shown that aluminum frequently exceeds SWQC and is thought to be derived from weathered Bandelier Tuff. Bandelier Tuff is a major geologic unit that forms the mesas and canyons on the Pajarito Plateau (LANL 2013, 239557). Mineral-bound aluminum is associated with poorly crystalline volcanic silica glass of Bandelier Tuff and, as the tuff weathers, the glass particles and associated aluminum-rich sediments are

entrained and transported by storm water runoff. Aluminum exceedances observed at E123 are most likely derived from Bandelier Tuff that form the hillslopes and side drainages surrounding the Sandia wetland.

Historically, the highest values of filtered copper were most often observed in storm water runoff at E121 and E122. In 2017, the average of the SWQC exceedances of copper at E121, E122, and E123 were approximately equivalent, ranging from 7.07 µg/L at E123 to 8.49 µg/L at E121. Gaging station E122 reported the highest maximum concentration (11.2 µg/L), suggesting copper in the wetlands is derived from the urban runoff from parking lots, roads, and buildings in TA-03.

Copper, lead, and zinc concentrations in storm water at E123 are generally the same or less than at E121 and E122. The Sandia wetland has not proven to be a source of the copper, lead, and zinc, and generally the average SWQC exceedances observed at E123 are less than those observed at E121 and E122. Zinc, which exceeded SWQC at E121 and E122 did not exceed SWQC at E123, indicating that zinc is attenuated as storm water flows through the wetland.

PCBs, historically used in hundreds of industrial and commercial applications in developed environments in the United States, are a common constituent in storm water discharging from developed environments. However, the maximum concentrations of PCBs at E121 and E122 are less than E123 for base flow and storm water, indicating the Sandia wetland may be a source of PCBs. The Sandia wetland contains a known inventory of PCBs as a result of historic spills at SWMU 03-056(c), a former transformer storage area. SWMU 03-056(c) is located just upgradient of E121, and PCB sediments from the SWMU may still be influencing the concentrations of PCBs at E121. Figure D-2.0-7 shows box plots of PCBs concentrations in storm water at E121, E122, and E123 for 2017 and the previous 5 yr. The plots show PCB concentrations within the range of historical data since the GCS was installed at all three gaging stations.

One sample exceeded SWQC for gross alpha at E123 on July 26, 2017. This was an intense storm event (1.0 in/30 min) and the suspended sediment concentration for a sample collected at the same time was 2,000 mg/L, indicating a turbid sample. Bandelier Tuff contains uranium and thorium, and gross alpha radioactivity concentrations in storm water are most likely derived from these alpha emitters (LANL 2013, 239557).

D-3.0 ANALYTICAL RESULTS FROM ALLUVIAL SYSTEM

Selected analytical results for water chemistry time-series data (filtered) from the alluvial sampling array are presented in Figures D-3.0-1 to D-3.0-8. Time-series plots are presented in the relative spatial distribution of the wells in the wetland (i.e., the upper plots are from the most northerly wells in each transect, ordered from west to east; the middle set of plots are from wells in the center of each transect, again ordered from west to east; and bottom plots are from the southernmost wells in each transect, in the same orientation) comprising four transects running north to south and spread out along the length of the wetland. Additionally, data for surface water entering the wetland at gaging station E121 and exiting the wetland at gaging station E123 are plotted at the western and easternmost parts of the wetland, respectively, serving as a comparison of input and output base flow chemistry. Differences between base flow data and alluvial groundwater data may indicate subsurface processes (e.g., reduction) and provide information about residence times in the alluvial system. Key analytes plotted include a major conservative anion (chloride); redox-sensitive species (sulfate, iron, manganese, ammonium, and sulfide); and key contaminants (dissolved arsenic and chromium) (Figures D-3.0-1 to D-3.0-8). Fe(II), As(III) and Cr(VI) speciated data were collected and are plotted along with the total iron, arsenic, and chromium, respectively (Figures D-3.0-4, D-3.0-7, and D-3.0-8).

D-3.1 Non-redox Sensitive Species

Species like chloride are not affected by the redox conditions of the wetland, providing information about changes in outfall chemistry and the connectivity between surface and alluvial groundwater. Chloride shows relatively constant concentrations at the wetland input and output surface water gaging stations. The chloride concentrations within the alluvial wells show some temporal variability with spikes in the February rounds, likely due to runoff from roads when salt is applied as a de-icing agent (Figure D-3.0-1). These spikes are most apparent in wells with more permeable sediment in the western most transect, SWA-2-4 and the wells of the eastern most transect, suggesting these locations are more strongly influenced by surface water infiltration.

D-3.2 Redox Sensitive Species

Redox sensitive species provide information on the degree of reduction happening in the wetland sediments. Concentrations of arsenic, manganese, iron, sulfide, and ammonium tend to be higher in the alluvial system than in surface water, indicating reducing conditions in the alluvial system. Conversely, sulfate, an oxidized species of sulfur, tends to be lower in the wetland than in surface water, also suggesting more reducing conditions in the alluvial system. Within the surface water system, concentrations at E121 and E123 are approximately the same for all redox sensitive species, other than Cr(VI) whose concentrations are lower at E123 (Figure D-3.0-8).

Most alluvial locations have lower sulfate concentrations than surface water input to the wetland, reflecting the strong reducing conditions in wetland sediments (Figure D-3.0-2). Locations with historically higher values of sulfate include: (1) SWA-1-2, which has coarse-grained and organic-poor sediment; (2) SWA-3-7 because of the shallow screening interval with the top of the screen at just 0.6 ft bgs compared to most wells in the wetland which are at least 3 ft bgs; and (3) SWA-4-10, SWA-4-11, and SWA-4-12, which were originally disturbed by the construction of the GCS. However, in the past few years, all locations, with exception of SWA-3-7, have observed a decrease and stabilization of sulfate concentrations, indicating increasingly reducing alluvial sediment conditions associated with the expansion of wetland vegetation and resaturation occurring at the head and terminus of the wetland. Locations SWA-2-5, SWA-2-6, and SWA-3-8 are particularly reducing based on lower sulfate concentrations relative to other locations. Location SWA-2-6 is in a very stagnant area based on observations of limited standing water with no apparent flow. Wells SWA-2-5 and SWA-3-8 are in or next to the central surface water flow path in the wetland but may be completed in tighter, more reducing sediments. The area of the easternmost transect was drier and more channelized before the GCS was constructed. Since the recovery from disturbance associated with the GCS, this transect has become more saturated and less channelized with the proliferation of vegetation, reflected in the observed decreases of sulfate, especially at SWA-4-10, indicating further stabilization of subsurface wetland conditions.

Sulfide, a reduced species of sulfur, has been detected throughout the wetland, further confirming the overall reducing nature of the system (Figure D-3.0-3). This is particularly clear when comparing sulfide concentrations in alluvial locations with those found in base flow where sulfide has not been detected. With sulfide near the bottom of the redox ladder, other species, including iron, arsenic, and chromium, are expected to be present primarily in their reduced forms, as observed in the speciated data (Figures D-3.0-4, D-3.0-7, and D-3.0-8). There appears to be a slight increase in sulfide at SWA-4-11 and SWA-4-12, this increasing trend is indicative of the stabilization of sediments and wetland conditions at the eastern-most transect post GCS construction. The lowest values of sulfide are observed at SWA-2-5 and SWA-2-6, however these locations seem to exemplify the most reducing conditions in the wetland through the other redox species. It's believed that sulfide may be precipitating because of the very reducing conditions such that dissolved sulfide is not present in the water samples.

Fe(II), the reduced form of iron, is the predominant form present in alluvial waters of the wetland, plotting on or just slightly below the total iron (Figure D-3.0-4). Total iron concentrations higher than Fe(II) are believed to be samples with colloidal Fe(III). There appears to be a drop in Fe(II) during the May 2017 round at multiple wells. Based on an unfavorable comparison between Fe(II) in a regular sample and its duplicate during this round at SWA-1-1 (the data were rejected), the Fe(II) results from the rest of this sampling round are considered suspect. A steady increase in iron concentrations over time is observed in SWA-1-3, SWA-2-6, SWA-3-7, and SWA-3-9. Increases in reduced iron suggest increases in reducing conditions. A stabilization of iron concentrations is observed in the easternmost downgradient transect over the last two years. The historically higher values for total iron in the easternmost transect are believed to be of colloidal iron, which has decreased as a result of the recovery from disturbance caused by the installation of the GCS, as suggested by other constituents.

All the locations appear to be strongly reducing with respect to manganese at the depth of screen completion (Figure D-3.0-5). Locations SWA-1-2 and SWA-1-3 have somewhat lower manganese concentrations, consistent with their shallow completion depths in sands and gravels. Small increasing trends of manganese were observed at SWA-3-7, SWA-3-8, and SWA-3-9 (Figure D-3.0-5). Most of the manganese is believed to be in its reduced form, with increases indicating increasing reducing conditions in alluvial sediment.

Ammonium concentrations are generally near or below the limit of detection in surface waters but are frequently detected in the alluvial system, confirming the reducing nature of wetland sediments (Figure D-3.0-6). Ammonium is stable under reducing conditions in the wetland and likely derives from mineralization of organic matter (e.g., dead cattail fronds). High concentrations of ammonium are not necessarily expected in the subsurface because of potential nutritive uptake by wetland plants. The stabilization and presence of ammonium over the last year in the wells of the easternmost transect and westernmost transect indicate the stabilization of sediment after the construction of the GCS, and the resaturation and greater presence of cattails at the head of the wetland, respectively.

Arsenic can exist as As(III) or As(V). As(III) is relatively mobile and should predominate under reducing conditions. As expected, within the range of analytical error, most of the total arsenic detected in analytical results from alluvial wells is As(III), confirming the reducing conditions of the wetland (Figure D-3.0-7). There is a decreasing trend in arsenic and As(III) through 2016 that suggests a reduction in mobility of the arsenic species as the reducing environment continues to persist and new inputs of organic matter that potentially bind arsenic accumulate (Wang and Mulligan 2006, 602277). However, in 2017 a continued decreasing trend in total arsenic is not observed and As(III) concentrations are not as similar to total arsenic concentrations as they had been previously. While the absolute variability in arsenic concentrations is small when comparing 2017 data to earlier data, these changes may reflect a change in analytical labs with a higher MDL for arsenic. The As(III) analyzed offsite at a different laboratory than that measuring total arsenic seems to follow the temporal decreasing trend in 2017. The discrepancy between total arsenic and As(III) is likely to be an analytical artifact as arsenic is further up on the redox ladder than sulfide which we observed in its reduced form in the wetland proper. However, if the quarterly data from last year is true, it's not an indication of oxidation of arsenic but of changes in incoming chemistry only observed at the input of the wetland, as the same increased trend of total arsenic is present at E121 (D-3.0-7).

Dissolved total chromium concentrations in the wetland alluvial system are quite high (the New Mexico Environment Department [NMED] groundwater standard for exceedance of chromium is 50 ppb [section D-3.4]) with significant spatial variation in chromium distribution, but predominantly reflects colloidal Cr(III) (Figure D-3.0-8). Given the colloidal nature of chromium, it is difficult to make meaningful spatial comparisons of total chromium, but locations SWA-1-2, SWA-1-3, SWA-4-10, and SWA-4-11 have higher concentrations on average, with the latter two, perhaps resulting from disturbance associated with

GCS construction in the easternmost transect. The reason for higher colloidal Cr(III) in the westernmost transect is not clear.

The concentrations of Cr(VI) measured in the alluvial system over the past 3 yr were nearly all at the detection limit or are nondetects (Figure D-3.0-8). The overall lack of Cr(VI) detections reflects the strong reducing conditions in the wetland. The highest detections of Cr(VI) concentration are at E121 and E122 with concentrations up to 11.5 µg/L in May 2015 at E122. These higher concentrations of Cr(VI) entering the wetland are believed to be from potable water derived from the regional aquifer and concentrated in the cooling towers (section D-2.0). There appear to be more Cr(VI) detects in alluvial groundwater during 2017; this increase is because of the lower minimum detection limit during 2017 (with a minimum detection level of 1 µg/L prior to May 2017 and 0.152 µg/L since May 2017). However, the values in the alluvial system are always significantly less than values at E121 and E122 suggesting that surface water infiltration is the source of the detects in the alluvial groundwater. E123, at the terminus of the wetland, has Cr(VI) below or just at the detection limit showing the great exchange and reduction in Cr(VI) as it passes through the wetland even when the concentrations are higher coming into the wetland.

D-3.3 Screening Alluvial Groundwater Results to Groundwater Standards

The alluvial system data from 2017 were screened to the levels required in the 2016 Compliance Order on Consent. Alluvial data were evaluated using the following screening process:

- Groundwater data are screened in accordance to Section IX of the Consent Order. For an individual substance, the lower of the New Mexico Water Quality Control Commission (NMWQCC) groundwater standard or U.S. Environmental Protection Agency (EPA) maximum contaminant level (MCL) is used as the screening value.
- If a NMWQCC groundwater standard or an MCL has not been established for a specific substance for which toxicological information is published, the NMED screening level for tap water is used as the groundwater screening value, using the July 2015 NMED screening levels for tap water. The NMED screening levels are for either a cancer- or noncancer-risk type. For the cancer-risk type, the screening levels are based on a 10^{-5} excess cancer risk.
- If an NMED screening level for tap water has not been established for a specific substance for which toxicological information is published, the EPA regional screening level for tap water is used as the groundwater screening value, using the May 2016 EPA regional screening levels for tap water. The EPA screening levels are for either a cancer- or noncancer-risk type. For the cancer-risk type, the Consent Order specifies screening at a 10^{-5} excess cancer risk. The EPA screening levels for tap water are for 10^{-6} excess cancer risk, so 10 times the EPA 10^{-6} screening levels is used in the screening process.

The screening standard exceedances for the alluvial system, including the screening value and screening value type, are presented in Table D-3.4-1.

All locations sampled with the exception of SWA-1-2 had iron exceedances greater than the screening value of 1000 µg/L and manganese exceedances greater than the screening value of 200 µg/L during the 2017 monitoring period. These exceedances are expected because the wetland is a reducing environment, and speciated Fe(II) data indicate that most, if not all, the iron in the alluvial system within the wetland is in its reduced form (section D-3.3). Manganese has very similar redox behavior as iron and is expected to be in its reduced state as well in the alluvial aquifer.

Arsenic exceedances ($> 10 \mu\text{g/L}$) were observed at two locations (SWA-2-5 and SWA-2-6) during the 2017 monitoring period. Speciated arsenic data indicate that most the aqueous arsenic in the alluvial system is As(III), the reduced mobile form. The alluvial aquifer is strongly reducing as indicated by the presence of sulfide and absence of oxygen. Once exposed to oxygen, As (III) quickly converts to As(V) and precipitates as or sorbs onto a solid mineral phase. As(III) was detected at all wells during each monitoring event, but always at levels less than total arsenic. This higher concentration of total arsenic is believed to be an artifact of the analysis, because of the very reducing conditions (presence of sulfide) all total arsenic is believed to be As(III) (see section D-3.2)

As discussed in section D-3.2, most of the total chromium in the alluvial aquifer is colloidal Cr(III), the nontoxic form with very low solubility. Exceedances of chromium occurred in wells SWA-1-2, SWA-4-10, and SWA-4-12 during the August 2017 sampling round. Cr(VI) was detected during this time but was never greater than the concentrations coming into the wetland from E121 and E122; concentrations which are believed to be from potable water derived from the regional aquifer and concentrated in the cooling towers (section D-2.0).

D-4.0 WATER-LEVEL RESULTS FROM ALLUVIAL SYSTEM

Water-level data was recorded at the twelve Sandia wetland alluvial wells during the 2017 calendar year continuously with a gap early in the year for instrument calibration. Water-level data are presented in Figure D-4.0-1 as a continuous record from 2016 through 2017. The plots are arranged within the figures to represent the spatial distribution of the alluvial locations in the wetland with the up gradient wells at the top of the figure. Daily flows at gaging station E121 and precipitation data from the weather station at E121.9 are plotted along with the alluvial groundwater-level data. Gaging station E121 represents the incoming flow to the wetland.

The water level results for 2017 were consistent with those of previous years. Temperatures were also consistent showing temporal changes with seasons and with less variation in wells located in the channel (SWA-2-5) and wells at a depth greater than 10 ft (SWA-1-1) (Figure D-4.0-2).

- SWA-1-1 (SCPZ-1), SWA-1-2 (SCPZ-2), and SWA-1-3 (SCPZ-3): The 2017 data showed continued rapid responses to changes in water levels as noted in previous years for this transect (top plot in Figure D-4.0-1). Water levels responded almost immediately to precipitation events (tenths of feet to 1.5 ft, depending on the size of the event). In addition, water levels responded quickly, but to a much lesser extent, to changes in base flow (driven by effluent releases at Outfalls 001 and 03A027), confirming the aquifer material in this narrow transect is relatively transmissive and storage is minimal.
- SWA-2-4 (SCPZ-4), SWA-2-5 (SCPZ-5), and SWA-2-6 (SCPZ-6): In 2017, water levels at the second transect (second plot from top in Figure D-4.0-1) also responded almost immediately to precipitation and showed much lower responses to variations in flow at gaging station E121. The variations are generally only a few tenths of a foot and are short-lived. The stability of water levels in this transect reflects the saturated conditions that occur in this part of the wetland. Surface flow spreads across a broad area in this well-vegetated transect. The fine-grained alluvial material has a lower hydraulic conductivity such that it neither drains nor fills rapidly, resulting in extremely flat water-level data. Temperatures begin to fluctuate diurnally during the winter months and is hypothesized to be a result of the lack of evapotranspiration from dominant vegetation.

- SWA-3-7, SWA-3-8 (SCPZ-8), and SWA-3-9 (SCPZ-9): In 2017, water levels at the third transect (third plot from top in Figure D-4.0-1) showed similar responses to those observed in the past. Water levels show rapid responses to both precipitation events and to outfall-driven changes in base flow. The near-instantaneous response to precipitation events and variations in base flow imply a strong connection to flowing surface waters. Water levels drop during the summer months after the monsoon season has ended and is hypothesized to be a result of increased evapotranspiration from vegetation along this transect. Temperatures begin to follow a diurnal trend in the winter months once vegetation becomes dormant and evapotranspiration decreases along this transect.
- SWA-4-10 (SCPZ-10), SWA-4-11 (SCPZ-11B), and SWA-4-12 (SCPZ-12): In 2017, water levels in 2017 (bottom plot in Figure D-4.0-1) responded quickly to both precipitation events and to variations in outfall flows (as measured by gaging station E121). Again, drops in water level have been observed in this transect during the summers. It appears the drop in water levels occurs after the monsoon season has ended and little precipitation occurs. This drop in precipitation coincides with the highest annual temperatures recorded in wetland waters (Figure D-4.0-2) and is hypothesized to result from increased evapotranspiration from vegetation.

D-5.0 REFERENCES

The following reference list includes documents cited in this appendix. Parenthetical information following each reference provides the author(s), publication date, and ERID or ESHID. This information is also included in text citations. ERIDs were assigned by the Associate Directorate for Environmental Management's (ADEM's) Records Processing Facility (IDs through 599999), and ESHIDs are assigned by the Environment, Safety, and Health Directorate (IDs 600000 and above). IDs are used to locate documents in the Laboratory's Electronic Document Management System and in the Master Reference Set. The NMED Hazardous Waste Bureau and ADEM maintain copies of the Master Reference Set. The set ensures that NMED has the references to review documents. The set is updated when new references are cited in documents.

- Blake, W.D., F.E. Goff, A.I. Adams, and D. Counce, May 1, 1995. "Environmental Geochemistry for Surface and Subsurface Waters in the Pajarito Plateau and Outlying Areas, New Mexico," Los Alamos National Laboratory report LA-12912-MS, Los Alamos, New Mexico. (Blake et al. 1995, 049931)
- LANL (Los Alamos National Laboratory), May 2007. "Groundwater Background Investigation Report, Revision 3," Los Alamos National Laboratory document LA-UR-07-2853, Los Alamos, New Mexico. (LANL 2007, 095817)
- LANL (Los Alamos National Laboratory), October 2009. "Investigation Report for Sandia Canyon," Los Alamos National Laboratory document LA-UR-09-6450, Los Alamos, New Mexico. (LANL 2009, 107453)
- LANL (Los Alamos National Laboratory), May 2011. "Interim Measures Work Plan for Stabilization of the Sandia Canyon Wetland," Los Alamos National Laboratory document LA-UR-11-2186, Los Alamos, New Mexico. (LANL 2011, 203454)
- LANL (Los Alamos National Laboratory), May 2012. "Polychlorinated Biphenyls in Precipitation and Stormwater within the Upper Rio Grande Watershed," Los Alamos National Laboratory document LA-UR-12-1081, Los Alamos, New Mexico. (LANL 2012, 219767)

- LANL (Los Alamos National Laboratory), April 2013. "Background Metals Concentrations and Radioactivity in Storm Water on the Pajarito Plateau, Northern New Mexico," Los Alamos National Laboratory document LA-UR-13-22841, Los Alamos, New Mexico. (LANL 2013, 239557)
- LANL (Los Alamos National Laboratory), June 2014. "Sandia Wetland Performance Report, Baseline Conditions 2012–2014," Los Alamos National Laboratory document LA-UR-14-24271, Los Alamos, New Mexico. (LANL 2014, 257590)
- Mahler, B.J., P.C. Van Metre, J.L. Crane, A.W. Watts, M. Scoggins, and E.S. Williams, 2012. "Coal-Tar-Based Pavement Sealcoat and PAHs: Implications for the Environment, Human Health, and Stormwater Management," *Environmental Science & Technology*, Vol. 46, pp. 3039-3045. (Mahler et al. 2012, 602275)
- Rogge, W.F., L.M. Hildemann, M.A. Mazurek, and G.R. Cass, 1993. "Sources of Fine Organic Aerosol. 3. Road Dust, Tire Debris, and Organometallic Brake Lining Dust: Roads as Sources and Sinks," *Environmental Science & Technology*, Vol. 27, pp. 1892-1904. (Wolfgang et al. 1993, 602276)
- Wang, S., and C.N. Mulligan, 2006. "Effect of Natural Organic Matter on Arsenic Release from Soils and Sediments into Groundwater," *Environmental Geochemistry and Health*, Vol. 28, pp. 197-214. (Wang and Mulligan 2006, 602277)
- Yunker, M.B., R.W. Macdonald, R. Vingarzan, R.H. Mitchell, D. Goyette, and S. Sylvestre, 2002. "PAHs in the Fraser River Basin: A Critical Appraisal of PAH Ratios as Indicators of PAH Source and Composition," *Organic Chemistry*, Vol. 33, pp. 489-515. (Yunker et al. 2002, 602278)

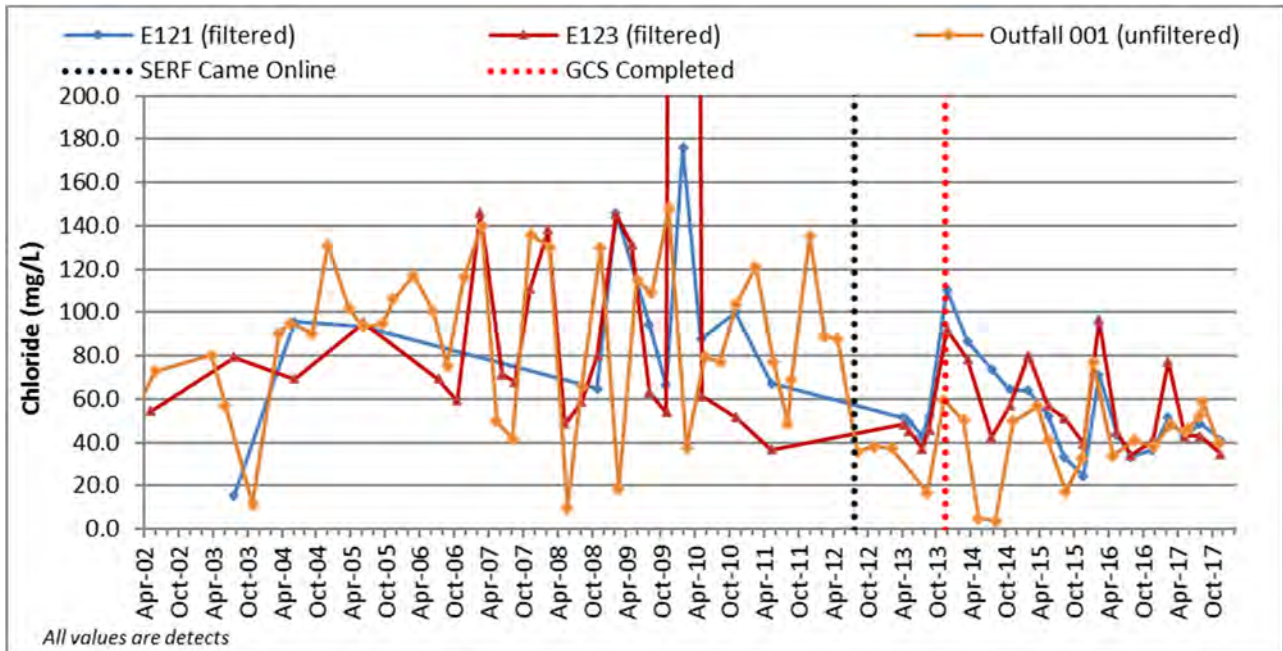
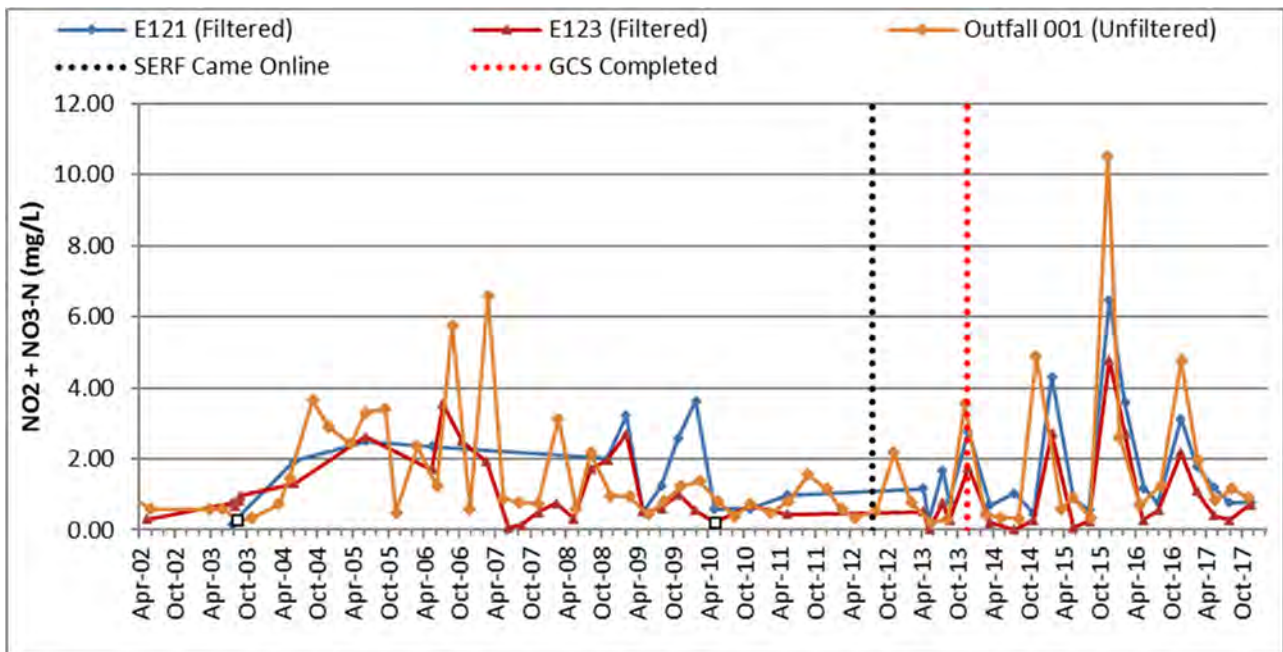


Figure D-2.0-1 Time-series plot showing chloride concentrations at gaging stations E121 and E123 and National Pollutant Discharge Elimination System- (NPDES-) permitted Outfall 001



Notes: Final values for nitrate from Outfall 001 from 11/23/15 include initial analysis at 10.5 mg/L and reanalysis at 8.99 mg/L. The reanalysis exceeded the holding time. All open symbols are non-detects. Nondetect values are estimates when above the MDL; otherwise values equal to half the MDL are used.

Figure D-2.0-2 Time-series plot showing nitrate plus nitrite as nitrogen concentrations at gaging stations E121 and E123 and NPDES Outfall 001

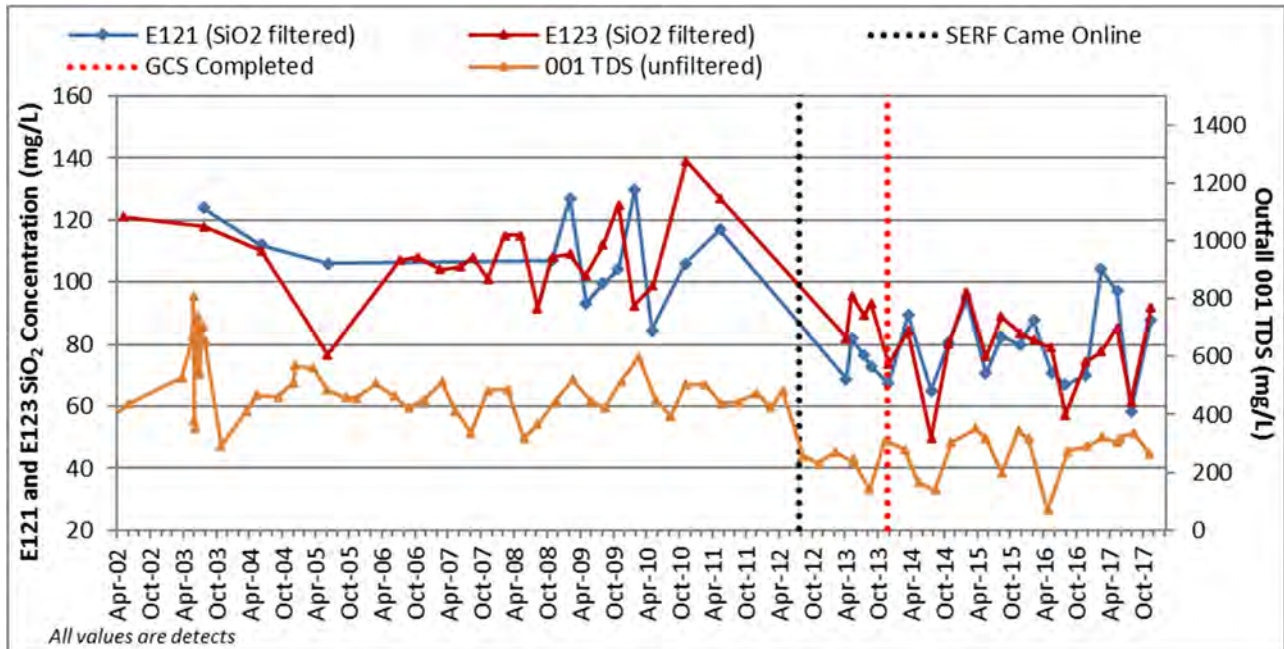
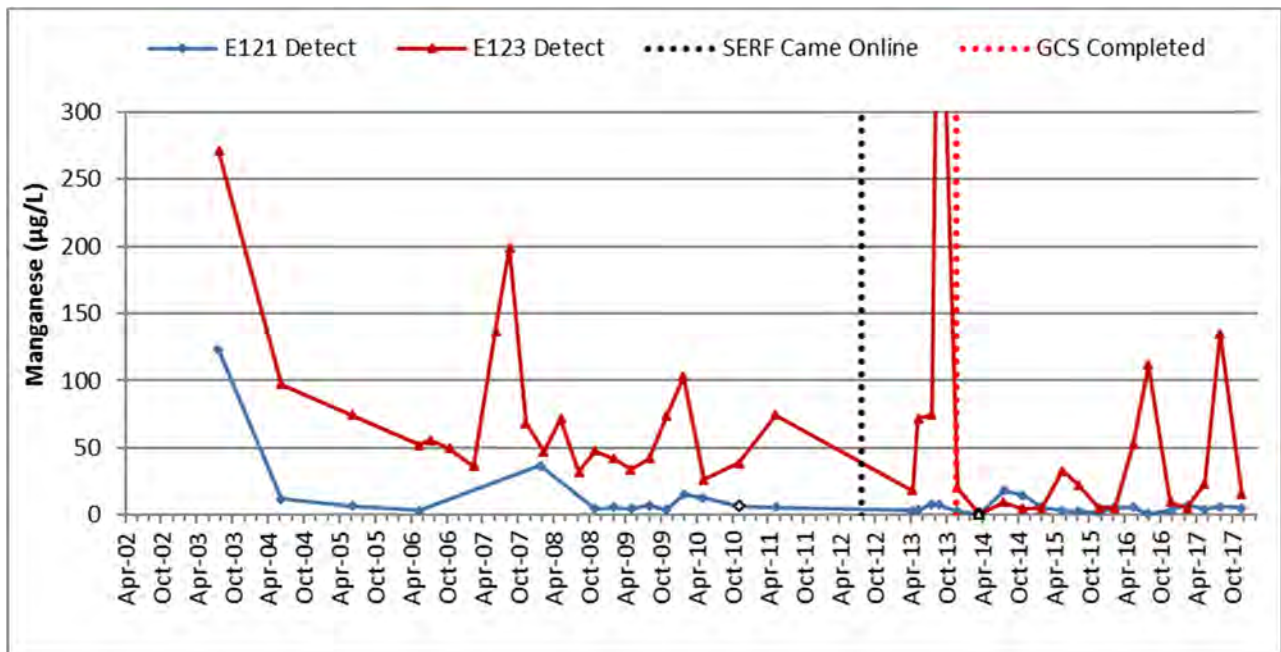
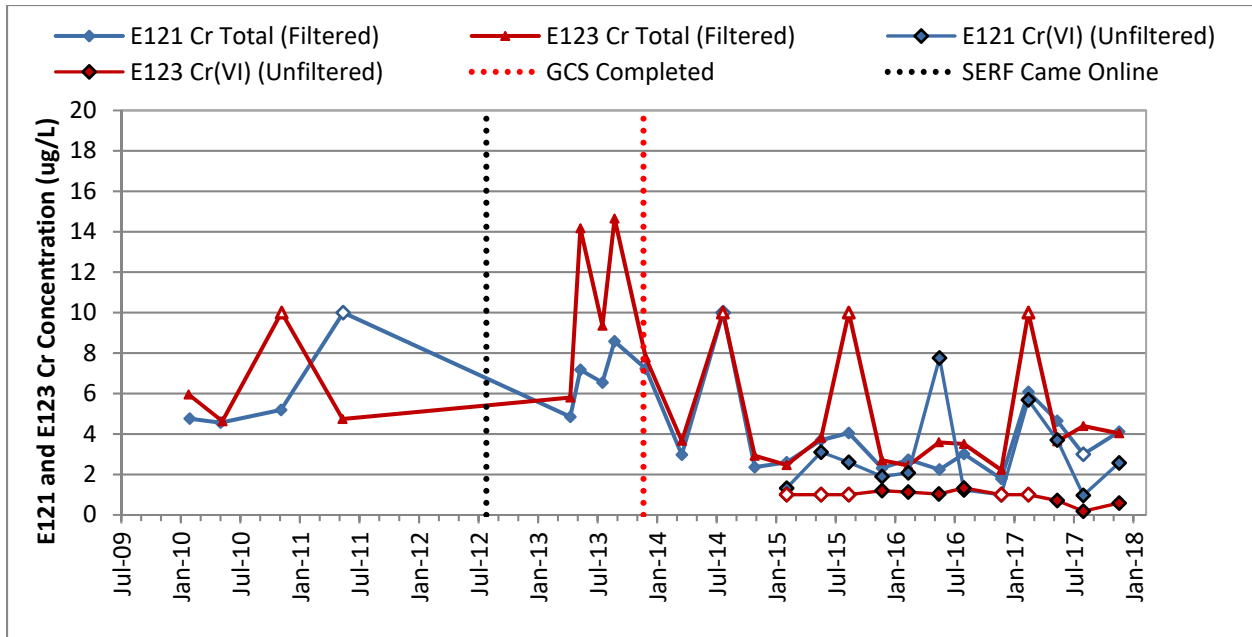


Figure D-2.0-3 Time-series plot showing silicon dioxide concentrations and TDS at gaging stations E121 and E123 and NPDES Outfall 001



Note: The highest concentration of manganese plots off the scale of the chart and was 495.5 µg/L on August 30, 2013. All open symbols are nondetections.

Figure D-2.0-4 Time-series plot showing manganese concentrations at gaging stations E121 and E123



Notes: The small concentrations of Cr(VI) versus total chromium illustrate that most of the chromium within the wetland is colloidal Cr(III). Cr(VI) shows multiple detects in base flow into the wetland but is largely attenuated within the wetland with only a few detects near the detection limit at E123. Method detection limit (MDL) at gaging stations for Cr(VI) is 1 µg/L through the February 2017 round, post the May 2017 round the MDL at gaging stations for Cr(VI) is 0.152 µg/L. Cr(VI) at NPDES Outfall 001 was a nondetection with a MDL of 3 µg/L (not shown on plot). All open symbols are nondetections.

Figure D-2.0-5 Time-series plot showing total chromium and Cr(VI) concentrations at gaging stations E121 and E123.

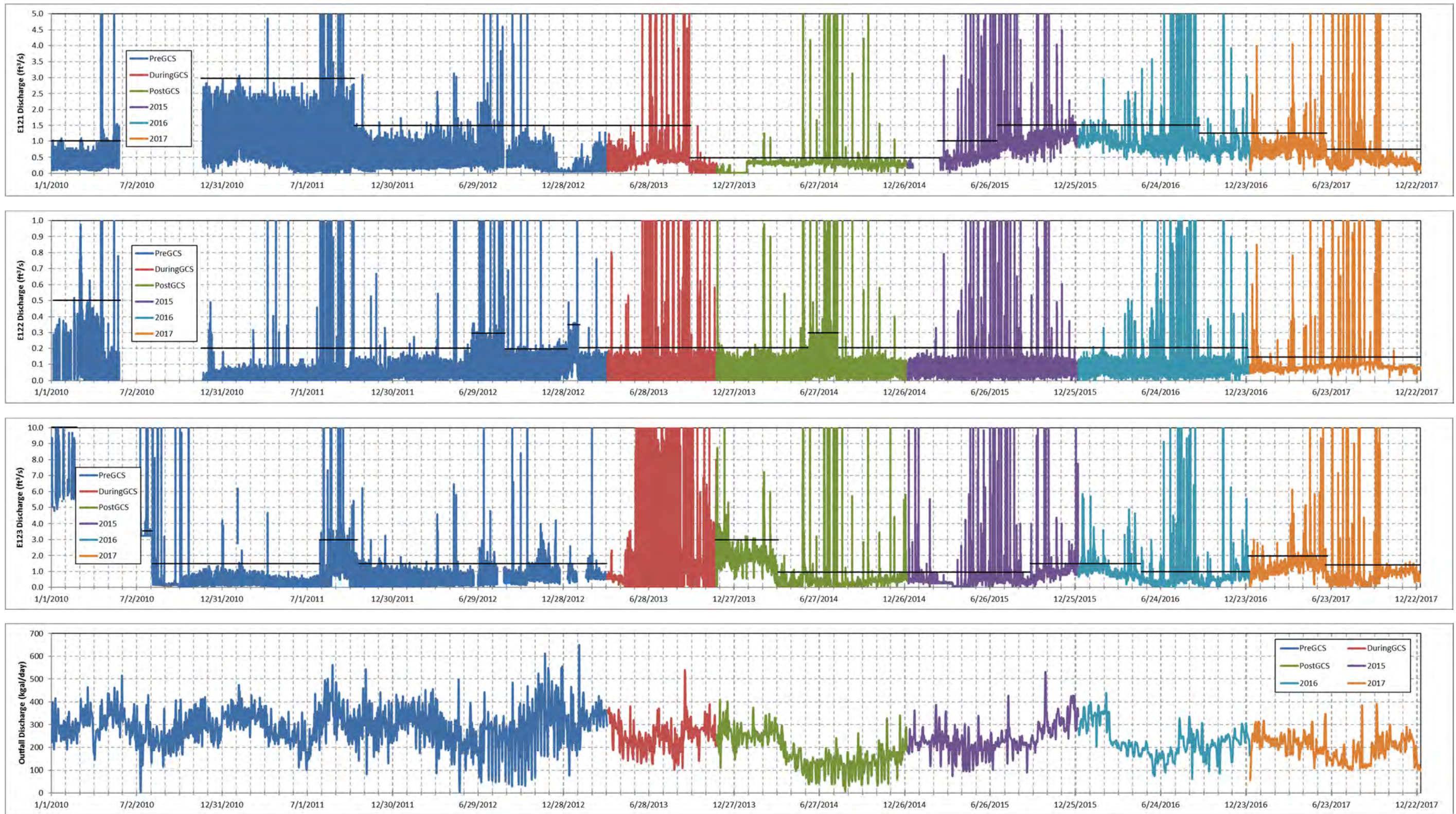


Figure D-2.0-6 Time-series plots from 2010 to 2017 showing discharge at E121, E122, and E123 and total discharge from Outfalls 001, 03A027, and 03A199; solid black horizontal lines indicate approximate base flow discharge at the surface-water gaging stations, which vary throughout the 8-yr period

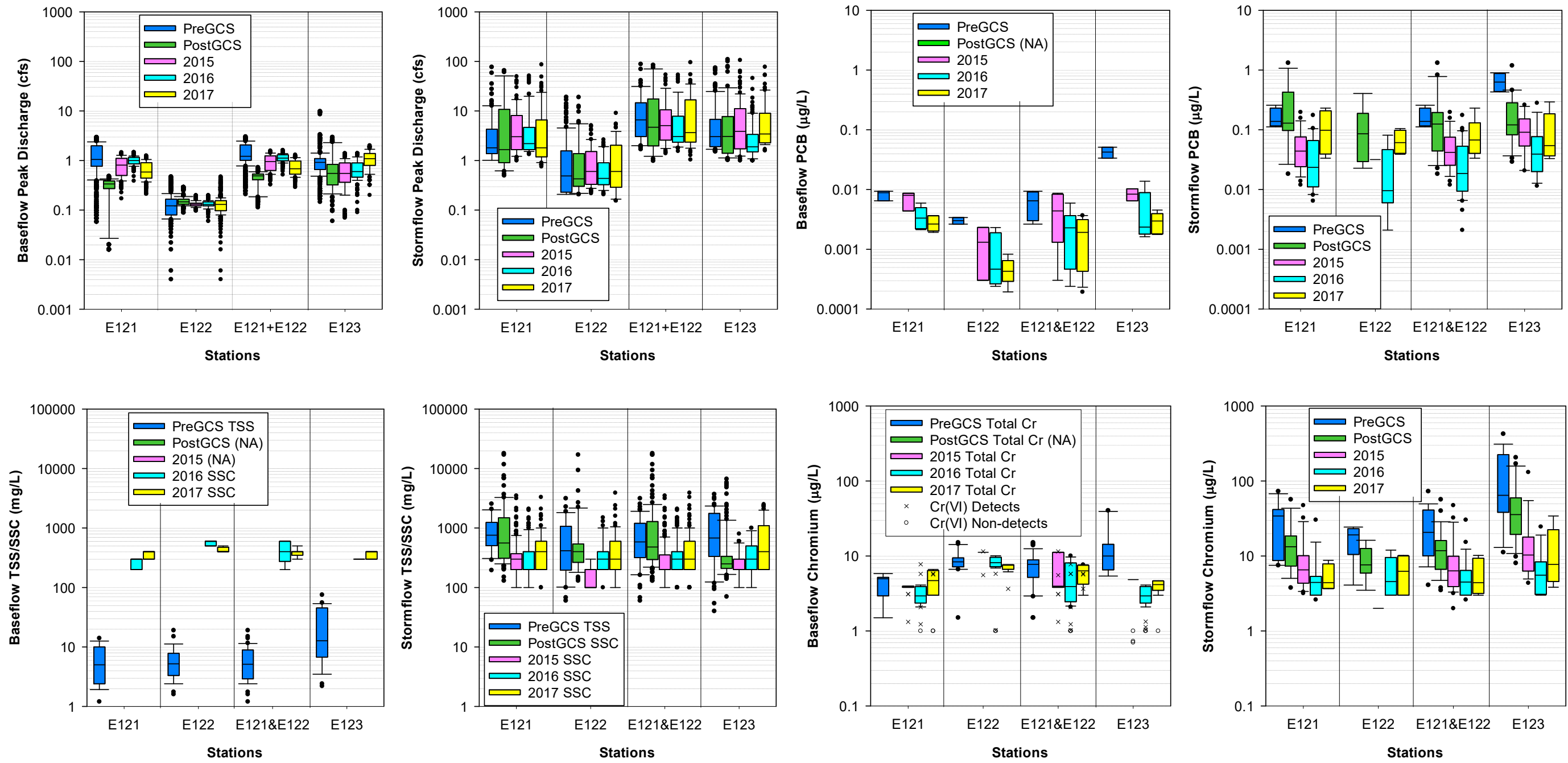


Figure D-2.0-7 Box-and-whisker plots of peak discharge, TSS/SSC, PCBs, unfiltered chromium and Cr(VI), and PAHs for base flow and storm flow at gaging stations E121, E122, and E123, pre- and post-construction of the GCS, respectively, in 2015, 2016, and 2017. (NA = Not analyzed.)

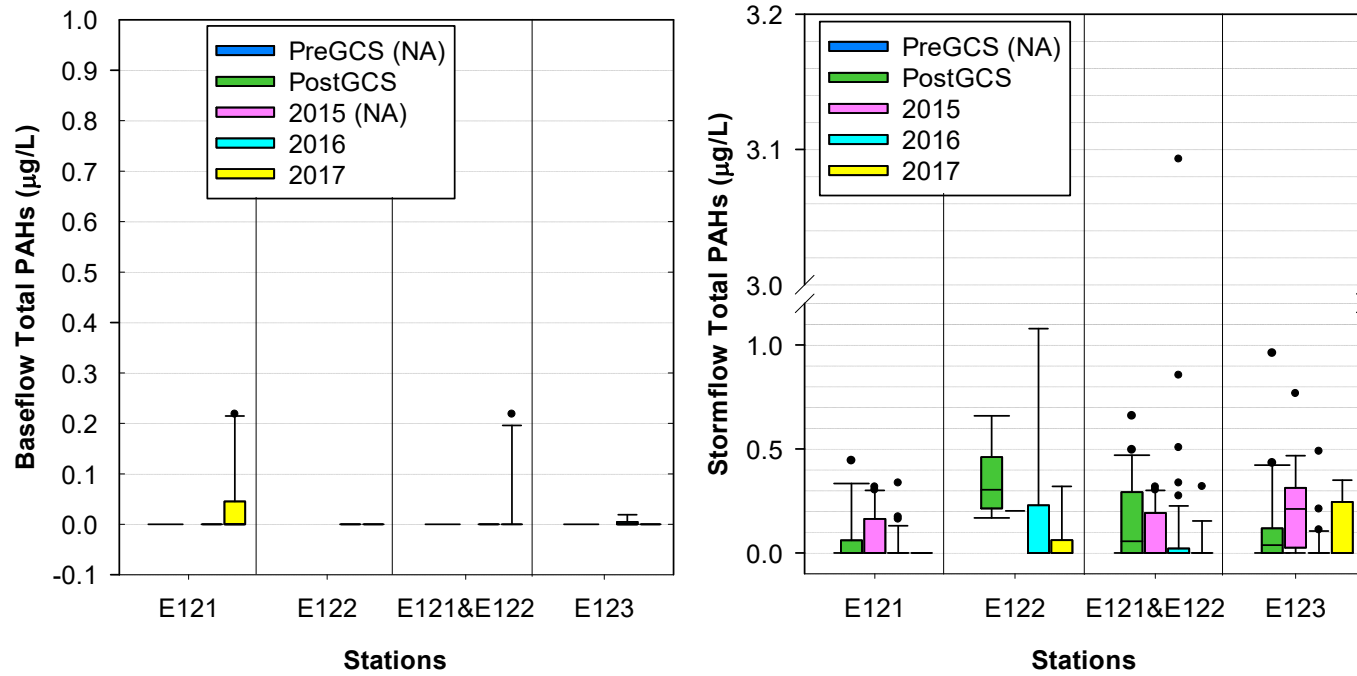


Figure D-2.0-7 (continued) Box-and-whisker plots of peak discharge TSS/SSC, total PCBs, unfiltered chromium and Cr(VI), and total PAHs for base flow and storm flow at gaging stations E121, E122, and E123, pre- and post-construction of the GCS, respectively, in 2015, 2016, and 2017. (NA = Not analyzed.)

D-20

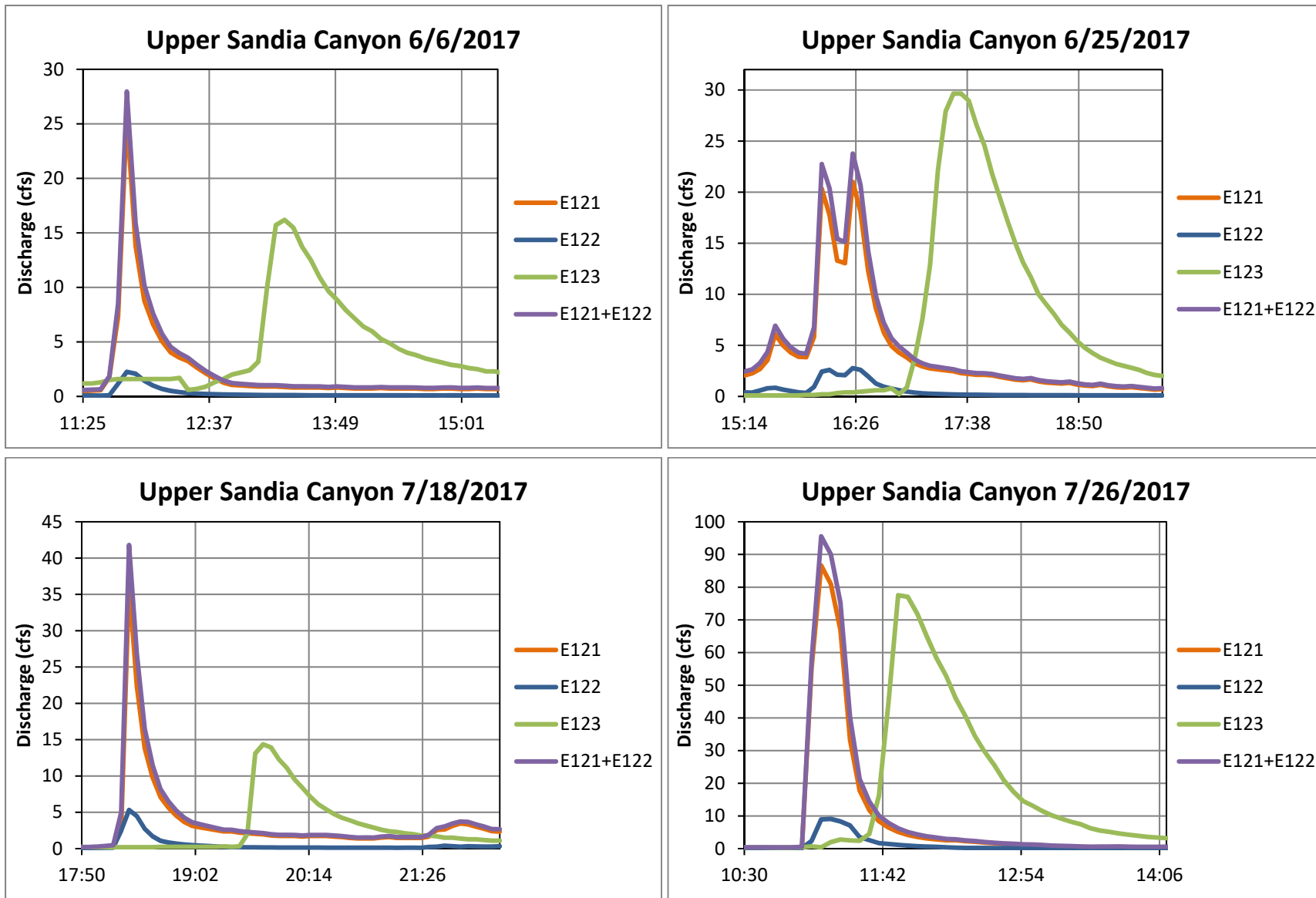


Figure D-2.0-8 Hydrographs of storm water discharge at E121, E122, and E123 during each sample-triggering storm event in 2017

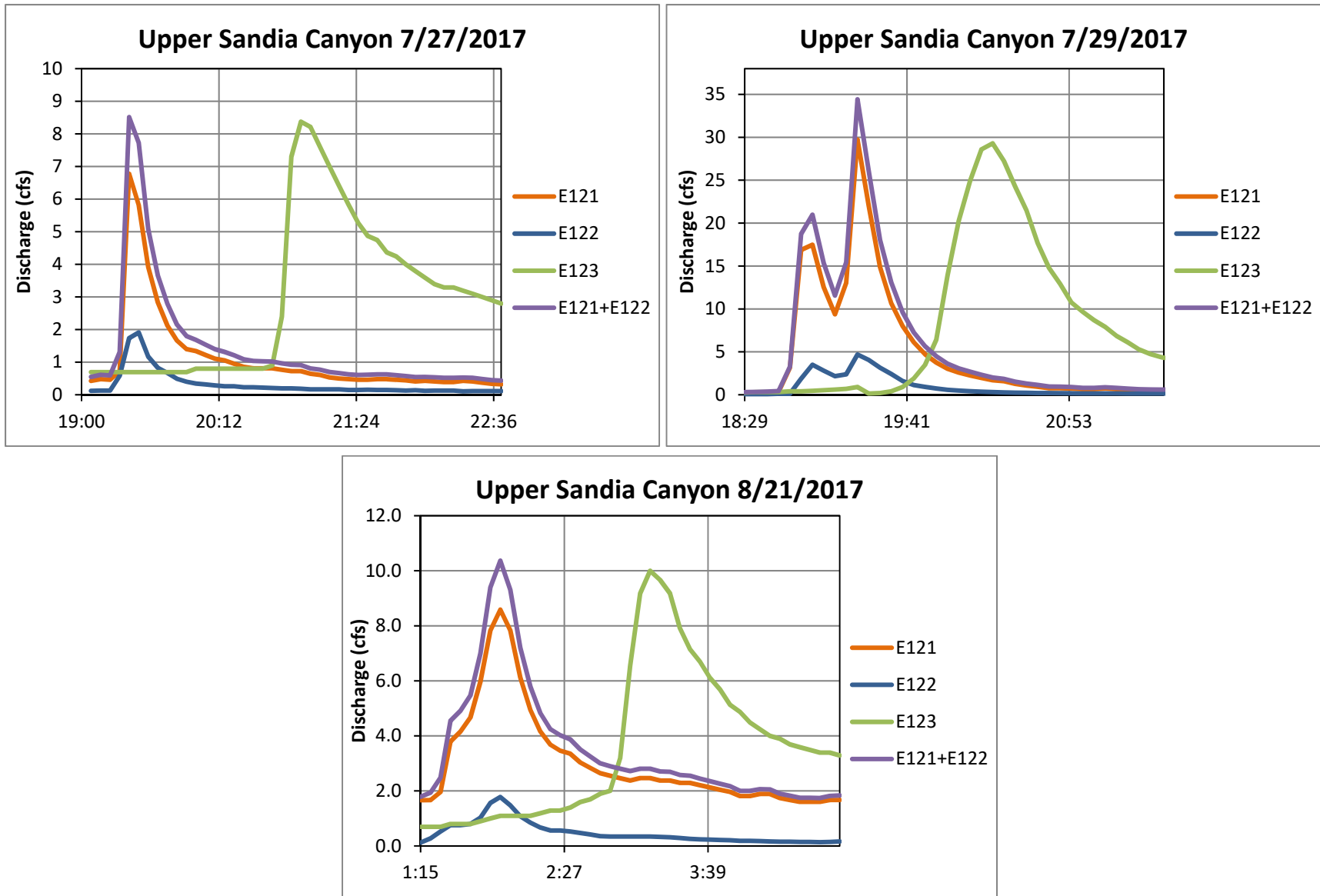


Figure D-2.0-8 (continued)

Hydrographs of storm water discharge at E121, E122, and E123 during each sample-triggering storm event in 2017

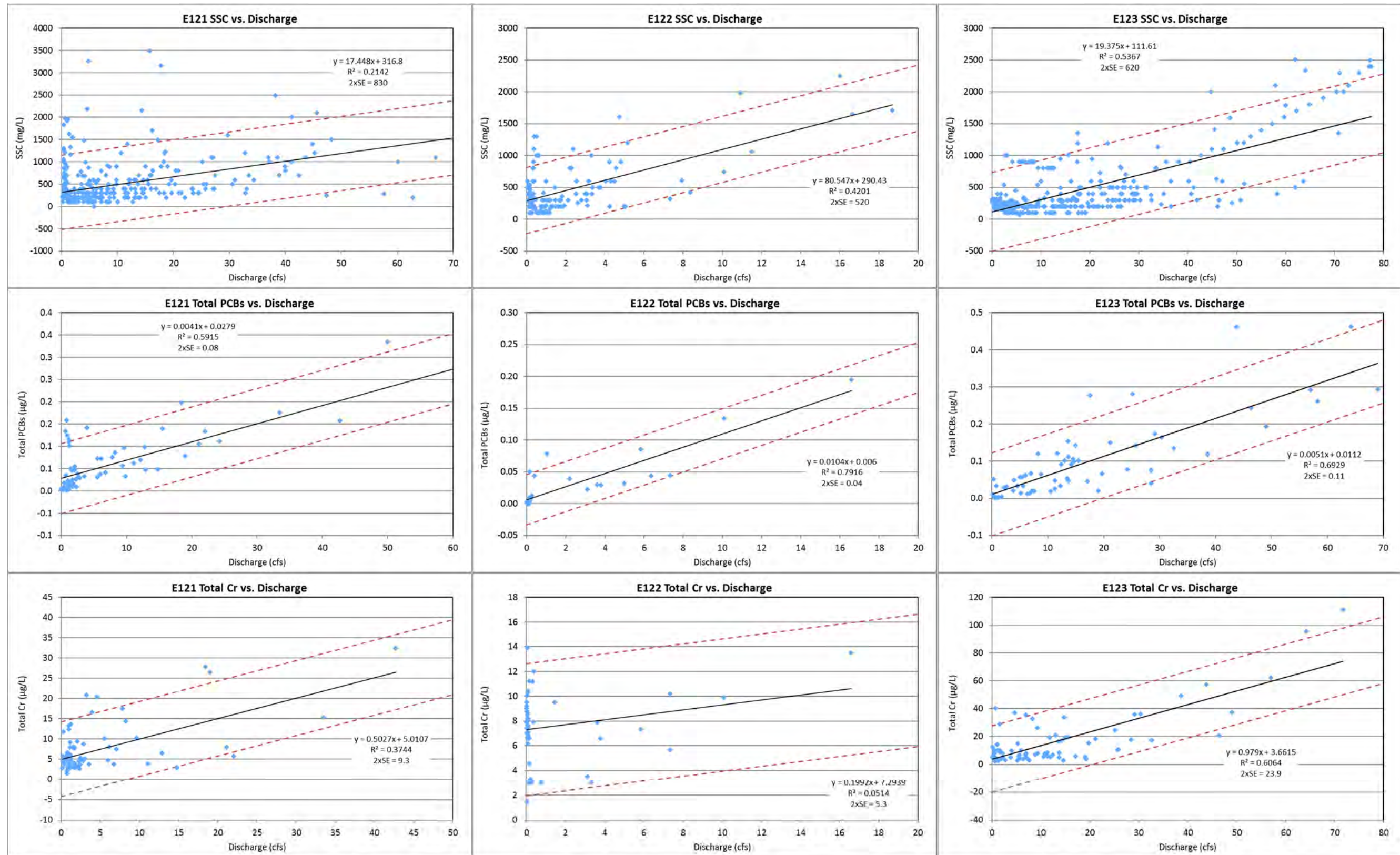


Figure D-2.0-9 Storm- and base flow discharge correlations with SSC, total PCBs, total chromium, and total PAHs from 2014 to 2017 at E121, E122, and E123 with standardized residual outliers removed; the red dashed lines are 2 times the standard error (2×SE) of the estimate, as noted with the equation of the line and the Pearson’s correlation coefficient (R²)

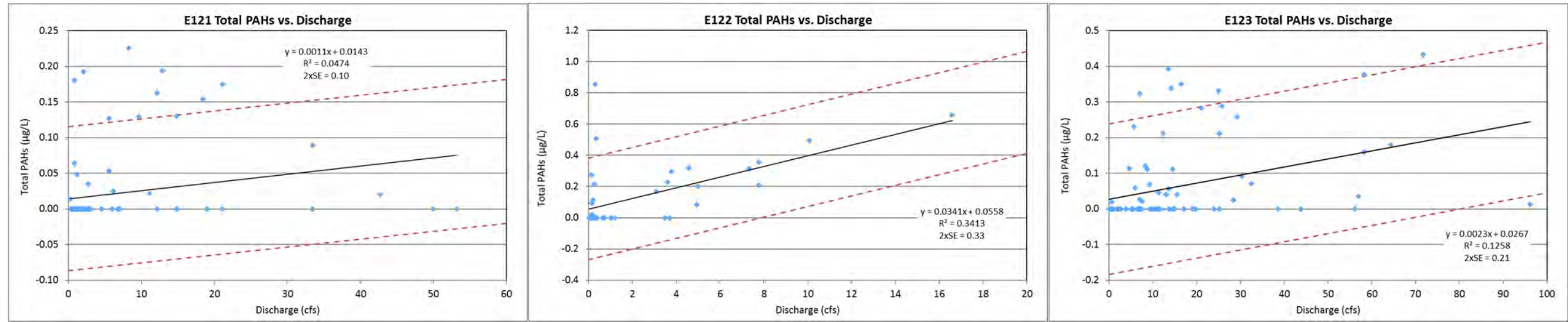


Figure D-2.0-9 (continued) Storm- and base flow discharge correlations with SSC, total PCBs, total chromium, and total PAHs from 2014 to 2017 at E121, E122, and E123 with standardized residual outliers removed; the red dashed lines are 2 times the standard error (2×SE) of the estimate, as noted with the equation of the line and the Pearson’s correlation coefficient (R²)

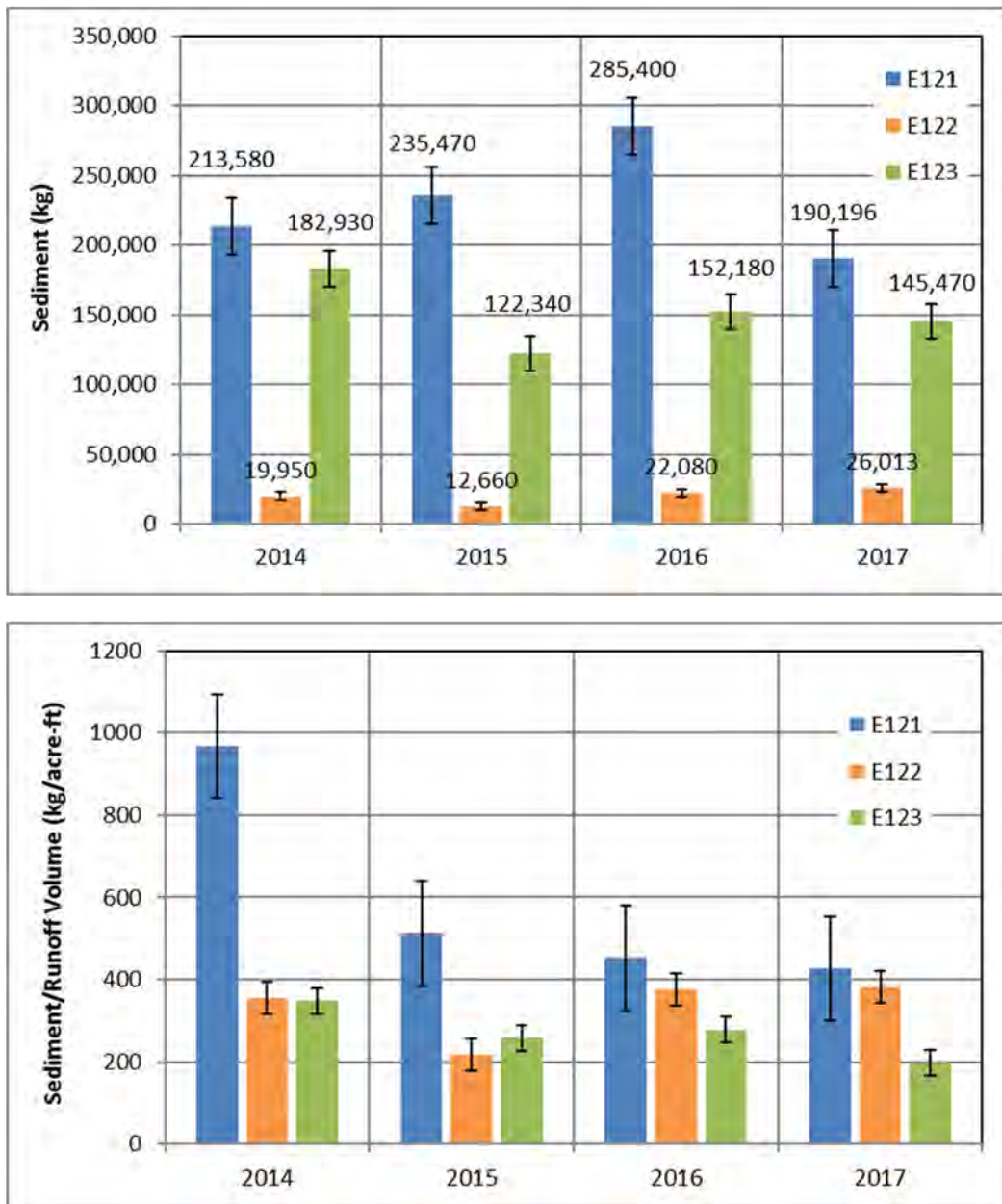


Figure D-2.0-10 Annual mass flux (top) and annual mass flux normalized by runoff volume (bottom) for sediment at gaging stations E121 (blue), E122 (orange), and E123 (green) from 2014 to 2017. Gaging stations E121 and E122 represent inputs into the wetland, and E123 represents output from the wetland. Error bars represent the standard error of the mean.

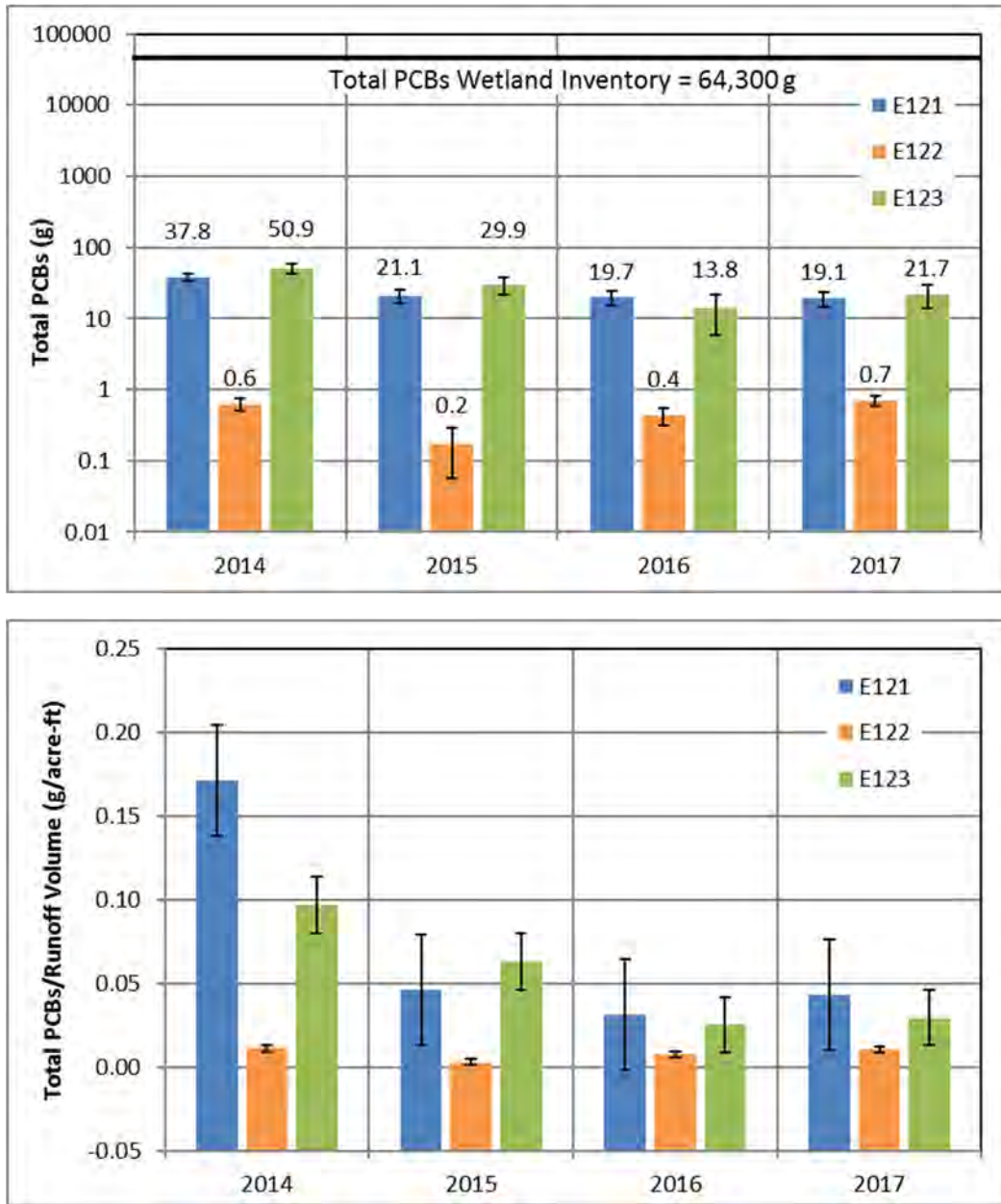


Figure D-2.0-11 Annual mass flux (top) and annual mass flux normalized by runoff volume (bottom) for total PCBs at gaging stations E121 (blue), E122 (orange), and E123 (green) from 2014 to 2017. Gaging stations E121 and E122 represent inputs into the wetland, and E123 represents output from the wetland. Error bars represent the standard error of the mean.

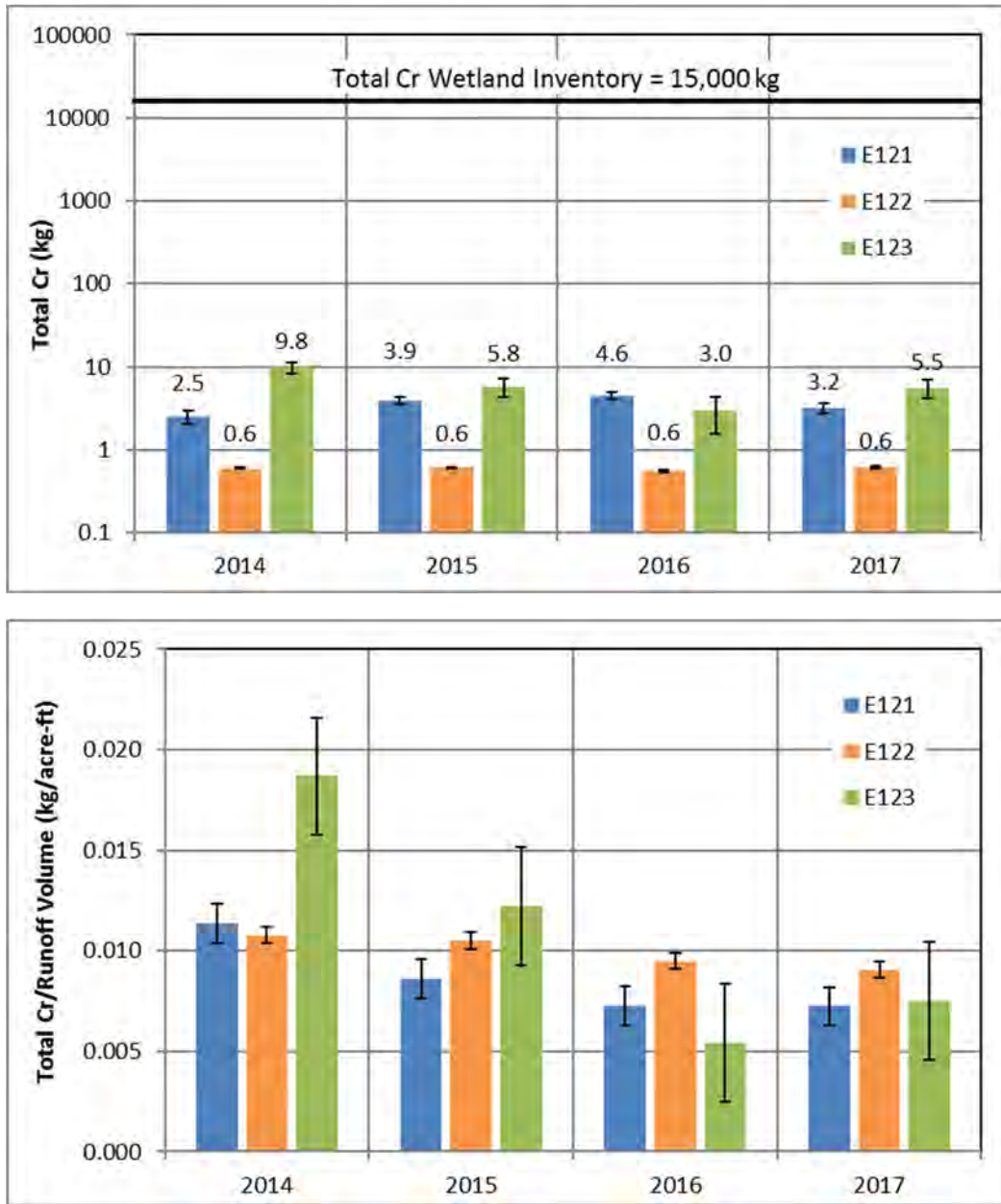


Figure D-2.0-12 Annual mass flux (top) and annual mass flux normalized by runoff volume (bottom) for total chromium at gaging stations E121 (blue), E122 (orange), and E123 (green) from 2014 to 2017. Gaging stations E121 and E122 represent inputs into the wetland, and E123 represents output from the wetland. Error bars represent the standard error of the mean.

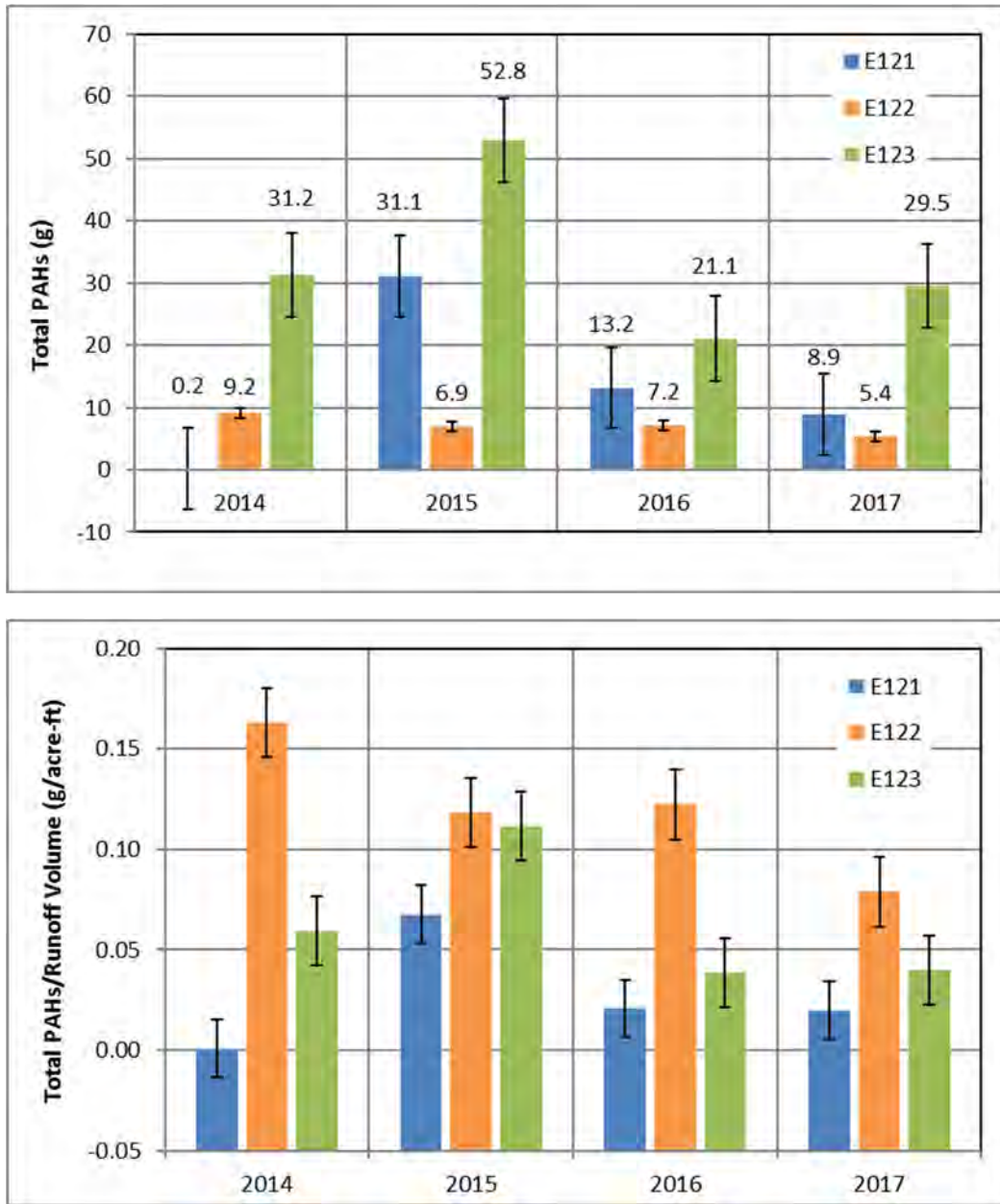
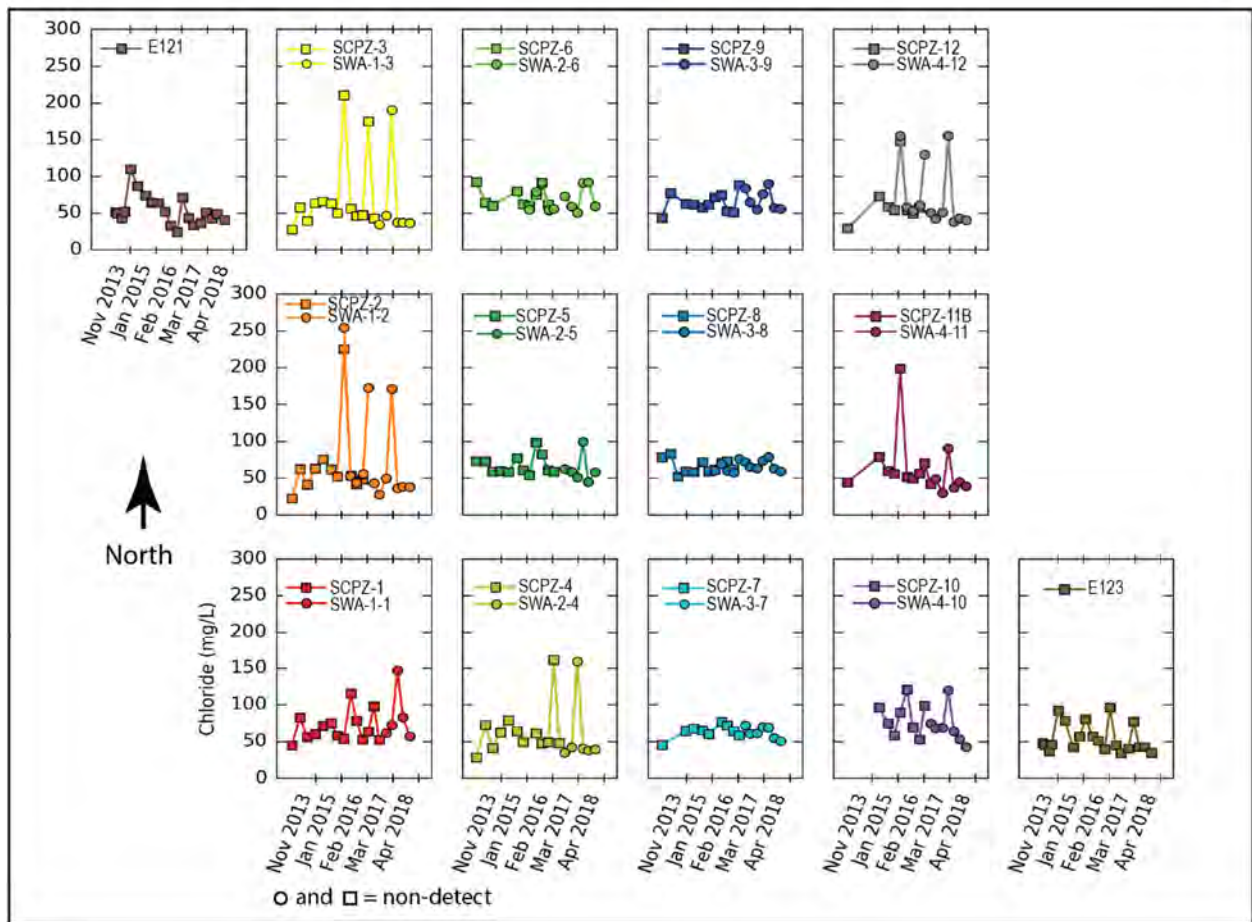
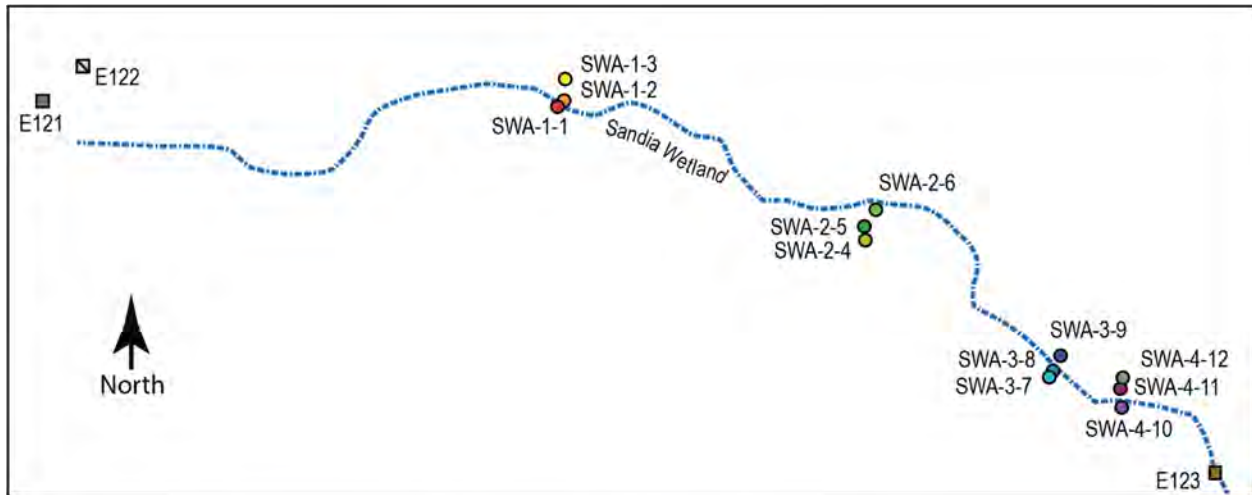
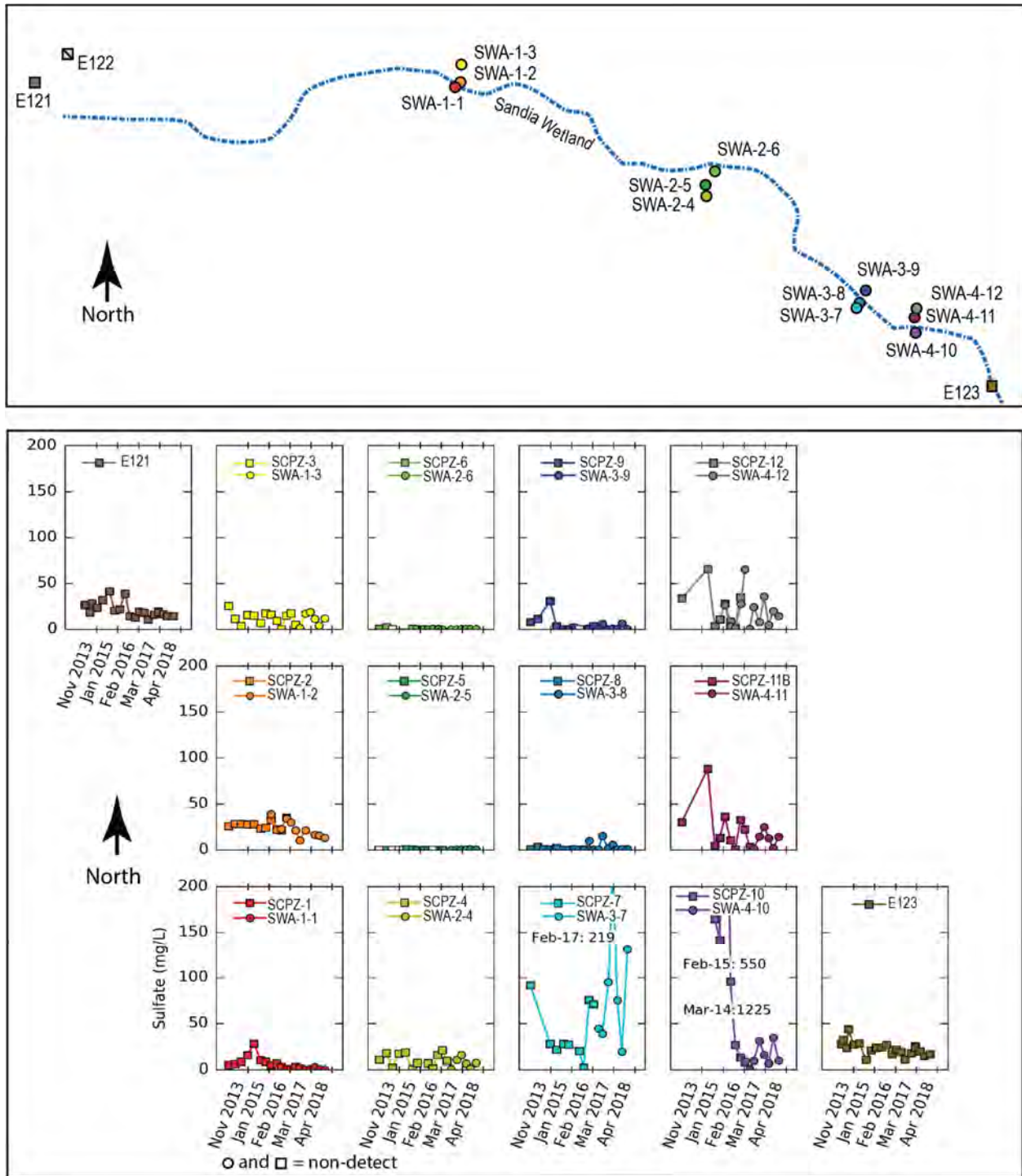


Figure D-2.0-13 Annual mass flux (top) and annual mass flux normalized by runoff volume (bottom) for total PAHs at gaging stations E121 (blue), E122 (orange), and E123 (green) from 2014 to 2017. Gaging stations E121 and E122 represent inputs into the wetland, and E123 represents output from the wetland. Error bars represent the standard error of the mean.



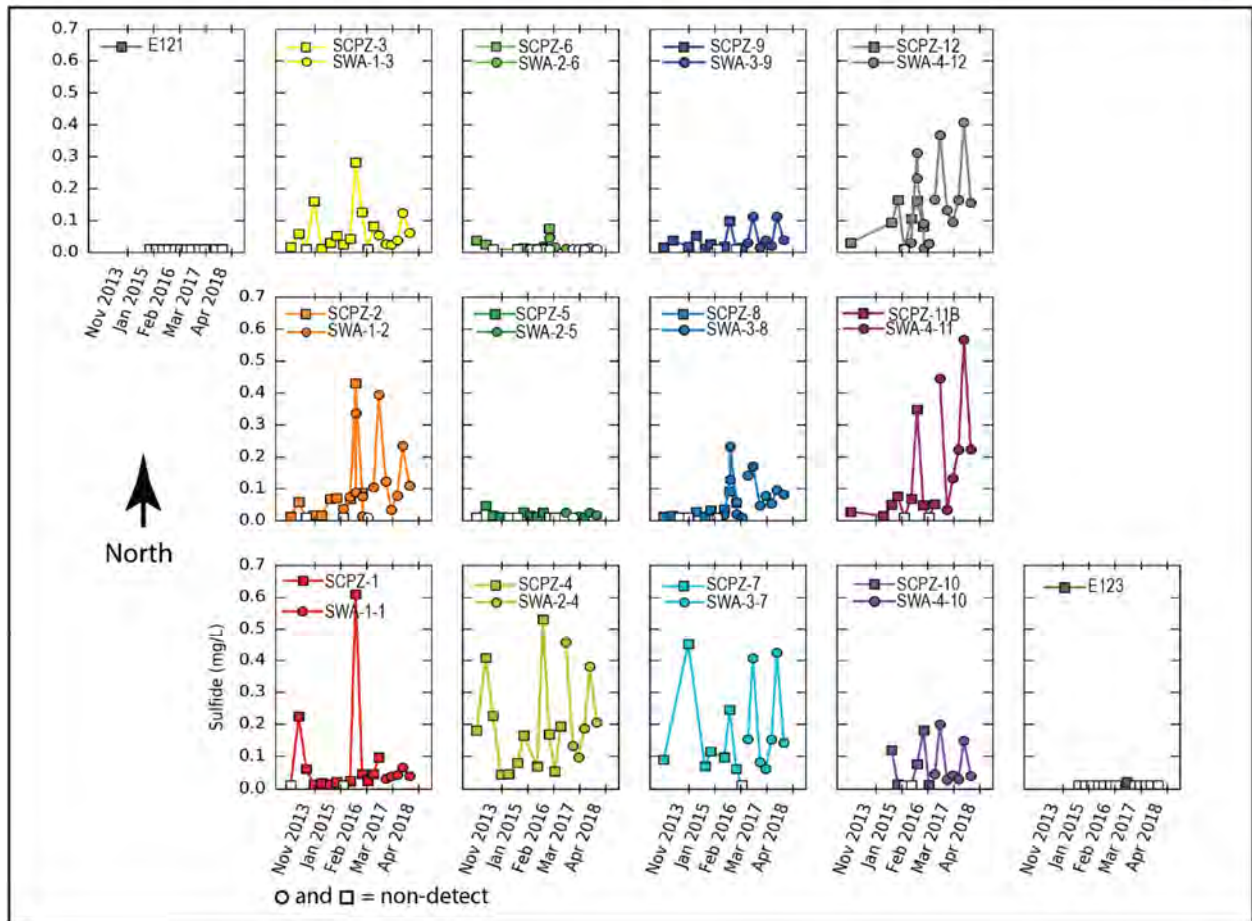
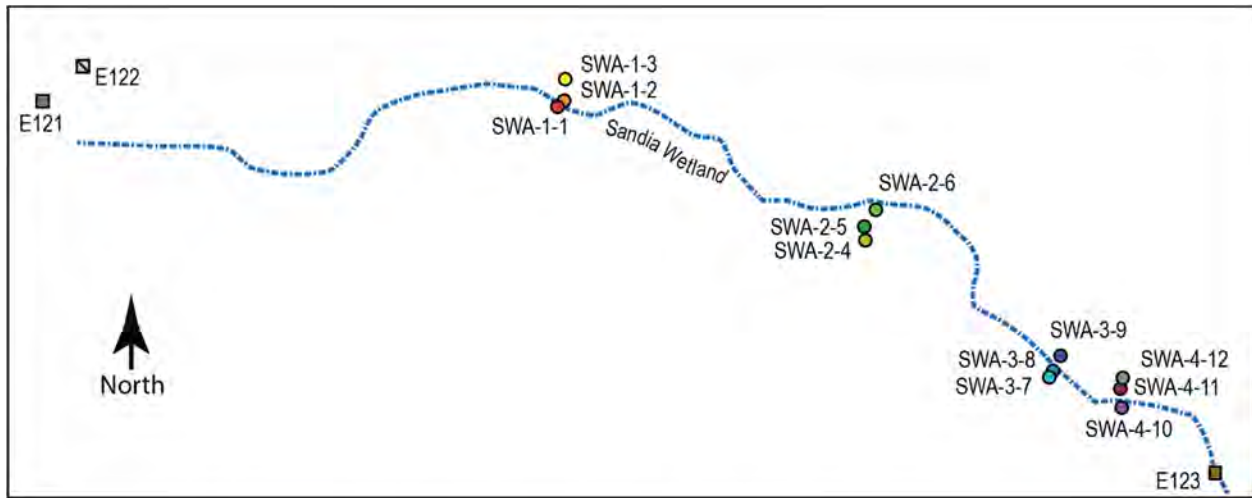
Notes: Surface water stations include E121, E122 (plot not shown), and E123. Piezometers are labeled with the prefix SCPZ (square symbols), and alluvial wells are labeled with the prefix SWA (circle symbols). The plots are arranged in four transects from west to east. Data are plotted for the full period of wetland monitoring. Nondetects are plotted as the MDL with open symbols. The map above is not to scale, but shows approximate sampling locations in relation to the approximate thalweg (blue dashed line).

Figure D-3.0-1 Chloride concentrations in Sandia wetland surface water and alluvial system



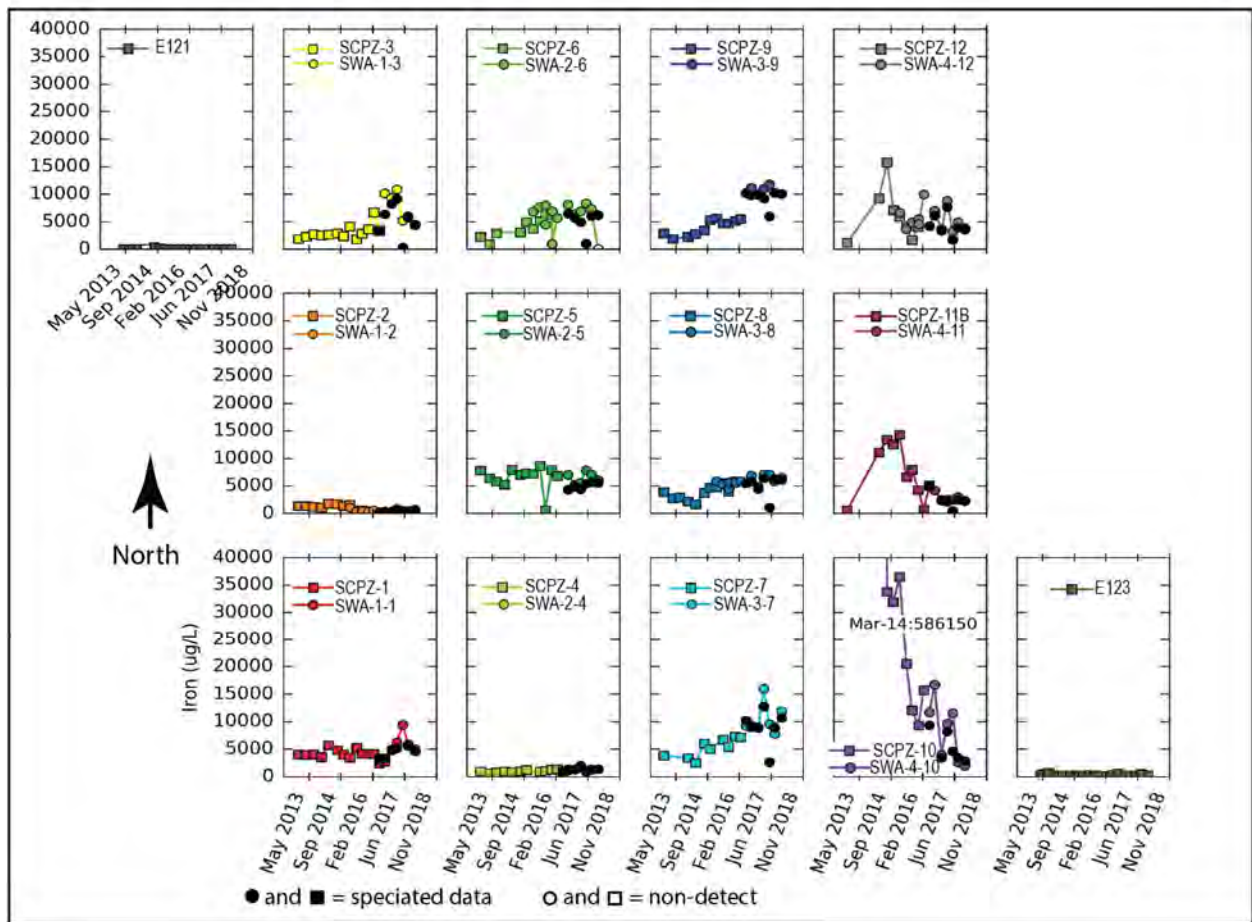
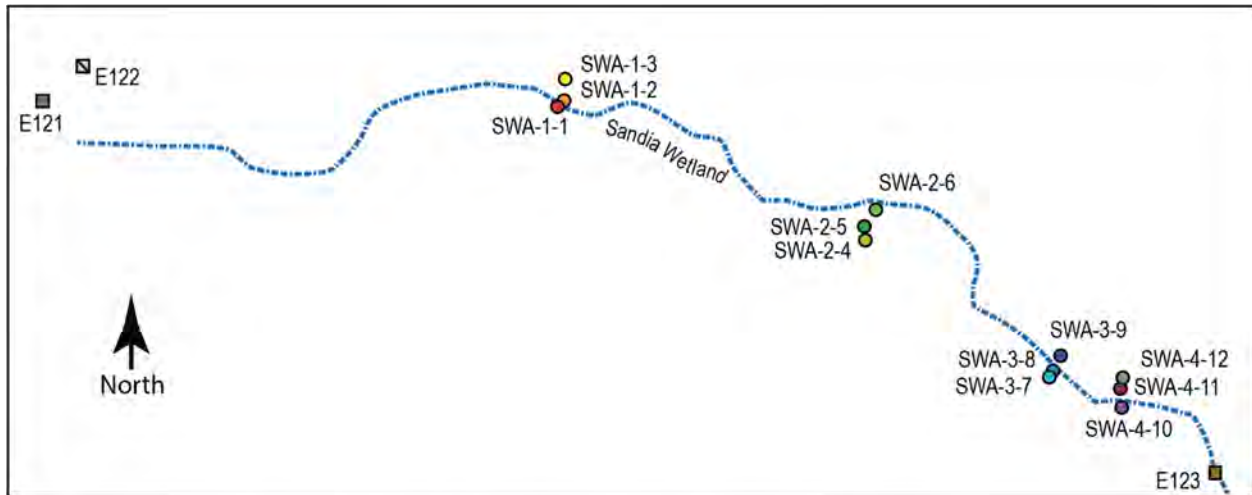
Notes: Surface water stations include E121, E122 (plot not shown), and E123. Piezometers are labeled with the prefix SCPZ (square symbols), and alluvial wells are labeled with the prefix SWA (circle symbols). The plots are arranged in four transects from west to east. Data are plotted for the full period of wetland monitoring. Nondetects are plotted as the MDL with open symbols. The map above is not to scale but shows approximate sampling locations in relation to the approximate thalweg (blue dashed line).

Figure D-3.0-2 Sulfate concentrations in Sandia wetland surface water and alluvial system



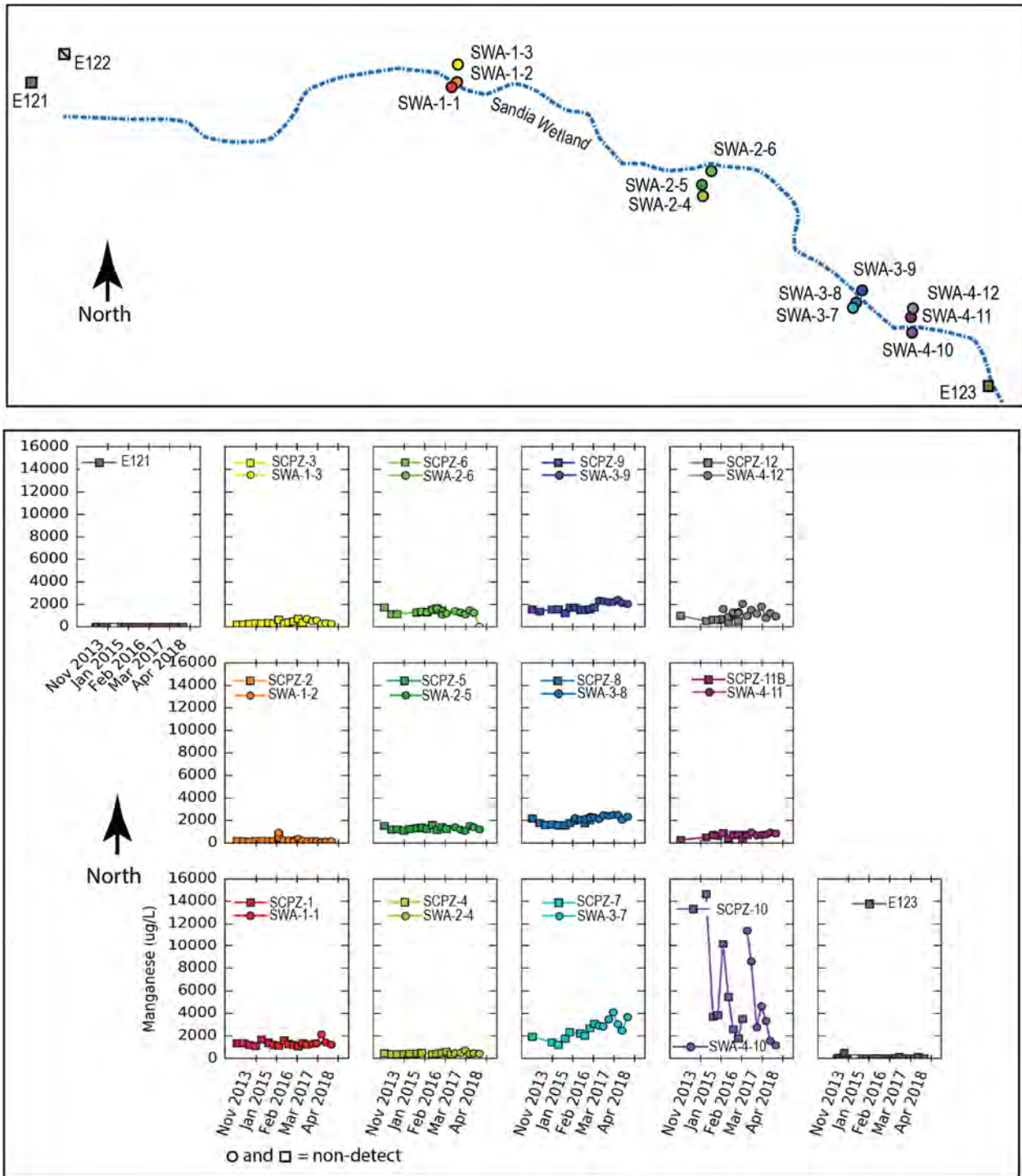
Notes: Surface water stations include E121, E122 (plot not shown), and E123. Piezometers are labeled with the prefix SCPZ (square symbols), and alluvial wells are labeled with the prefix SWA (circle symbols). The plots are arranged in four transects from west to east. Data are plotted for the full period of wetland monitoring. Nondetects are plotted as the MDL with open symbols. The map above is not to scale but shows approximate sampling locations in relation to the approximate thalweg (blue dashed line).

Figure D-3.0-3 Sulfide concentrations in Sandia wetland surface water and alluvial system



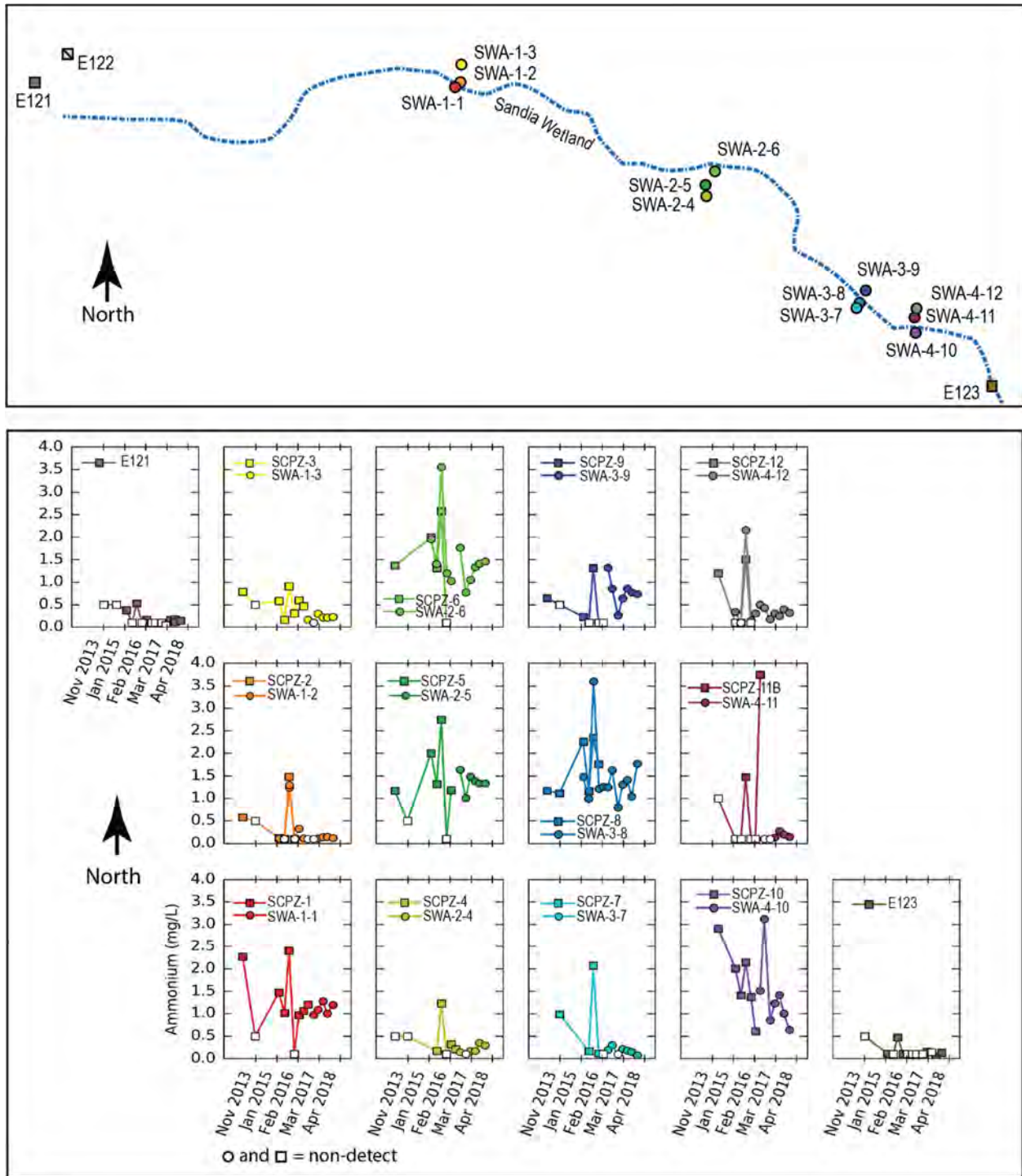
Notes: Surface water stations include E121, E122 (plot not shown), and E123. Piezometers are labeled with the prefix SCPZ (square symbols), and alluvial wells are labeled with the prefix SWA (circle symbols). The plots are arranged in four transects from west to east. Data are plotted for the full period of wetland monitoring. Nondetects are plotted as the MDL with open symbols. Total iron is represented with colored symbols and Fe(11) with black symbols. The map above is not to scale but shows approximate sampling locations in relation to the approximate thalweg (blue dashed line).

Figure D-3.0-4 Iron concentrations in Sandia wetland surface water and alluvial system



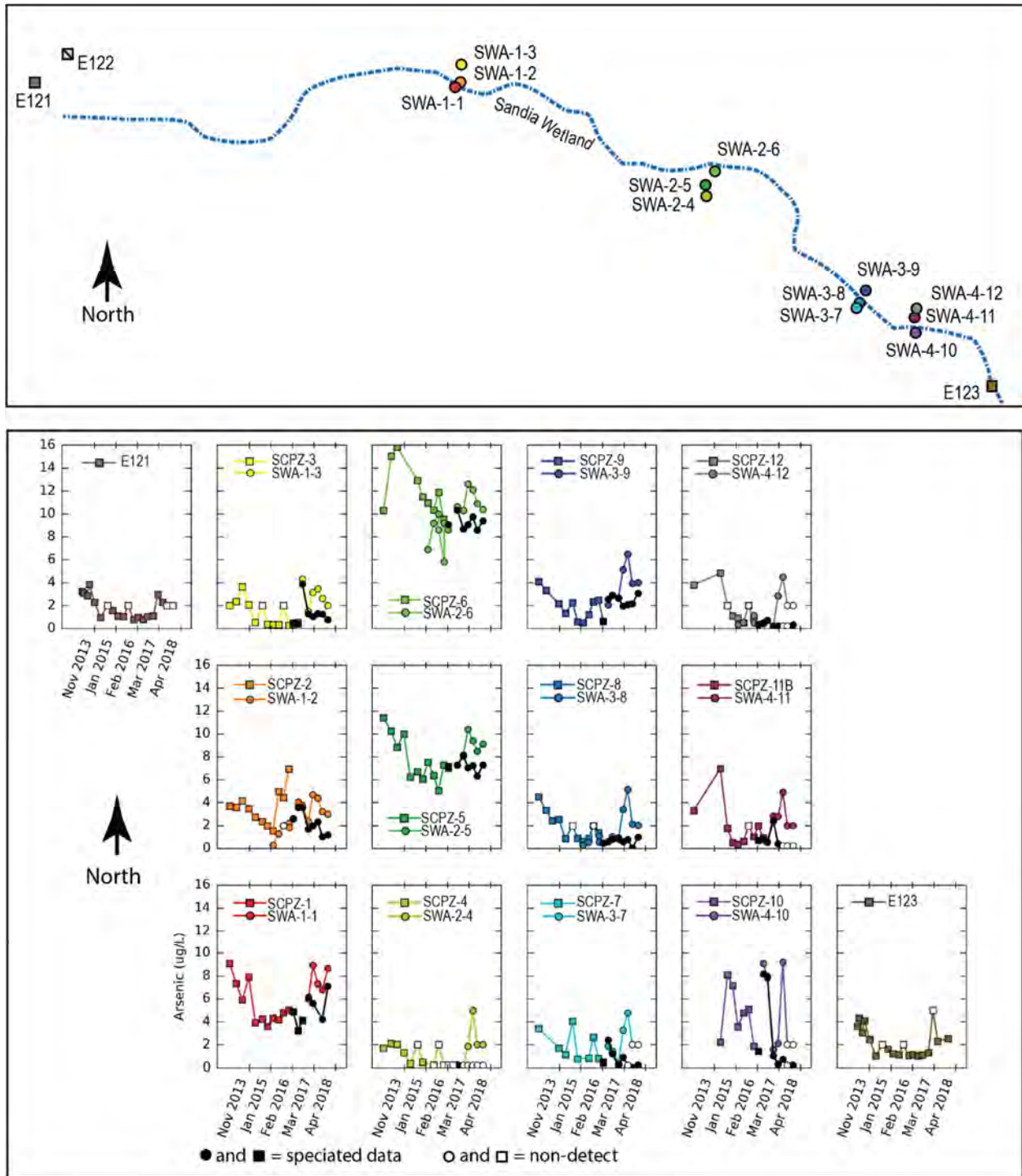
Notes: Surface water stations include E121, E122 (plot not shown), and E123. Piezometers are labeled with the prefix SCPZ (square symbols), and alluvial wells are labeled with the prefix SWA (circle symbols). The plots are arranged in four transects from west to east. Data are plotted for the full period of wetland monitoring. Nondetects are plotted as the MDL with open symbols. The map above is not to scale but shows approximate sampling locations in relation to the approximate thalweg (blue dashed line).

Figure D-3.0-5 Manganese concentrations in Sandia wetland surface water and alluvial system



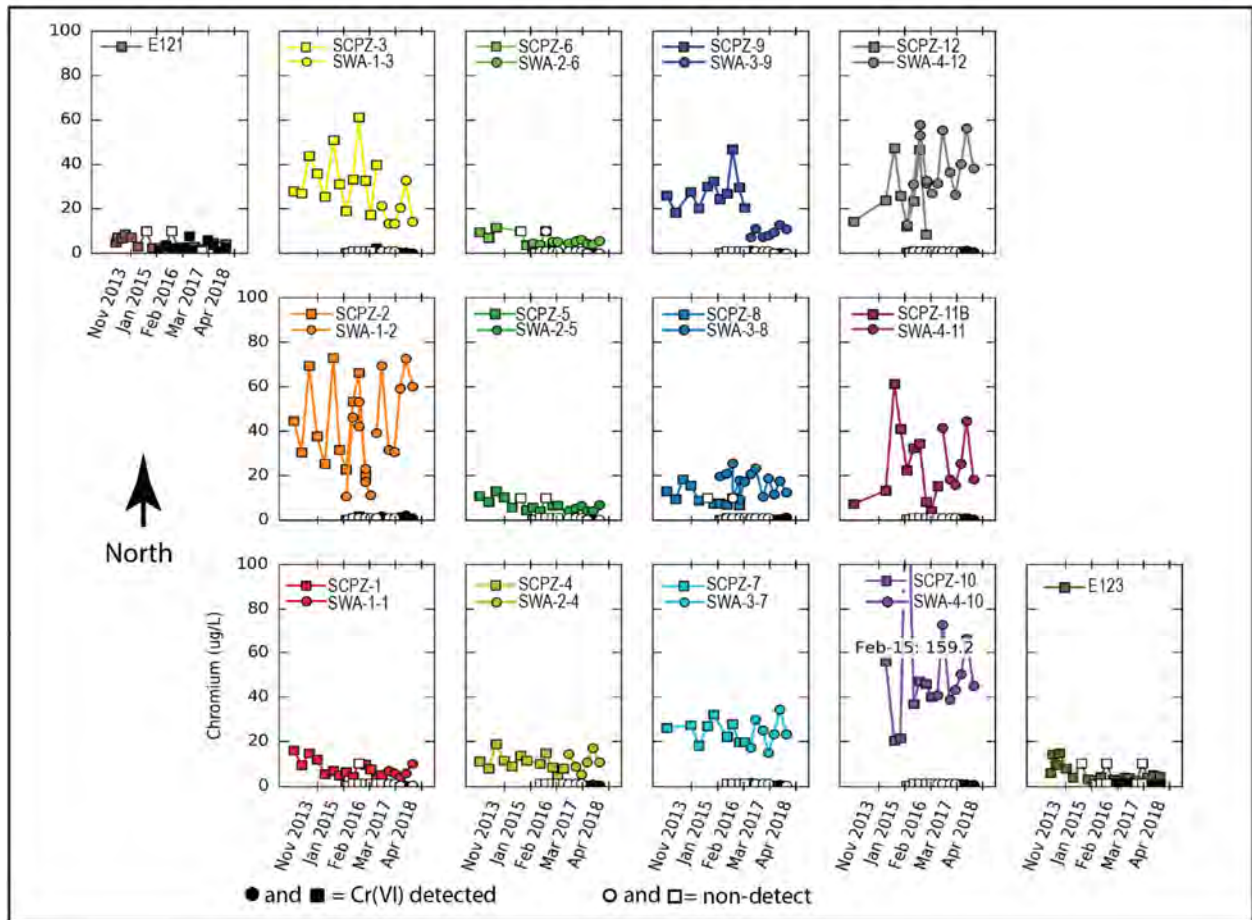
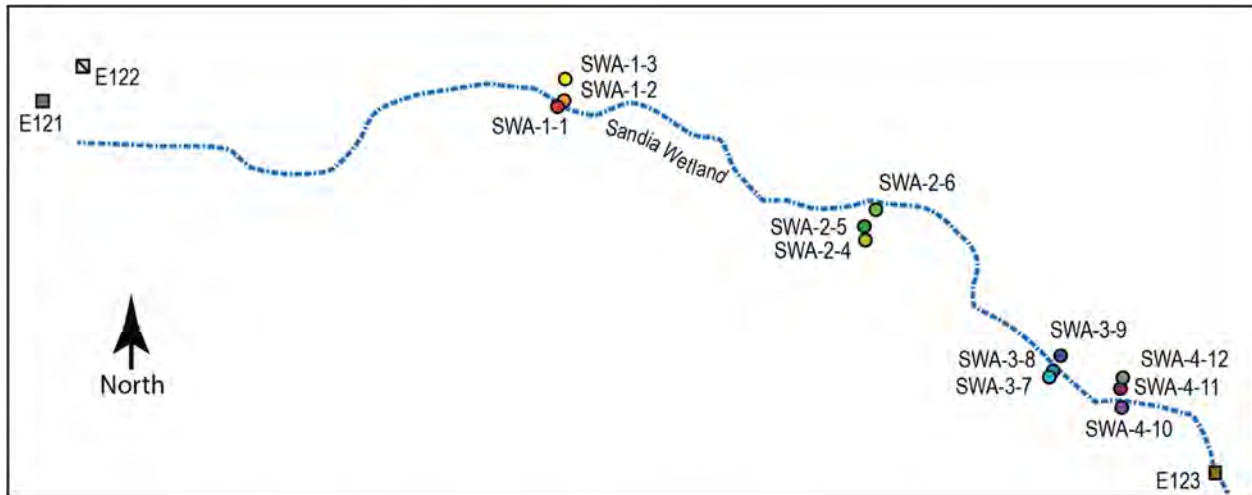
Notes: Surface water stations include E121, E122 (plot not shown), and E123. Piezometers are labeled with the prefix SCPZ (square symbols), and alluvial wells are labeled with the prefix SWA (circle symbols). The plots are arranged in four transects from west to east. Data are plotted for the full period of wetland monitoring. Nondetects are plotted as the MDL with open symbols. The map above is not to scale but shows approximate sampling locations in relation to the approximate thalweg (blue dashed line).

Figure D-3.0-6 Ammonium concentrations in Sandia wetland surface water and alluvial system



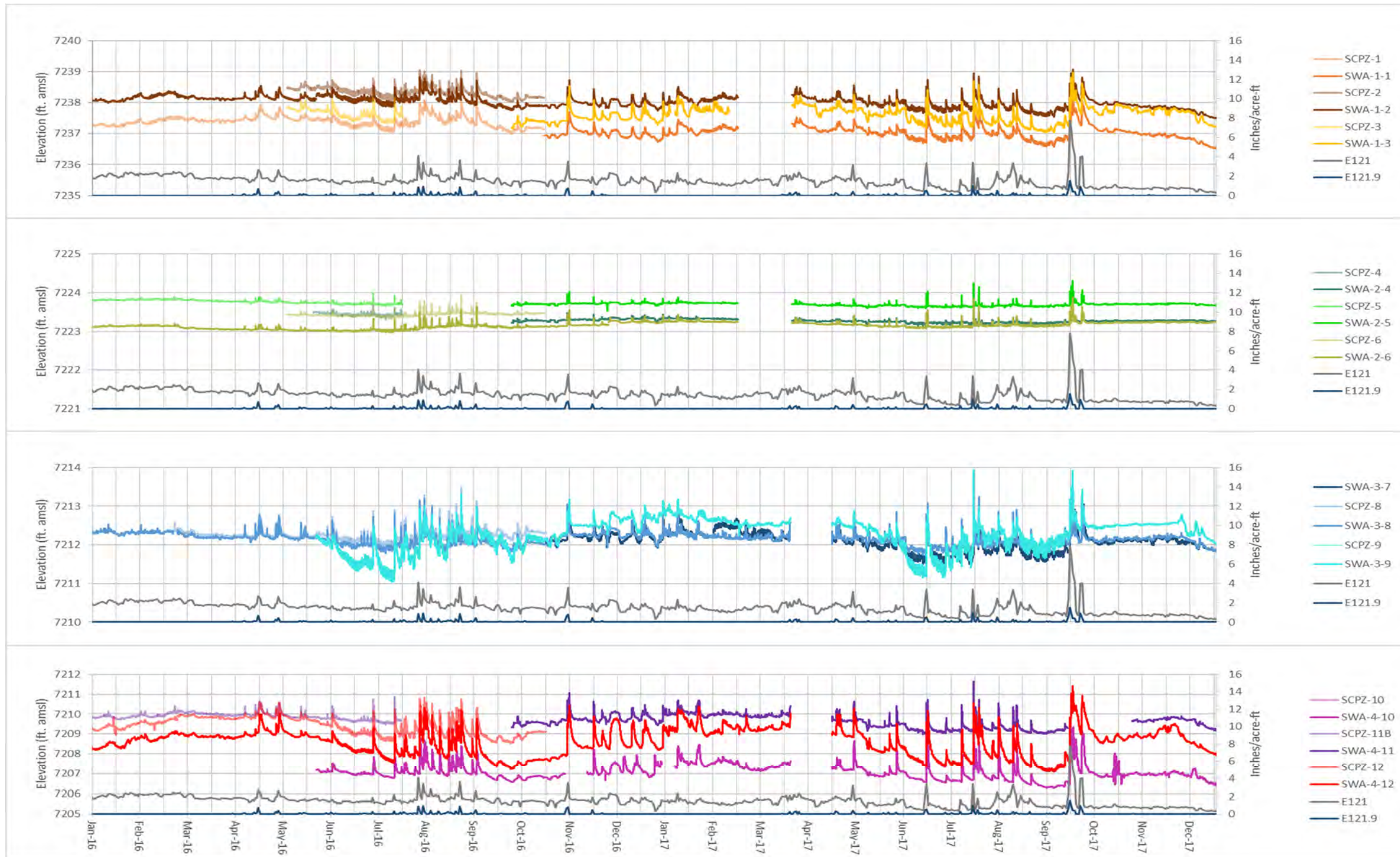
Notes: Surface water stations include E121, E122 (plot not shown), and E123. Piezometers are labeled with the prefix SCPZ (square symbols), and alluvial wells are labeled with the prefix SWA (circle symbols). The plots are arranged in four transects from west to east. Data are plotted for the full period of wetland monitoring. Nondetects are plotted as the MDL with open symbols. Total arsenic is represented with the colored symbols and As(III) with black symbols. The symbol with deviation in the upper right corners of the alluvial location plots shows the analytical error between total and speciated arsenic. The map above is not to scale but shows approximate sampling locations in relation to the approximate thalweg (blue dashed line).

Figure D-3.0-7 Arsenic concentrations in Sandia wetland surface water and alluvial system



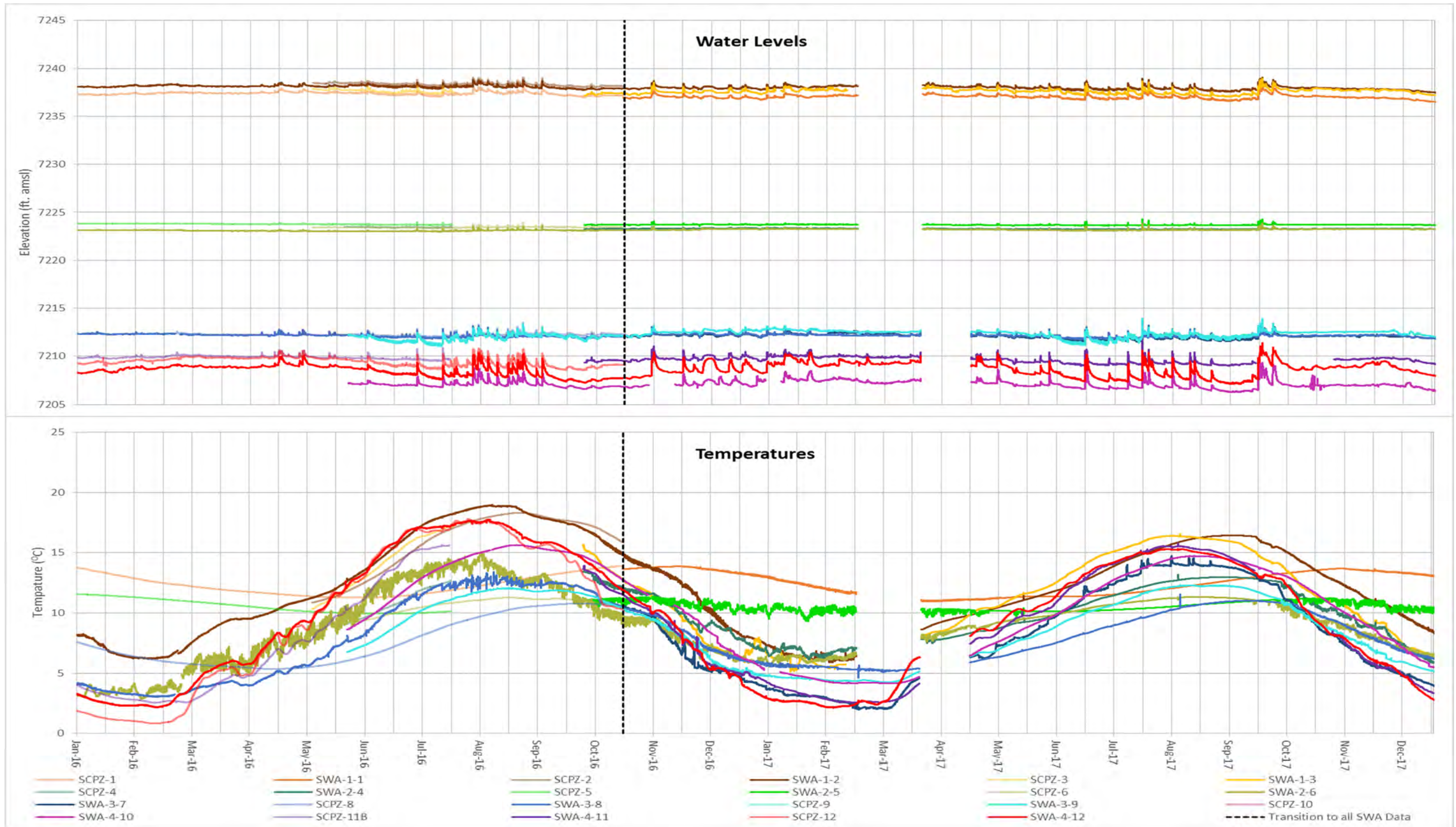
Notes: Surface water stations include E121, E122 (plot not shown), and E123. Piezometers are labeled with the prefix SCPZ (square symbols), and alluvial wells are labeled with the prefix SWA (circle symbols). The plots are arranged in four transects from west to east. Data are plotted for the full period of wetland monitoring. Nondetects are plotted as the MDL with open symbols. Total chromium is represented with the colored symbols and Cr(VI) with black symbols. The map above is not to scale but shows approximate sampling locations in relation to the approximate thalweg (blue dashed line).

Figure D-3.0-8 Chromium concentrations in Sandia wetland surface water and alluvial system



Notes: Water levels collected in the Sandia wetland were at times adjusted for reference value calculation errors and then checked against manual measurements taken in the field during sampling events. Most adjustments were made in response to inaccurate values of the wells inner/outer casing elevations and calculation errors when defining the new reference level. All changes made were made following standard operating procedure ER-SOP-20231, "Groundwater-Level Data Processing, Review, and Validation".

Figure D-4.0-1 Water levels recorded by sondes located in the alluvial system plotted with precipitation data from the E121.9 weather station and total daily volume of flow in surface water gaging station E121 in 2016 and 2017



Notes: The sonde in SWA-4-11 had software malfunction errors during mid-September 2017 and was replaced in November 2017.

Figure D-4.0-2 Time series of water level and temperature in alluvial system in 2016 and 2017

Table D-2.0-1
Travel Time of Flood Bore, Peak Discharge, Increase or Decrease
in Peak Discharge, and Percent Change in Peak Discharge from Upgradient
to Downgradient of the Wetland for Each Sample-Triggering Storm Event in 2017

Date	Travel Time from E121 to E123 (min)	Peak Discharge (cfs)		+/- ^a	% ^b	Travel Time from E122 to E123 (min)	Peak Discharge (cfs)		+/-	%
		E121	E123				E122	E123		
6/6	90	26	16	-	38	90	2.3	16	+	86
6/25	85	20	30	+	33	65	2.8	30	+	91
7/18	85	36	14	-	61	85	5.3	14	+	62
7/26	45	87	78	-	10	40	9.1	78	+	88
7/27	90	6.8	8.4	+	19	85	1.9	8.4	+	77
7/29	65	30	29	-	3	65	4.7	29	+	84
8/21	75	9	10	+	14	75	1.8	10	+	82
Min	45	6.8	8.4	— ^c	3	40	1.8	8.4	—	62
Mean	76	31	26	—	26	72	4.0	26	—	81
Max	90	87	78	—	61	90	9.1	78	—	91

^a + = Increase; - = decrease.

^b % = Percent change in peak discharge.

^c — = Result is not applicable.

Table D-2.0-2
Calculated Sediment Yield and Runoff Volume at Gaging Stations
E121, E122, and E123 for Each Sample-Triggering Storm Event from 2014 to 2017

Station	Date	Sediment Yield (ton)	Sediment Volume (yd ³)	Runoff Volume (acre-feet)	Peak Discharge (cfs)
2017					
E121	6/6/2017	0.70	0.31	0.8	26
E121	6/25/2017	0.71	0.32	1.7	21
E121	7/18/2017	0.48	0.22	1.5	36
E121	7/26/2017	4.09	1.83	2.8	87
E121	7/29/2017	0.88	0.40	1.4	30
E122	7/18/2017	0.11	0.05	0.2	5
E122	7/27/2017	0.02	0.01	0.1	2
E122	7/29/2017	0.13	0.06	0.3	5
E122	8/21/2017	<0.01	<0.01	0.2	2
E123	6/25/2017	1.10	0.49	2.9	30
E123	7/26/2017	8.79	3.94	6.2	78
E123	7/29/2017	0.64	0.29	2.7	29
2016					
E121	7/1/2016	0.36	0.16	0.8	22
E121	7/15/2016	0.26	0.12	1.2	22
E121	7/31/2016	1.80	0.81	2.7	47
E121	8/3/2016	0.34	0.15	1.6	37
E121	8/27/2016	1.57	0.70	1.9	51
E121	9/6/2016	0.75	0.34	1.5	40
E121	11/4/2016	0.15	0.07	0.8	8.4
E122	10/3/2016	0.02	0.01	0.1	22
E122	10/8/2016	0.01	0.01	0.1	22
E122	11/4/2016	0.03	0.01	0.1	47
E123	7/31/2016	0.34	0.15	4.0	46
E123	8/3/2016	2.10	0.94	2.9	13
E123	8/27/2016	0.54	0.24	3.3	28
E123	9/6/2016	0.15	0.07	3.1	18
E123	11/5–11/6/2016	0.16	0.07	3.4	15
2015					
E121	6/1/2015	0.45	0.20	1.7	20
E121	6/26/2015	3.88	1.74	1.3	18
E121	7/3/2015	0.71	0.32	1.6	30
E121	7/15–7/16/2015	0.50	0.22	1.3	39
E121	7/20–7/21/2015	1.62	0.73	4.0	50
E121	7/29–7/30/2015	0.38	0.17	2.2	14
E121	7/31/2015	0.27	0.12	1.1	9.2
E121	8/17/2015	0.45	0.20	1.6	36
E121	10/23–10/24/2015	0.38	0.17	2.0	28
E122	10/23–10/24/2015	0.07	0.03	0.4	5.1

Table D-2.0-2 (continued)

2015 (continued)					
E123	7/3/2015	1.26	0.56	3.9	35
E123	7/20–7/21/2015	2.58	1.16	10.6	64
E123	7/29–7/30/2015	0.84	0.37	5.8	29
E123	8/8/2015	0.15	0.07	1.8	16
E123	8/17/2015	1.06	0.47	3.2	38
E123	10/20/2015	0.25	0.11	1.9	16
E123	10/23/2015	1.19	0.53	4.6	48
2014					
E121	7/7/2014	0.84	0.38	2.3	63
E121	7/14–7/15/2014	0.19	0.09	0.7	4.8
E121	7/15–7/16/2014	1.64	0.73	0.6	10
E121	7/19/2014	3.22	1.44	0.6	11
E121	7/27–7/28/2014	0.57	0.26	0.9	29
E121	7/31/2014	15.4	6.91	2.9	66
E122	7/8/2014	0.60	0.27	1.0	10
E122	7/27–7/28/2014	0.05	0.02	0.6	6.2
E122	7/29/2014	0.73	0.33	1.2	12
E122	7/31/2014	1.55	0.69	1.0	19
E123	5/23/2014	1.62	0.73	2.7	18
E123	7/7/2014	4.12	1.84	6.4	80
E123	7/8/2014	18.2	8.14	7.0	76
E123	7/15–7/16/2014	2.01	0.90	3.1	20
E123	7/19/2014	0.39	0.17	1.7	18
E123	7/29/2014	7.36	3.30	7.5	62
E123	7/31/2014	28.6	12.8	7.2	109

**Table D-2.1-1
Analytical Exceedances in Surface Water at Gaging Stations E121, E122, and E123**

Location	Location alias	Date	Sample Time	Analyte	Sample Type ^a	Sample Purpose ^b	Field Prep Code ^c	Result	Unit	MDL ^d	PQL ^e	Screening Level	Screening Level Type	Comments
Sandia right fork at Pwr Plant	E121	7/18/2017	10:50	Total PCB	WS	REG	UF	0.14	ug/L	NA ^f	NA	0.014	WH ^g	
Sandia right fork at Pwr Plant	E121	7/18/2017	10:50	Total PCB	WS	FD	UF	0.14	ug/L	NA	NA	0.014	Aquatic Life Chronic ^h	
Sandia right fork at Pwr Plant	E121	7/26/2017	10:24	Total PCB	WS	REG	UF	0.231	ug/L	NA	NA	0.014	Aquatic Life Chronic	
Sandia right fork at Pwr Plant	E121	7/26/2017	11:40	Total PCB	WS	REG	UF	0.231	ug/L	NA	NA	0.00064	Aquatic Life HH-OO ⁱ	
Sandia right fork at Pwr Plant	E121	6/6/2017	10:24	Zinc	WS	FD	F	35.9	ug/L	3.3	10	33.4	Aquatic Life Chronic	measured hardness used
Sandia right fork at Pwr Plant	E121	7/18/2017	11:40	Zinc	WS	REG	F	25.5	ug/L	3.3	10	24.7	Aquatic Life Chronic	measured hardness used
Sandia right fork at Pwr Plant	E121	6/6/2017	12:49	Aluminum	WT	REG	F	270	ug/L	19.3	50	196	Aquatic Life Chronic	measured hardness used
Sandia right fork at Pwr Plant	E121	6/6/2017	20:00	Aluminum	WT	REG	UF	459	ug/L	19.3	50	196	Aquatic Life Chronic	measured hardness used
Sandia right fork at Pwr Plant	E121	7/18/2017	12:10	Aluminum	WT	REG	UF	2160	ug/L	19.3	50	125	Aquatic Life Chronic	measured hardness used
Sandia right fork at Pwr Plant	E121	7/18/2017	19:19	Aluminum	WT	REG	F	317	ug/L	19.3	50	125	Aquatic Life Chronic	measured hardness used
Sandia right fork at Pwr Plant	E121	7/26/2017	12:10	Aluminum	WT	REG	F	721	ug/L	19.3	50	223	Aquatic Life Chronic	measured hardness used
Sandia right fork at Pwr Plant	E121	7/26/2017	20:00	Aluminum	WT	REG	UF	2910	ug/L	19.3	50	223	Aquatic Life Chronic	measured hardness used
Sandia right fork at Pwr Plant	E121	7/29/2017	12:49	Aluminum	WT	REG	F	416	ug/L	19.3	50	80.3	Aquatic Life Chronic	measured hardness used
Sandia right fork at Pwr Plant	E121	7/29/2017	19:19	Aluminum	WT	REG	UF	1900	ug/L	19.3	50	80.3	Aquatic Life Chronic	measured hardness used
Sandia right fork at Pwr Plant	E121	6/6/2017	12:10	Copper	WT	REG	F	8.49	ug/L	0.3	1	2.66	Aquatic Life Chronic	measured hardness used
Sandia right fork at Pwr Plant	E121	7/18/2017	19:19	Copper	WT	REG	F	6.13	ug/L	0.3	1	2.01	Aquatic Life Chronic	measured hardness used
Sandia right fork at Pwr Plant	E121	7/26/2017	20:00	Copper	WT	REG	F	7.24	ug/L	0.3	1	2.89	Aquatic Life Chronic	measured hardness used
Sandia right fork at Pwr Plant	E121	7/29/2017	12:49	Copper	WT	REG	F	4.43	ug/L	0.3	1	1.53	Aquatic Life Chronic	measured hardness used
Sandia right fork at Pwr Plant	E121	7/26/2017	20:00	Lead	WT	REG	F	0.933	ug/L	0.5	2	0.58	Aquatic Life Chronic	measured hardness used
Sandia right fork at Pwr Plant	E121	7/29/2017	12:10	Lead	WT	REG	F	0.528	ug/L	0.5	2	0.249	Aquatic Life Chronic	measured hardness used
Sandia right fork at Pwr Plant	E121	2/22/2017	11:20	Total PCB	WT	REG	UF	0.00362	ug/L	NA	NA	0.00064	Aquatic Life HH-OO	
Sandia right fork at Pwr Plant	E121	2/22/2017	11:59	Total PCB	WT	REG	UF	0.00367	ug/L	NA	NA	0.00064	Aquatic Life HH-OO	
Sandia right fork at Pwr Plant	E121	5/22/2017	11:20	Total PCB	WT	REG	UF	0.00315	ug/L	NA	NA	0.00064	Aquatic Life HH-OO	
Sandia right fork at Pwr Plant	E121	6/6/2017	11:20	Total PCB	WT	REG	UF	0.0335	ug/L	NA	NA	0.00064	Aquatic Life HH-OO	
Sandia right fork at Pwr Plant	E121	6/6/2017	19:10	Total PCB	WT	REG	UF	0.0335	ug/L	NA	NA	0.014	WH	
Sandia right fork at Pwr Plant	E121	6/6/2017	19:10	Total PCB	WT	REG	UF	0.0335	ug/L	NA	NA	0.014	Aquatic Life Chronic	
Sandia right fork at Pwr Plant	E121	7/18/2017	19:10	Total PCB	WT	REG	UF	0.14	ug/L	NA	NA	0.00064	Aquatic Life HH-OO	
Sandia right fork at Pwr Plant	E121	7/26/2017	18:29	Total PCB	WT	REG	UF	0.231	ug/L	NA	NA	0.014	WH	
Sandia right fork at Pwr Plant	E121	7/29/2017	18:29	Total PCB	WT	REG	UF	0.0568	ug/L	NA	NA	0.014	Aquatic Life Chronic	
Sandia right fork at Pwr Plant	E121	7/29/2017	18:29	Total PCB	WT	REG	UF	0.0568	ug/L	NA	NA	0.00064	Aquatic Life HH-OO	
Sandia right fork at Pwr Plant	E121	7/29/2017	20:00	Total PCB	WT	REG	UF	0.0568	ug/L	NA	NA	0.014	WH	
Sandia right fork at Pwr Plant	E121	8/10/2017	12:10	Total PCB	WT	REG	UF	0.00205	ug/L	NA	NA	0.00064	Aquatic Life HH-OO	
Sandia right fork at Pwr Plant	E121	8/10/2017	19:19	Total PCB	WT	REG	UF	0.00215	ug/L	NA	NA	0.00064	Aquatic Life HH-OO	
Sandia right fork at Pwr Plant	E121	11/28/2017	12:49	Total PCB	WT	REG	UF	0.00192	ug/L	NA	NA	0.00064	Aquatic Life HH-OO	
Sandia right fork at Pwr Plant	E121	7/26/2017	11:59	Zinc	WT	REG	F	49.2	ug/L	3.3	10	36.3	Aquatic Life Chronic	measured hardness used
Sandia right fork at Pwr Plant	E121	7/29/2017	11:59	Zinc	WT	REG	F	24.2	ug/L	3.3	10	18.4	Aquatic Life Chronic	measured hardness used
South Fork of Sandia at E122	E122	2/22/2017	11:41	Total PCB	WS	REG	UF	0.000827	ug/L	NA	NA	0.00064	Aquatic Life HH-OO	
Sandia left fork at Asph Plant	E122	7/18/2017	18:37	Aluminum	WT	REG	UF	9030	ug/L	19.3	50	138	Aquatic Life Chronic	measured hardness used

Table D-2.1-1 (continued)
Analytical Exceedances in Surface Water at Gaging Stations E121, E122, and E123

Location	Location alias	Date	Sample Time	Analyte	Sample Type ^a	Sample Purpose ^b	Field Prep Code ^c	Result	Unit	MDL ^d	PQL ^e	Screening Level	Screening Level Type	Comments
Sandia left fork at Asph Plant	E122	7/18/2017	19:17	Aluminum	WT	REG	F	610	ug/L	19.3	50	138	Aquatic Life Chronic	measured hardness used
Sandia left fork at Asph Plant	E122	7/26/2017	02:12	Aluminum	WT	REG	F	917	ug/L	19.3	50	161	Aquatic Life Chronic	measured hardness used
Sandia left fork at Asph Plant	E122	7/26/2017	11:24	Aluminum	WT	REG	UF	8870	ug/L	19.3	50	161	Aquatic Life Chronic	measured hardness used
Sandia left fork at Asph Plant	E122	7/29/2017	02:12	Aluminum	WT	REG	UF	1020	ug/L	19.3	50	99.2	Aquatic Life Chronic	measured hardness used
Sandia left fork at Asph Plant	E122	7/29/2017	11:24	Aluminum	WT	REG	F	482	ug/L	19.3	50	99.2	Aquatic Life Chronic	measured hardness used
Sandia left fork at Asph Plant	E122	8/21/2017	18:37	Aluminum	WT	REG	UF	1260	ug/L	19.3	50	61.8	Aquatic Life Chronic	measured hardness used
Sandia left fork at Asph Plant	E122	8/21/2017	19:17	Aluminum	WT	REG	F	300	ug/L	19.3	50	61.8	Aquatic Life Chronic	measured hardness used
Sandia left fork at Asph Plant	E122	7/18/2017	19:17	Copper	WT	REG	F	11.2	ug/L	0.3	1	2.14	Aquatic Life Chronic	measured hardness used
Sandia left fork at Asph Plant	E122	7/26/2017	11:24	Copper	WT	REG	F	5.2	ug/L	0.3	1	2.35	Aquatic Life Chronic	measured hardness used
Sandia left fork at Asph Plant	E122	7/29/2017	02:12	Copper	WT	REG	F	4.62	ug/L	0.3	1	1.74	Aquatic Life Chronic	measured hardness used
Sandia left fork at Asph Plant	E122	8/21/2017	18:37	Copper	WT	REG	F	7.59	ug/L	0.3	1	1.29	Aquatic Life Chronic	measured hardness used
Sandia left fork at Asph Plant	E122	7/18/2017	18:37	Lead	WT	REG	F	0.823	ug/L	0.5	2	0.39	Aquatic Life Chronic	measured hardness used
Sandia left fork at Asph Plant	E122	7/26/2017	11:24	Lead	WT	REG	F	1.03	ug/L	0.5	2	0.442	Aquatic Life Chronic	measured hardness used
Sandia left fork at Asph Plant	E122	7/29/2017	19:17	Lead	WT	REG	F	0.572	ug/L	0.5	2	0.297	Aquatic Life Chronic	measured hardness used
Sandia left fork at Asph Plant	E122	8/21/2017	02:12	Lead	WT	REG	F	0.582	ug/L	0.5	2	0.2	Aquatic Life Chronic	measured hardness used
Sandia left fork at Asph Plant	E122	7/18/2017	02:06	Total PCB	WT	REG	UF	0.105	ug/L	NA	NA	0.00064	Aquatic Life HH-OO	
Sandia left fork at Asph Plant	E122	7/18/2017	19:11	Total PCB	WT	REG	UF	0.105	ug/L	NA	NA	0.014	WH	
Sandia left fork at Asph Plant	E122	7/18/2017	19:11	Total PCB	WT	REG	UF	0.105	ug/L	NA	NA	0.014	Aquatic Life Chronic	
Sandia left fork at Asph Plant	E122	7/26/2017	18:31	Total PCB	WT	REG	UF	0.0441	ug/L	NA	NA	0.014	WH	
Sandia left fork at Asph Plant	E122	7/26/2017	18:31	Total PCB	WT	REG	UF	0.0441	ug/L	NA	NA	0.014	Aquatic Life Chronic	
Sandia left fork at Asph Plant	E122	7/26/2017	19:11	Total PCB	WT	REG	UF	0.0441	ug/L	NA	NA	0.00064	Aquatic Life HH-OO	
Sandia left fork at Asph Plant	E122	7/29/2017	11:26	Total PCB	WT	REG	UF	0.039	ug/L	NA	NA	0.014	WH	
Sandia left fork at Asph Plant	E122	7/29/2017	11:26	Total PCB	WT	REG	UF	0.039	ug/L	NA	NA	0.014	Aquatic Life Chronic	
Sandia left fork at Asph Plant	E122	7/29/2017	18:31	Total PCB	WT	REG	UF	0.039	ug/L	NA	NA	0.00064	Aquatic Life HH-OO	
Sandia left fork at Asph Plant	E122	8/21/2017	02:12	Total PCB	WT	REG	UF	0.0782	ug/L	NA	NA	0.014	Aquatic Life Chronic	
Sandia left fork at Asph Plant	E122	8/21/2017	11:26	Total PCB	WT	REG	UF	0.0782	ug/L	NA	NA	0.00064	Aquatic Life HH-OO	
Sandia left fork at Asph Plant	E122	8/21/2017	18:37	Total PCB	WT	REG	UF	0.0782	ug/L	NA	NA	0.014	WH	
Sandia left fork at Asph Plant	E122	7/18/2017	02:06	Zinc	WT	REG	F	39.4	ug/L	3.3	10	26.4	Aquatic Life Chronic	measured hardness used
Sandia left fork at Asph Plant	E122	8/21/2017	02:06	Zinc	WT	REG	F	36.8	ug/L	3.3	10	15.5	Aquatic Life Chronic	measured hardness used
Sandia below Wetlands	E123	6/6/2017	13:43	Total PCB	WS	REG	UF	0.0544	ug/L	NA	NA	0.014	WH	
Sandia below Wetlands	E123	6/25/2017	09:47	Total PCB	WS	REG	UF	0.0404	ug/L	NA	NA	0.00064	Aquatic Life HH-OO	
Sandia below Wetlands	E123	6/25/2017	12:26	Total PCB	WS	FD	UF	0.0404	ug/L	NA	NA	0.014	WH	
Sandia below Wetlands	E123	6/25/2017	12:26	Total PCB	WS	REG	UF	0.0404	ug/L	NA	NA	0.014	Aquatic Life Chronic	
Sandia below Wetlands	E123	7/29/2017	12:16	Total PCB	WS	REG	UF	0.0777	ug/L	NA	NA	0.00064	Aquatic Life HH-OO	
Sandia below Wetlands	E123	6/6/2017	12:08	Aluminum	WT	REG	F	420	ug/L	19.3	50	283	Aquatic Life Chronic	measured hardness used
Sandia below Wetlands	E123	6/6/2017	13:37	Aluminum	WT	REG	UF	990	ug/L	19.3	50	283	Aquatic Life Chronic	measured hardness used
Sandia below Wetlands	E123	6/25/2017	17:47	Aluminum	WT	REG	F	229	ug/L	19.3	50	165	Aquatic Life Chronic	measured hardness used
Sandia below Wetlands	E123	6/25/2017	20:01	Aluminum	WT	REG	UF	2500	ug/L	19.3	50	165	Aquatic Life Chronic	measured hardness used

Table D-2.1-1 (continued)
Analytical Exceedances in Surface Water at Gaging Stations E121, E122, and E123

Location	Location alias	Date	Sample Time	Analyte	Sample Type ^a	Sample Purpose ^b	Field Prep Code ^c	Result	Unit	MDL ^d	PQL ^e	Screening Level	Screening Level Type	Comments
Sandia below Wetlands	E123	7/18/2017	17:47	Aluminum	WT	REG	F	191	ug/L	19.3	50	165	Aquatic Life Chronic	measured hardness used
Sandia below Wetlands	E123	7/18/2017	20:38	Aluminum	WT	REG	UF	2210	ug/L	19.3	50	165	Aquatic Life Chronic	measured hardness used
Sandia below Wetlands	E123	7/26/2017	20:01	Aluminum	WT	REG	F	988	ug/L	19.3	50	164	Aquatic Life Chronic	measured hardness used
Sandia below Wetlands	E123	7/26/2017	20:38	Aluminum	WT	REG	UF	27700	ug/L	19.3	50	164	Aquatic Life Chronic	measured hardness used
Sandia below Wetlands	E123	7/29/2017	12:08	Aluminum	WT	REG	F	477	ug/L	19.3	50	104	Aquatic Life Chronic	measured hardness used
Sandia below Wetlands	E123	7/29/2017	13:37	Aluminum	WT	REG	UF	2150	ug/L	19.3	50	104	Aquatic Life Chronic	measured hardness used
Sandia below Wetlands	E123	6/6/2017	12:08	Copper	WT	REG	F	5.63	ug/L	0.3	1	3.35	Aquatic Life Chronic	measured hardness used
Sandia below Wetlands	E123	6/25/2017	17:47	Copper	WT	REG	F	8.68	ug/L	0.3	1	2.39	Aquatic Life Chronic	measured hardness used
Sandia below Wetlands	E123	7/18/2017	20:38	Copper	WT	REG	F	6.92	ug/L	0.3	1	2.39	Aquatic Life Chronic	measured hardness used
Sandia below Wetlands	E123	7/26/2017	20:01	Copper	WT	REG	F	4.16	ug/L	0.3	1	2.38	Aquatic Life Chronic	measured hardness used
Sandia below Wetlands	E123	7/29/2017	13:37	Copper	WT	REG	F	4.64	ug/L	0.3	1	1.79	Aquatic Life Chronic	measured hardness used
Sandia below Wetlands	E123	7/26/2017	20:38	Gross alpha	WT	REG	UF	33.6	pCi/L	NA	NA	15	LW ^j	
Sandia below Wetlands	E123	6/25/2017	17:41	Lead	WT	REG	F	0.526	ug/L	0.5	2	0.452	Aquatic Life Chronic	measured hardness used
Sandia below Wetlands	E123	7/18/2017	17:47	Lead	WT	REG	F	0.615	ug/L	0.5	2	0.452	Aquatic Life Chronic	measured hardness used
Sandia below Wetlands	E123	7/26/2017	20:01	Lead	WT	REG	F	1.2	ug/L	0.5	2	0.449	Aquatic Life Chronic	measured hardness used
Sandia below Wetlands	E123	7/29/2017	12:08	Lead	WT	REG	F	0.629	ug/L	0.5	2	0.308	Aquatic Life Chronic	measured hardness used
Sandia below Wetlands	E123	2/22/2017	12:14	Total PCB	WT	REG	UF	0.00297	ug/L	NA	NA	0.00064	Aquatic Life HH-OO	
Sandia below Wetlands	E123	5/22/2017	12:02	Total PCB	WT	REG	UF	0.00452	ug/L	NA	NA	0.00064	Aquatic Life HH-OO	
Sandia below Wetlands	E123	6/6/2017	12:02	Total PCB	WT	REG	UF	0.0544	ug/L	NA	NA	0.014	Aquatic Life Chronic	
Sandia below Wetlands	E123	6/6/2017	12:02	Total PCB	WT	REG	UF	0.0544	ug/L	NA	NA	0.00064	Aquatic Life HH-OO	
Sandia below Wetlands	E123	7/18/2017	13:31	Total PCB	WT	REG	UF	0.033	ug/L	NA	NA	0.014	WH	
Sandia below Wetlands	E123	7/18/2017	13:31	Total PCB	WT	REG	UF	0.033	ug/L	NA	NA	0.014	Aquatic Life Chronic	
Sandia below Wetlands	E123	7/18/2017	13:31	Total PCB	WT	REG	UF	0.033	ug/L	NA	NA	0.00064	Aquatic Life HH-OO	
Sandia below Wetlands	E123	7/26/2017	19:55	Total PCB	WT	REG	UF	0.293	ug/L	NA	NA	0.014	WH	
Sandia below Wetlands	E123	7/26/2017	19:55	Total PCB	WT	REG	UF	0.293	ug/L	NA	NA	0.014	Aquatic Life Chronic	
Sandia below Wetlands	E123	7/26/2017	19:55	Total PCB	WT	REG	UF	0.293	ug/L	NA	NA	0.00064	Aquatic Life HH-OO	
Sandia below Wetlands	E123	7/29/2017	20:30	Total PCB	WT	REG	UF	0.0777	ug/L	NA	NA	0.014	WH	
Sandia below Wetlands	E123	7/29/2017	20:30	Total PCB	WT	REG	UF	0.0777	ug/L	NA	NA	0.014	Aquatic Life Chronic	
Sandia below Wetlands	E123	8/10/2017	20:30	Total PCB	WT	REG	UF	0.00337	ug/L	NA	NA	0.00064	Aquatic Life HH-OO	
Sandia below Wetlands	E123	11/28/2017	17:41	Total PCB	WT	REG	UF	0.00177	ug/L	NA	NA	0.00064	Aquatic Life HH-OO	
Sandia below Wetlands	E123	11/28/2017	17:41	Total PCB	WT	REG	UF	0.00184	ug/L	NA	NA	0.00064	Aquatic Life HH-OO	

Note: Shaded rows indicate base flow, unshaded rows indicate storm flow.

^a W and WS = Base flow water; WT = storm water.

^b REG = Regular investigative sample; FD = field duplicate.

^c F = Filtered using 0.45-µm pore size; UF = nonfiltered.

^d MDL = Method detection limit.

^e PQL = Practical quantitation limit.

^f NA = Not available.

^g WH = Wildlife Habitat Standard.

^h Aquatic Life Chronic = NMWQCC Aquatic Life Standards Chronic. Aquatic Life HH-OO = Human Health Organism Only Aquatic Life Standard.

ⁱ Aquatic Life HH-OO = Human Health Organism Only Aquatic Life Standard.

^j LW = Livestock Watering Standard.

**Table D-2.1-2
Summary of 2017 Base Flow and Storm Water SWQC Exceedances**

Location	Media Type	Filtration	Analyte	Total Samples	Number of Samples Exceeding SWQC	Average of Sample Results Exceeding SWQC	Maximum Sample Results Exceeding SWQC	Units
E121	Base Flow	UF ^a	Total PCB	6	6	0.00276	0.00367	ug/L
E122	Base Flow	UF	Total PCB	5	1	0.00083	0.000827	ug/L
E123	Base Flow	UF	Total PCB	5	5	0.00289	0.00452	ug/L
E121	Storm water	F ^b	Aluminum	4	4	431	721	ug/L
E122	Storm water	F	Aluminum	4	4	577	917	ug/L
E123	Storm water	F	Aluminum	5	5	461	988	ug/L
E121	Storm water	UF	Aluminum	4	4	1857	2910	ug/L
E122	Storm water	UF	Aluminum	4	4	5045	9030	ug/L
E123	Storm water	UF	Aluminum	5	5	7110	27700	ug/L
E121	Storm water	F	Copper	4	4	6.57	8.49	ug/L
E122	Storm water	F	Copper	4	4	7.15	11.2	ug/L
E123	Storm water	F	Copper	5	5	6.01	8.68	ug/L
E123	Storm water	UF	Gross alpha	5	1	33.6	33.6	pCi/L
E121	Storm water	F	Lead	4	1	0.933	0.933	ug/L
E122	Storm water	F	Lead	4	4	0.752	1.03	ug/L
E123	Storm water	F	Lead	5	5	0.720	1.2	ug/L
E121	Storm water	UF	Total PCB	4	4	0.11533	0.231	ug/L
E122	Storm water	UF	Total PCB	4	4	0.06658	0.105	ug/L
E123	Storm water	UF	Total PCB	5	5	0.09970	0.293	ug/L
E121	Storm water	F	Zinc	4	2	42.6	49.2	ug/L
E122	Storm water	F	Zinc	4	2	38.1	39.4	ug/L

^a UF = Non-filtered.

^b F = Filtration using 0.45- μ m pore size.

**Table D-3.4-1
Analytical Exceedances in the Alluvial System**

Location	Date	Analyte	Field Prep Code ^a	Result	Unit	MDL ^b	Screening Value	Screening Value Type ^c
SWA-1-1	2/23/2017	Iron	F	6180	µg/L	30	1000	NM GW STD
SWA-1-1	5/24/2017	Iron	F	9370	µg/L	30	1000	NM GW STD
SWA-1-1	8/16/2017	Iron	F	5890	µg/L	30	1000	NM GW STD
SWA-1-1	11/29/2017	Iron	F	5010	µg/L	30	1000	NM GW STD
SWA-1-1	2/23/2017	Manganese	F	1350	µg/L	2	200	NM GW STD
SWA-1-1	5/24/2017	Manganese	F	2130	µg/L	2	200	NM GW STD
SWA-1-1	8/16/2017	Manganese	F	1420	µg/L	2	200	NM GW STD
SWA-1-1	11/29/2017	Manganese	F	1220	µg/L	2	200	NM GW STD
SWA-1-2	5/24/2017	Chromium	F	59.1	µg/L	3	50	NM GW STD
SWA-1-2	8/16/2017	Chromium	F	72.6	µg/L	3	50	NM GW STD
SWA-1-2	11/29/2017	Chromium	F	60.1	µg/L	3	50	NM GW STD
SWA-1-3	2/23/2017	Iron	F	10900	µg/L	30	1000	NM GW STD
SWA-1-3	5/24/2017	Iron	F	5170	µg/L	30	1000	NM GW STD
SWA-1-3	8/16/2017	Iron	F	5990	µg/L	30	1000	NM GW STD
SWA-1-3	11/29/2017	Iron	F	4500	µg/L	30	1000	NM GW STD
SWA-1-3	2/23/2017	Manganese	F	575	µg/L	2	200	NM GW STD
SWA-1-3	5/24/2017	Manganese	F	276	µg/L	2	200	NM GW STD
SWA-1-3	8/16/2017	Manganese	F	307	µg/L	2	200	NM GW STD
SWA-1-3	11/29/2017	Manganese	F	298	µg/L	2	200	NM GW STD
SWA-2-4	2/23/2017	Iron	F	1950	µg/L	30	1000	NM GW STD
SWA-2-4	8/15/2017	Iron	F	1300	µg/L	30	1000	NM GW STD
SWA-2-4	11/29/2017	Iron	F	1290	µg/L	30	1000	NM GW STD
SWA-2-4	2/23/2017	Manganese	F	733	µg/L	2	200	NM GW STD
SWA-2-4	5/24/2017	Manganese	F	395	µg/L	2	200	NM GW STD
SWA-2-4	8/15/2017	Manganese	F	470	µg/L	2	200	NM GW STD
SWA-2-4	11/29/2017	Manganese	F	450	µg/L	2	200	NM GW STD
SWA-2-5	2/23/2017	Arsenic	F	10.4	µg/L	1.7	10	EPA MCL
SWA-2-5	2/23/2017	Iron	F	5530	µg/L	30	1000	NM GW STD
SWA-2-5	5/24/2017	Iron	F	7840	µg/L	30	1000	NM GW STD
SWA-2-5	8/15/2017	Iron	F	7080	µg/L	30	1000	NM GW STD
SWA-2-5	11/29/2017	Iron	F	5990	µg/L	30	1000	NM GW STD
SWA-2-5	2/23/2017	Manganese	F	1070	µg/L	2	200	NM GW STD
SWA-2-5	5/24/2017	Manganese	F	1520	µg/L	2	200	NM GW STD
SWA-2-5	8/15/2017	Manganese	F	1370	µg/L	2	200	NM GW STD
SWA-2-5	11/29/2017	Manganese	F	1200	µg/L	2	200	NM GW STD
SWA-2-6	2/23/2017	Arsenic	F	12.6	µg/L	1.7	10	EPA MCL
SWA-2-6	5/24/2017	Arsenic	F	12.1	µg/L	2	10	EPA MCL

Table D-3.4-1 (continued)

Location	Date	Analyte	Field Prep Code ^a	Result	Unit	MDL ^b	Screening Value	Screening Value Type ^c
SWA-2-6	8/15/2017	Arsenic	F	10.9	µg/L	2	10	EPA MCL
SWA-2-6	11/29/2017	Arsenic	F	10.4	µg/L	2	10	EPA MCL
SWA-2-6	2/23/2017	Iron	F	6910	µg/L	30	1000	NM GW STD
SWA-2-6	5/24/2017	Iron	F	8310	µg/L	30	1000	NM GW STD
SWA-2-6	8/15/2017	Iron	F	7320	µg/L	30	1000	NM GW STD
SWA-2-6	2/23/2017	Manganese	F	1120	µg/L	2	200	NM GW STD
SWA-2-6	5/24/2017	Manganese	F	1490	µg/L	2	200	NM GW STD
SWA-2-6	8/15/2017	Manganese	F	1260	µg/L	2	200	NM GW STD
SWA-3-7	2/24/2017	Iron	F	16000	µg/L	30	1000	NM GW STD
SWA-3-7	5/23/2017	Iron	F	9520	µg/L	30	1000	NM GW STD
SWA-3-7	8/16/2017	Iron	F	7760	µg/L	30	1000	NM GW STD
SWA-3-7	11/30/2017	Iron	F	11900	µg/L	30	1000	NM GW STD
SWA-3-7	2/24/2017	Manganese	F	4090	µg/L	2	200	NM GW STD
SWA-3-7	5/23/2017	Manganese	F	3040	µg/L	2	200	NM GW STD
SWA-3-7	8/16/2017	Manganese	F	2470	µg/L	2	200	NM GW STD
SWA-3-7	11/30/2017	Manganese	F	3670	µg/L	2	200	NM GW STD
SWA-3-8	2/24/2017	Iron	F	7100	µg/L	30	1000	NM GW STD
SWA-3-8	5/23/2017	Iron	F	7060	µg/L	30	1000	NM GW STD
SWA-3-8	8/16/2017	Iron	F	5830	µg/L	30	1000	NM GW STD
SWA-3-8	11/30/2017	Iron	F	6490	µg/L	30	1000	NM GW STD
SWA-3-8	2/24/2017	Manganese	F	2490	µg/L	2	200	NM GW STD
SWA-3-8	5/23/2017	Manganese	F	2480	µg/L	2	200	NM GW STD
SWA-3-8	8/16/2017	Manganese	F	2070	µg/L	2	200	NM GW STD
SWA-3-8	11/30/2017	Manganese	F	2330	µg/L	2	200	NM GW STD
SWA-3-9	2/24/2017	Iron	F	11000	µg/L	30	1000	NM GW STD
SWA-3-9	5/23/2017	Iron	F	11800	µg/L	30	1000	NM GW STD
SWA-3-9	8/16/2017	Iron	F	10200	µg/L	30	1000	NM GW STD
SWA-3-9	11/30/2017	Iron	F	10100	µg/L	30	1000	NM GW STD
SWA-3-9	2/24/2017	Manganese	F	2200	µg/L	2	200	NM GW STD
SWA-3-9	5/23/2017	Manganese	F	2410	µg/L	2	200	NM GW STD
SWA-3-9	8/16/2017	Manganese	F	2120	µg/L	2	200	NM GW STD
SWA-3-9	11/30/2017	Manganese	F	2050	µg/L	2	200	NM GW STD
SWA-4-10	5/23/2017	Chromium	F	50.2	µg/L	3	50	NM GW STD
SWA-4-10	8/15/2017	Chromium	F	66.7	µg/L	3	50	NM GW STD
SWA-4-10	2/24/2017	Iron	F	9590	µg/L	30	1000	NM GW STD
SWA-4-10	5/23/2017	Iron	F	11500	µg/L	30	1000	NM GW STD
SWA-4-10	8/15/2017	Iron	F	2610	µg/L	30	1000	NM GW STD
SWA-4-10	11/30/2017	Iron	F	1990	µg/L	30	1000	NM GW STD

Table D-3.4-1 (continued)

Location	Date	Analyte	Field Prep Code ^a	Result	Unit	MDL ^b	Screening Value	Screening Value Type ^c
SWA-4-10	2/24/2017	Manganese	F	4640	µg/L	2	200	NM GW STD
SWA-4-10	5/23/2017	Manganese	F	3340	µg/L	2	200	NM GW STD
SWA-4-10	8/15/2017	Manganese	F	1570	µg/L	2	200	NM GW STD
SWA-4-10	11/30/2017	Manganese	F	1170	µg/L	2	200	NM GW STD
SWA-4-11	2/24/2017	Iron	F	2510	µg/L	30	1000	NM GW STD
SWA-4-11	5/23/2017	Iron	F	2500	µg/L	30	1000	NM GW STD
SWA-4-11	8/15/2017	Iron	F	2980	µg/L	30	1000	NM GW STD
SWA-4-11	11/30/2017	Iron	F	2250	µg/L	30	1000	NM GW STD
SWA-4-11	2/24/2017	Manganese	F	696	µg/L	2	200	NM GW STD
SWA-4-11	5/23/2017	Manganese	F	741	µg/L	2	200	NM GW STD
SWA-4-11	8/15/2017	Manganese	F	924	µg/L	2	200	NM GW STD
SWA-4-11	11/30/2017	Manganese	F	838	µg/L	2	200	NM GW STD
SWA-4-12	8/15/2017	Chromium	F	56.2	µg/L	3	50	NM GW STD
SWA-4-12	2/24/2017	Iron	F	8810	µg/L	30	1000	NM GW STD
SWA-4-12	5/23/2017	Iron	F	3230	µg/L	30	1000	NM GW STD
SWA-4-12	8/15/2017	Iron	F	4920	µg/L	30	1000	NM GW STD
SWA-4-12	11/30/2017	Iron	F	3870	µg/L	30	1000	NM GW STD
SWA-4-12	2/24/2017	Manganese	F	1820	µg/L	2	200	NM GW STD
SWA-4-12	5/23/2017	Manganese	F	788	µg/L	2	200	NM GW STD
SWA-4-12	8/15/2017	Manganese	F	1220	µg/L	2	200	NM GW STD
SWA-4-12	11/30/2017	Manganese	F	945	µg/L	2	200	NM GW STD

Note: All values with 5.21 as the MDL had a dilution factor of 10, but this has been accounted for in the results.

^a F = Filtered using 0.45-µm pore size.

^b MDL = Method detection limit.

^c EPA regional screening levels for tap water.

Appendix E

2017 Watershed Mitigations Inspections

E-1.0 INTRODUCTION

Watershed storm water controls and grade-control structures (GCSs) are inspected twice a year and after significant flow events (greater than 50 cubic feet per second at locations with gaging stations). These inspections are completed to ensure watershed mitigations are functioning properly and to determine if maintenance is required. Examples of items evaluated during inspections include:

- debris/sediment accumulation that could impede operation
- water levels behind retention structures
- physical damage of structure, or failure of structural components
- undermining, piping, flanking, settling, movement, or breaching of structure
- vegetation establishment and vegetation that may negatively impact structural components
- rodent damage
- vandalism, and
- erosion.

The photographs in this appendix show the 2017 May and October inspections of watershed mitigations in Sandia Canyon. Each group of photographs is associated with a specific feature (e.g., standpipe, weir, upstream, downstream, vegetated cover) that could develop issues. The photographs are in chronological order and depict the features throughout 2017. Photographs of features were taken to mirror previous inspection photos as closely as possible. Certain findings were discovered as the year progressed and thus appear later during the year.

In 2017, Sandia GCS downstream gage did not record significant flow events. Therefore, two regular inspections were conducted. The inspections demonstrate that wetland plantings were dormant in the first quarter and flourished once the growing season set in.

The photographs in the appendix illustrate the health of the wetland in and around the GCS, revegetation of adjacent slopes, and the best management practices in place to help maintain the integrity of the GCS and its associated wetland vegetation.

Additional data on the position of the channel thalweg in the area of the GCS can be found in Appendix B. Quantitative data from vegetation perimeter mapping in and around the GCS can be found in Appendix C.

E-2.0 CONTROLS INSTALLED IN 2017

In early 2017, a side drainage upstream of the GCS was found to be contributing sediment to the wetland. The drainage receives storm water runoff from impervious areas in TA-3 and TA-60. The runoff created a large erosion feature and an alluvial fan that was beginning to spread into the wetland. Starting in August 2017, several storm water controls were installed at this location to capture and reduce storm water flow velocity and energy. The controls consisted of two log check dams, a flow spreader made from locally sourced trees, and a line of coir logs. Construction was completed in September 2017.

During an inspection in December 2017, damage to the log check dams and flow spreader were found. The site received significant runoff after the final construction inspection in September 2017 and the October GCS inspection. The backwater effect caused by the log check dams caused the flow to move into the subsurface, displaced the log check dam's scour protection, and created a preferential flow path

beneath the dams. Several of the logs making up the flow spreader were also displaced, as they were trenched in, not anchored. The original design failed to account for the highly porous nature of the alluvial channel bed material and misjudged the energy head created by reducing the runoff.

Maintenance on the new controls was completed in January 2018. The log check dams were modified by adding a percolation prevention cut-off wall made of riprap, crushed stone, and geotextile fabric placed subsurface and downstream of the spillways. The log check dam scour protection was replaced with gabion mattresses filled with riprap and crushed stone and buried under native channel material. The displaced logs making up the flow spreader were replaced and anchored with riprap. Riprap was also added to any areas where channelization was occurring to promote sheet flow and prevent further channelization.

Because the control installation occurred near the end of the FY2017, they were not included in the 2017 GCS inspections; however, photographs of the new controls, damaged controls, and repaired controls are included below.

E-2.1 Newly-Installed Side-Drainage Controls Upstream of GCS



Figure E-2.1-1 September 2017: The two log check dams were installed to capture sediment originating from an erosion feature upgradient of the controls. Picture looking toward the wetland/downstream.



Figure E-2.1-2 September 2017: View of newly installed log check dams looking upstream



Figure E-2.1-3 December 2017: View of failed log check dams with displaced scour protection logs. Looking upstream.



Figure E-2.1-4 January 2018: View of repaired log check dams with additional riprap erosion protection. Looking downstream.



Figure E-2.1-5 September 2017: A line of coir logs were installed to allow for both velocity dissipation and sediment capture.



Figure E-2.1-6 September 2017: Logs were trenched end-to-end to create a flow spreader. This control will encourage sheet flow into the wetland, rather than allowing more erosive concentrated flows. Looking west.



Figure E-2.1-7 December 2017: Flow spreader logs displaced during flow event. Logs were replaced and keyed in with riprap during January 2018 maintenance. Looking east.

E-3.0 SANDIA CANYON GCS INSPECTION PHOTOGRAPHS

E-3.1 GCS South Bank- Upper Structure



Figure E-3.1-1 May 2017: South bank of vegetation. Vegetation starting to become established on south bank. No erosion present.



Figure E-3.1-2 October 2017: Vegetation shows improving density of wetland-type vegetation and grasses along the south bank.

E-3.2 GCS North Bank- Upper Structure



Figure E-3.2-1 May 2017: Vegetation dormant showing good stability and density.



Figure E-3.2-2 October 2017: Partial establishment of vegetation on north embankment turf-reinforcement mat.

E-3.3 GCS Wetland- Upper Structure



Figure E-3.3-1 May 2017: Minor channelization occurring near bank but vegetation growth has significantly increased compared to prior season. Continue to monitor. No evidence of cracking or spalling on concrete wall.



Figure E-3.3-2 October 2017: Channelization has decreased since last visit (May 2017). Wetland vegetation has aided in dispersing upstream flow throughout wetland.

E-3.4 GCS South Bank-Middle Structure



Figure E-3.4-1 May 2017: Wetland vegetation well established. Vegetative cover on slope at roughly 50 percent. No evidence of erosion.



Figure E-3.4-2 October 2017: Vegetation cover on slope far more established since last inspection (May 2017). Cover now at 100 percent. No evidence of erosion.

E-3.5 GCS Wetland- Middle Structure



Figure E-3.5-1 May 2017: Wetland vegetation well established. Dispersing flow evenly throughout GCS. No evidence of channelization. No evidence of cracking or spalling on concrete wall.



Figure E-3.5-2 October 2017: Wetland vegetation further established since last site visit (May 2017). No further changes since last site visit.

E-3.6 GCS South Bank- Lower Structure



Figure E-3.6-1 May 2017: Slight vegetation establishment in rip rap. Structure is working as designed with no evidence of channelization.



Figure E-3.6-2 October 2017: No change in site condition since last visit (May 2017).

E-3.7 GCS Cascade Structure



Figure E-3.7-1 May 2017: Cascade structure working as designed. No evidence of rock displacement. No evidence of erosion in/near cascade pool.



Figure E-3.7-2 October 2017: No change in site condition since last inspection (May 2017).

E-2.3 GCS Upper Run-on Defense Cell Barriers



Figure E-3.8-1 May 2017: Upper defense at roughly 50 percent capacity. Los Alamos County upgradient best management practice reducing sediment flow to control. Defense cell operating as designed.



Figure E-3.8-2 October 2017: Slightly less capacity than last site inspection. Control still has capacity for sediment capture. Better established vegetation on downgradient hill-slope since last visit.

E-3.9 GCS Lower Run-on Defense Cell Barriers



Figure E-3.9-1 May 2017: Lower defense cell at 20 percent of capacity. Site stability has allowed for established vegetation growth.



Figure E-3.9-2 October 2017: No change in capacity since last site visit (May 2017). Vegetation slightly more established since last inspection.

Appendix F

*Analytical Data and 5-Min Stage,
Discharge, and Precipitation Data
(on CD included with this document)*

